Inzicht in het reactiemechanisme van industriële processen in de zeolietkatalyse via kwantumchemische technieken

Unraveling the Reaction Mechanism of Industrial Processes in Zeolite Catalysis: a Quantum Chemical Approach

David Lesthaeghe

Promotoren: dr. ir. V. Van Speybroeck, prof. dr. ir. G. B. Marin
Proefschrift ingediend tot het behalen van de graad van
Doctor in de Ingenieurswetenschappen

Vakgroep Subatomaire en Stralingsfysica
Voorzitter: prof. dr. D. Ryckbosch
Faculteit Wetenschappen
Academiejaar 2006 - 2007

UNIVERSITEIT GENT

ISBN 978-90-8578-144-8
NUR 913, 928
Wettelijk depot: D/2007/10.500/18

Center for
Molecular Modeling

Dit onderzoekswerk werd uitgevoerd binnen het Centrum voor Moleculaire Modellering
Hoofd onderzoekseenheid: prof. dr. M. Waroquier

To An & Colin

Leden van de examencommissie

Voorzitter

prof. Luc Taerwe, Academisch Secretaris

Leescommissie

prof. James Haw (University of Southern California, Los Angeles, USA)
prof. Pascal Van Der Voort (WE06)
prof. Rutger van Santen (Technische Universiteit Eindhoven, Nederland)
dr. ir. Veronique Van Speybroeck (WE05), promotor
prof. Michel Waroquier (WE05)

Overige leden

prof. Paul Geerlings (Vrije Universiteit Brussel)
prof. Jacques Grootjans (IR12)
prof. Guy Marin (IR12), promotor
prof. Johan Martens (Katholieke Universiteit Leuven)
prof. Dimitri Van Neck (WE05), secretaris

Contents

Preface xiii

Summary xvii

Samenvatting xxiii

1 Introduction 1

2 Terminology and methodology 7

2.1 Zeolites and zeotype materials 7
2.1.1 Shape selectivity 8
2.1.2 Isomorphic substitution 9
2.1.3 Catalytic cycle 9
2.2 Quantum chemical methods 11
2.3 Approximations in model space 13
2.3.1 Cluster approach 14
2.3.2 Periodic approach 15
2.3.3 QM/MM approach 16
2.3.4 Overview 18
2.4 Chemical kinetics 20
2.4.1 The Arrhenius equation 21
2.4.2 Transition State Theory 21

3 The methanol-to-olefin process 27

3.1 Introduction 27
3.1.1 Controversy surrounding the reaction mechanism 29
3.2 Direct mechanisms 29
3.2.1 Pre-equilibrium phase 32
3.2.2 Trimethyl oxonium ion 32
3.2.3 First bottleneck: ylide and carbene intermediates 36
3.2.4 Second bottleneck: methane/formaldehyde route 37
3.2.5 Third bottleneck: concerted C-C coupling 37
3.2.6 Complete failure 38

3.3 Hydrocarbon pool proposal . . . 39
3.3.1 Experimental observations . . . 39
3.3.2 The supramolecular catalyst . . . 40
3.3.3 Initiating step . . . 43
3.4 Conclusions . . . 45

Published papers on the MTO process **47**
3.5 Chem. Phys. Lett. 417, 2006, 309-315 . . . 49
3.6 Angew. Chem. Int. Ed. 45, 2006, 1714-1719 . . . 59
3.7 Ind. Eng. Chem. Res. 46, 2007, published online . . . 67
3.8 Angew. Chem. Int. Ed. 46, 2007, 1311-1314 . . . 77
3.9 Stud. Surf. Sci. Catal., 2007, in press . . . 83

4 Organic functionalized zeolites **95**

4.1 Introduction . . . 95
4.2 Methylene functionalization . . . 96
4.2.1 Water and ammonia adsorption . . . 97
4.2.2 Charge compensation . . . 98
4.2.3 Proton mobility . . . 99
4.3 Amine functionalization . . . 99
4.3.1 Proton mobility . . . 100
4.3.2 Characterization of acid/base properties . . . 101
4.3.3 Test reaction: alkoxide formation in the MTO process . . . 103
4.3.4 Alkoxide vs. alkylammonium formation . . . 105
4.3.5 Test set for theoretical procedures . . . 109
4.4 Conclusions . . . 109

Published papers on organic functionalization **113**
4.5 Microporous Mesoporous Mater. 96, 2006, 350-356 . . . 115
4.6 J. Am. Chem. Soc. 126, 2004, 9162-9163 . . . 125
4.7 J. Phys. Chem. B 109, 2005, 7952-7960 . . . 129
4.8 Chem. Phys. Lett. 419, 2006, 10-15 . . . 141
4.9 J. Phys. Chem. C 111, 2007, 3028-3037 . . . 149

5 Conclusions and perspectives **163**

The road ahead . . . 165

N Nederlandstalige appendix **169**

N.1 Algemene inleiding . . . 169
N.2 Terminologie en methodiek . . . 170
N.2.1 Zeolieten en zeotype materialen . . . 170
N.2.2 Kwantumchemische benaderingen . . . 172
N.2.3 Atomaire modelkeuzes voor uitgebreide systemen . . . 173
N.2.4 Chemische kinetiek . . . 175
N.3 Conversie van methanol naar lichte olefines . . . 177
N.3.1 Situering . . . 177
N.3.2 Directe mechanismes . . . 179

N.3.3 De hydrocarbon pool hypothese 183
N.4 Organische functionalisering van zeolieten 186
N.4.1 Situering 187
N.4.2 Methyleen-gesubstitueerde zeolieten 187
N.4.3 Amine-gesubstitueerde zeolieten 188
N.5 Algemeen besluit 193

Bibliography **197**

Preface

Before you lies not just the product of three years of research, but this work marks only one of the many milestones in what has been a major transition period for me, both professionally and personally. It cannot be considered as the isolated achievement of just one person: many people have played a role in it and deserve a word of gratitude.

When I started my PhD, prof. dr. Michel Waroquier and dr. ir. Veronique Van Speybroeck simply asked me 'to do something with zeolites'. While at the time it was an enormous challenge to be the first in our group to figure out what zeolites actually were, let alone model them, in retrospect this carte blanche really gave me the freedom to develop my own ideas. I would like to thank Michel, who always believed in me, who continuously stimulated my research and who scraped together the funds so I could go to any conference that might be useful. Driving with him along the spectacular San Francisco coast line and the Golden Gate Bridge remains one of the highlights of these last few years! Furthermore, I have the utmost respect for his courage in boldly switching in mid-career from nuclear physics to developing a new, more chemically oriented, research group. I also have a lot of gratitude to Veronique, who is the main reason behind this switch and who is currently the cornerstone of our group, for the boundless enthusiasm with which she introduced me into the world of molecular modeling. She has also spent many hours discussing results and meticulously proof-reading every single manuscript or conference abstract. In addition, I would like to thank prof. dr. ir. Guy Marin for providing the 'chemical link' to this thesis and for introducing me into the complex world of methanol-to-olefin (MTO) conversion. Furthermore, I am extremely grateful towards all members of the examination board for their enriching questions and constructive comments.

My co-workers at the Center for Molecular Modeling really made sure that the office was always a fun place to go to. First of all comes Karen, my work buddy,

with whom I have shared an office from the very first day of my Master thesis. Almost every day, our resounding laughter could be heard throughout the building. It was also great to have someone going through the same major life-course events to talk to. Karen, I wish you the best of luck in finishing your own PhD. The same goes for Karen H and my INW-colleagues Bart and Barbara, who were always up for a discussion, both work-related and personal. Furthermore, I did not venture into the complex world of heterogeneous catalysis on my own, but Toon and I took our first steps together. Who can forget our very first workshop in which we repeatedly trounced our Dutch counterparts at their own card games? Just recently, Peter has joined our small yet rapidly expanding zeolite club. Most importantly, I cannot imagine the Center for Molecular Modeling functioning properly without Toon and Ewald managing the computers so professionally.

An additional word of appreciation goes to all the members of our group for being such a jovial bunch. With many of you, I have great memories, with numerous ups and occasional downs (like the infamous Geneva stomach bug). The many social activities and baby showers keep our group young and vibrant. The technical staff, and Rudi in particular, also deserve a thank you for always being willing to help the clumsier among us. Apart from my colleagues, I would also like to thank my Master thesis students from last year, Bart and Gaella, and from this year, Annelies. Their feedback has taught me so much and guiding them has been an extremely rewarding experience. I wish them lots of luck in their current and future careers, be it in industry or in research. My mathematical friends were also the perfect partners for a weekly (or in my case often weakly) game of badminton to let off steam.

Outside the Center for Molecular Modeling there are several other people I am grateful to, in particular from the Ecole Polytechnique Fédérale de Lausanne and the University of Southern California. Prof. dr. Ursula Röthlisberger and Christian went out of their way to make me feel at home in Lausanne. It is a shame that I have not been able to finish the project we started at the same time as preparing this thesis, but let me reassure you: I have not given up on it. Finally, in just two days spent in Los Angeles with prof. dr. James Haw and his team, I learnt much more about MTO than I could ever have done by just reading papers. Since then, I have also had many interesting discussions with Dave regarding the trials and tribulations in modeling the MTO process. I sincerely hope that our collaboration may result in exciting new work.

Though I strongly fought it, I could not resist inheriting the fascination for scientific research that my parents (or 'Grandma' and 'Opa' as they are currently

referred to) passed on to me. It seems that 'Auntie' Claire is the only lucky one who got away! My mother gets a special thanks for being a tremendous help with the finer points of English. By now, she must be the only demographer on the globe who knows a lot about zeolites too. And of course I cannot forget to mention Etienne and Sonia, the other 'Opa' and 'Oma', who welcomed me into their family from day one and were always enthusiastic to baby-sit when deadlines needed to be met.

Since I started this PhD as a physicist, when reading this thesis you may well think to yourself: 'Now how does a physicist end up with this rather chemically oriented thesis?' As a beginning undergraduate in Belgium, who did not want to give up any of his interests in Mathematics, Physics and Chemistry, there was just one thing I could do: study Engineering and combine as many of these subjects as possible. It is not surprisingly, therefore, that I ended up in the relatively new and dynamic world of molecular modeling. At its core it was the frontier between Physics and Chemistry that drew me in, but in practice the fun of just 'fiddling with spheres and sticks' played an important role too. No sacrifices needed to be made, as I also kept my third interest, Mathematics, close by marriage.

This brings me to the two most important people in my life. An, what changes have we seen in these last few years! We have evolved from crazy high-school sweethearts who moved in together setting up a new apartment (in the Turtle-dove Street no less) right in the middle of an exam period, to a pair of responsible adults constantly trying to balance major personal projects with full-time professional careers. Thank you for being there for me all the way, and rest assured: your world of hexagons will always be a lot weirder than my zeolites! And finally Colin: you have only been in this world for less than a year, but I could not have coped with these final stressful months without having you to come home to. You are probably the most genuinely happy little fellow out there, and all worries disappear instantly when I see you smile. That is why I dedicate my thesis to both of you, and hope that one day little Colin might come up to me and ask: "Daddy, what is a zeolite really?".

For those of you who have been wondering what zeolites were from the onset of this preface, just read on...

Summary

Even though acidic zeolites form a crucial catalyst for many petrochemical processes, much of their fundamental reactive behavior is only superficially understood. Most often, catalysts are proposed on an 'ad hoc' basis, without a detailed understanding of their functioning on an atomic scale. It can indeed be difficult to identify the elementary steps of complex reaction networks from a purely experimental basis. For these issues, quantum chemical molecular modeling techniques provide an excellent complementary tool to laboratory data. This relatively new field of research has seen an enormous surge in popularity, mainly because of the rapid increase in computer power and the development of sufficiently accurate theoretical methods, which together make it possible now to model complex industrial processes. In this thesis, we use these modeling techniques for a detailed study on elementary reaction steps in zeolite catalysis. This summary gives only a very short overview of the work, and the interested reader is referred to the more elaborate full text or, for even more detail, to the research articles on which it is based, which are also included at the end of each relevant chapter.

In a preparatory chapter, several general terms and methods used throughout the thesis are introduced. First, two fundamental characteristics of zeolites that are vital in industrial catalysis - the topologically induced shape selectivity and the isomorphic substitution leading to a Brønsted acid site - are briefly explained. Then, the practical aspects of quantum chemical modeling of zeolites are discussed, with special attention given to the model space approximations that are necessary for such extended systems. Chemical reactions need to be modeled by computationally very demanding quantum chemical methods if we are to describe the changes in electronic binding pattern appropriately. Different approximations are possible, with an increase in accuracy usually accompanied by an increase in computational cost. Since zeolites are extended materials with a large number of atoms, a complete and accurate quantum chemical description of the entire system is not only extraordinarily demanding but also, at

the moment at least, simply not feasible. This issue has, however, led to the development recently of some advanced techniques that do allow an accurate description of at least the chemically active part of the system. Finally, since in this thesis the most important conclusions are based on rate coefficients, the basics of chemical kinetics are also introduced, describing the molecular-scale calculation of macroscopic quantities using transition state theory.

Subsequently one of the most intriguing substantive problems in heterogeneous catalysis is tackled: the reaction mechanism of the methanol-to-olefin process (MTO). First, a whole class of reaction mechanisms, the so-called direct mechanisms, are investigated, for which initial C-C coupling is taken to occur from C1 species only. Earlier theoretical studies tended to be fragmentary, typically investigating only a single reaction step rather than a complete pathway. Nevertheless, the existence of these individual reaction steps was often considered theoretical evidence for the direct proposal, even though no one had succeeded in defining a complete low-energy pathway. To resolve this complex issue, an extensive reaction scheme is presented in this thesis, including all the possible pathways and their constituent elementary reaction steps on a consistent basis. By combining the individual steps, it is demonstrated that the direct mechanism concept cannot explain the initial C-C coupling. Three bottlenecks are identified:

- the instability of ylide and carbene intermediates,
- the extremely slow conversion of a methane/formaldehyde mixture to ethanol, and
- the excessively high energy barriers for concerted C-C coupling steps.

Any alternative proposal, like the up-and-coming 'hydrocarbon pool' hypothesis, needs to provide C-C coupling steps that circumvent these bottlenecks.

The hydrocarbon pool model states that organic species trapped in the zeolite pores serve as building platforms, to which C1 species can attach methyl groups. The methylated species subsequently undergoes specific rearrangements and/or additional methylation steps, to finally split off light olefins. The original molecule is then regenerated by additional methylation steps. This way, the highly activated steps of the direct mechanisms could be bypassed. In this thesis, the initiating methylation (and at the same time C-C coupling) step is investigated. The results shed new light on the role of the zeolite framework in this process, and also in how the organic species and the inorganic zeolite cooperate as a supramolecular catalyst. The supramolecular picture is extended here by the explicit inclusion of previously omitted aspects like transition state shape selectivity and electronic stabilization of vital cationic intermediates by the zeolite

framework. We should definitely look beyond pure geometrical aspects since electronic embedding plays an equally important role.

Additional insight into the hydrocarbon pool hypothesis is, however, required for a guided optimization of the catalyst. A first step to catalyst improvement has already been made by investigating the effect that small organic groups built into the catalyst might have on the elementary reaction steps. Two such modifications - methylene and amine moieties that are iso-electronic with oxygen - are theoretically investigated here. The methylene moiety is one of the simplest organic groups that fits perfectly as a bridge between two silicon atoms to form the functional Si-CH_2-Si group. Even though such mesoporous organosilicate materials have been successfully synthesized before, only recently has a research team been able to synthesize methylene-substituted alumino-silicate zeolites. They failed to explain the observed framework defects, though, like the presence of end-standing Si-CH_3 groups. In this thesis the influence of the methylene moiety on fundamental adsorption properties is discussed for both neutral probe molecules and charge compensating cations. Additionally, we demonstrate how the combination of aluminum atoms (plus a Brønsted acid proton) with a methylene moiety will inevitably lead to protonation of the organic group and subsequent cleavage of the framework.

For similar amine-functionalized zeolites, this thesis also shows that protonation of the amine group will not necessarily lead to cleavage of the zeolite structure. Furthermore, Si-NH-Si moieties will provide additional basic sites, comparable to traditional Al-O-Si sites but not constrained to the aluminum tetrahedron. This enables more proton locations as well as the possibility of more favorable transition state geometries. This can result in a drastic reduction in energy barrier for those reactions which would otherwise have a highly strained transition state. Summarizing, we demonstrate how small organic modifications to the zeolite framework can have a considerable effect on the fundamental catalytic properties and MTO-related reactivity. However, neither methylene nor amine groups can be located on the aluminum tetrahedron without being automatically protonated, which in the case of methylene-modified zeolites even results in cleavage of the framework.

This thesis shows very clearly how theoretical modeling is capable of providing new insights into zeolite catalysis. The applications presented here are already located near the limits of what is currently feasible, considering computer power, method development and the current lack of insights into the possible supramolecular character of the system. The rapid evolution in this field of research, even within the time-scale of this thesis, makes it as good as certain that

further significant advances will soon be within reach, and the thesis closes with the identification of our high-priority research goals for the immediate future. Especially in identification of elementary reaction steps and optimization of the catalyst, there are still quite some challenges ahead.

Samenvatting

Zuur-gekatalyseerde reacties over zeolieten vormen een cruciale schakel in allerlei processen in de petrochemische industrie, maar hun reactief gedrag wordt vaak slechts oppervlakkig begrepen. Veelal worden katalysatoren 'ad hoc' voorgesteld, zonder een gedetailleerd begrip van hun werking op atomaire schaal. Voor complexe reactienetwerken is het vanuit experimenteel oogpunt immers vaak bijzonder moeilijk om de elementaire reactiestappen te identificeren. Het modelleren van moleculen en reacties door middel van kwantumchemische computersimulaties biedt daarom een hoogwaardig alternatief tot laboratoriumdata. Dit relatief jong onderzoeksgebied heeft de laatste jaren een enorme groei gekend door de grote toename aan computercapaciteit en de ontwikkeling van accurate theoretische methoden, die sinds kort ook toelaten om complexe processen van industrieel belang te bestuderen. In deze thesis zullen op basis van dergelijke methoden enkele belangrijke elementaire reactiestappen uit de zeoliet-katalyse gedetailleerd onderzocht worden. Deze samenvatting biedt slechts een uiterst beknopt overzicht van dit werk: de geïnteresseerde Nederlandstalige lezer wordt voor een meer diepgaande discussie verwezen naar de Nederlandstalige appendix. In het Engelstalig gedeelte van deze thesis wordt bovendien nog dieper op de resultaten ingegaan en alle details kunnen teruggevonden worden in de relevante onderzoeksartikels die in het Engelstalig gedeelte werden opgenomen.

In een eerste luik van deze thesis worden enkele algemene begrippen verduidelijkt, zodat ze nadien zonder verdere uitleg kunnen aangewend worden. Dit zijn in eerste instantie enkele cruciale eigenschappen die volgen uit de structuur en de samenstelling van zeolieten en zeotype materialen, zoals het optreden van vormselectiviteit en de aanwezigheid van Brønsted zure sites. Vervolgens worden ook de gebruikte kwantumchemische methoden aangebracht, met vooral aandacht voor de specifieke technieken die nodig zijn voor het modelleren van elementaire reactiestappen in uitgebreide systemen zoals zeolieten. Chemische reacties moeten immers via computationeel veeleisende kwantummechanische technieken behandeld worden om de drastische wijzigingen in het elektronisch

bindingspatroon correct te beschrijven. Verscheidene kwantumchemische benaderingen zijn in dit opzicht mogelijk, waarbij een hogere nauwkeurigheid meestal gepaard gaat met een hogere computationele kost. Zeolieten zijn bovendien zeer uitgestrekte materialen met een groot aantal atomen, waardoor een nauwkeurige kwantummechanische beschrijving van het volledige systeem binnen een aanvaardbare rekentijd gewoonweg niet haalbaar is. Deze problematiek heeft geleid tot de ontwikkeling van vergevorderde technieken die het toch mogelijk maken om een chemische reactie voldoende nauwkeurig te beschrijven binnen de huidige computationele beperkingen. Vermits bovendien in deze thesis de belangrijkste conclusies gebaseerd worden op de reactiesnelheid van cruciale stappen, wordt het berekenen van snelheidscoëfficiënten door middel van transitietoestandstheorie eveneens kort toegelicht.

Vervolgens wordt er ingegaan op een uiterst actuele problematiek: de zoektocht naar het reactiemechanisme van het methanol-to-olefin proces (MTO). In eerste instantie wordt een hele klasse van reactievoorstellen onderzocht, de zogenaamde 'directe' mechanismen, waarbij de initiële C-C koppeling enkel op basis van C1 species doorgaat. Door de extreme versnippering van eerdere theoretische studies en het brede spectrum aan kwantumchemische benaderingen en modelkeuzes, was rechtstreekse vergelijking tussen onderlinge resultaten tot voor kort onmogelijk. Deze individuele reacties werden steevast als bewijs aangevoerd voor de juistheid van dit model, maar er werd nooit ontegensprekelijk aangetoond dat de combinatie van deze elementaire stappen ook effectief een volledig succesvol reactiepad zou opleveren. Om dit complex probleem op te lossen, wordt in deze thesis een uitgebreid reactieschema geconstrueerd, met een consistente inclusie van alle relevante reactiepaden. Door de directe reactiestappen op deze manier te combineren, wordt aangetoond dat het vaak gesuggereerde directe mechanisme onmogelijk een verklaring kan bieden voor de initiële C-C koppeling. Drie knelpunten kunnen geïdentificeerd worden:

- de instabiliteit van de ylide of carbeen intermediairen,
- de uiterst trage omzetting van het methaan/formaldehyde mengsel naar ethanol,
- en de extreem hoge barrières voor geconcerteerde C-C koppelingsreacties.

Alternatieve hypothesen, zoals het in opmars zijnde 'hydrocarbon pool' model, zullen daarom C-C koppelingsreacties moeten voorzien die deze knelpunten omzeilen.

In de hydrocarbon pool hypothese wordt voorgesteld dat organische species in de zeolietporiën als stellingen fungeren waaraan C1 species methylgroepen kunnen hechten. Daarna ondergaat de organische molecule enkele gerichte herschikkin-

gen (desnoods met bijkomende methyleringsstappen) en worden lichte olefines afgesplitst. Verdere methylering regenereert de originele startmolecule. Op deze manier zouden de hoog-geactiveerde routes uit de directe mechanismen omzeild kunnen worden. In deze thesis wordt de initiërende methyleringsstap onderzocht, die tevens voor de initiële C-C koppeling zorgt. De resultaten hierover leveren nieuwe inzichten in de functie van het zeolietrooster en hoe het geheel van zeolietrooster en organisch actief centrum als een supramoleculair complex moet worden beschouwd. Het traditioneel beeld van deze supramolecule wordt verder uitgebreid met aspecten zoals vormselectiviteit op de transitietoestand en elektronische stabilisatie van cruciale kationen door het zeolietrooster. Blijkbaar moet er verder gekeken worden dan enkel naar geometrische aspecten en speelt de volledig elektronische inbedding een minstens even belangrijke rol. Bijkomend inzicht in het volledige hydrocarbon pool netwerk is echter nodig om de katalysator gericht te optimaliseren.

Een eerste stap naar optimalisatie van de katalysator wordt toch al gezet door in detail na te gaan op welke manier ingebouwde organische fragmenten in het zeolietrooster eerder gedefinieerde elementaire reactiestappen kunnen beïnvloeden. Eén van de meest eenvoudige organische groepen is de methyleen-groep, die perfect past als brug tussen twee silicium atomen en zo een functionele Si-CH_2-Si groep vormt. Hoewel eerder al gelijkaardige organosilica materialen gesynthetiseerd werden, is slechts uiterst recent een onderzoeksteam er in geslaagd om ook methyleen-gesubstitueerde aluminium-houdende zeolieten te produceren. Er kon tot nog toe echter geen verklaring gevonden worden voor de waargenomen imperfecties in het zeolietrooster, zoals de aanwezigheid van eindstandige Si-CH_3 groepen. In deze thesis wordt nagegaan wat de invloed van deze methyleengroep is op de adsorptie van typische probe-moleculen en ladingscompenserende ionen. Er zal bovendien duidelijk aangetoond worden dat de aanwezigheid van aluminium atomen rechtstreeks aanleiding geeft tot de eindstandige methylgroepen.

In gelijkaardige amine-gesubstitueerde zeolieten zullen de -NH- groepen roostergebonden blijven, ook na protonering. Ze zullen bovendien voor bijkomende basische sites zorgen die vergelijkbaar zijn met een traditionele Al-O-Si basische site, maar dan niet beperkt tot het aluminiumdefect. Dit laat bijkomende protonposities toe, alsook de mogelijkheid om meer gunstige transitietoestanden aan te nemen. Dit veroorzaakt een sterk reducerend effect op de reactiebarrière voor reacties die een anders te vervormde transitietoestand zouden vertonen. Globaal genomen toont deze thesis aan hoe kleine organische modificaties aan het zeolietrooster de fundamentele eigenschappen en MTO-gerelateerde reactiviteit op de nano-schaal kunnen beïnvloeden. Zowel methyleen als amine groepen

kunnen echter niet op aluminium tetraëders gesynthetiseerd worden zonder dat het zure proton de organische groep contamineert, en zelfs in het geval van methyleen-substituties aanleiding geeft tot klieven van het rooster.

Deze thesis geeft reeds een eerste indruk van de mogelijkheden die theoretische modellering biedt op het vlak van zuurgekatalyseerde reacties in zeolieten. De toepassingen die hier beschouwd worden, bevinden zich al op de limiet van wat huidig in dit onderzoeksdomein mogelijk is, zowel qua computerkracht, methodologie en de vertrouwdheid met het supramoleculair karakter. De snelle evolutie van dit onderzoeksdomein, zelfs tijdens dit doctoraatswerk, biedt rooskleurige perspectieven voor de toekomst. Vooral op het vlak van identificatie van elementaire reacties en optimalisatie van de katalysator staat er ons nog veel te wachten.

1 Introduction

While acid zeolite catalysts are abundantly used for all kinds of petrochemical processes, their exact reactive behavior is often only superficially understood. A detailed understanding of the elementary reaction steps that govern these processes is vital, though, for a directed search for improved catalysts. Obtaining a better understanding of the industrial processes involved is, therefore, not only an issue within the exact sciences, but also in applied research.

Numerous experimental methods, like NMR spectroscopy or gas chromatography - mass spectrometry, are ideally suited for obtaining initial insight into a subset of likely intermediates, but not into the elementary reaction steps themselves. Only by connecting these intermediates by proposing reaction links can one construct a probable reaction network. Since interpretation of these experimental data is based on an indirect evaluation of the elementary reactions, it is extremely difficult to obtain conclusive results for very complex reaction networks.

For those cases where experimental results are ambiguous, quantum chemical simulations provide an ideal complementary tool to laboratory data. The massive expansion in computing power of the last few years has led to a surge in the relatively new field of quantum chemical simulation, which is mostly based on cost-effective density functional theory methods (DFT). Guided by the intermediates proposed by experimentalists, these methods allow each individual reaction step to be simulated on an atomic scale. Several challenges within quantum chemical simulation remain, however, involving the complexity of the

process at hand and the constant trade-off between required methodology and computational limitations. Yet, even though the virtual DFT-microscope only provides a look at computer simulations rather than the real thing, this is probably the closest we will ever get to a molecular-scale view of the actual reaction. It is exactly from this perspective that this thesis will try to clarify one of the most intriguing problems in heterogeneous catalysis: unraveling the mechanism of the methanol-to-olefin process (or MTO for short).

The MTO process was originally developed as an alternative route from natural gas over methanol to synthetic gasoline (methanol-to-gasoline or MTG). However, right before gasoline production, an initial mixture of light olefins was also observed. Nowadays, it is this olefinic mixture which is considered important as a crucial petrochemical feedstock, and the further reaction to aromatics and alkanes is highly undesirable. Currently, methanol-to-olefin chemistry forms the crucial central step in the conversion of methane to polyolefins, in which the smallest organic building block is assembled to the larger building blocks that are essential for creating macromolecular polymers. While natural gas is the current main source for methanol production, conversion of biomass and/or waste to methanol permits a future shift in emphasis from finite to renewable resources.

The mechanism of the MTO process has baffled many prominent researchers, mainly because the answer was not to be found in the most obvious places. Most experimental and theoretical research was focused on the 'direct' mechanisms, in which the crucial C-C coupling step occurs directly through co-reaction of two or more C1 species like methanol. In this thesis, however, strong theoretical evidence will be presented on the failure of all the direct mechanisms, additionally identifying where and why these more obvious routes go wrong. Fortunately, an alternative 'hydrocarbon pool' route which operates independently from direct C-C coupling reactions, has been experimentally proposed. Even though this hydrocarbon pool hypothesis might have seemed a little far-fetched at the time it was originally suggested, it remains the last of many proposals left to be consistently backed up by recent experimental findings. The hydrocarbon pool hypothesis states principally that in the zeolite pores there is some kind of organic species present that acts as a building platform: with help of the acidic zeolite framework, methyl groups from methanol are continuously added on to the organic scaffolding. After several internal rearrangements of this organic molecule and/or additional methylation steps, ethene and propene can be split off from the building platform. This reaction mechanism forms an enormous challenge for experimentalists and theoreticians alike, not only because of the

immense number of reactions which intertwine to form a tangled network, but also because the organic hydrocarbon pool species and the inorganic zeolite lattice constantly interact as a supramolecular complex. Taking into account that there are numerous zeolite topologies, which all interact differently with the many hydrocarbons present, further complicates the already challenging task. In this thesis, a theoretical study on the proposed critical initiating step for the hydrocarbon pool model will be presented, which - despite the fact that the initiating step forms only a tiny part of the complete network - will already reveal unexpected information regarding the role of shape selectivity and cation stability for different topologies.

Identification of the elementary reactions, and more specifically the rate-limiting steps, is particularly useful when improvements to the catalyst need to be made. In fact, for the MTO process, one of the industrial goals is a tailor-made catalyst that suppresses the secondary reactions forming the deactivating coke. Furthermore it would be highly practical if the ethene/propene selectivity could somehow be controlled: depending on the demand, production could be adequately shifted towards one or the other. One of the major modifications that have been suggested in the literature for all kinds of zeolite-catalyzed processes is the creation of so-called 'zeozymes'. By incorporating (preferably not too large) organic fragments directly into the inorganic zeolite framework it might be possible to combine the properties of industrial catalysts (like zeolites) with nature's own-made catalysts (enzymes), thus creating new materials with all kinds of highly exciting catalytic properties. Many such materials have been synthesized in the last few years, though only a very small subset have already proven their worth in actual applications. To test these seemingly promising materials, quantum chemical simulations can ideally be used as a virtual laboratory. In this thesis, we will demonstrate how even the simplest of modifications can alter the fundamental nature of a zeolite catalyst. Extensive investigation of typical properties and key reactions for both methylene and amine substitutions will clearly define the extent to which these moieties are capable of improving catalytic properties as well as provide guidelines for future synthesis.

With all this in mind, several research questions should be clearly formulated:

- Which methods are best suited to investigate extensive and complex reaction networks within current computational limitations?
- What are the best theoretically obtained parameters on which to base our conclusions?
- Is it possible to identify a complete direct reaction pathway between methanol and light olefins?

- If not, what kind of potentially interesting intermediates can be formed directly from methanol?
- Does the hydrocarbon pool model effectively provide more accessible pathways to C-C coupling compared to the direct routes?
- To what extent does zeolite topology influence the reactivity of the hydrocarbon pool?
- Can methylene substitutions improve fundamental catalytic properties like zeolite acidity?
- Can amine substitutions in the zeolite framework provide a stronger basic site?
- For what type of reactions in MTO chemistry might methylene or amine substitutions actually improve the catalyst?

These questions will be addressed both in the text of this thesis and in the accompanying articles.

Before outlining the structure of this thesis, a few general comments are needed. Firstly, we must note that this thesis is not a traditional monograph, but it is rather a synthesis based on research articles that have just been published or are in press in international peer-reviewed journals. The text provides a mere synoptic overview, while more detail can be found in the articles, which are embedded at the end of each chapter. References to these articles in the text take the form [art. 3.5] to distinguish them from references to the works of others, e.g. [1], listed in the Bibliography. Secondly, although our research is theoretical, we believe strongly in the complementarity of theoretical and experimental research. The text is aimed, therefore, at a public of both theoreticians and experimentalists. The relevance of certain sections and the appropriateness of the level and depth of their presentation will vary considerably depending on the individual reader's background. This is most especially the case for Chapter 2. Thirdly, the material in the main chapters is not organized chronologically, but rather by subject. Occasionally, therefore, the historical order is reversed. This is especially pronounced for the models used, which were more rudimentary at the outset, but became more advanced as this PhD neared its end. Even within the 4-year span in which these articles were published, both methodology and computational power have evolved rapidly. Where this could have been important for the conclusions in the text, we have employed the best available current method.

The thesis is structured as follows:

- In Chapter 2, an overview will be given of the quantum chemical techniques and model approximations currently most often used to simulate reactions in zeolites. Special attention will be given to the small cluster approach and the multi-level approach (QM/MM or QM-high/QM-low), both of which are employed throughout this thesis. The basic concepts of transition state theory, which is used to calculate rate coefficients, are also briefly introduced. More advanced techniques to calculate rates do exist (like molecular dynamics and Monte Carlo simulations), yet these are way beyond what is currently feasible for zeolites.
- In Chapter 3, the concepts introduced in Chapter 2 will be used to unravel the mechanism of the methanol-to-olefin process. The direct mechanism proposals will all be combined in an exhaustive and consistent scheme. Unlike most theoretical studies that only deal with reaction barriers, they will be evaluated on the basis of calculated rate coefficients. The initiating step for the alternative hydrocarbon pool hypothesis will also be studied and measured up to the direct C-C coupling steps. Furthermore, the effect of various zeolite topologies on the reaction kinetics will be monitored. The more detailed articles dealing with this specific topic and published in peer-reviewed journals are grouped at the end of this chapter.
- In Chapter 4, the knowledge obtained in the previous chapter will be employed to suggest organic modifications to the zeolite lattice. The reactivity of two such modifications, like methylene and amine moieties, will be extensively tested. Special focus is given to the combination of these moieties with an aluminum defect and their effect on proton location and mobility. For amine-substituted zeolites, typical reactions leading to an alkoxide will be compared to alkylammonium formation. Just like in the previous chapter, the more detailed published papers are brought together at the end of the chapter.
- The final chapter summarizes the general conclusions of this thesis, after which directions for future research are also suggested. To use a cliché, the results presented here are only the tip of what seems to be a massive iceberg...

2 Terminology and methodology

This chapter serves as a preparatory chapter, introducing the terminology and methodology that will be used throughout the rest of the thesis. As already mentioned in the Introduction, the relevance of various sections in this chapter will depend heavily on the individual reader's background. In an initial section, two fundamental characteristics of zeolites that are vital in industrial catalysis are briefly explained: the topologically induced shape selectivity and the isomorphic substitution leading to a Brønsted acid site. In the following sections, the practical aspects of modeling zeolites will be discussed, accompanied by many specific issues that arise. An overview will be given of the numerous quantum chemical approximations that can be made for a whole range of systems, after which focus is shifted towards the model choices that have to be made for extended structures in particular. In a final section, the basics of chemical kinetics will be introduced, describing the nanoscopic calculation of macroscopic quantities using the aforementioned approximations combined with transition state theory.

2.1 Zeolites and zeotype materials

Zeolites are nanoporous crystalline alumino-silicates, built from corner-sharing TO_4 (T=Si or Al) tetrahedra [1]. By connecting the tetrahedrally coordinated T-atoms along bridging oxygen atoms, one can build 4-rings, 5-rings and 6-rings that form the basis for complex 3-dimensional networks of channels and cages [2]. Since the constructed channels and cages are typically of molecular

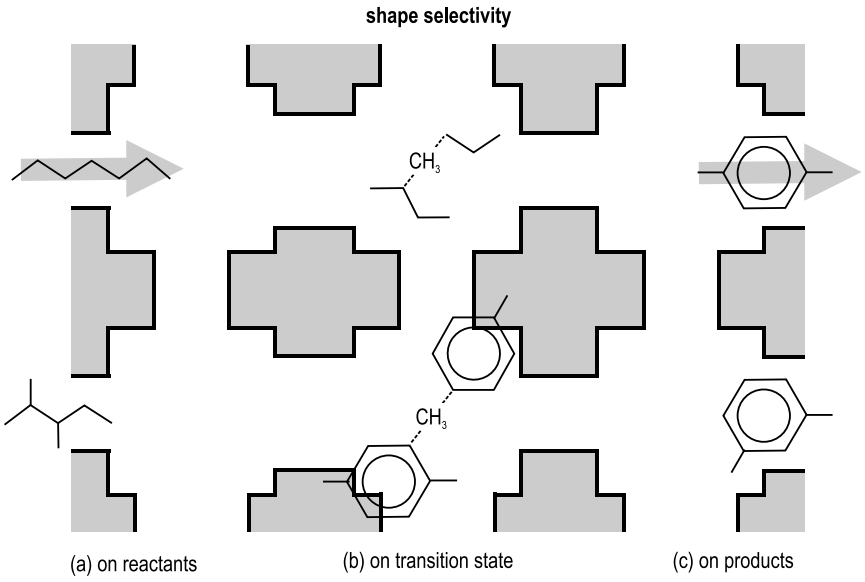

Figure 2.1: Fictitious zeolite structure illustrating different manifestations of shape selectivity.

size (0.2 - 1.2 nm), these materials are best known for their capacity to act as molecular sieves. This is best illustrated by their shape-selective properties [3, 4], classified by the nature of the molecule upon which the shape selective criteria are active. This molecule can be an initial reactant, a transition state for a chemical reaction, or the consequently formed products.

2.1.1 Shape selectivity

In Figure 2.1 these different categories are illustrated in a fictitious zeolite structure that contains both large and small channels. Figure 2.1(a) illustrates initial reactant selectivity: linear alkane reactants (above) can enter the pore and consequently reach the active site, while the small channel prevents branched alkanes (below) from entering the material. Restricted transition state shape selectivity, illustrated in Figure 2.1(b), is a different phenomenon: even though two para-xylene molecules might enter the cage along the wider channels, methyl transfer from one xylene to the other can occur only if there is sufficient space

available to accommodate the bulky transition state. Lastly, product shape selectivity is shown in Figure 2.1(c): para-xylene can exit the cages, while meta-xylene remains trapped in the cage and will consequently be absent from the product stream.

Apart from these rather traditional interpretations from a steric viewpoint, shape selectivity can also be expressed by a number of novel concepts. Among these are molecular traffic control, window effects, a directed adsorption of molecules at the active sites, inverse shape selectivity and pore mouth catalysis [5–7]. These concepts will not be discussed further here.

2.1.2 Isomorphic substitution

When, in a pure silica zeolite, a tetravalent silicon atom is replaced by a trivalent aluminum atom, this leads to a net negative charge on the system. This negative charge will be compensated by an extra-framework cation, such as an inorganic cation like Na^+ forming a Lewis acidic site, or by a Brønsted acidic proton (which will attach to one of the oxygen atoms neighboring the aluminum defect). The maximum number of aluminum substitutions is defined by the Löwenstein rule [8], stating that no two Al substitutions may occur on neighboring tetrahedral sites.

While only alumino-silicates are strictly classified as zeolites, similar materials like alumino-phosphates, zinco-silicates and titano-silicates with zeolite topologies are referred to as zeotype materials or as crystalline molecular sieves. For example, alumino-phosphates (or AlPOs) have strictly alternating Al and P tetrahedral units forming a neutral framework that lacks odd-numbered rings [9]. In AlPOs, substitution of the pentavalent phosphorus atom by a tetravalent silicon atom leads to silico-aluminophosphates (or SAPOs) which can contain a similar Si-OH-Al Brønsted acid site as in zeolites.

2.1.3 Catalytic cycle

Currently, zeolite and zeotype catalysts are widely used as catalysts in all kinds of petrochemical processes [10], such as isomerization, alkylation and cracking. The understanding and improvement of key reaction steps in such processes will form the main focus of this thesis. It is important to note, however, that elementary reactions in zeolites form just a single step in a complete catalytic cycle [11], as shown in Figure 2.2. Yet, modeling the reaction step is often more

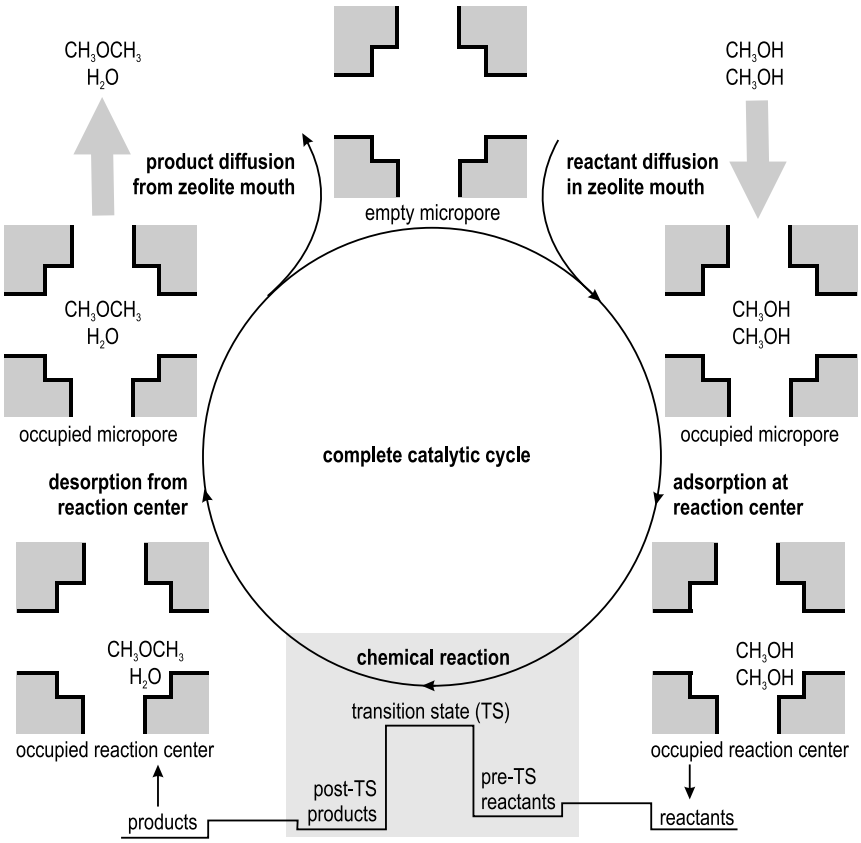

Figure 2.2: Complete cycle in zeolite catalysis, with the elementary reaction step shown in a grey rectangle (adapted from [11]).

demanding computationally than modeling the other steps.

Molecular adsorption steps, diffusion along the channels and desorption steps are best described by classical molecular mechanics (MM) methods, which are both highly accurate for these particular phenomena and computationally fast [12]. Moreover, a wide variety of newly generated force fields provide an excellent description of the long-range van der Waals interaction. Chemical reactions, on the other hand, are based on the activation and formation of chemical bonds, which coincide with a drastic rearrangement of the electronic structure. Reac-

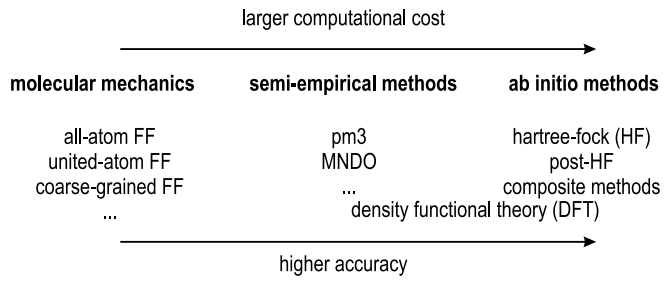

Figure 2.3: Overview of various chemical simulation methods.

tions are, therefore, more suitably described using the computationally much more demanding quantum-mechanical (QM) methods that describe the electronic structure more accurately.

Two main aspects need to be carefully chosen when modeling reactions in zeolites: on the one hand many different methods to describe the electronic binding pattern are widely available, and on the other hand different model systems can be used to simulate the extended zeolite framework.

2.2 Quantum chemical methods

One of the most important considerations when modeling reactions is the choice of an appropriate quantum chemical approximation. Computational chemistry is based on many different quantum-mechanical methods for solving the Schrödinger equation associated with the molecular Hamiltonian. Figure 2.3 gives an overview of the main classification of electronic structure methods, ranging from approximative but extremely fast (such as force fields) to highly accurate yet computationally demanding (such as composite methods).

Ab initio methods

Methods that do not include any semi-empirical parameters in their equations (i.e. are not fitted to experimental data) are called ab initio methods. This means that a particular approximation is rigorously defined on first principles and then solved within an error margin that is qualitatively known beforehand.

The simplest type of ab initio electronic structure calculation is the Hartree-Fock (HF) scheme. Many improvements to this scheme, known as post-Hartree-Fock methods, begin with a Hartree-Fock calculation and subsequently correct for electronic correlation [13]. Composite methods, on the other hand, are based on subsequent applications of various methods on the same system after which these intermediate values are extrapolated to a final solution which is within kJ mol^{-1} accuracy [14]. Even though they provide the most reliable results, composite methods are only feasible for very small systems.

Density functional theory

In density functional theory (DFT) [15], the total energy is expressed in terms of the total electron density rather than the wave function. DFT methods are often considered to be ab initio methods for determining the molecular electronic structure. However, many of the most common density functionals use parameters derived from empirical data, which means that, strictly, they should be called semi-empirical methods. DFT provides a very cost-effective method since a very accurate yet rapid QM calculation of the electronic structure is often possible. Because of this, the development of DFT-based software codes is the main reason behind the sudden surge in applications and developments in the field of molecular modeling.

Semi-empirical methods

Semi-empirical methods are based on the Hartree-Fock formalism, but make many approximations to reduce the computational cost by parameterizing from empirical data. They are crucial for treating large systems where DFT or the full Hartree-Fock method without these approximations is too expensive. In this thesis these methods will primarily be used to generate initial geometries or to describe border regions of the extended system. Examples of semi-empirical methods are MNDO (Modified Neglect of Diatomic Overlap) and pm3 (Parametric Method 3) [16, 17].

Molecular mechanics

In many cases, large molecular systems can be modeled successfully while avoiding quantum mechanical calculations entirely. Molecular mechanics simulations, for example, use a single classical expression (or force field) for the energy of a compound. All constants appearing in the equations must be obtained beforehand from fitting to experimental data or to ab initio calculations. All-atom

force fields provide parameters for each individual atom, including hydrogen, while united-atom force fields treat typical groups of atoms as a single interaction center, often lumping the light hydrogens together with the larger atoms to which they are bound. Coarse-grained force fields, which are frequently used in long-time biomolecular simulations, provide even more abstracted representations for increased computational efficiency. These methods are less suitable, though, to model a wide variety of chemical reactions.

2.3 Approximations in model space

A second, and an especially important problem when modeling zeolites is the choice of an appropriate model to simulate the extended zeolite framework. Zeolites are bulky materials that contain an enormous number of atoms, which impedes the search for methods that adequately describe these complex systems within reasonable computer time. New force fields for zeolites are constantly being developed, allowing rapid optimization of almost any zeolite framework structure and numerous adsorbed species [12]. But because they are parameterized around equilibrium situations, they are useless when describing the complex electronic changes accompanying the activation and formation of chemical bonds. And while the standard QM methods currently available are ideally suited for isolated molecules in the gas-phase (with an upper limit of approximately 200-500 atoms), the enormous computational cost renders them impractical for extended systems like zeolites.

This issue has led to several new developments in computational chemistry, all of which attempt to provide an accurate description of the chemical reactivity of extended systems at a reasonable computational cost. In the remainder of this chapter, a brief overview will be given of the main methods that have been commonly applied in zeolite chemistry. Many of these techniques have also been regularly applied to other extended systems that suffer from this scaling issue: e.g. chemical reactions in solvent, in biomolecular structures, or in surface catalysis. Only in the last decade have we been able to model reactions in zeolites, not only by taking full advantage of these special new techniques, but also by the highly increased computing power and the development of DFT.

When further investigating suitable methods used to describe reactions in zeolites, it is crucial to mention that, while long-range electrostatic contributions play a limited role, short-range electrostatic contributions dominate the interaction energy of molecules with the zeolite host [18]. Moreover, charge can

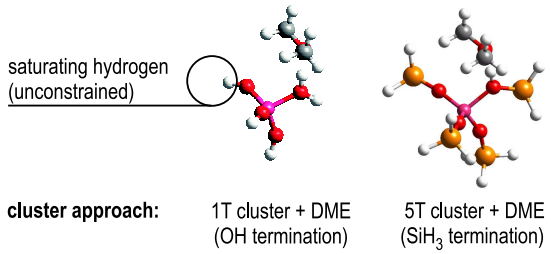

Figure 2.4: Small QM clusters cut from the zeolite framework, representing the active site [art. 3.7].

easily be spread out over the framework [19] and adsorbed molecules will interact mainly with the more diffuse zeolite oxygen atoms [20]. For adsorbed hydrocarbons, the van der Waals contribution will also play a major role, yet this contribution is not always properly incorporated within current DFT descriptions [21]. Chemical bonding, on the other hand, will be dominated by covalent interaction. It is important to note that the many current shortcomings in theoretical modeling of reactions in zeolites are more often due to model assumptions than to quantum chemical approximations [11].

2.3.1 Cluster approach

The cluster technique is the simplest and most wide-spread method used to model reactions in zeolites. In this approach, the chemically active part is simply cut away from the zeolite framework. Since this action inevitably involves cleavage of several covalent Si-O bonds, the resulting cluster would be chemically unstable, unless additional capping hydrogen atoms are used to saturate the dangling bonds. Figure 2.4 shows both a silicon-free 1T cluster with OH-termination on the aluminum atom and a larger 5T cluster with H termination on the silicon atoms. For zeolites containing planar ring structures, a ring-shaped cluster is often used.

The main advantage of this method is the limited number of atoms that are taken into account. This permits the use of highly accurate levels of theory (such as advanced DFT functionals) within reasonable computer time. Nevertheless, as the zeolite is modeled merely by a small gas-phase molecule, it is clear that the cluster method can never guarantee a complete description of the

entire system, especially when the zeolite framework significantly affects reaction kinetics.

Two main problems arise when the cluster method is used:

Relaxation of the cluster: If the saturating hydrogen atoms are left unconstrained during geometry optimization procedures, the zeolite cluster will act as a completely free gas-phase molecule. In reality, though, the cluster is embedded in a more rigid zeolite framework and relaxation is severely hampered. Constraining the cluster by keeping the saturating hydrogen atoms at fixed positions only partially solves this problem: especially for small clusters, the constraints might result in a cluster that is too rigid. Furthermore, the vibrational frequencies of stationary points calculated with constrained clusters will be soiled by parasitic negative eigenvalues, which impede a straightforward calculation of rate coefficients.

Long-range effects: All long-range effects, such as dispersive interaction of an adsorbed molecule with the framework, electrostatic stabilization of charged intermediates, or shape selectivity effects by the framework, are completely neglected in the small cluster approach.

When we compared small cluster results with more advanced techniques, energy barriers were found to be generally well reproduced, even in the small cluster approach [art. 3.5]. Historically, this relatively good agreement between cluster calculations and experiments has often been observed for energy barriers, mainly because of the strong covalent nature of the zeolite lattice. Only for a very limited number of reactions, particularly when bulky molecules and/or charged intermediates are formed, is a larger model required to obtain correct reaction barriers [art. 3.5].

2.3.2 Periodic approach

At the other extreme, fully periodic QM software codes provide the most natural description of a zeolite, since no arbitrary cuts of the structure are required. Furthermore, as opposed to reactions in solution, the crystal structures of heterogeneous catalysts are often well-known beforehand. However, the industrially most important zeolites are often built from rather large unit cells: for example, the unit cell of ZSM-5 contains no less than 288 atoms. The corresponding computational cost is too high for practical purposes, which is the main reason why periodic calculations on zeolites are currently still limited to systems with very small unit cells like CHA, as illustrated in Figure 2.5. Even then, typical

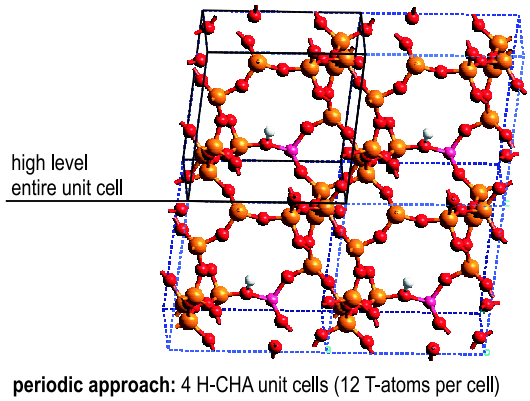

Figure 2.5: Unit cells of chabazite as used in a full QM periodic approach [art. 3.7].

periodic artifacts or large incorporated species necessitate the use of a larger supercell, which is often too big to be efficiently handled within a full QM approach. Furthermore, implementation of the latest functionals in periodic codes is still in a developmental phase, which means that the main strength of periodic codes will only fully emerge in the next few years.

2.3.3 QM/MM approach

Ideally, a QM zeolite cluster would be extended until all necessary framework effects are taken into account, but these clusters are too large to be described fully at a high QM level. In this case, a 'divide-and-conquer' strategy is able to provide the most efficient solution: the relatively small active site and all guest-molecules are treated at the necessary high QM level (high-level or HL region), while the larger surrounding framework - which does not actively participate in the reaction - can be described at a computationally much faster low QM level (QM-high/QM-low approach) or even by a molecular mechanical (MM) force field (QM/MM approach), both denoted as the lower-level or LL region. This separation of the system into two parts is demonstrated on a 46T cluster (built around a HL 5T cluster) cut from H-ZSM5 in Figure 2.6. There are quite a number of QM/MM software packages available, such as the QM/Pot method [22, 23] which was designed specifically for zeolites. In this thesis, however, we

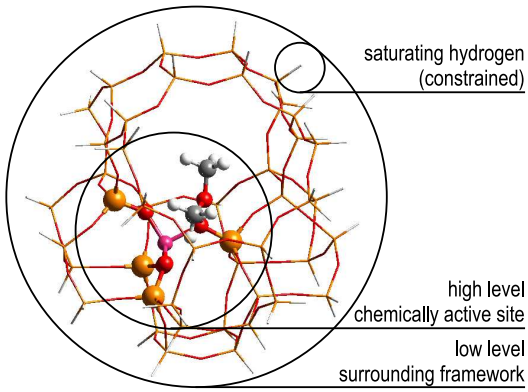

ONIOM approach: 5T:46T H-ZSM5 cluster + DME

Figure 2.6: 2-layered cluster cut from the MFI topology [art. 3.7].

will use a QM-high/QM-low approach with the ONIOM method [24] as currently implemented in the Gaussian software package [25], because of its more adequate treatment of the surrounding framework. The Gaussian code has furthermore proven its worth in many areas of quantum-chemical simulation (e.g. through efficient transition state search algorithms) and it is currently well beyond the early developmental phase.

ONIOM method

The ONIOM method is basically a multi-level method, which allows for inclusion of the zeolite framework at moderate additional computational cost [24]. The ONIOM method also allows QM-high/QM-low as well as QM/MM calculations, since any HL/LL combination can be chosen. Even though originally developed for biomolecular systems, the ONIOM method is currently widely used in zeolite chemistry [26–30], as it has been shown to be very a robust method [31]. Furthermore, it provides results as accurate as those of full periodic calculations, but at a significantly lower computational cost [32].

In the ONIOM method, the molecular system is divided into two subsystems. The entire system is called the real system (Inner region I + outer region O),

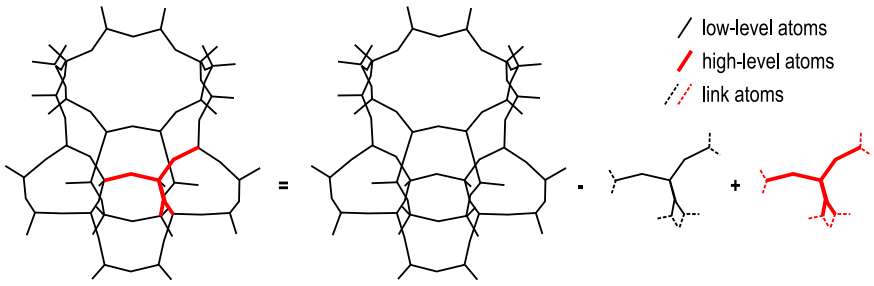

Figure 2.7: Subtraction scheme for 2-layered ONIOM calculation

while the smaller reactive part is called the model subsystem (Inner system I + Link region L). The Link region comprises the saturating hydrogen atoms that are placed on the broken bonds between the Inner and Outer regions.

The ONIOM energy is calculated from a subtraction scheme as illustrated in Figure 2.7:

$$E_{target} \approx E^{LL}_{real} - E^{LL}_{model} + E^{HL}_{model}$$

The ONIOM method is a mechanical embedding method, which means that electrostatic interactions between the HL and LL region are not updated during the calculation of the HL region.

2.3.4 Overview

An overview of the techniques discussed - ranging from low cost cluster methods to computationally demanding fully periodic methods - is given in Figure 2.8. Each type of technique is rated here on eight major output characteristics, five of which are of the utmost importance in the context of this thesis. At one extreme, despite its limitations, the small cluster approach is an ideal tool for studying localized effects, and this technique is especially useful when a quick qualitative interpretation is needed. Before applying more advanced methods, cluster calculations will always be used to obtain initial insight into the reaction mechanism or as a fast tool to obtain initial transition state geometries. At the other extreme, although the full periodic approach has many advantages, it will not be used in this thesis, mainly because of its inability to perform calculations

larger computational cost →

very important (less important) aspects for this work:	QM cluster	QM/MM	QM-high/QM-low	QM periodic
geometries	++	+++	+++	+++
qualitative results	+	+++	+++	+++
(quantitative results)	-	+++	+++	+++
framework electrostatics	-	+	+++	+++
(van der Waals contributions)	-	+++	-	-
steric constraints	-	+++	+++	+++
applicable to many topologies	+++	+++	+++	+
(no arbitrary cuts)	-	-	-	+++

Figure 2.8: Performance of the main DFT-based techniques used in zeolite catalysis.

on a wide range of industrially important zeolite structures. However, explicit inclusion of the framework is vital when studying the hydrocarbon pool route in methanol-to-olefin catalysis, which is space-demanding and based on carbenium-ion intermediates. Since in this case a reliable description of the electrostatic interaction between charged intermediate and zeolite framework is essential, we use QM-high/QM-low ONIOM calculations whenever necessary.

Level-of-theory used here for the cluster approach

The size of the cluster used will depend mainly on the application and on the computer facilities at hand. At a minimum, a 4T cluster should be used to guarantee a reasonable description of the acid site and both directly available base sites. In this thesis, cluster calculations will mostly be performed on SiH_3 terminated pentatetrahedral (5T) clusters (Figure 2.4). These clusters are left unconstrained to verify the true nature of all stationary points (i.e. one and only one imaginary eigenfrequency for the transition state and no imaginary eigenfrequencies for minima on the potential energy surface). DFT calculations will be performed using the B3LYP functional [33] as implemented in the Gaussian03 software package [25]. This functional has been found to provide the best results compared to high-level post-Hartree Fock MP2 calculations [34]. Various Pople

type basis sets [35] will most often be used, ranging from the small 6-31g(d) basis set to the more extensive 6-311++g(d,p) set.

Level-of-theory used here for the ONIOM method

Whenever necessary, the 5T cluster approach will be extended to a 5T high-level cluster embedded in a 41T low-level cluster using a QM-high/QM-low ONIOM approach to include the bulk electrostatic effects induced by the zeolite framework. This 46T model (illustrated in Figure 2.6) is considered to be large enough to cover all important framework effects on both the active site and the adsorbate [36]. As suggested from comparison with periodic calculations [32], the B3LYP functional will be used for the high-level QM-high region. The low-level QM-low region will be optimized using the semi-empirical MNDO method, and a single-point energy calculation will consequently be performed using the Hartree-Fock method. For this larger cluster, saturating H-atoms in the Outer region will be constrained to prevent the cages and channel intersections from collapsing.

2.4 Chemical kinetics

In standard calculations by the methods described, temperature effects are implicitly excluded. To take temperature rigorously into account, one should perform molecular dynamics calculations at various temperatures. Crucial reaction steps are often rare events though, and the probability of simulating at least one such event is extremely low. The application of this type of calculation to zeolites lies just beyond the edge of what is feasible at the moment. To partially solve this problem, kinetic parameters will be calculated using transition state theory as described in this section.

Chemical kinetics is the general term in physical chemistry used to describe all studies related to the velocity at which chemical systems evolve to their equilibrium state. In this section, the basics of calculating unimolecular rate coefficients, which can be linked directly to macroscopically measurable quantities, are briefly discussed. Since in this thesis the prior adsorption of the reagent on the active site is not considered, the combination of the zeolite framework with the adsorbed species can be considered as a single supramolecule which undergoes a unimolecular reaction to give a new supramolecule. Within this approximation, the calculated rates - which are therefore considered per ideally

occupied reaction center - can be considered as an upper limit to the overall reaction rates.

2.4.1 The Arrhenius equation

The dependence of the reaction rate v of a unimolecular reaction on the concentration of the reactants c_R (in $m^{-3}\ mol\ s^{-1}$) and temperature T (in K) is given by the following rate equation:

$$v = k(T)c_R$$

with $k(T)$ the temperature-dependent rate coefficient (in s^{-1}). In most cases, the rate coefficient (and consequently also the reaction rate) will increase exponentially with increased temperature. Within limited temperature intervals, this temperature dependence is empirically defined by the Arrhenius rate equation:

$$k(T) = Ae^{-E_a/RT}$$

with R the universal gas constant, E_a the activation energy and A the pre-exponential factor. The activation energy can be interpreted as the minimum energy required for the reaction to proceed and the exponential expression gives the fraction of molecules that actually possess this energy as obtained through a Boltzmann distribution. Nevertheless, just because the reactant contains the right amount of energy, this generally does not guarantee a successful reaction since specific orientation effects will also play an important role. This aspect is included in the pre-exponential factor A, which will be more rigorously defined through Transition State Theory.

2.4.2 Transition State Theory

Transition State Theory (TST) or Theory of the Activated Complex, which was developed as early as 1935 [37, 38] is unique in the sense that not a single new theory has been able to capture both its simplicity and accuracy. In principle, all possible trajectories for a chemical reaction should be calculated, after which averaging them out would lead to the reaction rate. However, because of the excessive number of calculations needed in this approach, it is simply not computationally feasible. TST, on the other hand, significantly reduces the number of calculations needed to link microscopic and macroscopic entities using several model assumptions. Fundamentally, TST states that there is a

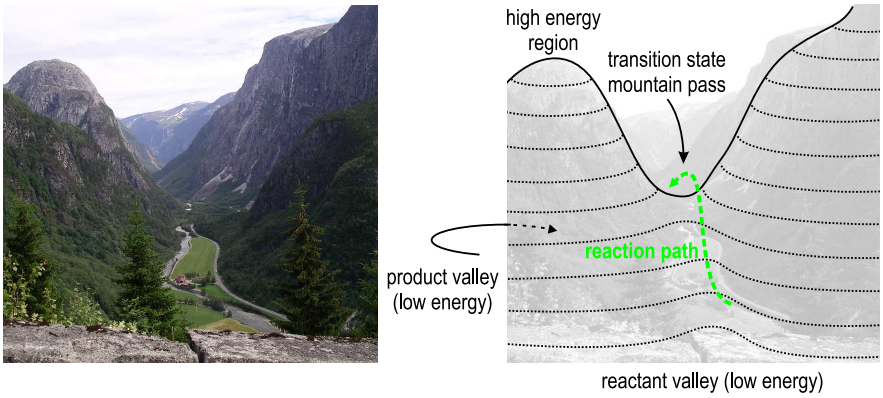

Figure 2.9: Analogy between a mountainous landscape and the potential energy surface illustrating Transition State Theory.

single critical point (called the transition state or activated complex) that lies on every successful reaction path. Furthermore, this saddle-point is a minimum energy conformer in all degrees of freedom, except in the reaction coordinate for which it is a maximum (this is best illustrated by the concept of a mountain pass, as shown in Figure 2.9). In conventional Transition State Theory (CTST) several additional assumptions are made:

- Once the transition state point is crossed towards the product valley, the system does not return to the reactant valley. In practice, this means that no multiple crossings of the dividing surface are considered.
- There is a quasi-equilibrium between the transition state and the reactant, as well as among the reactants, even though the system itself is not equilibrated.
- The motion corresponding to the crossing of the mountain pass can be separated from all other motions.
- The motion corresponding to the crossing of the mountain pass can be modeled classically (i.e. without inclusion of QM effects like tunneling).

The power of TST lies in the fact that, instead of a full dynamic evaluation of the reaction path, calculation of the rate coefficient is limited to just three stationary points: reactant, transition state and product. The forward reaction rate is for example given by:

$$k(T) = \frac{k_B T}{h} \frac{q_\ddagger(T)}{q_R(T)} e^{-\Delta E_0/k_B T}$$

with k_B Boltzmann's constant, h Planck's constant, $q_\ddagger$ and q_R the temperature-dependent molecular partition functions of the transition state (excluding the motion along the reaction coordinate) and reactants respectively, and ΔE_0 the energy barrier at 0 Kelvin.

$$\Delta E_0 = E_0^\ddagger - E_0^R$$

The required energies and partition functions are determined from the ab initio calculations. For the evaluation of the molecular partition functions, the vibrational, rotational, translational and electronic motions are assumed to be decoupled:

$$q(T) = q_{elec} \cdot q_{trans} \cdot q_{vib} \cdot q_{rot}$$

The electronic partition function q_{elec} is approximated by unity, since in the Born-Oppenheimer approximation the molecule is assumed to be in its ground-state configuration. For gas phase reactions, the translational partition function is usually given by that of an ideal gas:

$$q_{trans} = \left(\frac{2\pi m k_B T}{h^2}\right)^{3/2} \quad \text{(per unit volume)}$$

The vibrational partition functions are expressed within the 'Harmonic Oscillator' (HO) approximation. In this picture, the total vibrational motion for a non-linear molecule with N atoms is approximated by a sum of 3N-6 independent harmonic oscillators, each corresponding to one of the normal modes of the molecule. As a result q_{vib} can be factorized as follows:

$$q_{vib} = \prod_{i=1}^{3N-6} q_{vib,i} = \prod_{i=1}^{3N-6} \frac{1}{1 - e^{-h\nu_i/k_B T}}$$

with $q_{vib,i}$ the partition function of each individual harmonic oscillator with vibrational frequency ν_i. Note that the zero point energy contribution $e^{-h\nu_i/2k_B T}$ to the vibrational partition function is lifted out, as it is already taken up in the molecular energy difference ΔE_0. Finally the rotational partition function corresponds to the external rotation of the global rigid molecule. Usually, an overall

approximation of the partition function of a non-linear polyatomic molecule is applied:

$$q_{rot} = \frac{\pi^{1/2}}{\sigma}(\frac{8\pi^2 k_B T}{h^2})^{3/2}(I_X I_Y I_Z)^{1/2}$$

In this formula, σ is the symmetry number of the molecule that represents the number of indistinguishable orientations. I_X, I_Y and I_Z are the three principal moments of inertia of the rigid molecule.

After plotting the obtained rate coefficient in a ln(k) vs. 1/T diagram for a specific temperature interval, the temperature-dependence can be approximated by an Arrhenius plot allowing extrapolation of the macroscopical parameters A and E_a. When comparing reaction steps that differ ever so slightly in reaction mechanism and molecular geometries, the pre-exponential contribution is often neglected and qualitative evaluation is made solely on the basis of ΔE_0.

It is important to note here that for extended systems like zeolites, rate constants are rarely calculated except for a handful of papers [39–41], and discussion is centered almost exclusively on variations in ΔE_0. Furthermore, once certain atoms have been constrained (e.g. in the ONIOM approach), the residual negative eigenvalues should be eliminated from calculation of the partition functions. This problem can be avoided by attributing an infinite mass to all constrained atoms during the frequency calculation, thus performing a partial Hessian vibrational analysis.

3 The methanol-to-olefin process

In this chapter, the theoretical techniques described in the previous chapter are used to resolve a strongly debated problem in heterogeneous catalysis: the mechanism of the methanol-to-olefin process. After a brief introduction to the subject, the 30-year-old controversy regarding the MTO reaction mechanism is discussed. The historically important direct reaction proposals are then fully analyzed, after which their inability to account for experimental observations is confirmed. The focus is subsequently shifted to the alternative hydrocarbon pool proposal, for which a theoretical study on the critical initiating step provides new insights into shape selectivity and the supramolecular character of the catalyst. A final section summarizes the conclusions and sums up suggestions for future research.

3.1 Introduction

Light olefins, which are traditionally obtained by steam cracking of crude oil fractions, are vital components in the petrochemical industry [42]. However, because the world's finite oil reserves will not be able to meet the ever-increasing demand for oil-based chemicals (and polyolefins in particular), developments currently focus on technologies that are based on alternative natural sources [43]. In the conversion of raw materials to polyolefins from methane, the methanol-to-olefins (MTO) process is a crucial step: methanol can be made from almost any gasifiable carbonaceous material, following which MTO technology converts methanol to crucial petrochemical feedstock like ethene and propene [44–46].

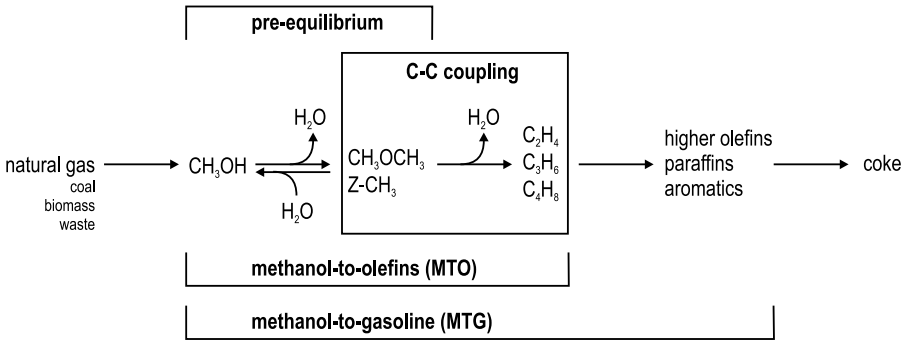

Figure 3.1: Conversion of methanol to light olefins through the MTO process.

The production of methanol currently occurs mainly through steam reforming of natural gas, making great use of otherwise stranded natural gas reserves. Alternatives, like the conversion of biomass and waste to methanol, might also gain interest, mainly because these novel technologies form a closed carbon-cycle, independent of the decline in fossil fuel reserves. By subsequently applying MTO technology to the methanol produced, one could make almost anything out of methanol that can currently be made out of crude oil!

Figure 3.1 is a schematic presentation of the entire route, with the MTO process centrally situated. The conversion of methanol is known to start with bimolecular dehydration to dimethyl ether (DME). Subsequently, this pre-equilibrium mixture consisting of methanol, DME and water can be processed to olefins (MTO) or even further to high-octane gasoline (methanol-to-gasoline or MTG). Framework-bound methoxide species (noted as Z-CH_3) are also formed in the pre-equilibrium stage [47–49], though their role as an active species is highly disputed [50–52]. Finally, coke deposition leads to catalyst deactivation.

While several different acidic zeolite and zeotype structures, like HZSM-5 and HSAPO-34 respectively, are well-known MTO catalysts, a major target is the design and development of an improved catalyst. This material should not only exhibit superior activity towards olefin formation, but it should also suppress the secondary reactions that form alkanes and aromatics and lead to deactivation of the catalyst by coke formation. A third important goal is control of product selectivity, i.e. the ethene/propene ratio, so that production can be adjusted to

meet the specific market demands at any given time.

3.1.1 Controversy surrounding the reaction mechanism

In the search for control of product selectivity, a detailed understanding of the MTO reaction mechanism is vital. Quite remarkably, though, the actual mechanism has been a hugely challenging problem for more than 30 years [46]. Much remains uncertain and the literature is replete with different and often conflicting propositions. The main question is how the initial C-C coupling occurs from C1 species like methanol and DME. Until very recently, speculation centered mainly on mechanisms based on the 'direct' formation of small olefins from only methanol, DME and other single-carbon derivatives. This has led to more than 20 distinct mechanistic proposals with all kinds of reactive intermediates, such as ylides, carbenium ions and radicals [46].

Recently, however, experimental studies provided evidence that extensively purified methanol is unreactive under standard MTO conditions [53], which is in complete disagreement with the direct mechanism proposals. A viable alternative is given by the 'hydrocarbon pool' model [54, 55], in which some kind of (originally undefined) hydrocarbon pool species trapped in the zeolite pores undergoes methylation and subsequent olefin elimination. Lately, this proposal has systematically gained in experimental and theoretical support, with cyclic carbenium ions and methylbenzenes advocated as key species [56–58]. However, it remained unclear both why the numerous direct mechanisms proposed fail to explain consistent formation of ethene and what role certain directly formed intermediates or impurities in the methanol feed might play in combination with the hydrocarbon pool. Furthermore, the elementary reaction steps in the hydrocarbon pool model and the effect of the zeolite environment upon them are still poorly understood.

3.2 Direct mechanisms

While experimental methods are often impractical for evaluating individual reaction steps, theoretical methods are ideally suited for uncovering the underlying mechanism of the MTO process on an atomic scale. Over the years, not only have many experimentally suggested direct mechanisms been intensively tested by theoretical calculations, but numerous new potential routes have sprouted from theoretician's minds as well.

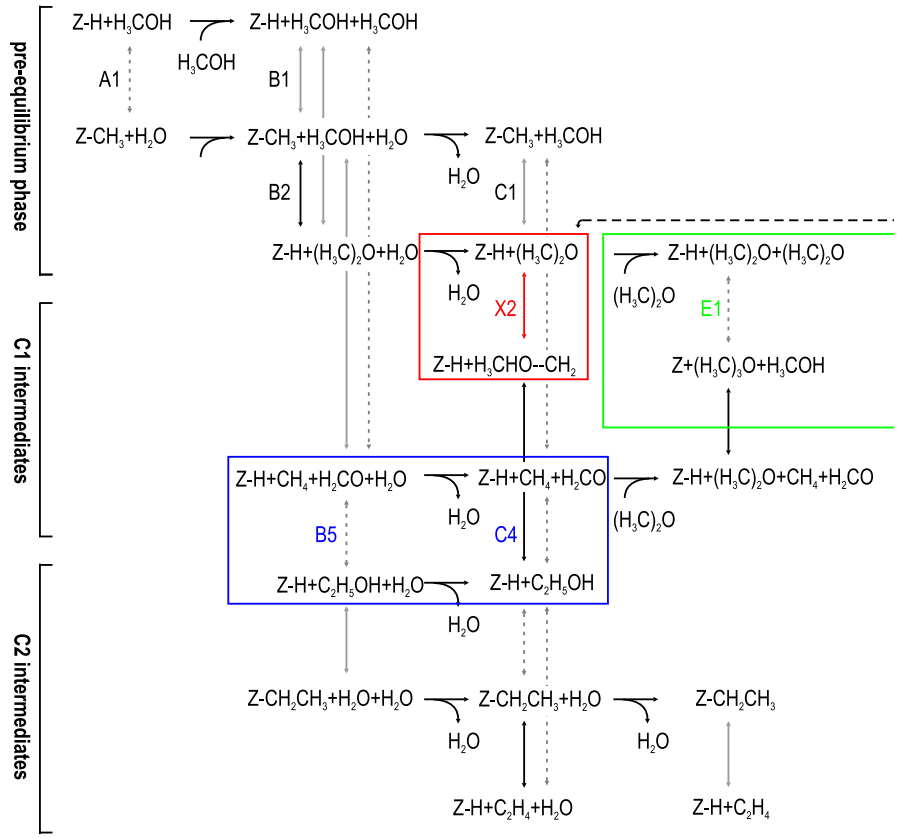

Figure 3.2: Reaction scheme containing elementary direct reaction steps from methanol to ethene [art. 3.6].

Until recently, however, theoretical calculations on the direct mechanisms tended to be severely fragmentary and widely scattered as most analyzed just part of a single potential direct route. Moreover, straightforward comparison of results was cumbersome or even impossible, due to the wide variety of methods employed. Only a handful of landmark papers suggested and compared multiple direct routes [59, 60], and these were (because of more pressing computational limitations at the time) limited to low level of theory calculations on extremely small 1T/3T zeolite clusters. Furthermore, conclusions were mostly based on theoretical reaction barriers rather than on reaction rate coefficients, which combine both energetic and entropic contributions. The mere existence of individual

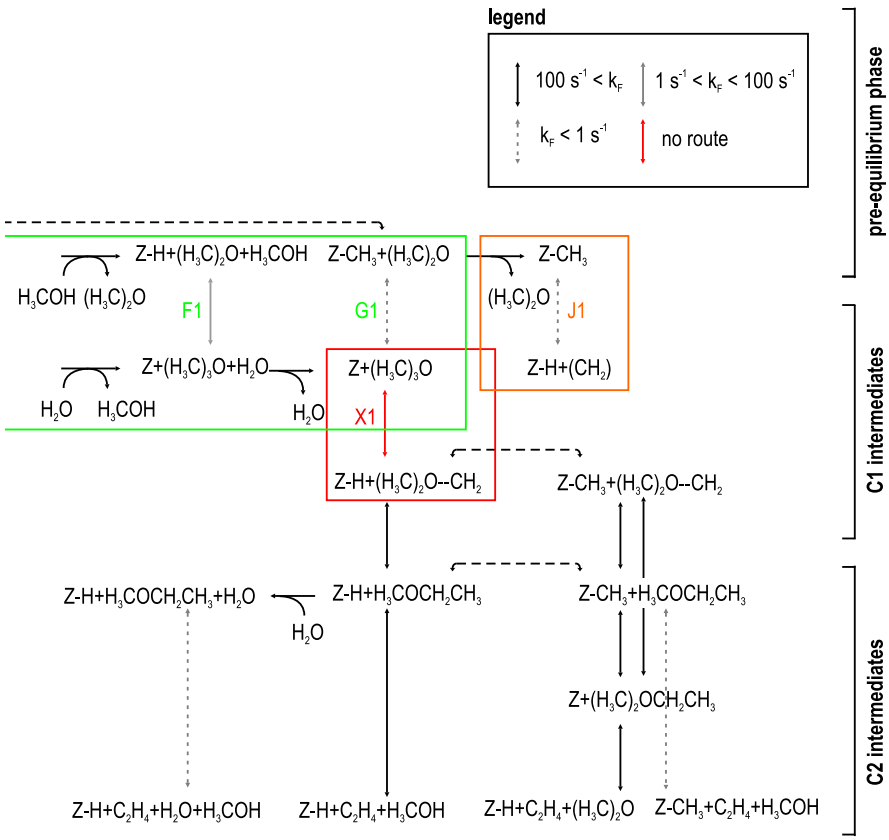

Figure 3.2: Reaction scheme containing elementary direct reaction steps from methanol to ethene (continued) [art. 3.6].

direct reactions demonstrated in many theoretical papers was always considered strong evidence for the direct mechanism proposal. There was never a theoretical guarantee, though, that the direct mechanisms came together to form a complete route that actually proceeds under reaction conditions.

To resolve this complex issue once and for all, an extensive reaction scheme had to be constructed, tying together a large variety of possible direct reactions and even including several previously overlooked, parallel pathways. This scheme - minus the reaction steps that have a forward and reverse energy bar-

rier higher than 200 kJ mol^{-1} - is shown in Figure 3.2 [art. 3.6]. Table 3.1 lists the individual reaction steps and gives selected key references for the various reactions together with the code numbers we use for ease of reference in the text. Table 3.2 gives the detailed kinetic parameters for these steps. On the basis of not only reaction barriers at 0 K but also rate coefficients at 720 K (obtained from TST, as described in Section 2.4.2) at the 5T level, the bottlenecks in the direct mechanism proposal can be identified. This chapter will focus on the most deep-rooted direct mechanism proposals that have received the strongest experimental attention, namely the oxonium ylide, carbene, and methane-formaldehyde routes. The steps shown in a box in Figure 3.2 will be discussed in more detail in the following sections.

3.2.1 Pre-equilibrium phase

As shown in Figure 3.1, the conversion of methanol is known to start with rapid dehydration to DME. This step proceeds either via an intermediate methoxide species Z-CH_3 and methanol, or through co-reaction of a methanol dimer, as presented in the top left corner of Figure 3.2. A two-step pathway is facilitated by methanol or water successively lowering reaction barriers as 'assisting molecules' (steps B1 and B2), allowing for more favorable transition state geometries than without assisting molecules (steps A1 and C1).

This first pre-equilibrium phase in the MTO-process has been extremely well-documented from a theoretical viewpoint, ranging from very small, yet pioneering cluster calculations [61–63] to more recent fully periodic DFT calculations [64–66]. All studies revealed similar conclusions on the mechanism independent of the method used, and this pre-equilibrium phase is currently very well understood. From our calculated rate coefficients using the 5T approach in Table 3.1, it is clear that the steps with assisting molecules have higher rate coefficients than those without and that both dimethyl ether and framework-bound methoxide groups will be formed [art. 3.6]. This pre-equilibrium, however, does not yet provide the highly sought-after carbon-carbon bond.

3.2.2 Trimethyl oxonium ion

From the initial mixture, a direct formation of the trimethyl oxonium ion (TMO) has been proposed through nucleophilic attack by adsorbed DME on a framework-bound methoxide species (step G1) or through co-reaction of DME and methanol (F1) [59, 60]. Alternatively, TMO could also be formed through

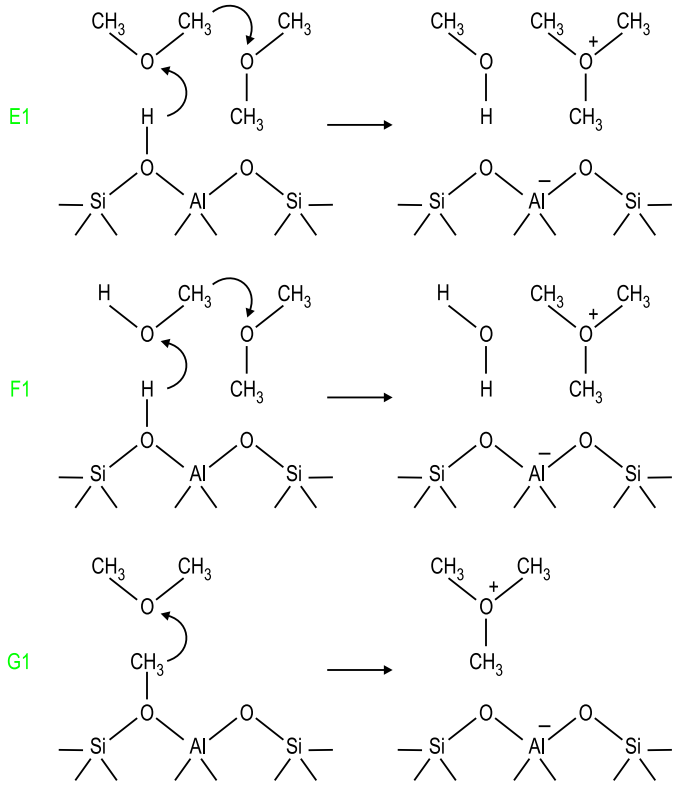

Figure 3.3: Different routes to trimethyl oxonium ion (TMO) formation from the pre-equilibrium mixture [art. 3.7].

co-reaction of two DME molecules (E1). All routes to TMO are situated in the green rectangle in Figure 3.2 and are illustrated schematically in Figure 3.3.

From the 5T cluster results, it seems that TMO is a relatively unstable intermediate. At this point, we should note that the 5T cluster approach is not always sufficient. Positively charged TMO, for example, forms an ion-pair with the negative aluminum defect and cannot, therefore, be adequately described in the small cluster approach (as previously explained in Section 2.3.4). However, our ONIOM calculations on larger 46T clusters confirm that TMO is additionally stabilized by the zeolite framework by approximately 70 kJ mol^{-1} [art. 3.5].

reactants	products	ref.	code
Z-H+H_3COH	Z-CH_3+H_2O	[61–63]	A1
Z-H+H_3COH+H_3COH	Z-CH_3+H_3COH+H_2O	[62, 63]	B1
Z-CH_3+H_3COH+H_2O	Z-H+$(H_3C)_2O$+H_2O	[63]	B2
Z-H+H_3COH+H_3COH	Z-H+$(H_3C)_2O$+H_2O	[63–66]	B3
Z-CH_3+H_3COH+H_2O	Z-H+CH_4+H_2CO+H_2O	-	B4
Z-H+CH_4+H_2CO+H_2O	Z-H+C_2H_5OH+H_2O	[67, 68]	B5
Z-H+C_2H_5OH+H_2O	Z-CH_2-CH_3+H_2O+H_2O	[60]	B6
Z-H+H_3COH+H_3COH	Z-H+CH_4+H_2CO+H_2O	[67, 68]	B7
Z-CH_3+H_3COH	Z-H+$(H_3C)_2O$	[63]	C1
Z-H+H_3CHO–CH_2	Z-H+C_2H_5OH	-	C2
Z-CH_3+H_3COH	Z-H+CH_4+H_2CO	[59, 60]	C3
Z-H+CH_4+H_2CO	Z-H+C_2H_5OH	[59]	C4
Z-H+C_2H_5OH	Z-CH_2-CH_3+H_2O	[60]	C5
Z-CH_2-CH_3+H_2O	Z-H+C_2H_4+H_2O	[60]	C6
Z-H+C_2H_5OH	Z-H+C_2H_4+H_2O	[59, 60]	C7
Z-H+$(H_3C)_2O$	Z-H+H_3CHO–CH_2	-	X2
Z-CH_2-CH_3	Z-H+C_2H_4	[60]	D1
Z-H+$(H_3C)_2O$+$(H_3C)_2O$	Z+$(H_3C)_3O$+H_3COH	-	E1
Z+$(H_3C)_3O$+H_3COH	Z-H+$(H_3C)_2O$+CH_4+H_2CO	-	E2
Z-H+$(H_3C)_2O$+H_3COH	Z+$(H_3C)_3O$+H_2O	[60]	F1
Z-CH_3+$(H_3C)_2O$	Z+$(H_3C)_3O$	[59, 60]	G1
Z-H+$(H_3C)_2O$–CH_2	Z-H+$H_3COCH_2CH_3$	-	G2
Z-H+$H_3COCH_2CH_3$	Z-H+C_2H_4+H_3COH	-	G3
Z+$(H_3C)_3O$	Z-H+$(H_3C)_2O$–CH_2	[59]	X1
Z-H+$H_3COCH_2CH_3$+H_2O	Z-H+C_2H_4+H_2O+H_3COH	[60]	H1
Z-CH_3+$(H_3C)_2O$–CH_2	Z-CH_3+$H_3COCH_2CH_3$	-	I1
Z-CH_3+$H_3COCH_2CH_3$	Z+$(H_3C)_2OCH_2CH_3$	-	I2
Z-CH_3+$(H_3C)_2O$–CH_2	Z+$(H_3C)_2OCH_2CH_3$	-	I3
Z+$(H_3C)_2OCH_2CH_3$	Z-H+C_2H_4+$(H_3C)_2O$	-	I4
Z-CH_3+$H_3COCH_2CH_3$	Z-CH_3+C_2H_4+H_3COH	-	I5
Z-CH_3	Z-H+(CH_2)	[69]	J1

Table 3.1: Overview of individual reaction steps with selected key references and letter code [art. 3.7].

code	forward E_a (kJ mol^{-1})	forward A (s^{-1})	forward k (s^{-1})	reverse E_a (kJ mol^{-1})	reverse A (s^{-1})	reverse k (s^{-1})
A1	223.6	3.44E+12	2.1E−04	176.2	1.50E+12	2.5E−01
B1	142.3	9.87E+11	4.7E+01	95.7	1.29E+12	1.5E+05
B2	84.8	1.14E+11	8.1E+04	155.0	4.64E+10	2.7E−01
B3	129.7	1.27E+10	5.0E+00	153.4	6.77E+09	5.1E−02
B4	146.8	1.79E+11	4.0E+00	185.1	1.10E+06	4.1E−08
B5	173.7	4.84E+05	1.2E−07	231.5	2.93E+10	4.7E−07
B6	147.2	1.05E+11	2.2E+00	93.1	2.08E+12	3.7E+05
B7	196.4	1.24E+11	6.9E−04	188.1	9.86E+05	2.2E−08
C1	141.0	6.99E+11	4.1E+01	187.6	3.65E+10	8.9E−04
C2	129.3	9.93E+13	4.1E+04	545.2	1.12E+14	3.2E−26
C3	189.9	4.31E+11	7.2E−03	221.6	3.15E+06	2.6E−10
C4	172.6	5.81E+06	1.7E−06	233.4	1.33E+12	1.6E−05
C5	198.0	6.84E+12	3.0E−02	148.5	7.95E+13	1.3E+03
C6	139.4	2.46E+12	1.9E+02	83.5	5.27E+08	4.6E+02
C7	193.2	7.94E+13	7.7E−01	87.8	1.98E+11	8.5E+04
X2	-	-	0.0E+00	-	-	0.0E+00
D1	153.0	3.83E+12	3.0E+01	89.4	2.89E+09	9.4E+02
E1	135.7	6.81E+09	9.7E−01	28.2	4.42E+10	4.0E+08
E2	105.7	1.83E+11	3.9E+03	208.4	1.66E+05	1.3E−10
F1	147.3	5.70E+11	1.2E+01	12.7	4.35E+11	5.2E+10
G1	120.5	2.98E+08	5.4E−01	52.9	2.29E+14	3.3E+10
G2	117.9	5.31E+13	1.5E+05	470.5	2.24E+11	1.6E−23
G3	113.8	4.53E+10	2.5E+02	80.8	5.77E+10	8.0E+04
X1	-	-	0.0E+00	-	-	0.0E+00
H1	159.2	2.25E+11	6.4E−01	115.2	6.32E+08	2.8E+00
I1	130.4	1.02E+14	3.5E+04	521.3	1.02E+14	1.5E−24
I2	127.6	5.62E+11	3.1E+02	49.7	4.67E+15	1.2E+12
I3	18.9	1.56E+12	6.6E+10	331.9	1.30E+16	1.1E−08
I4	84.7	2.55E+14	1.8E+08	127.1	1.62E+07	9.6E−03
I5	281.2	9.17E+11	3.6E−09	193.1	1.46E+10	1.4E−04
J1	244.8	3.08E+11	5.3E−07	51.9	3.16E+12	5.5E+08

Table 3.2: Kinetic parameters of forward and reverse reactions at 720K, calculated at the B3LYP/6-31g(d) level on 5T clusters [art. 3.7].

A similar result was obtained through periodic calculations in the chabazite topology [70]. Adjusted energies using the ONIOM technique reveal two parallel routes with a barrier below 100 kJ mol^{-1}, providing theoretical evidence for TMO remaining an important lowly activated product formed directly from the equilibrium mixture [art. 3.7].

3.2.3 First bottleneck: ylide and carbene intermediates

The main difficulties arise once TMO is effectively formed and oxonium ylides (a carbene group coordinated to methanol or DME) are the next suggested intermediates (red rectangles in Figure 3.2). For instance, once TMO is successfully formed, it might be deprotonated by an adjacent basic site to form dimethyl oxonium methylide (DOMY) [art. 3.5]. The next step (forming the desired carbon-carbon bond) could be an intramolecular Stevens' rearrangement to methylethyl ether, or an intermolecular methylation, forming the ethyldimethyl oxonium ion. However, even using the ONIOM method on large 46T clusters there is no possible route X1 to be found from TMO to DOMY [art. 3.5]. Moreover, even though the zeolite framework offers supplementary stabilization for TMO, the same conclusion does not hold for the ylide, which results in DOMY being a highly energetic species. Methyl oxonium methylide (MOMY) is also a suggested intermediate. Adsorbed dimethyl ether could form a dimethyl oxonium ion (DMO), after which it would be deprotonated to MOMY [71]. A Stevens-type rearrangement would lead to ethanol, forming the required carbon-carbon bond. Yet again, this step X2 is non-existent and MOMY is highly unstable [art. 3.5]. Generally speaking, the oxygen bridge is insufficiently basic to form the desired ylides. Alternative pathways based on oxonium ylides are also highly improbable because of these unattainable species.

A somewhat different type of carbene, which is incorporated into the framework, can be formed by deprotonation of a framework-bound methyl group, as shown by the brown rectangle in Figure 3.2. Previous investigations of this step found a relatively unstable carbene and an extremely high reaction barrier [69]. Because of this, the rate coefficients for the formation of this framework-coordinated carbene (step J1 in Table 3.2) are extremely low [art. 3.6].

This analysis shows that the severe instability and the corresponding non-existence of not only the ylides but also the framework-coordinated carbene form a first main bottleneck for the direct approach in MTO chemistry [art. 3.6]. An experimental H/D exchange study has just recently confirmed the effective non-existence of these exotic species [50].

3.2.4 Second bottleneck: methane/formaldehyde route

Alternatively, there are multiple potential routes to methane and formaldehyde, starting from two methanol molecules, from a surface methoxide species and methanol or from TMO jointly adsorbed with methanol. The methane/formaldehyde route has been widely hailed as a possible MTO route, not only in small cluster calculations [59], but also in periodic molecular dynamics simulations [67, 68].

Once formed, however, only extremely slow reactions lead to the formation of ethanol (blue rectangle in Figure 3.2). As is clear from the steps B5 and C4 in Table 3.2, the rate coefficient for this step in particular is not determined mainly by the activation energy E_a but by the very small pre-exponential factor A, reflecting the major decrease in entropy that accompanies this reaction [art. 3.7]. This substantiates the importance of basing conclusions on reaction rates rather than solely on barriers. From ethanol, ethene could quite rapidly be formed, the fastest route running along a framework-bound ethoxide species and subsequent ethene production. Nevertheless, even though methane and formaldehyde will undoubtedly be formed, the conversion of this mixture to ethanol proceeds too slowly to be considered viable [art. 3.7]. The failure of methane and formaldehyde to easily convert to a C2 species forms the second main bottleneck in the direct mechanism proposal.

3.2.5 Third bottleneck: concerted C-C coupling

In order not to overcrowd Figure 3.2, conversions showing both forward and reverse barriers larger than 200 kJ mol^{-1} (which would not proceed in either direction) are not shown. However, a closer investigation of these reaction steps reveals crucial information on their failure [art. 3.6]. They all seem to follow a similar concerted reaction mechanism and share a common reason for being unsuccessful. A general model is shown in Figure 3.4 (left diagram), representing the steps that were too highly activated to be incorporated: a hydrogen abstraction from a methanol/DME methyl group by a zeolite basic oxygen bridge (possibly assisted by a water vehicle molecule) combined with the formation of a carbon-carbon bond with a methanol/DME/TMO/framework-bound methyl-group [art. 3.6]. Many of these concerted steps were first studied in a pioneering 1T cluster study [60], which even then already reported rather high reaction barriers. The unprotonated oxygen bridge lacks the strong basic character needed to activate the highly covalent carbon-hydrogen bond.

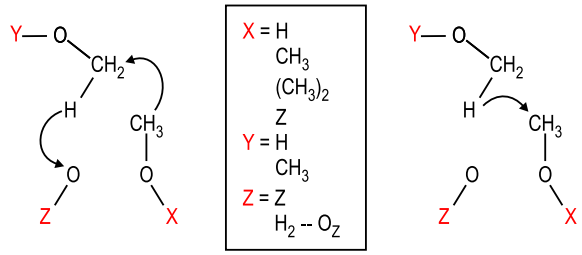

Figure 3.4: Reactions with a high energy barrier corresponding to concerted carbon-carbon coupling and carbon-hydrogen bond activation by zeolite basic oxygen O_Z (left diagram). Competing protonation of the methyl group forming methane (right diagram) will proceed far more rapidly.

A much faster competing reaction is preferred, forming methane instead (right diagram in Figure 3.4). This outspoken formation of methane is quite similar to what has been observed in molecular dynamics simulations [67, 68]. As mentioned above, though, the mixture of methane and formaldehyde does not succeed in supplying the first carbon-carbon bond. Thus, these concerted reactions form the third, and final bottleneck of the direct mechanism proposal.

3.2.6 Complete failure

Theoretical identification and clarification of all direct mechanisms behind the methanol-to-olefin process has been performed by not only giving an overview of the many individual reactions suggested in the literature, but by also calculating and recombining every single step in each pathway to allow for an overall picture and for direct comparison between the individual steps. The consistency of the scheme has allowed the critical reaction steps to be identified, and more advanced calculations using an embedding technique have been performed when necessary, as was the case for TMO. Moreover, the importance of basing conclusions on reaction rate coefficients rather than just barriers has been clearly demonstrated. As long as reaction barriers for partial pathways remained scattered over the literature, it seemed that there were multiple possibilities for direct conversion of methanol to ethene. Yet, the combination of these results in a complete network shows that no complete direct pathway from methanol leading all the way to ethene (or to any C2 intermediate) exists.

Hopefully, this theoretical conclusion ends some of the existing controversy surrounding the direct mechanisms. Alternatives to the direct mechanism concept, like the 'hydrocarbon pool' proposal, should be based on reactions and intermediates that somehow bypass the bottlenecks.

3.3 Hydrocarbon pool proposal

The most likely alternative to the direct mechanisms is provided by the hydrocarbon pool (HP) proposal, in which organic species trapped in the zeolite pores serve as a platform to which C1 species can attach (e.g. through repeated methylation by methanol), following which internal rearrangements and/or additional methylation leads to splitting off of olefins [54, 55]. Further methylation steps would then regenerate the original HP and close the catalytic cycle. By using this organic scaffolding to build the C2 species upon, the high-energy intermediates proposed in the 'direct' mechanisms can possibly be bypassed.

3.3.1 Experimental observations

The elementary steps governing this HP process are still not well understood, however, mainly because secondary reactions consume and mask the primary products, severely complicating interpretation of experimental data. Theoretical methods provide an ideal tool to unravel this complex network of reactions, as individual reaction steps can be modeled separately and consistently. The basic assumption for the calculations is the general consensus on a hydrocarbon pool consisting mainly of polymethylbenzenes, which are abundantly observed under MTO conditions [72, 73]. Furthermore, these polymethylbenzenes have been shown to be active for olefin formation independent of the zeotype catalyst chosen [74–77]. There is also strong experimental evidence for cyclic resonance-stabilized tertiary cations as persistent species in the pores, such as cyclopentenyl and pentamethylbenzenium cations in HZSM-5 [56, 78] and hexamethylbenzenium and heptamethylbenzenium (7MB+) cations in HBeta [79, 80]. *Gem*-dimethylbenzenium cations in particular have been observed by in situ ^{13}C solid-state NMR in alumino-silicates and form the main starting point from which commonly proposed hydrocarbon pool routes - such as the 'paring' and 'side-chain' mechanisms - originate [57]. In Figure 3.5 this initiating step is illustrated by a one-step geminal methylation of hexamethylbenzene (HMB) by methanol to form the heptamethylbenzenium cation (7MB$^+$). A third 'tropylium' route is more speculative, and has received much less attention.

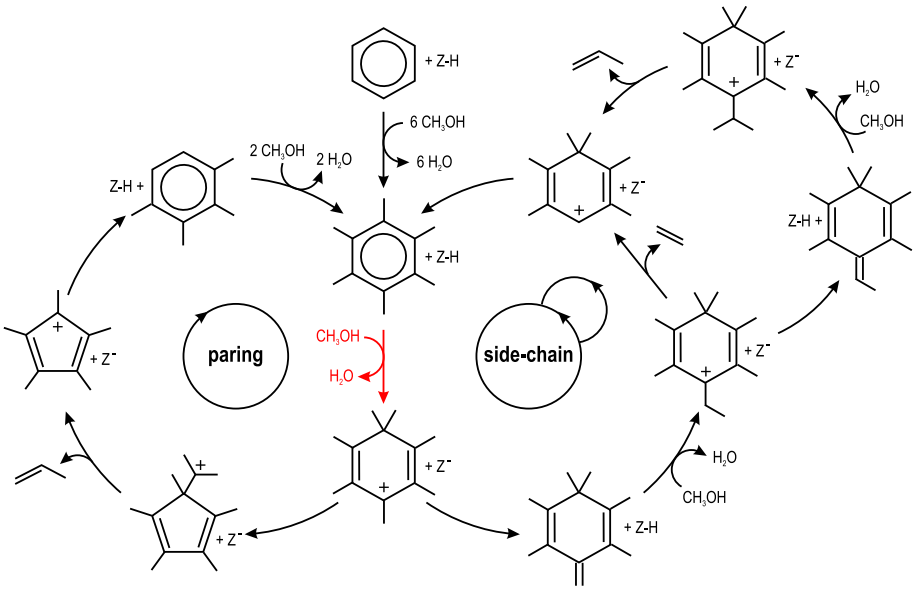

Figure 3.5: Catalytic cycles for paring and side-chain mechanisms leading to ethene/propene production from methanol. The initiating step is shown in red.

3.3.2 The supramolecular catalyst

Due to the complexity of the HP proposal, Haw and co-workers suggested that the catalyst should not be considered as a typical acid zeolite framework acting as a mere container for the hydrocarbon pool, but rather that each cage with all included organic and inorganic species should be seen as a supramolecule [81]. The nature and catalytic behavior of various supramolecular sites for MTO conversion is defined by the complex interplay between the inorganic framework, the organic hydrocarbon pool species and several additional factors. Figure 3.6 presents an overview of all the separate contributions, which, when combined, will define the active HP species as well as the reaction mechanism and the products that will consequently be formed.

With respect to the inorganic framework, zeolite composition (Figure 3.6.F1) is a first important factor. Although traditionally alumino-silicates (like HZSM-5) are most often considered, certain zeotype silico-aluminophosphates (like HSAPO-34) also show excellent MTO activity. Furthermore, the silico-alumino-

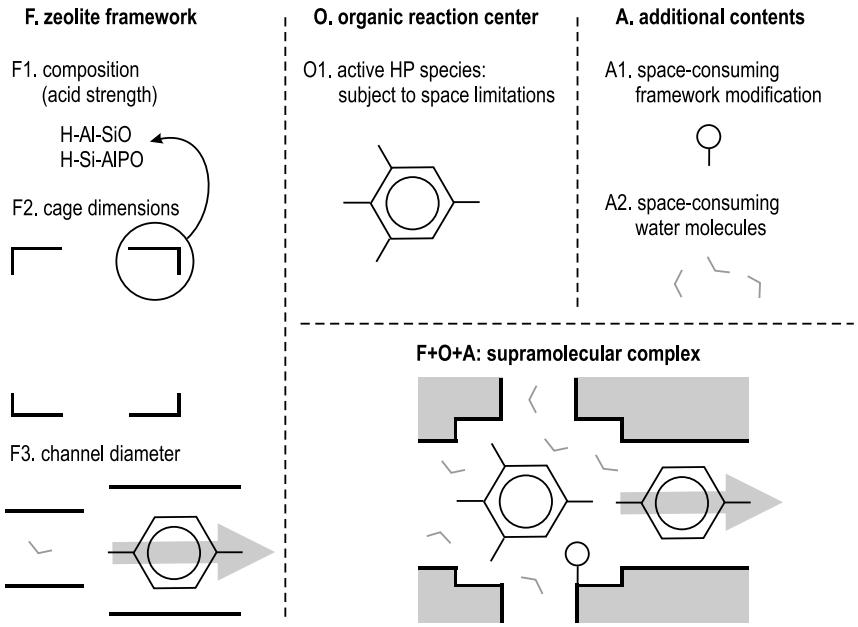

Figure 3.6: Separate contributions to the supramolecular catalyst (adapted from [81]).

phosphate composition leads to a lower, relatively moderate, acidic strength, which has the great advantage of suppressing the secondary reactions. Since the HP mechanism is a space-demanding process, pore architecture and shape selectivity will also play a crucial role. The cage dimensions (Figure 3.6.F2) will define both the maximum volume and shape allowed for bulky molecules. Channel diameters (Figure 3.6.F3), on the other hand, will control diffusion: small channels or windows will only allow small molecules like methanol/water and ethene/propene to enter and exit the cages, thus providing a basis for both reactant and product shape selectivity. In HSAPO-34, which has rather large cages compared to the small windows, the organic HP species has to be formed through ship-in-a-bottle synthesis. Furthermore, once it is formed, it remains trapped in the cage. Therefore, HSAPO-34 will only properly function as an MTO catalyst once coke formation has already started.

The organic reaction center (Figure 3.6.O1) is essential for an active MTO catalyst, as it acts as a platform upon which C-C bonds can be made and broken, as

illustrated in Figure 3.5. Without this platform, C-C coupling can only occur via the direct mechanisms for which rate coefficients are too low. Different organic components will exhibit different activity and different product selectivity, so establishment and modification of this species is crucial towards understanding and obtaining product control. In the case of polymethylbenzenes as an active HP species, for example, increasing the number of methyl groups is believed to significantly decrease the barrier to olefin synthesis, but at the same time to lead also to higher propene selectivity [82].

The number of methyl substitutions on a methylbenzene, and as a consequence also product distribution, will depend on the other ingredients shown in Figure 3.6. The degree of methylation depends mainly on the space available, which is determined predominantly by the cage dimensions. The cage dimensions can, however, also be tailored by additional space-consuming contents, such as inorganic framework modification or additional adsorbed molecules. Control of the spatial arrangement of cages with diverse functionality is, therefore, one of the ultimate goals in MTO catalysis. Post-synthesis modification with tetramethylphosphonium cations has succeeded in occupying cage volume and/or block windows and channels (Figure 3.6.A1), increasing the ethene/propene ratio [83]. Using another post-synthesis modification technique, silanation and disilanation of HSAPO-34 has led to an increase in light olefin/paraffin ratio and a decrease in coke formation [84]. Essential space can also be occupied by non-framework-bound molecules. For example, a higher loading of water leads to a reduction of free space (Figure 3.6.A2) and an increase in ethene/propene ratio [82].

Failure of direct mechanisms from topological viewpoint

The supramolecular premise of a bulky HP molecule in the zeolite pores shown in Figure 3.6 implies that zeolites with very small cages that are unable to host this space-demanding process, should not demonstrate any MTO activity whatsoever. Recently, this hypothesis was put to the test by performing experiments on systematically selected framework structures with varying pore and channel sizes [85]. These results confirmed that the MTO reaction only takes place on zeolites that allow the hydrocarbon pool mechanism to work, i.e. zeolites with larger cages (like CHA) or zeolites where channel intersections (like MFI) can also serve as an extended space for reactive intermediates. This important experimental verification of small cages providing an inactive MTO catalyst was attributed to transition state shape selectivity. Experimental claims to transition state shape selectivity are, ideally, verified by theoretical methods, since

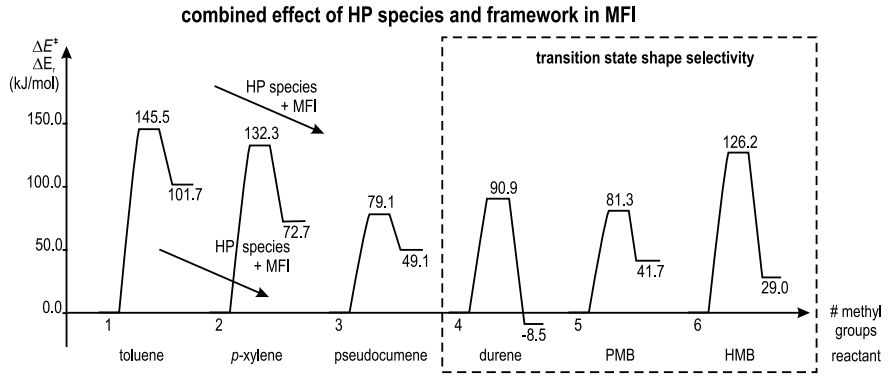

Figure 3.7: Energy barriers demonstrating transition state shape selectivity for *gem*-methylation of polymethylbenzenes [art. 3.8].

these are more suited for elucidating the extent to which the local shape of the pore influences local reaction rates [86, 87]. For the initiating step forming crucial cationic intermediates, the experimental claim to transition state shape selectivity will be theoretically confirmed in the following paragraph.

3.3.3 Initiating step

The initiating step of both hydrocarbon pool cycles is the geminal methylation of a methylbenzene by methanol. Alternatively methylation can also occur from DME or from a framework-bound methoxide. In Figure 3.5, only the routes from hexamethylbenzene are shown, but lower methylbenzenes can just as well undergo similar steps. We repeat that product distribution is defined by the number of methyl groups on the active hydrocarbon pool species: propene is favored by methylbenzenes with four to six methyl groups, while ethene is predominantly formed from the lower methylbenzenes [82]. Since the hydrocarbon pool mechanism involves bulky cyclic intermediates, it is also a space-demanding process. Therefore, zeolite topology is crucial in defining the hydrocarbon pool, resulting in a strong topological dependence of product distribution. For the initiating step highlighted in Figure 3.5, two main contributions play an important role: not only shape selectivity but also electrostatic stabilization effects of the zeolite framework on crucial cationic intermediates.

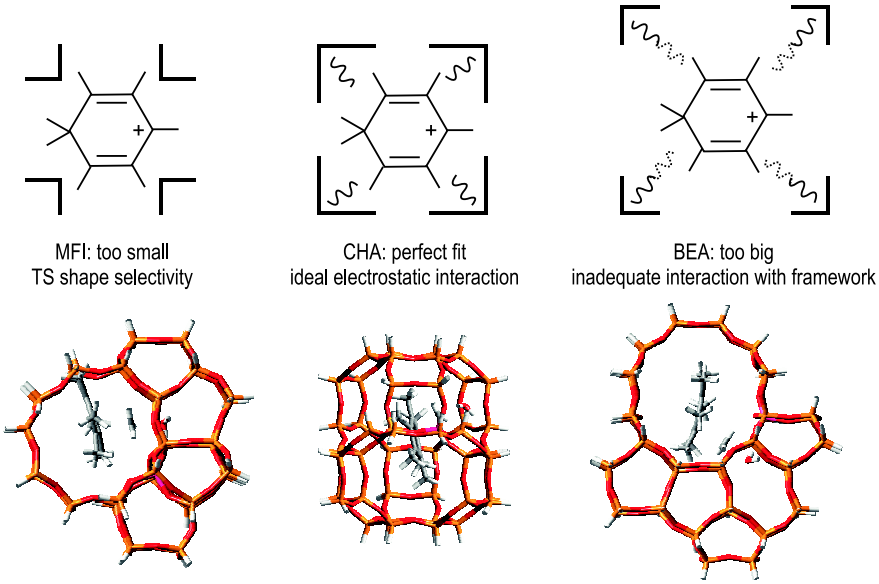

Figure 3.8: Refinement of the supramolecular picture: importance of the electrostatic effect of the zeolite topology on the carbenium ion product (top) and transition state shape selectivity (bottom), both for *gem*-methylation of hexamethylbenzene [art. 3.9].

Transition shape selectivity

For a zeolite with medium sized cages, or in the case of MFI medium sized channel intersections, there is inadequate volume for the higher *gem*-dimethylbenzenium cations to be formed [art. 3.8]. The lower methylbenzenes on the other hand do not suffer from these imposed restrictions (shown in Figure 3.7). Neither the size of the methylbenzene reactant nor that of the *gem*-dimethylbenzenium cation product is crucial, but the activity of a HP molecule is governed largely by the size of the transition state leading to the geminal methyl group, and as such will be subject to transition state shape selectivity [art. 3.8] (illustrated in Figure 3.8). This theoretical prediction was confirmed when experimental results demonstrated that even though the higher methylbenzenes are present in MFI, they are virtually unreactive and ethene appears to be formed exclusively from the lower methylbenzenes [88]. Most importantly, even if an aromatic HP platform is present, it can only perform as an active species for olefin production if the surrounding conditions allow favorable tran-

sition states as well.

Cationic intermediates

For a zeolite with larger cages (like CHA) there is adequate space, not only for the bulky HP species, but also for the transition state leading to heptamethylbenzenium ion formation. Furthermore, as shown in Figure 3.8, the encapsulating cage provides ideal electrostatic stabilization of this ion, resulting in a very low barrier to formation of this species [art. 3.8]. Adding solvent molecules or inorganic features would reduce the amount of methyl substitutions and increase ethene selectivity, while simultaneously slightly reducing catalytic activity. In a zeolite like HBeta, on the other hand, the cages are too big to provide the necessary electrostatic stabilization (illustrated in Figure 3.8) [art. 3.8]. Although there is enough space for the heptamethylbenzenium ion to be formed, it is relatively unstable with respect to the neutral species. This is in accordance with the electronic confinement effect, which is more pronounced when guest molecules and the cavity are closer in size [89].

Both the stability and ease of formation of crucial cationic intermediates in the hydrocarbon pool model will be largely influenced by the catalyst's topology. This will also directly govern the route which will be followed. Transition state shape selectivity and electrostatic stabilization by the zeolite framework are, therefore, important extensions to the previously outlined supramolecular picture.

3.4 Conclusions

Our theoretical work has firmly demonstrated that the frequently suggested direct mechanisms all fail to explain initial C-C coupling in the methanol-to-olefin process. Three critical points can be identified:

- firstly the instability of the ylide or carbene intermediates
- secondly the low conversion rates of methane and formaldehyde to ethanol
- and thirdly the concerted carbon-carbon coupling reactions, which convert to the formation of methane and formaldehyde instead.

This means that our focus should be shifted to alternative proposals. Our theoretical calculations on the initiating step of the hydrocarbon pool model have clearly illustrated the extent to which the organic hydrocarbon pool species and

the inorganic zeolite framework cooperate as a supramolecular catalyst. This makes alternative C-C coupling pathways with lower energy barriers than those in the direct mechanisms possible.

Both hydrocarbon pool species and zeolite topology play a crucial role in the reaction kinetics for the first C-C bond formation, to the extent that there might not be just one methanol-to-olefin mechanism, but several separate mechanisms tailored to each different zeotype material. The supramolecular picture as earlier developed [81] has been extended here by stating that not only the traditional concepts of reactant and product shape selectivity need to be taken into account, but that transition state shape selectivity will play a far more important role than either of these. Furthermore, we have illustrated the effect of pore size and shape on the stability and ease of formation for crucial cationic intermediates and have demonstrated the importance of electronic confinement effects. Unlike often postulated, topology effects go much further than just a matter of available space.

From here, we need further theoretical insights into the effect of zeolite topology and composition on the entire hydrocarbon pool route. At this point, firm theoretical proof of an entire reaction network is not yet present. Since conclusions should be based on reaction rates for extended systems because of the supramolecular aspect, theoretical modeling of the entire hydrocarbon pool network is a far more ambitious goal than modeling the direct mechanisms. Ideally, we would combine the knowledge obtained from both theory and experiment to create a fine-tuned local spatial environment that optimizes catalytic activity, improves product selectivity and simultaneously suppresses the undesired secondary reactions. Since the methanol-to-olefin process is a key step in the switch from fossil fuels to green chemistry [43], additional insights into the mechanism are highly desirable. Strong interaction between experimental and theoretical research is needed if we are to achieve these insights in a cost-effective way.

Published papers on the MTO process

article 3.5

D. Lesthaeghe, V. Van Speybroeck, G.B. Marin, M. Waroquier

What role do oxonium ions and ylides play in the ZSM-5 catalysed methanol-to-olefin process?

Chem. Phys. Lett. 417, **2006**, 309-315

No way, José: Oxonium ylides are the key species in the often proposed direct mechanisms for C-C coupling in the methanol-to-olefin process. However, these intermediates are highly energetic and thus unattainable at relevant temperatures. Even though the zeolite framework assists in stabilizing the preceding trimethyl oxonium ion, it does not similarly affect the dimethyl oxonium methylide nor the methyl oxonium methylide.

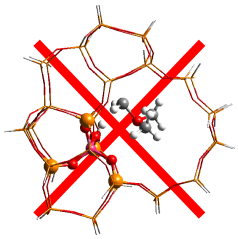

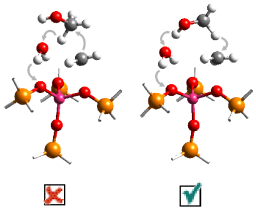

You are the weakest link, goodbye! An extensive number of individual steps from direct mechanisms in the methanol-to-olefin process are tied together in an integrated scheme, allowing simple identification of the weakest links. Theoretical calculations show that a combined pathway from methanol directly to ethylene does not exist and that no carbon-carbon bond can be formed along the way.

article 3.6

D. Lesthaeghe, V. Van Speybroeck, G.B. Marin, M. Waroquier

Understanding the failure of direct C-C coupling in the zeolite-catalyzed methanol-to-olefin process

Angew. Chem. Int. Ed. 45, **2006**, 1714-1719

article 3.7

D. Lesthaeghe, V. Van Speybroeck, G.B. Marin, M. Waroquier

The rise and fall of direct mechanisms in methanol-to-olefin catalysis: an overview of theoretical contributions

Ind. Eng. Chem. Res. 46, **2007**, published online

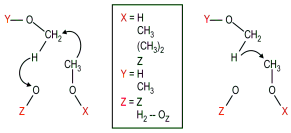

End of an era: Based on the results in [art. 3.6], this review-style article gives a more detailed overview of the theoretical contributions that initially supported the direct mechanism proposal, but which finally culminated in its demise. Special attention is given to the most deep-rooted direct mechanism proposals, namely the oxonium ylide, carbene, and methane-formaldehyde routes.

Must fit like a glove: The initiating step for olefin formation from methanol in zeolites is strongly dependent on specific combinations of organic hydrocarbon pool species and zeolite topology. If the cages are too large, neutral species are favored over reactive cations. If the cage is too small, transition state shape selectivity poses severe limitations on the reactivity of bulkier species.

article 3.8

D. Lesthaeghe, B. De Sterck, V. Van Speybroeck, G.B. Marin, M. Waroquier

Zeolite shape selectivity in the gem-methylation of aromatic hydrocarbons

Angew. Chem. Int. Ed. 46, **2007**, 1311-1314

article 3.9

D. Lesthaeghe, V. Van Speybroeck, G.B. Marin, M. Waroquier

Refinement of the supramolecular concept in methanol-to-olefin catalysis

Stud. Surf. Sci. Catal. **2007**, submitted

One plus one equals three: Combining the organic hydrocarbon pool with the inorganic framework unleashes a wide variety of interactions. Based on the results in [art. 3.8], the current supramolecular picture is refined in this review article. An overview of previously defined contributions is extended with the role of transition state shape selectivity and framework electrostatic stabilization on crucial cationic intermediates.

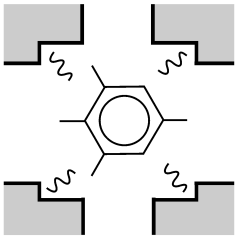

3.5

What role do oxonium ions and oxonium ylides play in the ZSM-5 catalysed methanol-to-olefin process?

D. Lesthaeghe, V. Van Speybroeck, G.B. Marin, M. Waroquier
Chemical Physics Letters 417, **2006**, 309-315.

---

article 3.5

D. Lesthaeghe, V. Van Speybroeck, G.B. Marin, M. Waroquier

What role do oxonium ions and ylides play in the ZSM-5 catalysed methanol-to-olefin process?

Chem. Phys. Lett. 417, **2006**, 309-315

No way, José: Oxonium ylides are the key species in the often proposed direct mechanisms for C-C coupling in the methanol-to-olefin process. However, these intermediates are highly energetic and thus unattainable at relevant temperatures. Even though the zeolite framework assists in stabilizing the preceding trimethyl oxonium ion, it does not similarly affect the dimethyl oxonium methylide nor the methyl oxonium methylide.

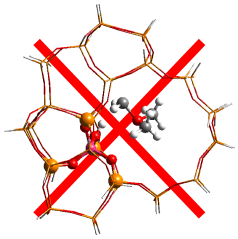

Available online at www.sciencedirect.com
SCIENCE DIRECT®
Chemical Physics Letters 417 (2006) 309–315
CHEMICAL PHYSICS LETTERS
www.elsevier.com/locate/cplett

What role do oxonium ions and oxonium ylides play in the ZSM-5 catalysed methanol-to-olefin process?

D. Lesthaeghe [a], V. Van Speybroeck [a], G.B. Marin [b], M. Waroquier [a,*]

[a] *Center for Molecular Modeling, Laboratory of Theoretical Physics, Ghent University, Proeftuinstraat 86, B-9000 Gent, Belgium*
[b] *Laboratorium voor Petrochemische Techniek, Ghent University, Krijgslaan 281-S5, B-9000 Gent, Belgium*

Received 26 August 2005; in final form 21 September 2005
Available online 2 November 2005

Abstract

The adsorption properties and possible rearrangements of several proposed oxonium ylides and oxonium ions in protonated ZSM-5 are studied using the 2-layered ONIOM(B3LYP/6-31+g(d,p):HF/3-21g) approach. We show that both methyl oxonium methylide and dimethyl oxonium methylide are highly energetic species and unlikely to be intermediates in the formation of a carbon–carbon bond as the zeolite lattice does not offer supplementary stabilisation. The trimethyl oxonium and ethyldimethyl oxonium ions, however, are distinctly stabilised by the surrounding ZSM-5 framework, which does not impose steric constraints on further intermolecular reactions.
© 2005 Elsevier B.V. All rights reserved.

1. Introduction

The methanol-to-olefin (MTO) process on zeolite H-ZSM-5 has been the focus of intensive research efforts from both industrial and academic viewpoints. Much remains uncertain, however, and the literature is replete with different and often conflicting propositions. The key step is the formation of the first carbon–carbon bond, for which more than 20 distinct mechanistic proposals have been suggested [1]. Of all the direct mechanisms, the oxonium ylide proposal [2] has received the strongest experimental attention. However, recent research has suggested that direct mechanisms might not be responsible for the sudden boost in hydrocarbon formation after all [3]. A viable alternative is given by the 'hydrocarbon pool' model as proposed by Dahl and Kolboe [4], in which impurities in the zeolite undergo methylation and subsequent olefin elimination. Lately, this proposal has gained in experimental and theoretical support, advocating cyclic carbenium ions and methylbenzenes as key species [5–7]. However, it still remains unclear both why the numerous direct mechanisms proposed fail to explain consistent formation of ethylene and what role certain directly formed intermediates might play in combination with the hydrocarbon pool.

The conversion of methanol is known to start with bimolecular dehydration to dimethyl ether (DME). Subsequently, an equilibrium mixture consisting of methanol, DME and water is converted to light olefins through carbon–carbon bond formation. Framework-bound methoxy species (in this Letter noted as ZEO-CH3) also seem to play a key role as an initial ingredient [8].

In this Letter, we will focus on possible oxonium ion and oxonium ylide intermediates, often reoccurring in direct mechanism proposals. Van den Berg et al. [2] postulated that dimethyl ether interacts with a zeolite Brønsted acid site (noted as ZEO-H) to form the dimethyl oxonium ion (DMO), which reacts further with another DME molecule to form the trimethyl oxonium ion (TMO). As schematically shown in Fig. 1, Olah [9] proposed a direct formation of TMO through nucleophilic attack by adsorbed DME on a framework-bound methoxide species. The formation of TMO is then followed by deprotonation by an adjacent basic site to form dimethyl oxonium methylide (DOMY). The next step (leading to the first carbon–carbon bond) would be either an intramolecular Stevens' rearrangement, leading to the formation of methylethyl ether (MEE), or an intermolecular methylation, leading to the formation of the

* Corresponding author.
E-mail address: michel.waroquier@ugent.be (M. Waroquier).

0009-2614/$ - see front matter © 2005 Elsevier B.V. All rights reserved.
doi:10.1016/j.cplett.2005.09.136

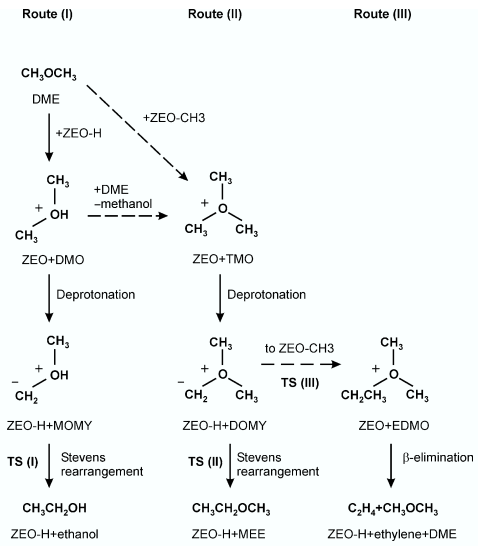

Fig. 1. Reaction scheme including oxonium ions and oxonium ylides.

ethyldimethyl oxonium ion (EDMO). The ethyldimethyl oxonium ion readily undergoes β-elimination forming ethylene and DME, the latter re-entering the condensation reaction.

Olefin formation through this suggested route would lead to the parallel formation of DME. However, Dewaele et al. [10] observed the parallel formation of water instead, and suggested that methyl oxonium methylide (MOMY) might be a possible intermediate. They proposed that adsorbed DME would first form a dimethyl oxonium ion (DMO), which would be deprotonated to MOMY. A Stevens-type rearrangement would then lead to the creation of ethanol, forming the required carbon–carbon bond.

We will focus on the formation of these oxonium ions and ylides, as they can be held directly responsible for the first carbon–carbon bond formation. The ylides can undergo Stevens' rearrangement, for which we will calculate energy barriers, but can also act as a nucleophilic form of carbon, a carbene coordinated to dimethylether (in the case of DOMY) or a carbene coordinated to methanol (MOMY). We will compare the ground state energies of the oxonium ions and oxonium ylides as shown in Fig. 1 with more stable intermediates like dimethyl ether, ethanol and methylethyl ether, and verify whether the ylide species are likely to persist within the aluminosilica framework. Furthermore, we will investigate whether the zeolite environment plays a major role in stabilising the oxonium ions.

2. Methods

2.1. Computational details

Full geometry optimizations for minimum energy and transition-state structures were performed within the GAUSSIAN03 software package [11] using density functional theory (DFT). Zygmunt et al. [12] assessed the applicability of various readily available functionals for studying molecular adsorption in small zeolite clusters and found that Becke's three-parameter B3LYP exchange-correlation functional [13] yields intermolecular energies and vibrational frequencies similar to those obtained using MP2. Their final conclusion states that the B3LYP functional is the best choice for DFT treatment of small zeolite clusters. The double ζ level basis set 6-31+g(d,p) was used, which includes polarisation and diffuse functions.

As we are dealing with adsorption properties of ion pairs, special attention must be given to the bulk electrostatic effects induced by the zeolite framework. Small QM cluster results were, therefore, compared to more advanced calculations using the 2-layered ONIOM approach, as developed by Morokuma and co-workers [14]. Recently, Solans-Monfort et al. [15] compared adsorption properties of NH_3 and H_2O in acidic chabazite, using both the ONIOM2 scheme and fully periodic calculations, and found that long-range effects do not extend too far, even

when ion pairs are involved. Their major conclusion states that the ONIOM(B3LYP:MNDO) level provides similar geometries to those obtained through periodic calculations, while accurate adsorption energies can be obtained through a single-point energy calculation at the ONIOM-(B3LYP:HF/3-21g) level of theory on the ONIOM-(B3LYP:MNDO) geometries. Their study shows that the ONIOM scheme provides a computationally attractive alternative to more expensive periodic calculations. In this Letter, we report the first application of this specific procedure extended to more advanced adsorption complexes in the clusters described in the following section.

2.2. Cluster selection

The large unit cell of ZSM-5 (288 atoms) impedes ab initio periodic calculations, which is why we resorted to hybrid high/low-level methods on zeolite clusters. For the fully high-level DFT calculations, the active site was modelled by a pentatetrahedral (5T) cluster. For this 5T cluster no geometric constraints were imposed to verify the true nature of stationary points, i.e., absolute minima or saddle points. At this level of approximation we obtain molecular-type systems with atoms having a higher degree of freedom than the real active sites that are embedded in a solid framework. As a result, artificial deformations of this limited model might occur, possibly altering the energetics [16,17], which is why we performed additional high/low-level calculations on larger clusters.

For the hybrid high/low-level study the active site was modelled by the same 5T cluster, surrounded by the low-level region. The combined high/low-level zeolite clusters were cut out of the crystallographic structure of ZSM-5, the predominant commercially used catalyst for the MTO process. Two specific clusters were chosen, containing 30 T-atoms and 46 T-atoms, respectively. The 46T model is

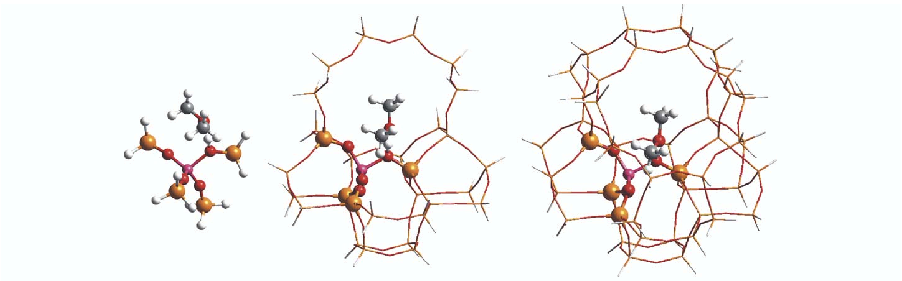

Fig. 2. From left to right: 5T, 30T, 46T models of zeolite H-ZSM-5 containing adsorbed DME. Low-level bonds are represented by cylinders, while the high-level active centre is shown in the ball/stick representation.

Table 1
Energies (in kJ/mol) of intermediates relative to a chosen reference state for different cluster sizes

Cluster size	5T	30T		46T	
High-level	B3LYP/6-31+g(d,p)	B3LYP/6-31+g(d,p)		B3LYP/6-31+g(d,p)	
Low-level	–	MNDO	HF/3-21g	MNDO	HF/3-21g
Route (I)					
ZEO-H + DME	0.0	0.0	0.0	0.0	0.0
ZEO-H + MOMY	355.1	340.8	365.6	363.2	374.0
ZEO-H + ethanol	−54.3	−63.8	−47.2	−56.9	−48.9
ΔE[TS(I)]	134.7	145.0	134.0	137.2	133.0
Route (II)					
ZEO-CH3 + DME	0.0	0.0	0.0	0.0	0.0
$ZEO^- + TMO^+$	73.8	55.4	−17.6	81.8	7.7
ZEO-H + DOMY	315.1	315.6	313.0	355.2	317.6
ZEO-H + MEE	−96.7	−99.1	−116.9	−58.4	−101.6
ΔE[TS(II)]	112.3	139.1	130.3	137.2	133.0
Route (III)					
ZEO-CH3 + DOMY	0.0	0.0	0.0	0.0	0.0
$ZEO^- + EDMO^+$	−302.1	−267.1	−389.1	−306.0	−380.5
ΔE[TS(III)]	26.3	23.5	≈0	8.1	≈0

Forward reaction barriers (in kJ/mol) for routes (I) to (III) are given by ΔE[TS(I)] to ΔE[TS(III)], respectively (as defined in Fig. 1). Energies at the B3LYP/6-31+g(d,p):HF/3-21g level of theory are calculated on optimised B3LYP/6-31+g(d,p):MNDO geometries.

Table 2
Adsorption energies (in kJ/mol) of different species at the B3LYP:6-31+g(d,p) and the B3LYP/6-31+g(d,p):HF/3-21g level of theory for 5T and 30T/46T clusters, respectively

Cluster size	5T	30T	46T
Route (I)			
ZEO-H + DME	−58.3	−73.4	−77.8
ZEO-H + MOMY	−59.2	−63.7	−59.7
ZEO-H + ethanol	−69.1	−77.1	−83.2
Route (II)			
ZEO-CH3 + DME	−9.9	−16.7	−21.3
$ZEO^- + TMO^+$	−338.6	−332.4	−356.2
ZEO-H + DOMY	−34.2	−36.3	−56.6
ZEO-H + MEE	−58.8	−79.1	−88.7
Route (III)			
ZEO-CH3 + DOMY	−22.1	−28.4	−22.5
$ZEO^- + EDMO^+$	−321.8	−313.9	−343.9

considered to be large enough to cover all important framework effects on both the active site and the adsorbate [18]. The different cluster models cut out of ZSM-5 are shown in Fig. 2.

Dangling bonds, which in the authentic zeolite would connect the cluster with the rest of the solid, were saturated with hydrogen atoms in order to preserve electrostatic neutrality and spin multiplicity. For the 30T and 46T clusters these hydrogen atoms were held fixed in crystallographic positions, while all other low-level atoms were left unconstrained. A single Si/Al substitution was considered, located at the intersection of the main and sinusoidal channels, thus easily accessible to adsorbates.

3. Results and discussion

Energies (in kJ/mol) of all intermediates and transition states relative to chosen reference states are shown in Table 1. Routes (I) to (III) refer to the definitions given in Fig. 1. We will start by discussing the often proposed pathway via DOMY in detail, corresponding to route (II). There is evidence from solid-state NMR that the trimethyl oxonium ion (TMO) is present following the adsorption of methanol [19], and this experimental proof has also been backed up by numerous theoretical calculations. The latter are, how-

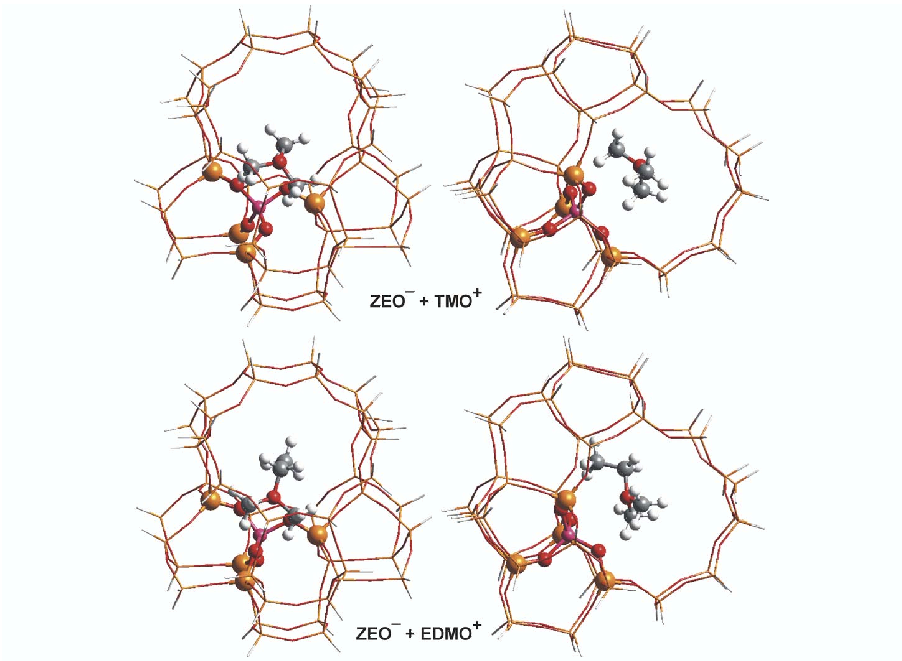

Fig. 3. Trimethyl oxonium ion (TMO) and ethyldimethyl oxonium ion (EDMO) in the negatively charged 46T cluster, viewed through sinusoidal and straight channels of ZSM-5. Distances between the oxonium oxygen atom and the framework aluminium are 4.15 and 3.63 Å, respectively.

ever, mostly conducted on small clusters [20], which neglect all effects of the surrounding zeolite framework. Our small 5T cluster (showing the same shortcomings) would suggest that methylation leading to TMO is endothermic by 73.8 kJ/mol, while the larger clusters show TMO to be comparable in energy with respect to DME and a framework methoxy group. Shah et al. [21] mention a similar stabilising effect for fully periodic calculations on chabasite, which is known for its relatively small unit cell (36 atoms).

In Table 2 we have summarised the adsorption energies of all species, defined as $E_{ads} = E(\text{zeo} + \text{ads}) - E(\text{zeo}) - E(\text{ads})$. The most eye-catching result is the extremely high adsorption energy of positively charged TMO (more than 300 kJ/mol). This is due to the ion-pair nature of TMO in contact with the negatively charged aluminium defect, and will restrict TMO to the aluminium site. While TMO is centrally locked in the cavity of chabasite [21], the accommodation within the larger pores of ZSM-5, as shown in Fig. 3, reveals that diffusion of a second molecule to TMO is not hampered by steric constraints. Any reaction with this second molecule nearby would not be restricted by the zeolite framework, implying that TMO can act as a viable source of methyl groups within the hydrocarbon pool model, as an alternative to framework methoxy species.

Shah et al. [21] also concluded that no local minimum for the ylide species exists within the microporous environment. They did not, however, perform transition state searches, and allowed for the possibility of an ylide species to exist as a transition state. Likewise, we were unable to form DOMY starting from the TMO, and we continuously observed back-donation of the proton from the zeolite to the oxonium ion. The proton affinity of the aluminium defect appears to be insufficient to deprotonate TMO. We were also unsuccessful in locating a transition state corresponding to this bond cleavage.

Tajima et al. [22] performed 3T cluster calculations at the HF/3-21g level of theory, and found DOMY as a local minimum, albeit a highly unstable species. In their study, possible stabilising effects of the zeolite framework were not considered. We succeeded in locating a similar stable configuration of DOMY, however it is clear from the orientation of the CH_2 group in Fig. 4 that this species cannot be directly formed by deprotonation of TMO. Furthermore,

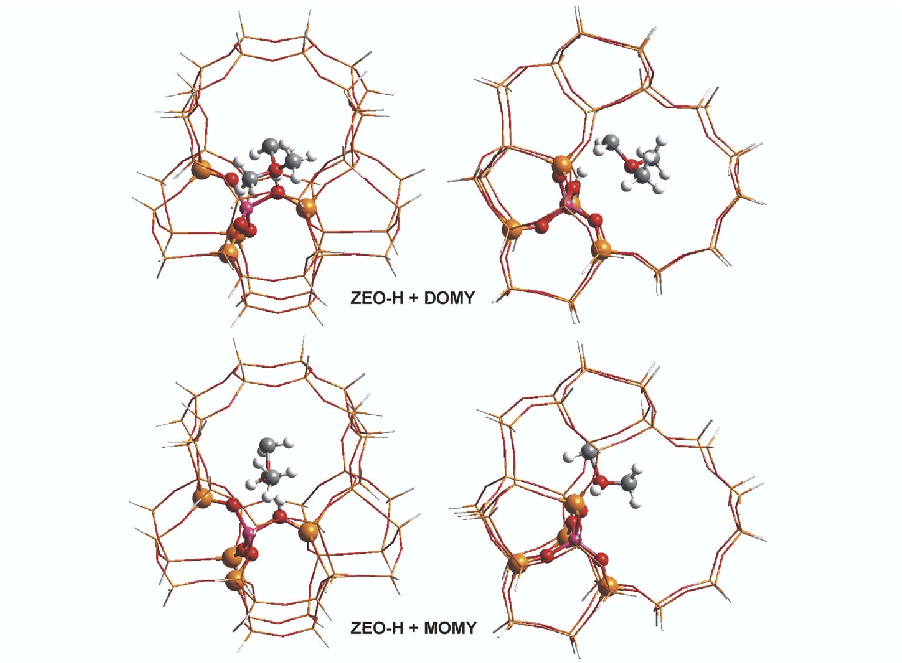

Fig. 4. Dimethyl oxonium methylide (DOMY) and methyl oxonium methylide (MOMY) in the 46T cluster, viewed through sinusoidal and straight channels of ZSM-5. Distances between the ylide oxygen atom and the framework aluminium are 4.11 and 3.37 Å, respectively.

Table 1 shows that the oxonium ylide is not additionally stabilised when larger parts of the zeolite framework are taken into account.

Olah [23] suggested through labelling experiments that the ylide undergoes bimolecular methylation along route (III), rather than an intramolecular Stevens' rearrangement. The subsequent methylation of the dimethyl oxonium ylide species would form an ethyldimethyl oxonium ion (EDMO). This reaction is extremely exothermic as well as quasi barrier free, which is why we expect this reaction to occur instantaneously. However, this mechanism requires migration of DOMY to a nearby framework-bound methoxy site. Due to the relative instability of the ylide, we highly doubt that this species would be sufficiently long-living to be able to migrate to a neighbouring methoxy site and that the formation of EDMO is likely to proceed. Notwithstanding, EDMO could be formed through a different, unknown pathway and is a stable species in the zeolite environment, as shown in Table 1. Just as in the case of TMO, this oxonium ion is highly stabilised by the zeolite framework. It is also clear that the B3LYP/6-31+g(d,p):MNDO level of theory underestimates the adsorption energy compared to the single point B3LYP/6-31+g(d,p):HF/3-21g calculations.

For the alternative route (I) through methyl oxonium methylide (MOMY), no previous theoretical work exists. In contrast to other oxonium ions TMO and EDMO, we found the dimethyl oxonium ion (DMO), which is in fact protonated DME, to be unstable near the zeolite active site. We did find a local minimum for the ylide, once more corresponding to a highly unstable species by more than 300 kJ/mol. Moreover, this species is again not additionally stabilised by the zeolite framework. Geometric considerations (Fig. 4), as well as the lack of a suitable transition state, lead us to believe that a deprotonation reaction of DME resulting in this ylide does not exist. Yet again there remains a major doubt on the zeolite's ability to abstract a carbon-bound proton from the oxonium ion to form the desired ylide.

As a general remark regarding cluster size, it is clear from these results that, while incorporating larger parts of the zeolite significantly influences absolute energies, it does not drastically alter energy differences. The 5T cluster energies are remarkably similar to the 30T and 46T results. In this case, even small cluster models, being the crudest of approximations, are capable of providing qualitative information. Notable exceptions are the stable oxonium ions, TMO and EDMO, for which the HF correction has a significant impact in stabilizing these species. This effect is overlooked at the B3LYP:MNDO level of theory, demonstrating the absolute necessity of the additional B3LYP:HF single point energy calculation for ion pairs.

4. Conclusions

We performed theoretical calculations on the adsorption properties and possible rearrangements of oxonium ylides and oxonium ions in protonated ZSM-5. Small cluster results reveal that the proposed ylides are local minima on the potential energy surface, but are highly unstable. Furthermore, by comparing small QM cluster calculations to more extensive ONIOM2 calculations, we conclude that the zeolite framework does not aid in stabilising these species. Therefore, it is highly unlikely that oxonium ylides play a significant role in the methanol-to-olefin process.

On the other hand, trimethyl oxonium (TMO) and ethyldimethyl oxonium (EDMO) ions are without a doubt stable species in the zeolite framework, while dimethyl oxonium ion (DMO) is not. We were unable to find a reaction path corresponding to a base-induced deprotonation of these ions resulting in the formation of oxonium ylides, and can conclude that the zeolite conjugate base is too weak in order to cleave the carbon–hydrogen bond. Excluding alternative pathways, EDMO is formed from DOMY, which is why we believe TMO to be the only realistically stable intermediate studied.

We provide solid proof that no ethylene can be formed through oxonium ylides, and our findings correspond to the fact that direct mechanisms fail in explaining the MTO process. Looking at stable intermediates interacting with the hydrocarbon pool, we have strong evidence that TMO can play at least an equally crucial role as a methyl-donating agent as methoxide groups. Other oxonium ions like DMO and EDMO are either unstable or formed through an oxonium ylide and are expected to play no role whatsoever in the hydrocarbon pool.

Acknowledgement

This work is supported by the Fund for Scientific Research – Flanders (FWO) and the Research Board of Ghent University.

References

[1] M. Stocker, Micropor. Mesopor. Mater. 29 (1999) 3.
[2] J.P. Van den Berg, J.P. Wolthuizen, J.H.C. Van Hooff, in: L.V. Reed (Ed.), Proceedings of the Fifth International Conference on Zeolites, Heyden, London, 1980, p. 649.
[3] W.G. Song, D.M. Marcus, H. Fu, J.O. Ehresmann, J.F. Haw, J. Am. Chem. Soc. 124 (2002) 3844.
[4] I.M. Dahl, S. Kolboe, J. Catal. 149 (1994) 458.
[5] J.F. Haw, J.B. Nicholas, W.G. Song, F. Deng, Z.K. Wang, T. Xu, C.S. Heneghan, J. Am. Chem. Soc. 122 (2000) 4763.
[6] B. Arstad, J.B. Nicholas, J.F. Haw, J. Am. Chem. Soc. 126 (2004) 2991.
[7] M. Bjorgen, U. Olsbye, S. Svelle, S. Kolboe, Catal. Lett. 93 (2004) 37.
[8] W. Wang, A. Buchholz, M. Seiler, M. Hunger, J. Am. Chem. Soc. 125 (2003) 15260.
[9] G.A. Olah, H. Doggweiler, J.D. Felberg, S. Frohlich, M.J. Grdina, R. Karpeles, T. Keumi, S. Inaba, W.M. Ip, K. Lammertsma, G. Salem, D.C. Tabor, J. Am. Chem. Soc. 106 (1984) 2143.
[10] O. Dewaele, V.L. Geers, G.F. Froment, G.B. Marin, Chem. Eng. Sci. 54 (1999) 4385.
[11] M.J. Frisch et al., Gaussian 03, Revision B.03, Gaussian Inc., Wallingford, CT, 2004.

[12] S.A. Zygmunt, R.M. Mueller, L.A. Curtiss, L.E. Iton, J. Mol. Struct. (Theochem) 430 (1998) 9.
[13] A.D. Becke, J. Chem. Phys. 98 (1993) 5648.
[14] S. Dapprich, I. Komaromi, K.S. Byun, K. Morokuma, M.J. Frisch, J. Mol. Struct. (Theochem) 461 (1999) 1.
[15] X. Solans-Monfort, M. Sodupe, V. Branchadell, J. Sauer, R. Orlando, P. Ugliengo, J. Phys. Chem. B 109 (2005) 3539.
[16] D. Lesthaeghe, V. Van Speybroeck, M. Waroquier, J. Am. Chem. Soc. 126 (2004) 9162.
[17] D. Lesthaeghe, V. Van Speybroeck, G.B. Marin, M. Waroquier, J. Phys. Chem. B 109 (2005) 7952.
[18] C. Raksakoon, J. Limtrakul, J. Mol. Struct. (Theochem) 631 (2003) 147.
[19] E.J. Munson, A.A. Kheir, N.D. Lazo, J.F. Haw, J. Phys. Chem. 96 (1992) 7740.
[20] S.R. Blaszkowski, R.A. van Santen, J. Am. Chem. Soc. 119 (1997) 5020.
[21] R. Shah, J.D. Gale, M.C. Payne, J. Phys. Chem. B 101 (1997) 4787.
[22] N. Tajima, T. Tsuneda, F. Toyama, K. Hirao, J. Am. Chem. Soc. 120 (1998) 8222.
[23] G.A. Olah, H. Doggweiler, J.D. Felberg, J. Org. Chem. 49 (1984) 2116.

3.6

Understanding the failure of direct C-C coupling in the zeolite-catalyzed methanol-to-olefin process

D. Lesthaeghe, V. Van Speybroeck, G.B. Marin, M. Waroquier
Angewandte Chemie - International Edition 45, **2006**, 1714-1719.

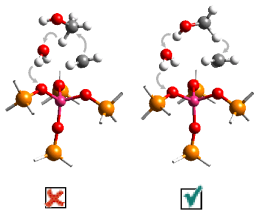

You are the weakest link, goodbye!
An extensive number of individual steps from direct mechanisms in the methanol-to-olefin process are tied together in an integrated scheme, allowing simple identification of the weakest links. Theoretical calculations show that a combined pathway from methanol directly to ethylene does not exist and that no carbon-carbon bond can be formed along the way.

article 3.6

D. Lesthaeghe, V. Van Speybroeck, G.B. Marin, M. Waroquier

Understanding the failure of direct C-C coupling in the zeolite-catalyzed methanol-to-olefin process

Angew. Chem. Int. Ed. 45, **2006**, 1714-1719

Zeolites

DOI: 10.1002/anie.200503824

Understanding the Failure of Direct C–C Coupling in the Zeolite-Catalyzed Methanol-to-Olefin Process**

*David Lesthaeghe, Veronique Van Speybroeck, Guy B. Marin, and Michel Waroquier**

The mechanism of the methanol-to-olefin (MTO) process on zeolite H-ZSM-5 has been the source of significant debate by both industrial and academic researchers. Much still remains uncertain, and the literature is replete with diverse and often conflicting propositions. A crucial step is the formation of the first carbon–carbon bond, for which more than 20 distinct mechanistic proposals exist.[1] Early research focused mainly on mechanisms based on the direct formation of small olefins from only methanol and methanol derivatives. Advanced theoretical calculations on these "direct mechanisms" are fragmented throughout the literature, and straightforward comparison is cumbersome owing to the large array of methods employed. Only a handful of papers suggest and compare multiple direct routes,[2,3] but these are limited to low levels of theory calculations on extremely small 1T/3T zeolite clusters.

Recent developments suggest, however, that direct mechanisms might not be responsible for the observed boost in hydrocarbon synthesis.[4] A plausible alternative is given by the "hydrocarbon pool" model,[4,5] in which impurities in the mixture undergo repeated methylation and subsequent olefin elimination. This latter proposal is consistently gaining experimental and theoretical support, which advocates methylbenzenes and methylcyclopentenyl cations as key species.[6,7] Because of an observed kinetic induction period preceding the hydrocarbon formation, the hydrocarbon pool model implies that reactions occurring during this induction period need not necessarily be similar to those on a working catalyst. It is still unresolved, though, which—if any—induction reactions give rise to the hydrocarbon pool.

As the literature currently stands, two important questions regarding direct mechanisms remain unanswered: 1) From a theoretical viewpoint it is still unclear why the numerous proposed direct mechanisms should fail in consistent production of ethylene. 2) From a more practical perspective, it is still unknown what role certain directly formed intermediates might play both during the induction period and during hydrocarbon synthesis. Although experimental methods are often incapable of evaluating individual reaction steps, DFT-based calculations can provide these answers.

An extensive scheme is proposed, tying together a large variety of possible direct reactions, which include several previously overlooked, parallel pathways. On the basis of calculated adsorption energies, reaction barriers (at 0 K), and rate coefficients (at 720 K), it is possible to deduce whether ethylene can be produced from only methanol, and which stable intermediates might be formed directly to finally enhance our understanding of the first carbon–carbon bond formation.

Our aim was to integrate a whole range of reactions in an orderly and concise manner, as shown in Scheme 1. The adsorbed species form the main building blocks, with the total adsorption energy (in kJ mol^{-1}) shown in brackets. Horizontal movement between these species corresponds to adsorption or desorption of a required molecule. Vertical arrows represent an elementary reaction step for which both forward and reverse intrinsic energy barrier heights at 0 K (in kJ mol^{-1}) as well as rate coefficients at 720 K (in s^{-1}) are included. For simple referencing purposes, each reaction step is identified by a specific code. The starting point (top left corner) is a single methanol molecule adsorbed near the acid site Z-H, leading finally to the creation of ethylene (bottom row). For clarity, we omit connections for which both the forward and reverse reactions are highly activated ($\Delta E_0 >$ 200 kJ mol^{-1}) and which are therefore unlikely to proceed in either direction.

The conversion of methanol is known to start with rapid dehydration to dimethyl ether (DME). This proceeds either via an intermediate methoxide species Z-CH_3 (reactions coded A1/B1/B2/C1),[8] or through co-reaction of a methanol dimer (B3). The two-step pathway B1/B2 is facilitated by methanol/water successively lowering the reaction barriers as "assisting molecules", allowing more-favorable transition-state geometries. This first preequilibrium phase in the methanol-to-olefin process is theoretically well documented, ranging from small clusters[9–11] to fully periodic DFT calculations,[12–14] which all lead to similar conclusions.

From this initial mixture, the direct formation of the trimethyl oxonium ion (TMO) has been proposed through nucleophilic attack by adsorbed DME on a framework-bound methoxide species (G1).[15] Alternatively, TMO can also be formed through co-reaction of two DME molecules (E1) or DME and methanol (F1). Owing to the extremely low reverse reaction barriers, one would at first glance expect TMO to be an exceptionally short-lived intermediate. However, positively charged TMO forms an ion pair with the negative aluminum defect, and therefore cannot be adequately described in the small cluster approach. Our previous ONIOM calculations, however, have shown that TMO is additionally stabilized by the zeolite framework,[16] a similar result to that obtained through periodic calculations in chabazite,[17] and that TMO remains an important product formed directly from the equilibrium mixture.

[*] Ir. D. Lesthaeghe, Dr. Ir. V. Van Speybroeck, Prof. Dr. M. Waroquier
Center for Molecular Modeling
Ghent University
Proeftuinstraat 86, 9000 Gent (Belgium)
Fax: (+32) 9-264-6697
E-mail: michel.waroquier@ugent.be
Prof. Dr. Ir. G. B. Marin
Laboratorium voor Petrochemische Techniek
Ghent University
Krijgslaan 281-S5, 9000 Gent (Belgium)

[**] This work was supported by the Fund for Scientific Research–Flanders (FWO) and the Research Board of Ghent University.

© 2006 Wiley-VCH Verlag GmbH & Co. KGaA, Weinheim

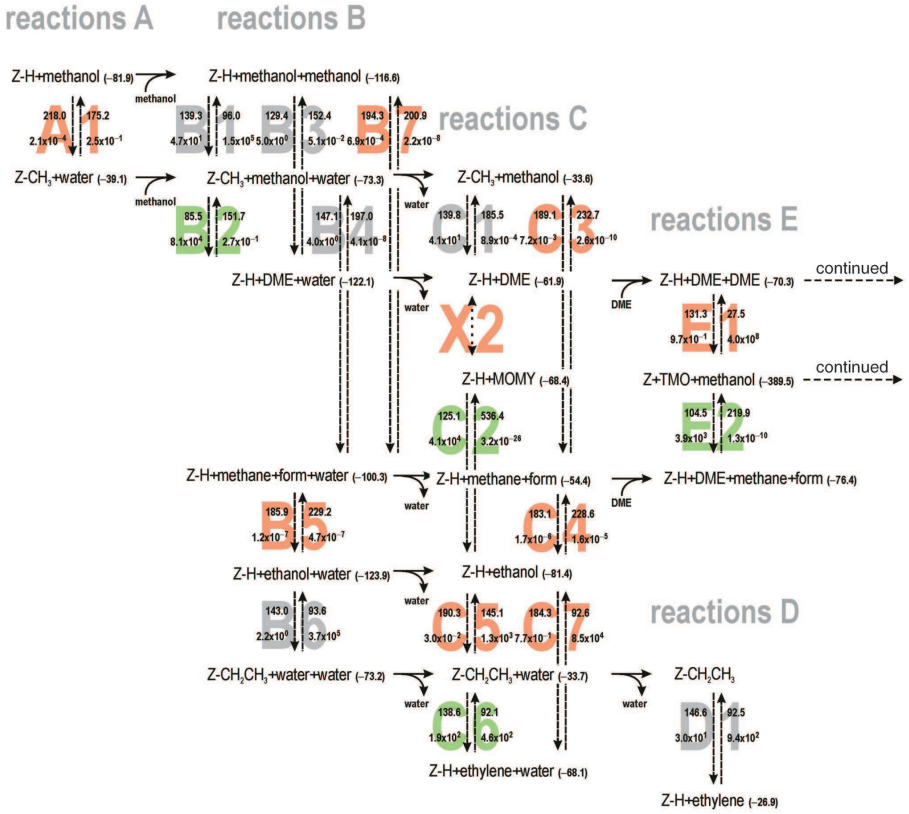

Scheme 1. Direct routes in the methanol-to-olefin process. Horizontal arrows correspond to an adsorption/desorption step, vertical arrows denote a reaction step. Intrinsic energy barriers at 0 K are shown in kJ mol^{-1}, rate coefficients at 720 K are expressed in s^{-1}.

Once TMO is successfully formed, it might be deprotonated by an adjacent basic site (reaction step X1) to form dimethyl oxonium methylide (DOMY).[15] The next step is an intramolecular Stevens rearrangement (G2/I1) to methyl ethyl ether (MEE) or an intermolecular methylation (I2/I3) to form the ethyl dimethyl oxonium ion (EDMO). EDMO readily undergoes β elimination to form ethylene and dimethyl ether (I4). From MEE, several alternative pathways lead directly to ethylene (H1/G3/I5). However, our previous work has shown that there is no possible route from TMO to DOMY (X1).[16] Moreover, the zeolite framework does not offer any supplementary stabilization, which results in DOMY being a highly energetic species.

Alternatively, methyl oxonium methylide (MOMY) has been proposed as a possible intermediate.[18] Adsorbed dimethyl ether could form a dimethyl oxonium ion (DMO), after which it would be deprotonated to MOMY (X2). A Stevens-type rearrangement would lead to ethanol (C2), thus forming the required carbon–carbon bond. Yet again, we have found this step to be non-existent and MOMY to be highly unstable.[16] An altogether different ylide, incorporated into the framework, can be formed by deprotonation of a framework-bound methyl group (J1).[19] This step was found to be highly activated as well.

Generally speaking, the oxygen bridge seems to be insufficiently basic to form the desired ylides. We also state that alternative pathways based on oxonium ylides are highly improbable owing to the high instability of these species. The instability of the ylides consequently rules out the role of MEE as a crucial intermediate as well as the pathway through EDMO.

There are several routes to methane and formaldehyde (form), starting from two methanol molecules (B7),[3] from a surface methoxy species and methanol (B4/C3), or from TMO

 © 2006 Wiley-VCH Verlag GmbH & Co. KGaA, Weinheim

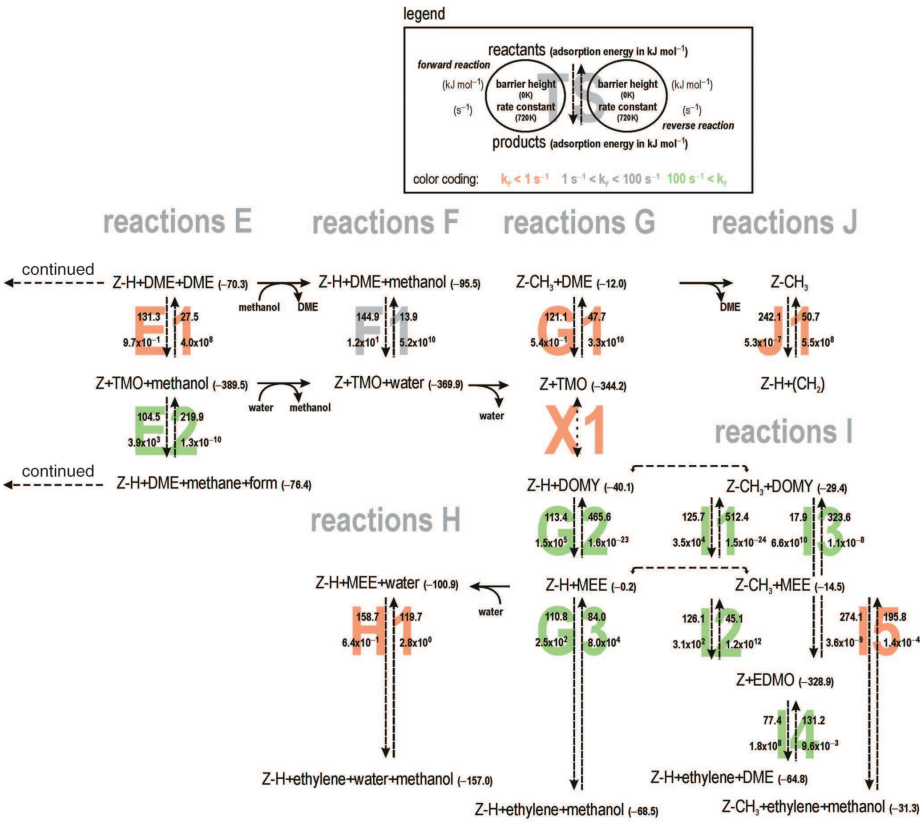

Scheme 1. (Continued).

jointly adsorbed with methanol (E2). Once formed, however, only extremely high reaction barriers (B5/C4) allow the formation of ethanol. From ethanol, ethylene could be immediately formed (C7), but the fastest routes would be through the formation of a framework-bound ethoxide species (B6/C5) and subsequent ethylene production (C6/D1).

As mentioned earlier, conversions showing both forward and reverse barriers larger than 200 kJ mol^{-1} are not shown in Scheme 1, and a closer investigation of the omitted reaction steps is necessary. In Figure 1 (blue arrows) we show a model representing the steps that were too highly activated to be incorporated, as they all follow a similar concerted reaction mechanism: hydrogen abstraction from a methanol/DME methyl group by a zeolite basic oxygen bridge (alternatively assisted by a water "vehicle molecule") combined with the formation of a carbon–carbon bond with a methanol/DME/

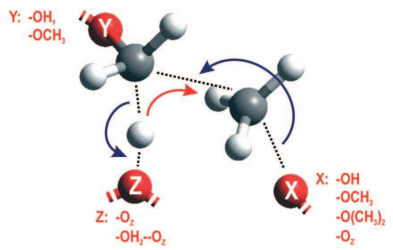

Figure 1. Highly activated reactions corresponding to concerted C–C bond formation and C–H bond breaking by zeolite basic oxygen O_Z (blue arrows). Protonation of the methyl group to form methane (red arrow) is observed instead.

 © 2006 Wiley-VCH Verlag GmbH & Co. KGaA, Weinheim

TMO/framework-bound methyl group. The unprotonated oxygen bridge apparently lacks the strong basic character needed to break the highly covalent C–H bond. An equally strong C–H bond is preferably formed, which is why the system evolves to a nearby transition state, thus leading to methane instead (red arrow in Figure 1). This is similar to observations in molecular-dynamics simulations.[20,21] These concerted reactions form the main bottleneck of the direct mechanism proposal, whereas currently suggested hydrocarbon pool reactions avoid similar concerted steps through the formation of an intermediate carbenium ion.

In conclusion, a large set of direct mechanisms (>80 stationary points) in the MTO process was studied theoretically, providing both rate coefficients at 720 K and reaction barriers at 0 K. Direct comparisons allowed the qualitative evaluation of which steps are likely to proceed. The crucial reaction steps were identified, into which further research is currently underway.

We failed to find a successive pathway from methanol leading all the way to ethylene (or to any intermediate containing a C–C bond), which is in accordance with methanol/DME not being noticeably reactive on H-ZSM-5 in the absence of organic impurities that provide a primordial hydrocarbon pool.[22] From our results, two bottlenecks can be clearly identified: on the one hand the instability of the ylide intermediates and on the other hand the high energy barriers for the often proposed concerted C–C bond-formation reactions, both of which are a direct result of the weak basic character of the zeolite oxygen bridge. It is also possible to define clearly which intermediate species are likely to be directly formed and may consequently interact with the hydrocarbon pool. These intermediates are not limited solely to the mixture of methanol with well-known condensation products DME and water but also TMO, which might act as a viable source of methyl groups, together with methane and formaldehyde.

Summarizing our conclusions, we have tied the numerously proposed reaction mechanisms together to find that not a single combination of direct reaction steps can link methanol to ethylene. This theoretical conclusion provides strong additional support for alternative proposals,[4–7] which bypass the highly activated concerted steps.

Methods Section

Geometry optimizations were performed on pentatetrahedral (5T) clusters with the Gaussian 03 package[23] at the B3LYP/6-31g(d) level of theory.[24–26] The cluster selection was motivated by the large amount of species taken into account (more than 80 distinctly different stationary points). Moreover, our recent study using ONIOM calculations on extended 30T and 46T clusters showed that the energy profile is only significantly altered in the case of adsorbed ion pairs.[16] Initial interpretation on the 5T level allowed us to evaluate which reactions require further detailed investigation. The cluster was left unconstrained to verify the true nature of stationary points, and zero-point energy (ZPE) corrections were included. Starting from transition-state geometries, the quasi-IRC approach allowed the product geometries to be acquired.[27] Rate coefficients were obtained by using transition-state theory (TST) by calculating the partition functions at 720 K. As elementary reaction steps were considered separately from adsorption/desorption requirements, only intrinsic energy barriers are shown (in kJ mol^{-1}): $\Delta E_0 = E_0$(transition state) $- E_0$(adsorbed reactants). Additionally, each elementary reaction was modeled assuming prior adsorption of necessary reagents, resulting in intrinsic rate coefficients (in s^{-1}).

Received: October 28, 2005
Revised: November 29, 2005
Published online: February 14, 2006

Keywords: ab initio calculations · C–C coupling · heterogeneous catalysis · methanol-to-olefin process · zeolites

[1] M. Stöcker, *Microporous Mesoporous Mater.* **1999**, *29*, 3–48.
[2] S. R. Blaszkowski, R. A. van Santen, *J. Am. Chem. Soc.* **1997**, *119*, 5020–5027.
[3] N. Tajima, T. Tsuneda, F. Toyama, K. Hirao, *J. Am. Chem. Soc.* **1998**, *120*, 8222–8229.
[4] W. Song, D. M. Marcus, H. Fu, J. O. Ehresmann, J. F. Haw, *J. Am. Chem. Soc.* **2002**, *124*, 3844–3845.
[5] I. M. Dahl, S. Kolboe, *J. Catal.* **1994**, *149*, 458–464.
[6] J. F. Haw, J. B. Nicholas, W. Song, F. Deng, Z. Wang, T. Xu, C. S. Heneghan, *J. Am. Chem. Soc.* **2000**, *122*, 4763–4775.
[7] B. Arstad, J. B. Nicholas, J. F. Haw, *J. Am. Chem. Soc.* **2004**, *126*, 2991–3001.
[8] W. Wang, A. Buchholz, M. Seiler, M. Hunger, *J. Am. Chem. Soc.* **2003**, *125*, 15260–15267.
[9] C. M. Zicovich-Wilson, P. Viruela, A. Corma, *J. Phys. Chem.* **1995**, *99*, 13224–13231.
[10] P. E. Sinclair, C. R. A. Catlow, *J. Chem. Soc. Faraday Trans.* **1997**, *93*, 333–345.
[11] S. R. Blaszkowski, R. A. van Santen, *J. Phys. Chem. B* **1997**, *101*, 2292–2305.
[12] E. Sandre, M. C. Payne, J. D. Gale, *Chem. Commun.* **1998**, 2445–2446.
[13] M. Hytha, I. Stich, J. D. Gale, K. Terakura, M. C. Payne, *Chem. Eur. J.* **2001**, *7*, 2521–2527.
[14] M. C. Payne, M. Hytha, I. Stich, J. D. Gale, K. Terakura, *Microporous Mesoporous Mater.* **2001**, *48*, 375–381.
[15] G. A. Olah, H. Doggweiler, J. D. Felberg, S. Frohlich, M. J. Grdina, R. Karpeles, T. Keumi, S. I. Inaba, W. M. Ip, K. Lammertsma, G. Salem, D. C. Tabor, *J. Am. Chem. Soc.* **1984**, *106*, 2143–2149.
[16] D. Lesthaeghe, V. Van Speybroeck, G. B. Marin, M. Waroquier, *Chem. Phys. Lett.* **2006**, *417*, 309–315.
[17] R. Shah, J. D. Gale, M. C. Payne, *J. Phys. Chem. B* **1997**, *101*, 4787–4797.
[18] O. Dewaele, V. L. Geers, G. F. Froment, G. B. Marin, *Chem. Eng. Sci.* **1999**, *54*, 4385–4395.
[19] P. E. Sinclair, C. R. A. Catlow, *J. Phys. Chem. B* **1997**, *101*, 295–298.
[20] C. Lo, C. A. Giurumescu, R. Radhakrishnan, B. L. Trout, *Mol. Phys.* **2004**, *102*, 281–288.
[21] C. S. Lo, R. Radhakrishnan, B. L. Trout, *Catal. Today* **2005**, *105*, 93–105.
[22] J. F. Haw, D. M. Marcus in *Handbook of Zeolite Science and Technology* (Eds.: S. M. Auerbach, K. A. Carrado, P. K. Dutta), Marcel Dekker, New York, **2003**, pp. 833–866.
[23] Gaussian 03, Revision B.03, M. J. Frisch, G. W. Trucks, H. B. Schlegel, G. E. Scuseria, M. A. Robb, J. R. Cheeseman, J. A. Montgomery, Jr., T. Vreven, K. N. Kudin, J. C. Burant, J. M. Millam, S. S. Iyengar, J. Tomasi, V. Barone, B. Mennucci, M. Cossi, G. Scalmani, N. Rega, G. A. Petersson, H. Nakatsuji, M. Hada, M. Ehara, K. Toyota, R. Fukuda, J. Hasegawa, M. Ishida, T. Nakajima, Y. Honda, O. Kitao, H. Nakai, M. Klene, X. Li, J. E. Knox, H. P. Hratchian, J. B. Cross, V. Bakken, C. Adamo, J. Jaramillo, R. Gomperts, R. E. Stratmann, O. Yazyev, A. J.

 © 2006 Wiley-VCH Verlag GmbH & Co. KGaA, Weinheim

Austin, R. Cammi, C. Pomelli, J. W. Ochterski, P. Y. Ayala, K. Morokuma, G. A. Voth, P. Salvador, J. J. Dannenberg, V. G. Zakrzewski, S. Dapprich, A. D. Daniels, M. C. Strain, O. Farkas, D. K. Malick, A. D. Rabuck, K. Raghavachari, J. B. Foresman, J. V. Ortiz, Q. Cui, A. G. Baboul, S. Clifford, J. Cioslowski, B. B. Stefanov, G. Liu, A. Liashenko, P. Piskorz, I. Komaromi, R. L. Martin, D. J. Fox, T. Keith, M. A. Al-Laham, C. Y. Peng, A. Nanayakkara, M. Challacombe, P. M. W. Gill, B. Johnson, W. Chen, M. W. Wong, C. Gonzalez, J. A. Pople, Gaussian, Inc., Wallingford CT, **2003**.

[24] A. D. Becke, *J. Chem. Phys.* **1993**, *98*, 5648 – 5652.

[25] S. A. Zygmunt, R. M. Mueller, L. A. Curtiss, L. E. Iton, *J. Mol. Struct.* **1998**, *430*, 9 – 16.

[26] D. Lesthaeghe, V. Van Speybroeck, M. Waroquier, *J. Am. Chem. Soc.* **2004**, *126*, 9162 – 9163.

[27] S. Svelle, B. Arstad, S. Kolboe, O. Swang, *J. Phys. Chem. B* **2003**, *107*, 9281 – 9289.

 © 2006 Wiley-VCH Verlag GmbH & Co. KGaA, Weinheim

3.7

The rise and fall of direct mechanisms in methanol-to-olefin catalysis: an overview of theoretical contributions

D. Lesthaeghe, V. Van Speybroeck, G.B. Marin, M. Waroquier
Industrial & Engineering Chemistry Research 46, **2007**, published online.

---

article 3.7

D. Lesthaeghe, V. Van Speybroeck,
G.B. Marin, M. Waroquier

The rise and fall of direct mechanisms in methanol-to-olefin catalysis: an overview of theoretical contributions

Ind. Eng. Chem. Res. 46, **2007**,
published online

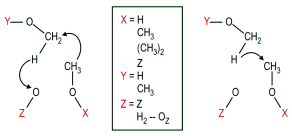

End of an era: Based on the results in [art. 3.6], this review-style article gives a more detailed overview of the theoretical contributions that initially supported the direct mechanism proposal, but which finally culminated in its demise. Special attention is given to the most deep-rooted direct mechanism proposals, namely the oxonium ylide, carbene, and methane-formaldehyde routes.

The Rise and Fall of Direct Mechanisms in Methanol-to-Olefin Catalysis: An Overview of Theoretical Contributions

David Lesthaeghe,*,† Veronique Van Speybroeck,† Guy B. Marin,‡ and Michel Waroquier*,†

Center for Molecular Modeling, Ghent University, Proeftuinstraat 86, B-9000 Gent, Belgium, and Laboratorium voor Petrochemische Techniek, Ghent University, Krijgslaan 281-S5, B-9000 Gent, Belgium

Over the past 30 years, the methanol-to-olefin (MTO) process on acidic zeolites has been subject to a vast number of studies from both industrial and academic researchers, leading to numerous controversies regarding the most probable reaction mechanism. Improvement of computational facilities during the past decade led to a sudden boost of theoretical contributions that, when considered individually, all seemed to provide reasonable evidence for partial pathways of the commonly proposed direct mechanisms. Not only the reactions suggested by experimental studies were investigated, but in addition novel potential routes were discovered by theoreticians as well. However, when all of the individual reactions scattered throughout the literature were recently combined, theoretically obtained rate coefficients turned out to show the exact opposite, that is, the complete failure of the direct mechanisms to produce ethylene from methanol only. In this paper, we give a detailed overview of the theoretical contributions that initially supported the direct mechanism proposal, but which finally culminated in its demise.

Introduction

Light olefins, which are vital components for the petrochemical industry, are traditionally obtained through the refinement of crude oil. However, the rapidly increasing demand for oil-based chemicals calls for the development of new technologies based on alternative natural sources. Among these processes, the zeolite-catalyzed methanol-to-hydrocarbons (MTH) technology[1] is one of the most promising as well as being currently ready for commercial use. MTH conversion starts from methanol, which on its turn can be made from synthesis gas ($CO + H_2$), formed by steam re-forming of natural gas, or even through conversion of any gasifiable carbonaceous material like biomass or waste. Although, in principle, bio-methanol could be used directly as motor fuel, MTH technology allows upgrading of bio-methanol to other fuels and even to chemicals in general.

Scheme 1 shows the catalytic conversion of methanol to a pre-equilibrium mixture containing dimethyl ether (DME) and water. This mixture can then be processed to olefins (methanol-to-olefins: MTO) or even further to high-octane gasoline (methanol-to-gasoline: MTG). Through this technology, methanol provides an excellent feedstock for the entire petrochemical industry: one could make almost anything out of methanol that can currently be made out of crude oil. In this paper, we will focus entirely on the MTO process, which is also assumed to initiate MTG conversion.

Quite remarkably, for more than 30 years the actual mechanism of the conversion of methanol to olefins in acidic zeolites has been the source of considerable debate, fueled by countless different and often conflicting propositions. The trickiest step to elucidate has always been the formation of the first carbon−carbon bond, for which more than 20 distinct mechanisms have been proposed.[1] Speculation mainly centered on mechanisms based on the "direct" formation of small olefins from only methanol, dimethyl ether, and other single-carbon derivates.[2,3] Even though current beliefs are steadily shifting toward alternative "hydrocarbon pool" proposals,[4] the direct mechanisms have received the most widespread attention, both from experiment and from theory.

Scheme 1. Conversion of Natural Gas, Biomass, or Waste to Fuels and Chemicals through the Methanol-to-Olefin Process (Z = Zeolite)

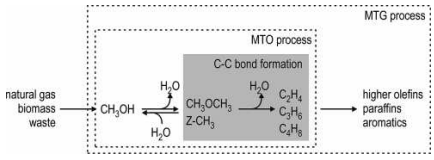

While experimental methods are often impractical for evaluating individual reaction steps, theoretical methods are ideally suited for uncovering the underlying mechanism of the MTO process. Theoretical calculations have experienced a huge boost over the past decade, mainly because of the development of rapid yet highly accurate methods such as density functional theory (DFT), improved parallelization algorithms, and increased computing power. Over the years, not only have many experimentally suggested mechanisms been intensively tested by theoretical calculations, but numerous new routes have sprouted from theoretician's minds as well. In this paper, we aim to give a complete and detailed overview of all of the theoretical contributions that, taken separately, initially supported the direct mechanism concept in MTO chemistry, but when considered in their entirety, also finally led to its downfall. Although still not universally accepted, this failure is in agreement with recent experimental observations.[5]

Until recently, theoretical calculations on the direct mechanisms tended to be fragmentary and severely scattered. Moreover, straightforward comparison was cumbersome due to the wide variety of methods employed. Only a handful of papers suggested and compared multiple direct routes,[2,3] but these were (due to historical reasons) limited to low level of theory

* To whom correspondence should be addressed. Tel.: +32 9 264 65 64 (D.L.), +32 9 264 65 59 (M.W.). Fax: +32 9 264 66 97 (D.L.), +32 9 264 66 97 (M.W.). E-mail: david.lesthaeghe@ugent.be (D.L.), michel.waroquier@ugent.be (M.W.).

† Center for Molecular Modeling.

‡ Laboratorium voor Petrochemische Techniek.

10.1021/ie0613974 CCC: $37.00 © xxxx American Chemical Society
Published on Web 02/20/2007 **PAGE EST: 6.8**

B

calculations on extremely small 1T/3T zeolite clusters, and they formed a nowhere near to complete survey. Furthermore, the focus was always solely on theoretical reaction barriers, rather than reaction rate coefficients, which combine both thermodynamic and entropic contributions. While the mere existence of individual direct reactions demonstrated in many theoretical papers was always considered strong evidence for the direct mechanism proposal, there was never a theoretical guarantee that the direct mechanisms came together to form a complete route that actually proceeds under reaction conditions.

To resolve this complex issue, we proposed an extensive reaction scheme (Scheme 2) in a recent communication,[6] tying together a large variety of possible direct reactions and even including several previously overlooked, parallel pathways. On the basis of not only reaction barriers at 0 K but also rate coefficients at 720 K (obtained from classical transition state theory) at the 5T level, we were able to deduce which stable intermediates are formed directly, and where bottlenecks in the direct mechanism proposal lie. In this paper, we will focus on the most deep-rooted direct mechanism proposals, the onium ylide, carbene, and methane-formaldehyde routes.

Computational Details

Zeolites are bulky materials and contain an enormous number of atoms, which impedes the search for methods that adequately describe these complex systems. New force fields for zeolites are constantly developed, allowing rapid optimization of almost any zeolite framework structure. However, these force fields are useless when describing bond breaking and bond formation. Classical force fields are thus incapable of modeling chemical reactions, and a quantum-mechanically (QM) based treatment of the electronic many-body problem is essential. Because of the enormous computational cost of current QM methods, especially for extended systems like zeolites, this has led to new developments in computational chemistry, which all attempt to provide an excellent description of chemical reactivity at a reasonable computational cost. In this paragraph, we will give a brief overview of three such methods that have been commonly applied in zeolite chemistry and the MTO process in particular.

The cluster technique is the simplest and most widespread method used to model reactions in zeolites. In this approach, the chemically active part is just cut from the zeolite framework. As this involves the breaking of several silicon−oxygen bonds, this cluster would be chemically unstable, were it not for additional hydrogen atoms placed to saturate the dangling bonds. Figure 1a shows both a silicon-free 1T cluster with H-termination on the oxygen atoms and a larger 5T cluster with H termination on the silicon atoms. For zeolites containing ring structures like CHA, a ring-shaped cluster is often used. The main advantage of this method is the limited amount of atoms that are taken into account. This permits the use of highly accurate levels of theory within reasonable time. On the other hand, it is clear that the cluster method does not guarantee a complete description of the system, especially not when zeolite framework effects play a crucial role on reaction kinetics. In a previous paper, we compared small cluster results to more advanced techniques and found that even in the small cluster approach energy barriers are generally well reproduced. Only for a very limited number of reactions where charged intermediates are formed is a larger model required to obtain correct reaction barriers.[7]

Ideally, the zeolite cluster would be extended until all necessary framework effects are taken into account. For these clusters that are consequently too large to be fully described at a high QM level, a "divide and conquer" strategy provides optimal results: the relatively small acid site and guest-molecules are treated at the necessary high QM level (high-level or HL region), while the larger surrounding framework (which does not actively participate in the reaction) can be described at a computationally much faster low QM level or even a force-field (low-level or LL region). This separation of the system is demonstrated on a 46T cluster (a HL 5 T-cluster and a LL 41 T-cluster) cut from H-ZSM5 in Figure 1b.[7,8] The ONIOM method as currently implemented in the Gaussian software package[9] is an example of a hybrid HL/LL method.

Finally, fully periodic QM software codes would seem to provide the most natural description of a zeolite system. However, the industrially most important zeolites are often built from rather large unit cells: for example, the unit cell of ZSM-5 contains no less than 288 atoms. The corresponding computational cost is too high for practical purposes, which is the main reason why periodic calculations on zeolites are currently still limited to systems with very small unit cells like CHA, as illustrated in Figure 1c, and will not be considered in this paper.

All calculated numerical values reported in this paper were obtained through density functional theory (DFT) calculations with the B3LYP functional within the Gaussian 03 software package.[9] Initial calculations were performed on frequently used pentatetrahedral (5T) clusters (Figure 1a). For certain key reaction steps where charged intermediates are formed, this approach was extended to a 5T high-level B3LYP cluster embedded in a 41T low-level QM cluster at the HF//MNDO level[7,8] using the ONIOM approach to include the bulk electrostatic effects induced by the zeolite framework. This 46T model (illustrated in Figure 1b), which was cut from the MFI crystallographic structure, is considered to be large enough to cover all important framework effects on both the active site and the adsorbate.

Results and Discussion

Our results confirm the well-documented first step, which is the development of a pre-equilibrium, as well as several other C1-species. Our work identifies, however, three bottlenecks, which prevent direct carbon−carbon coupling of these C1 species to C2-species.

Pre-equilibrium Phase. As shown in Scheme 1, the conversion of methanol is known to start with rapid dehydration to DME. This step proceeds either via an intermediate methoxide species Z-CH_3 and methanol or through co-reaction of a methanol dimer, as presented in the top left corner of Scheme 2. Single molecular dehydration of methanol is prohibited, but a two-step pathway is facilitated by methanol or water successively lowering reaction barriers, not as spectator or solvating molecules, but rather as "assisting molecules", allowing for more favorable transition-state geometries. This first pre-equilibrium phase in the MTO-process has been extremely well-documented from a theoretical viewpoint, ranging from very small, yet pioneering cluster calculations by Zicovich-Wilson et al.,[10] Sinclair et al.,[11] and Blaszkowski et al.[12] to more recent fully periodic DFT calculations by Payne and co-workers.[13−15] All studies revealed similar mechanisms independent of the method used, and this pre-equilibrium phase is currently very well understood. From our calculated rate coefficients using the 5T approach in Table 1, it is clear that especially the steps with assisting molecules have higher rate coefficients and both dimethyl ether and framework-bound methoxide groups will be formed. This is in perfect accordance with the experimental

C

Scheme 2. Combined Overview of All Direct Reactions, Starting from Methanol (Top Row) and Leading to the Formation of Ethylene (Bottom Row)[a]

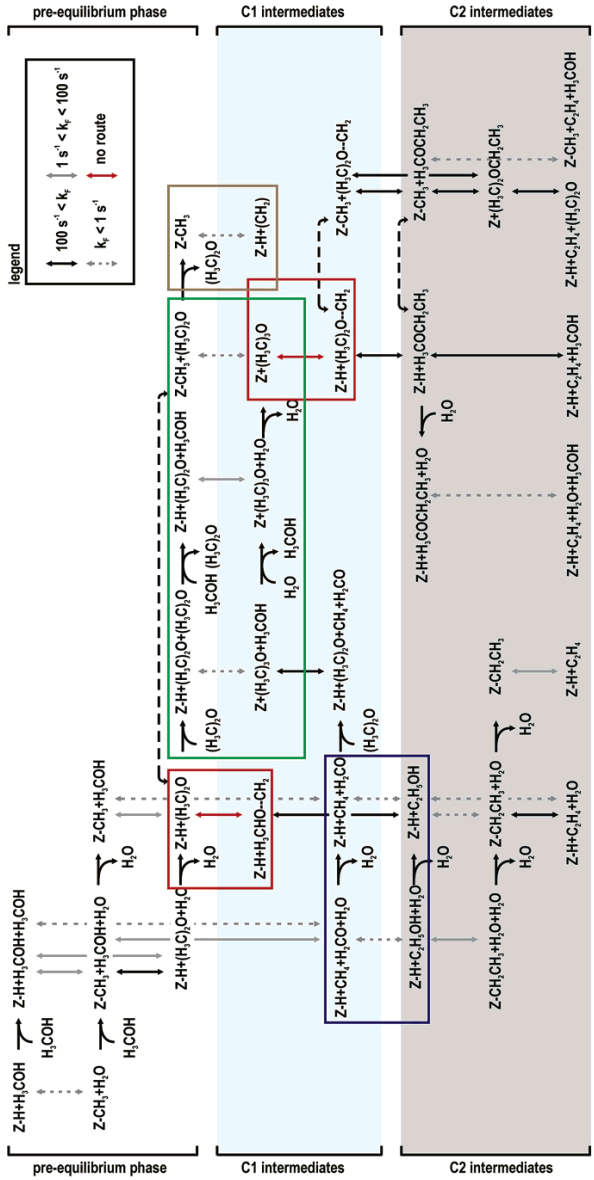

[a] Horizontal movement corresponds to the adsorption or desorption of a reactive molecule, while vertical arrows represent elementary reaction steps. The elementary reactions are divided into four categories based on the values of forward rate coefficients at 720 K (adapted from ref 6).

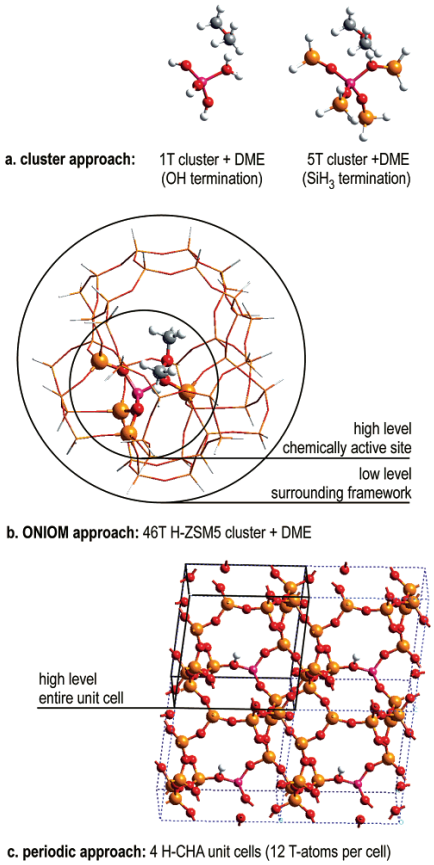

Figure 1. Various methodologies for theoretical calculations on zeolite systems.

observation of this pre-equilibrium preceding the olefin formation. This pre-equilibrium, however, does not yet provide the crucial and highly sought-after carbon−carbon bond.

Formation of the Trimethyl Oxonium Ion. From the initial mixture, a direct formation of the trimethyl oxonium ion (TMO) has been proposed through nucleophilic attack by adsorbed DME on a framework-bound methoxide species or through co-reaction of DME and methanol. These steps were respectively studied on 3T clusters by Tajima et al.[3] and 1T clusters by Blaszkowski et al.[2] Alternatively, TMO could also be formed through co-reaction of two DME molecules. All routes to TMO are situated in the green rectangle in Scheme 2 and are illustrated in more detail in Scheme 3. Because of the extremely low reverse reaction barriers (green rectangles in Table 1) observed in our 5T cluster calculations, one would at first glance expect TMO to be an exceptionally short-living intermediate. However, positively charged TMO forms an ion-pair with the negative aluminum defect and therefore cannot be adequately described

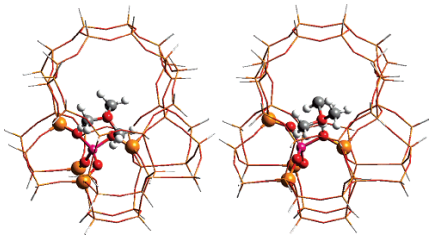

Figure 2. Trimethyl oxonium ion (TMO) and dimethyl oxonium methylide (DOMY) formed in H-ZSM-5 cage (46T cluster).

Scheme 3. Different Routes to Trimethyl Oxonium Ion (TMO) Formation from the Pre-equilibrium Mixture (Green Rectangle in Scheme 2)

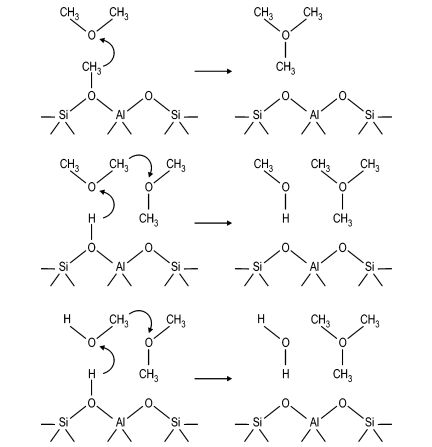

in the small cluster approach. Furthermore, our previous ONIOM calculations on larger 46T clusters demonstrated that TMO is additionally stabilized by the zeolite framework,[7] a result similar to that obtained through periodic calculations by Shah et al. in the chabazite topology.[16] In their periodic calculations, however, Shah et al. did not calculate any reaction barriers for the formation of TMO. To resolve this issue, we performed advanced calculations using the ONIOM technique, providing lower barriers. Adjusted energies (in kJ/mol) for all stationary points are shown in Table 2. Two parallel routes with a barrier below 100 kJ/mol provide theoretical evidence for TMO remaining an important product formed directly from the equilibrium mixture.

First Bottleneck: Ylide and Carbene Intermediates. The main difficulties arise, however, once TMO is effectively formed, and oxonium ylides (a carbene group coordinated to methanol or DME) are the next suggested intermediates (red rectangles in Scheme 2). For instance, once TMO is successfully formed, it might be deprotonated by an adjacent basic site to form dimethyl oxonium methylide (DOMY),[7] as shown in Figure 2. The next step (forming the desired carbon−carbon bond) could be an intramolecular Stevens' rearrangement to methylethyl ether (MEE), or an intermolecular methylation, forming the ethyldimethyl oxonium ion (EDMO), as shown in

E

Table 1. Kinetic Parameters of Both Forward and Reverse Reactions, Calculated in Reference 6 at the B3LYP/6-31g(d) Level on 5T Zeolite Clusters[a]

reactants	products	forward E_a (kJ/mol) 670-770K	forward A (1/s) 670-770K	forward k (1/s) 720K	reverse E_a (kJ/mol) 670-770K	reverse A (1/s) 670-770K	reverse k (1/s) 720K	other ref.
Z-H+H_2COH	Z-CH_3+H_2O	223.6	3.44E+12	2.1E-04	176.2	1.50E+12	2.5E-01	10-12
Z-H+H_2COH+H_2COH	Z-CH_3+H_2COH+H_2O	142.3	9.87E+11	4.7E+01	95.7	1.29E+12	1.5E+05	11-12
Z-CH_3+H_2COH+H_2O	Z-H+$(H_2C)_2O$+H_2O	84.8	1.14E+11	8.1E+04	155.0	4.64E+10	2.7E-01	12
Z-H+H_2COH+H_2COH	Z-H+$(H_2C)_2O$+H_2O	129.7	1.27E+10	5.0E+00	153.4	6.77E+09	5.1E-02	12-15
Z-CH_3+H_2COH+H_2O	Z-H+CH_4+H_2CO+H_2O	146.8	1.79E+11	4.0E+00	185.1	1.10E+06	4.1E-08	-
Z-H+CH_4+H_2CO+H_2O	Z-H+C_2H_5OH+H_2O	173.7	4.84E+05	1.2E-07	231.5	2.93E+10	4.7E-07	19-20
Z-H+C_2H_5OH+H_2O	Z-CH_3-CH_3+H_2O+H_2O	147.2	1.05E+11	2.2E+00	93.1	2.08E+12	3.7E+05	2
Z-H+H_3COH+H_3COH	Z-H+CH_4+H_2CO+H_2O	196.4	1.24E+11	6.9E-04	188.1	9.86E+05	2.2E-08	19-20
Z-CH_3+H_2COH	Z-H+$(H_2C)_2O$	141.0	6.99E+11	4.1E+01	187.6	3.65E+10	8.9E-04	12
Z-H+H_2CHO--CH_3	Z-H+C_2H_5OH	129.3	9.93E+13	4.1E+04	545.2	1.12E+14	3.2E-26	7
Z-CH_3+H_2COH	Z-H+CH_4+H_2CO	189.9	4.31E+11	7.2E-03	221.6	3.15E+06	2.6E-10	2-3
Z-H+CH_4+H_2CO	Z-H+C_2H_5OH	172.6	5.81E+06	1.7E-06	233.4	1.33E+12	1.6E-05	3
Z-H+C_2H_5OH	Z-CH_3-CH_3+H_2O	198.0	6.84E+12	3.0E-02	148.5	7.95E+13	1.3E+03	2
Z-CH_3-CH_3+H_2O	Z-H+C_2H_4+H_2O	139.4	2.46E+12	1.9E+02	83.5	5.27E+08	4.6E+02	2
Z-H+C_2H_5OH	Z-H+C_2H_4+H_2O	193.2	7.94E+13	7.7E-01	87.8	1.98E+11	8.5E+04	2-3
Z-H+$(H_2C)_2O$	Z-H+H_2CHO--CH_3	-	-	0.0E+00	-	-	0.0E+00	7
Z-CH_3-CH_3	Z-H+C_2H_4	153.0	3.83E+12	3.0E+01	89.4	2.89E+09	9.4E+02	2
Z-H+$(H_2C)_2O$+$(H_2C)_2O$	Z+$(H_2C)_2O$+H_2COH	135.7	6.81E+09	9.7E-01	28.2	4.42E+10	4.0E+08	-
Z+$(H_2C)_2O$+H_2COH	Z-H+$(H_2C)_2O$+CH_4+H_2CO	105.7	1.83E+11	3.9E+03	208.4	1.66E+05	1.3E-10	-
Z-H+$(H_2C)_2O$+H_2COH	Z+$(H_2C)_2O$+H_2O	147.3	5.70E+11	1.2E+01	12.7	4.35E+11	5.2E+10	2
Z-CH_3+$(H_2C)_2O$	Z+$(H_2C)_2O$	120.5	2.98E+08	5.4E-01	52.9	2.29E+14	3.3E+10	2-3
Z-H+$(H_2C)_2O$--CH_3	Z-H+$H_2COCH_2CH_3$	117.9	5.31E+13	1.5E+05	470.5	2.24E+11	1.6E-23	7
Z-H+$H_2COCH_2CH_3$	Z-H+C_2H_4+H_2COH	113.8	4.53E+10	2.5E+02	80.8	5.77E+10	8.0E+04	-
Z+$(H_2C)_2O$	Z-H+$(H_2C)_2O$--CH_3	-	-	0.0E+00	-	-	0.0E+00	3,7
Z-H+$H_2COCH_2CH_3$+H_2O	Z-H+C_2H_4+H_2O+H_2COH	159.2	2.25E+11	6.4E-01	115.2	6.32E+08	2.8E+00	2
Z-CH_3+$(H_2C)_2O$--CH_3	Z-CH_3+$H_2COCH_2CH_3$	130.4	1.02E+14	3.5E+04	521.3	1.02E+14	1.5E-24	-
Z-CH_3+$H_2COCH_2CH_3$	Z+$(H_2C)_2OCH_2CH_3$	127.6	5.62E+11	3.1E+02	49.7	4.67E+15	1.2E+12	-
Z-CH_3+$(H_2C)_2O$--CH_3	Z+$(H_2C)_2OCH_2CH_3$	18.9	1.56E+12	6.6E+10	331.9	1.30E+16	1.1E-08	7
Z+$(H_2C)_2OCH_2CH_3$	Z-H+C_2H_4+$(H_2C)_2O$	84.7	2.55E+14	1.8E+08	127.1	1.62E+07	9.6E-03	-
Z-CH_3+$H_2COCH_2CH_3$	Z-CH_3+C_2H_4+H_2COH	281.2	9.17E+11	3.6E-09	193.1	1.46E+10	1.4E-04	-
Z-CH_3	Z-H+(CH_2)	244.8	3.08E+11	5.3E-07	51.9	3.16E+12	5.5E+08	17

[a] References to other theoretical papers covering each specific reaction barrier (but not the corresponding rate coefficient) are given in the right-hand column. Colored rectangles highlight the crucial reactions from Scheme 2.

Table 2. Energies of Stationary Points (in kJ/mol) for the Formation of TMO in a 46T H-ZSM5 Model at the B3LYP/6-31+g(d,p):HF/6-31+g(d,p)//B3LYP/6-31+g(d,p):MNDO Level

trimethyl oxonium ion (TMO) formation	
Z-CH_3 + DME	0.0
transition state	96.6
Z^- + TMO^+	27.7
Z−H + DME + DME	0.0
transition state	132.3
Z^- + TMO^+ + CH_3OH	22.0
Z−H + DME + CH_3OH	0.0
transition state	94.0
Z^- + TMO^+ + H_2O	31.6

Scheme 4. The ethyldimethyl oxonium ion readily undergoes β-elimination, forming ethylene and dimethylether. From MEE, there exist several alternative pathways leading directly to ethylene. However, our previous work using the ONIOM method on large 46T clusters has shown that there is no possible route from TMO to DOMY.[7] Moreover, even though the zeolite framework offers supplementary stabilization for TMO, this does not hold for the ylide, which results in DOMY being a highly energetic species.

Methyl oxonium methylide (MOMY) is also a possible candidate. Adsorbed dimethyl ether could form a dimethyl oxonium ion (DMO), after which it would be deprotonated to MOMY. A Stevens-type rearrangement would lead to ethanol, forming the required carbon−carbon bond. Yet again, we have found this step to be nonexistent and MOMY to be highly unstable.[7] Generally speaking, we find the oxygen bridge to be

Scheme 4. Possible Routes from DME to Ylides and Subsequent Carbon−Carbon Coupling. (Adapted from Reference 7)

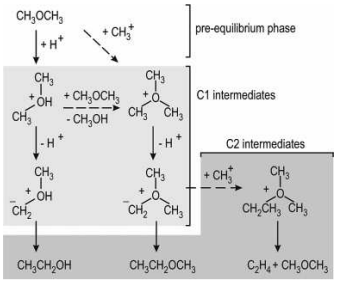

F

Scheme 5. Formation of a Framework-Bound Carbene

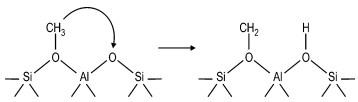

Scheme 6. Formation of Ethanol from Methane and Formaldehyde

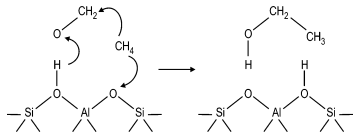

insufficiently basic to form the desired ylides. Alternative pathways based on oxonium ylides are also highly improbable due to the high instability of these species. This consequently rules out the role of MEE as a crucial intermediate as well as the pathway through EDMO.

An altogether different type of carbene, which is incorporated into the framework, can be formed by deprotonation of a framework-bound methyl group, as shown by the brown rectangle in Scheme 2 and schematically depicted in Scheme 5. Sinclair and Catlow investigated this step and found a relatively unstable carbene and an extremely high reaction barrier.[17] Our rate coefficients for the formation of this framework-coordinated carbene are extremely low (brown rectangle in Table 1), corresponding with the high reaction barrier of this step.

The severe instability and the corresponding nonexistence of not only the ylides but also the framework-coordinated carbene form the first main bottleneck for the direct approach in MTO chemistry. Based on these theoretical results, an experimental H/D exchange study has just recently confirmed the nonexistence of these exotic species.[18]

Second Bottleneck: Methane/Formaldehyde Route. Alternatively, there are multiple potential routes to methane and formaldehyde, starting from two methanol molecules, from a surface methoxy species and methanol, or from TMO jointly adsorbed with methanol. The methane/formaldehyde route has been widely hailed as a possible MTO route, not only in small cluster calculations by Tajima et al.,[3] but also in molecular dynamics simulations by Lo et al.[19,20] Once formed, however, only extremely slow reactions lead to the formation of ethanol (blue rectangle in Scheme 2, detailed reaction in Scheme 6). From ethanol, ethylene could quite rapidly be formed, the fastest route running along a framework-bound ethoxide species and subsequent ethylene production. Nevertheless, even though methane and formaldehyde will undoubtedly be formed, the conversion of this mixture to ethanol proceeds too slowly to be considered viable. As is clear from the blue rectangles in Table 1, the rate coefficient for this step in particular is not mainly determined by the activation energy E_a, but more so by the very small pre-exponential factor A, reflecting the major decrease in entropy which accompanies this reaction. The failure of methane and formaldehyde to easily convert to a C2 species forms the second main bottleneck in the direct mechanism proposal.

Third Bottleneck: Extremely High Barrier for Concerted C−C Coupling. So as to not overcrowd Scheme 2, conversions showing both forward and reverse barriers larger than 200 kJ/mol (which would not proceed in either direction) are not shown in Scheme 2. However, a closer investigation of the omitted reaction steps reveals crucial information on the failure of these steps. As they all follow a similar concerted reaction mechanism, we show a general model in Scheme 7 (left diagram) representing the steps that had too high-energy barriers to be incorporated: a hydrogen abstraction from a methanol/DME methyl group by a zeolite basic oxygen bridge (possibly assisted by a water vehicle molecule) combined with the formation of a carbon−carbon bond with a methanol/DME/TMO/framework-bound methyl group.[6] Many of these concerted steps were first studied in the pioneering 1T cluster study by Blaszkowski et al.,[2] who even then already observed exceptionally high reaction barriers. The unprotonated oxygen bridge lacks the strong basic character needed to activate the highly covalent carbon−hydrogen bond. An equally strong carbon−hydrogen bond is preferably formed, which is why any perturbation of the transition state leads the system to automatically evolve to a nearby transition state, forming methane instead (right diagram in Scheme 7). This outspoken formation of methane is quite similar to what was observed in the molecular dynamics simulations by Lo et al.[19,20] As previously mentioned, though, the mixture of methane and formaldehyde does not succeed in supplying the first carbon−carbon bond. Thus, these prohibited concerted reactions form the third and final bottleneck of the direct mechanism proposal.

Scheme 7. Prohibited Reactions Corresponding to Concerted Carbon−Carbon Coupling and Carbon−Hydrogen Bond Activation by Zeolite Basic Oxygen O_Z (Left Diagram)[a]

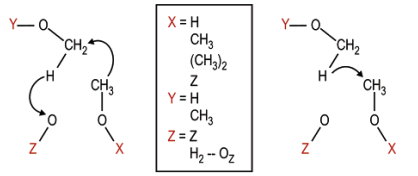

[a] Protonation of the methyl group forming methane (right diagram) will proceed far more rapidly (adapted from ref 6).

Conclusions

We have worked toward the theoretical identification and clarification of all direct mechanisms behind the methanol-to-olefin process by not only giving an overview of the many individual reactions suggested in the literature, but by also calculating and recombining every single step in each pathway to allow for an overall picture and for direct comparison between the individual steps. This has allowed for the crucial reaction steps to be identified, and more advanced calculations using an embedding technique have been performed when necessary.

As long as reaction barriers for partial pathways remained scattered over the literature, it seemed that there were multiple possibilities for direct conversion of methanol to ethylene. However, the combination of these results in complete pathways and calculation of rate coefficients as well as just barrier heights shows that no complete direct pathway from methanol leading all of the way to ethylene (or to any C2 intermediate) exists. Three critical points can be clearly recognized: first, the instability of the ylide or carbene intermediates, second, the low conversion rates of methane and formaldehyde to ethanol, and, third, the concerted carbon−carbon coupling reactions, which convert to the formation of methane and formaldehyde instead.

Hopefully, this theoretical conclusion ends some of the existing controversy surrounding the direct mechanisms. Al-

ternatives to the direct mechanism concept, like the "hydrocarbon pool" proposal, should be based on reactions and intermediates that somehow bypass the earlier-mentioned bottlenecks. As this alternative proposal is based on bulky and charged intermediates, topology effects will play a crucial role in reaction kinetics, and the small cluster approach will not be sufficient in its description.[21,22]

As the methanol-to-olefin process is a key step in the switch from fossil fuels to green chemistry,[23] additional insights into the mechanism to control product distribution would be highly desirable, yet only achievable through strong interaction between experimental and theoretical research.

Acknowledgment

This work is supported by the Fund for Scientific Research − Flanders (FWO) and the Research Board of Ghent University.

Literature Cited

(1) Stocker, M. Methanol-to-hydrocarbons: catalytic materials and their behavior. *Microporous Mesoporous Mater.* **1999**, *29*, 3−48.

(2) Blaszkowski, S. R.; van Santen, R. A. Theoretical study of C-C bond formation in the methanol-to-gasoline process. *J. Am. Chem. Soc.* **1997**, *119*, 5020−5027.

(3) Tajima, N.; Tsuneda, T.; Toyama, F.; Hirao, K. A new mechanism for the first carbon-carbon bond formation in the MTG process: A theoretical study. *J. Am. Chem. Soc.* **1998**, *120*, 8222−8229.

(4) Dahl, I. M.; Kolboe, S. On the reaction-mechanism for hydrocarbon formation from methanol over Sapo-34. 1. Isotopic labeling studies of the co-reaction of ethene and methanol. *J. Catal.* **1994**, *149*, 458−464.

(5) Song, W. G.; Marcus, D. M.; Fu, H.; Ehresmann, J. O.; Haw, J. F. An oft-studied reaction that may never have been: Direct catalytic conversion of methanol or dimethyl ether to hydrocarbons on the solid acids HZSM-5 or HSAPO-34. *J. Am. Chem. Soc.* **2002**, *124*, 3844−3845.

(6) Lesthaeghe, D.; Van Speybroeck, V.; Marin, G. B.; Waroquier, M. Understanding the failure of direct C-C coupling in the zeolite-catalyzed methanol-to-olefin process. *Angew. Chem.* **2006**, *118*, 1746−1751; *Angew. Chem., Int. Ed.* **2006**, *45*, 1714−1719.

(7) Lesthaeghe, D.; Van Speybroeck, V.; Marin, G. B.; Waroquier, M. What role do oxonium ions and oxonium ylides play in the ZSM-5 catalysed methanol-to-olefin process? *Chem. Phys. Lett.* **2006**, *417*, 309−315.

(8) Lesthaeghe, D.; Delcour, G.; Van Speybroeck, V.; Marin, G. B.; Waroquier, M. Theoretical study on the alteration of fundamental zeolite properties by methylene functionalization. *Microporous Mesoporous Mater.* **2006**, *96*, 350−356.

(9) Frisch, M. J.; Trucks, G. W.; Schlegel, H. B.; Scuseria, G. E.; Robb, M. A.; Cheeseman, J. R.; Montgomery, J. A., Jr.; Vreven, T.; Kudin, K. N.; Burant, J. C.; Millam, J. M.; Iyengar, S. S.; Tomasi, J.; Barone, V.; Mennucci, B.; Cossi, M.; Scalmani, G.; Rega, N.; Petersson, G. A.; Nakatsuji, H.; Hada, M.; Ehara, M.; Toyota, K.; Fukuda, R.; Hasegawa, J.; Ishida, M.; Nakajima, T.; Honda, Y.; Kitao, O.; Nakai, H.; Klene, M.; Li, X.; Knox, J. E.; Hratchian, H. P.; Cross, J. B.; Bakken, V.; Adamo, C.; Jaramillo, J.; Gomperts, R.; Stratmann, R. E.; Yazyev, O.; Austin, A. J.; Cammi, R.; Pomelli, C.; Ochterski, J. W.; Ayala, P. Y.; Morokuma, K.; Voth, G. A.; Salvador, P.; Dannenberg, J. J.; Zakrzewski, V. G.; Dapprich, S.; Daniels, A. D.; Strain, M. C.; Farkas, O.; Malick, D. K.; Rabuck, A. D.; Raghavachari, K.; Foresman, J. B.; Ortiz, J. V.; Cui, Q.; Baboul, A. G.; Clifford, S.; Cioslowski, J.; Stefanov, B. B.; Liu, G.; Liashenko, A.; Piskorz, P.; Komaromi, I.; Martin, R. L.; Fox, D. J.; Keith, T.; Al-Laham, M. A.; Peng, C. Y.; Nanayakkara, A.; Challacombe, M.; Gill, P. M. W.; Johnson, B.; Chen, W.; Wong, M. W.; Gonzalez, C.; Pople, J. A. *Gaussian 03*, revision B.03; Gaussian, Inc.: Wallingford, CT, 2003.

(10) Zicovich-Wilson, C. M.; Viruela, P.; Corma, A. Formation of surface methoxy groups on H-zeolites from methanol - a quantum-chemical study. *J. Phys. Chem.* **1995**, *99*, 13224−13231.

(11) Sinclair, P. E.; Catlow, C. R. A. Density functional theory calculations of adsorption and reactivity of methanol at alumino-silicate Bronsted acid centres. *J. Chem. Soc., Faraday Trans.* **1997**, *93*, 333−345.

(12) Blaszkowski, S. R.; van Santen, R. A. Theoretical study of the mechanism of surface methoxy and dimethyl ether formation from methanol catalyzed by zeolitic protons. *J. Phys. Chem. B* **1997**, *101*, 2292−2305.

(13) Sandré, E.; Payne, M. C.; Gale, J. D. First principles location of the transition state for formation of dimethyl ether in a zeolite. *Chem. Commun.* **1998**, 2445−2446.

(14) Payne, M. C.; Hytha, M.; Stich, I.; Gale, J. D.; Terakura, K. First principles calculation of the free energy barrier for the reaction of methanol in a zeolite catalyst. *Microporous Mesoporous Mater.* **2001**, *48*, 375−381.

(15) Hytha, M.; Stich, I.; Gale, J. D.; Terakura, K.; Payne, M. C. Thermodynamics of catalytic formation of dimethyl ether from methanol in acidic zeolites. *Chem.-Eur. J.* **2001**, *7*, 2521−2527.

(16) Shah, R.; Gale, J. D.; Payne, M. C. In situ study of reactive intermediates of methanol in zeolites from first principles calculations. *J. Phys. Chem. B* **1997**, *101*, 4787−4797.

(17) Sinclair, P. E.; Catlow, C. R. A. Generation of carbenes during methanol conversion over Bronsted acidic aluminosilicates. A computational study. *J. Phys. Chem. B* **1997**, *101*, 295−298.

(18) Marcus, D. M.; McLachlan, K. A.; Wildman, M. A.; Ehresmann, J. O.; Kletnieks, P. W.; Haw, J. F. Experimental evidence from H/D exchange studies for the failure of direct C-C coupling mechanisms in the methanol-to-olefin process catalyzed by HSAPO-34. *Angew. Chem.* **2006**, *118*, 3205−3208; *Angew. Chem., Int. Ed.* **2006**, *45*, 3133−3136.

(19) Lo, C.; Giurumescu, C. A.; Radhakrishnan, R.; Trout, B. L. Methanol coupling in the zeolite chabazite studied via Car-Parrinello molecular dynamics. *Mol. Phys.* **2004**, *102*, 281−288.

(20) Lo, C. S.; Radhakrishnan, R.; Trout, B. L. Application of transition path sampling methods in catalysis: A new mechanism for C-C bond formation in the methanol coupling reaction in chabazite. *Catal. Today* **2005**, *105*, 93−105.

(21) Svelle, S.; Joensen, F.; Nerlov, J.; Olsbye, U.; Lillerud, K.-P.; Kolboe, S.; Bjorgen, M. Conversion of methanol into hydrocarbons over zeolite H-ZSM-5: Ethene formation is mechanistically separated from the formation of higher alkenes. *J. Am. Chem. Soc.* **2006**, *128*, 14770−14771.

(22) Lesthaeghe, D.; De Sterck, B.; Van Speybroeck, V.; Marin, G. B.; Waroquier, M. Zeolite shape-selectivity in the *gem*-methylation of aromatic hydrocarbons. *Angew. Chem.* **2007**, *119*, 1333−1336; *Angew. Chem., Int. Ed.* **2007**, *46*, 1311−1314.

(23) Okkerse, C.; van Bekkum, H. From fossil to green. *Green Chem.* **1999**, *1*, 107−114.

Received for review October 31, 2006
Revised manuscript received December 22, 2006
Accepted January 9, 2007

IE0613974

3.8

Zeolite shape selectivity in the *gem*-methylation of aromatic hydrocarbons

D. Lesthaeghe, B. De Sterck, V. Van Speybroeck, G.B. Marin, M. Waroquier
Angewandte Chemie - International Edition 46, **2007**, 1311-1314.

Must fit like a glove: The initiating step for olefin formation from methanol in zeolites is strongly dependent on specific combinations of organic hydrocarbon pool species and zeolite topology. If the cages are too large, neutral species are favored over reactive cations. If the cage is too small, transition state shape selectivity poses severe limitations on the reactivity of bulkier species.

article 3.8

D. Lesthaeghe, B. De Sterck,
V. Van Speybroeck, G.B. Marin,
M. Waroquier

Zeolite shape selectivity in the gem-methylation of aromatic hydrocarbons

Angew. Chem. Int. Ed. 46, **2007**, 1311-1314

DOI: 10.1002/anie.200604309

Arene Methylation

Zeolite Shape-Selectivity in the *gem*-Methylation of Aromatic Hydrocarbons**

David Lesthaeghe, Bart De Sterck, Veronique Van Speybroeck, Guy B. Marin, and Michel Waroquier**

Herein, we explicitly demonstrate the importance of transition-state-shape selectivity for the conversion of methanol to light olefins (methanol-to-olefins or MTO). The MTO process in acidic zeolites is a prominent research topic, driven both by the possibility of monetizing stranded natural gas reserves, coal, or even biomass and by the ever-increasing demands for ethene derivatives.[1] For the last 30 years, the actual reaction mechanism of this process has been a topic of considerable debate, fueled by countless and often conflicting propositions.[1,2] Most efforts centered on mechanisms proposing "direct" formation of ethene from only methanol and C_1 derivates. Recently, however, experimental studies by Haw and co-workers[3,4] as well as our own theoretical results[5] provided strong evidence for the complete failure of the direct routes.

The most likely alternative, which is more in accordance with experimental observations,[6] is given by the "hydrocarbon-pool" (HP) proposal,[7,8] in which organic species trapped in the zeolite pores undergo repeated methylation followed by olefin elimination. To date, the elementary steps governing this process are not well understood. Ideally, experimental and theoretical efforts should complement each other in unraveling this complex network of reactions. A hydrocarbon pool consisting mainly of polymethylbenzenes has been shown to be active for olefin formation,[9,10] independent of the zeotype catalyst chosen.[11] Additionally, there is strong experimental evidence for cyclic resonance-stabilized cations as persistent species in the pores, such as cyclopentenyl and pentamethylbenzenium cations in HZSM-5[12,13] and hexamethylbenzenium and heptamethylbenzenium ($7MB^+$) cations in HBEA.[14,15] Geminal methylbenzenium ions form the main starting point from which commonly proposed HP routes (such as the "paring" and "side-chain" mechanisms) originate.[16] The heptamethylbenzenium cation, for example, is formed from hexamethylbenzene (HMB) through one-step geminal methylation by methanol as shown in Scheme 1.

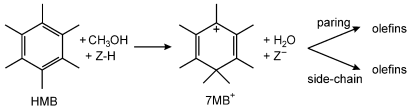

Scheme 1. Initiating step for the formation of olefins from hexamethylbenzene (HMB). Z = zeolite.

The product distribution is defined by the number of methyl groups on the active hydrocarbon-pool species: propene is favored by methylbenzenes with four to six methyl groups, while ethene is predominantly formed from the lower methylbenzenes.[17] As the hydrocarbon-pool mechanism involves bulky cyclic intermediates, it is also a space-demanding process. Therefore, zeolite topology is crucial in defining the hydrocarbon pool, resulting in a strong topological dependence of product distribution as well. The active catalyst is a combined organic–inorganic supramolecular complex of the zeolite framework and the hydrocarbon pool.[2]

Just recently, Cui et al. have reported experimental evidence for transition-state-shape selectivity in studies of methanol-to-olefin conversion on zeolites with varying pore size.[18] Experimental claims to transition-state-shape selectivity are, ideally, verified by theoretical methods,[19–21] since these are more suited for elucidating the extent to which the local shape of the pore influences local reaction rates. To the best of our knowledge, ours is the first theoretical study on the hydrocarbon-pool proposal to take topological concepts explicitly into account, by focusing on both the electrostatic stabilization and geometrical constraints of typical zeolite frameworks on key carbenium ions and transition states.

To separate the effects of hydrocarbon-pool species and zeolite topology, the geminal methylation of several methylbenzenes, ranging from toluene, over *p*-xylene, 1,2,4-trimethylbenzene (pseudocumene), 1,2,4,5-tetramethylbenzene (durene), and pentamethylbenzene (PMB) to hexamethylbenzene (HMB), was first modeled on 5T clusters. These small clusters represent any aluminosilicate and neglect all framework steric and electrostatic effects. Figure 1a shows the energy barriers and reaction energies for the methylation

[*] Ir. D. Lesthaeghe, Ir. B. De Sterck, Dr. Ir. V. Van Speybroeck, Prof. Dr. M. Waroquier
Center for Molecular Modeling
Ghent University
Proeftuinstraat 86, 9000 Gent (Belgium)
Fax: (+32) 9-264-6697
E-mail: david.lesthaeghe@ugent.be
michel.waroquier@ugent.be
Homepage: http://molmod.ugent.be
Prof. Dr. Ir. G. B. Marin
Laboratorium voor Petrochemische Techniek
Ghent University
Krijgslaan 281-S5, 9000 Gent (Belgium)

[**] This work is supported by the Fund for Scientific Research—Flanders (FWO) and the Research Board of Ghent University.

Supporting information for this article is available on the WWW under http://www.angewandte.org or from the author.

 © 2007 Wiley-VCH Verlag GmbH & Co. KGaA, Weinheim

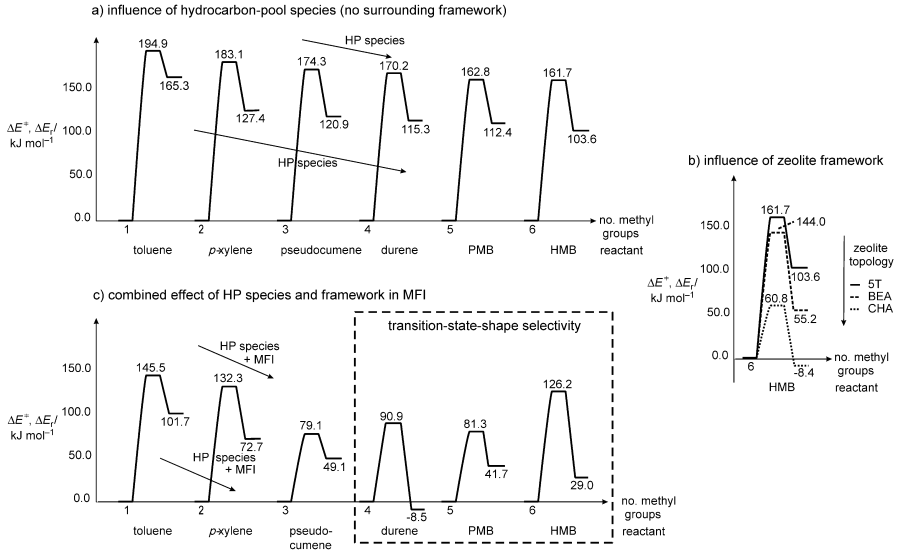

Figure 1. Barrier heights ΔE^{+} and reaction energies ΔE_r in kJ mol^{-1} for a) geminal methylation of different polymethylbenzenes in the 5T cluster, b) geminal methylation of hexamethylbenzene in the zeolite topologies BEA and CHA, and c) geminal methylation of different polymethylbenzenes in the space-limiting MFI structure.

of a series of polymethylbenzenes in the 5T cluster. A steady decrease in both the reaction barrier ΔE^{+} (from 194.9 to 161.7 kJ mol^{-1}) and the reaction energy ΔE_r (from 165.3 to 103.6 kJ mol^{-1}) is observed with the increasing number of methyl groups. Our results for HMB in 5T are similar to the values calculated earlier for HMB in 4T (169 kJ mol^{-1} and 108 kJ mol^{-1}).[22] While these results clearly illustrate the increase of reactivity for higher polymethylbenzenes, the barriers remain relatively high in absolute value. It is expected that the zeolite framework lends additional electrostatic stabilization to the ion pair formed by the cation and the negative aluminum defect.[23] Therefore, the calculations were extended to more advanced 44T and 46T clusters, which represent both the active site and the surrounding zeolite cage[23,24] for various industrially and academically important topologies, such as BEA, CHA, and MFI (shown in Figure 2).

The beta zeolite (BEA topology) has a large pore structure that allows direct introduction of large molecules such as hexamethylbenzene. It is an interesting topology for mechanistic studies, although it is not used as a commercial catalyst because of rapid coke formation and deactivation. Calculations with the BEA topology (Figure 1 b) shows an only slightly reduced reaction barrier of 144.0 kJ mol^{-1} and a reaction energy of 55.2 kJ mol^{-1}. As shown in Figure 2, the large cages in BEA provide limited electrostatic interaction with the organic species that are located centrally in the pores.

Modeling the aluminosilicate chabazite (CHA topology) is a first step towards the commercially important aluminophosphate HSAPO-34, which has the same topology as CHA but an entirely different composition. Composition effects should, however, be treated separately from pure topology effects, and these will be part of a future study. The CHA topology is a structure with spacious cages interconnected by small windows. Methylbenzenes are formed through a "ship-in-a-bottle" synthesis and remain trapped in the catalyst.[9] The calculations with the CHA topology (Figure 1 b) shows a spectacular reduction in energetics. The reaction barrier of merely 60.8 kJ mol^{-1} is easily surmountable, and the reaction energy of −8.4 kJ mol^{-1} even hints at an exothermic initiation of the hydrocarbon-pool cycle in chabazite. Apparently, the enclosing chabazite topology provides an ideal setting for this key reaction step. The term "inverse shape selectivity" immediately springs to mind, although this terminology is usually reserved for the preferential adsorption of neutral branched paraffins rather than for charged species.[25,26] Direct comparison between BEA and CHA clearly shows the strong difference between open and dense framework topologies in solvating this crucial intermediate.

Even though they differ greatly in cage dimensions, both beta and chabazite zeolites contain sufficiently large cages not to impose any geometric constraints on the transition state. This is not the case for HZSM-5, an industrially important

 © 2007 Wiley-VCH Verlag GmbH & Co. KGaA, Weinheim

zeolite exhibiting the medium-pore MFI topology containing two sets of intersecting channels. Durene is the largest polymethylbenzene that can be introduced directly along the narrow channels.[27] Although MFI does not boast spacious cages, HMB could be formed in the extended space available at the channel intersections. However, its diffusion and reactivity will be sterically restricted. This limited space imposes severe problems for the geminal methylation of methylbenzenes. The spatial demand of the transition state in particular is shown in Figure 2: the two-dimensional methylbenzene is extended perpendicularly into a third dimension in a typical S_N2-type methyl-exchange configuration, while the entire complex remains connected to the active site by hydrogen bonds and the aluminum negative charge, allowing little to no room for flexibility. Deformation of an optimal S_N2-type geometry will invariably lead to an increased reaction barrier.[28]

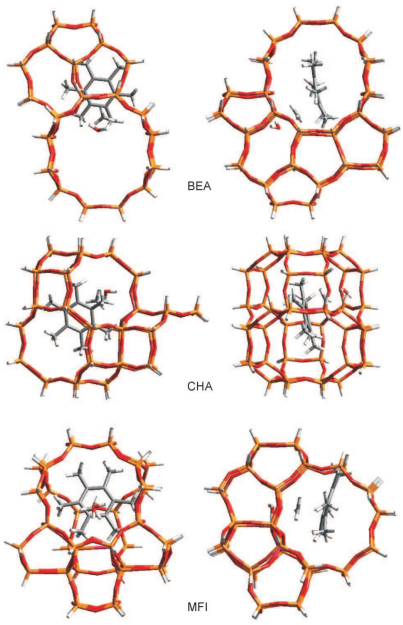

Figure 2. Transition-state geometries for the formation of heptamethylbenzenium in the BEA, CHA, and MFI zeolite topologies.

Not surprisingly, the reaction barrier in the MFI topology (Figure 1c) is strongly dependent on the number of methyl substituents. For small polymethylbenzenes a steady decrease in both reaction barrier (from 145.5 to 79.1 kJ mol^{-1}) and reaction energy (from 101.7 to 49.1 kJ mol^{-1}) is observed. From durene on, however, the transition state lacks sufficiently ample space to take on the optimal geometry, and the reaction barrier increases significantly to 90.9 kJ mol^{-1}. However, the pentamethylbenzenium ion, which is not as bulky as the transition state, is more stable than the neutral species by 8.5 kJ mol^{-1}. The geminal methylation of pseudocumene and pentamethylbenzene also has a low activation energy (79.1 and 81.3 kJ mol^{-1}) and provides more reactive species for subsequent steps. Each additional methyl group imposes a constant conflict between two opposing effects: on the one hand it leads to a more reactive hydrocarbon-pool species as well as stronger electrostatic interaction with the framework, and on the other hand it is subject to the geometric constraints imposed by the zeolite topology. For HMB this combination of contradictory contributions leads to a reaction barrier of 126.2 kJ mol^{-1} and reaction energy of 29.0 kJ mol^{-1}, which is located between the values obtained for BEA and CHA. In a small-pore catalyst like HZSM-5, the formation of large cations is severely restricted, and the hydrocarbon pool will most likely consist of less sterically demanding methylated benzenes or might even be based on the methylation of smaller branched olefins rather than bulkier methylbenzenes.[29,30]

We conclude that specific combinations of organic reaction centers and the inorganic framework cooperate effectively in stabilizing intermediates and transition states that would, if considered separately, be of excessively high energy. These results offer additional support for the hydrocarbon-pool model by providing a first step towards alternative low-energy pathways for reactions that would otherwise have very high-energy intermediates, as, for example, in the direct oxonium ylide or carbene proposals.[5] Without the solvating effect of the zeolite framework, the number of methyl substitutions on the benzene ring can account for only a relatively minor decrease in both barrier height and reaction energy. The zeolite topology, however, plays a major role in reaction kinetics. For the geminal methylation of hexamethylbenzene the following order of reactivity according to topology is observed: CHA $\gg$ MFI $>$ BEA. The chabazite cages provide the perfect surroundings for a surprisingly stable heptamethylbenzenium cation, while the large beta cages favor neutral species over cations. In the MFI framework, on the other hand, transition-state-shape selectivity takes over for the bulkier methylbenzenes, and lesser methylated cations are the most likely intermediates. Immediately after submission of this paper, a communication by Svelle et al. was published online, including experimental confirmation of the higher activity of the lower methylbenzenes in H-ZSM5.[31]

Further theoretical insights into the effect of zeolite topology are desperately needed, if only to guide development of novel materials with a fine-tuned local spatial environment that optimizes catalytic activity, improves product selectivity, and simultaneously reduces coke formation. Additional insights might even be obtained from enzyme or homogeneous catalysis rather than from traditional zeolite chemistry.[32] To achieve these common goals, strong interaction between experimental work and computational modeling is indispensable.

 © 2007 Wiley-VCH Verlag GmbH & Co. KGaA, Weinheim

Experimental Section

All geometry optimizations were performed with the Gaussian03 package.[33] The 5T cluster, treated at the B3LYP/6-31g(d) level of theory,[34] was left unconstrained to verify the true nature of all stationary points. Zero-point-energy (ZPE) corrections were included. Starting from transition-state geometries, the quasi-IRC approach allowed the reactant and product geometries to be acquired. The calculations on the BEA, CHA, and MFI topologies were performed on 44T or 46T clusters at the ONIOM(B3LYP/6-31 + g(d):HF/6-31 + g(d))//ONIOM(B3LYP/6-31 + g(d):MNDO) level of theory,[23,24] where the 5T zeolite active site as well as all organic species were considered at the high QM level. Only the saturating hydrogen atoms were fixed to prevent collapse of the cage. All other low-level framework atoms were allowed to fully adjust themselves to the large incorporated species. As elementary reaction steps were considered separately from adsorption/desorption requirements, only intrinsic energy barriers are shown in kJ mol^{-1}.

Received: October 20, 2006
Published online: January 4, 2007

Keywords: ab initio calculations · arenes · heterogeneous catalysis · methanol-to-olefin process · zeolites

[1] M. Stocker, *Microporous Mesoporous Mater.* **1999**, *29*, 3 – 48.
[2] J. F. Haw, W. G. Song, D. M. Marcus, J. B. Nicholas, *Acc. Chem. Res.* **2003**, *36*, 317 – 326.
[3] W. G. Song, D. M. Marcus, H. Fu, J. O. Ehresmann, J. F. Haw, *J. Am. Chem. Soc.* **2002**, *124*, 3844 – 3845.
[4] D. M. Marcus, K. A. McLachlan, M. A. Wildman, J. O. Ehresmann, P. W. Kletnieks, J. F. Haw, *Angew. Chem.* **2006**, *118*, 3205 – 3208; *Angew. Chem. Int. Ed.* **2006**, *45*, 3133 – 3136.
[5] D. Lesthaeghe, V. Van Speybroeck, G. B. Marin, M. Waroquier, *Angew. Chem.* **2006**, *118*, 1746 – 1751; *Angew. Chem. Int. Ed.* **2006**, *45*, 1714 – 1719.
[6] P. W. Goguen, T. Xu, D. H. Barich, T. W. Skloss, W. G. Song, Z. K. Wang, J. B. Nicholas, J. F. Haw, *J. Am. Chem. Soc.* **1998**, *120*, 2650 – 2651.
[7] R. M. Dessau, *J. Catal.* **1986**, *99*, 111 – 116.
[8] I. M. Dahl, S. Kolboe, *J. Catal.* **1994**, *149*, 458 – 464.
[9] W. G. Song, J. F. Haw, J. B. Nicholas, C. S. Heneghan, *J. Am. Chem. Soc.* **2000**, *122*, 10726 – 10727.
[10] B. Arstad, S. Kolboe, *J. Am. Chem. Soc.* **2001**, *123*, 8137 – 8138.
[11] U. Olsbye, M. Bjorgen, S. Svelle, K.-P. Lillerud, S. Kolboe, *Catal. Today* **2005**, *106*, 108 – 111.
[12] T. Xu, D. H. Barich, P. W. Goguen, W. G. Song, Z. K. Wang, J. B. Nicholas, J. F. Haw, *J. Am. Chem. Soc.* **1998**, *120*, 4025 – 4026.
[13] J. F. Haw, J. B. Nicholas, W. G. Song, F. Deng, Z. K. Wang, T. Xu, C. S. Heneghan, *J. Am. Chem. Soc.* **2000**, *122*, 4763 – 4775.
[14] M. Bjorgen, F. Bonino, S. Kolboe, K.-P. Lillerud, A. Zecchina, S. Bordiga, *J. Am. Chem. Soc.* **2003**, *125*, 15863 – 15868.
[15] W. G. Song, J. B. Nicholas, A. Sassi, J. F. Haw, *Catal. Lett.* **2002**, *81*, 49 – 53.
[16] B. Arstad, J. B. Nicholas, J. F. Haw, *J. Am. Chem. Soc.* **2004**, *126*, 2991 – 3001.
[17] W. Song, H. Fu, J. F. Haw, *J. Am. Chem. Soc.* **2001**, *123*, 4749 – 4754.
[18] Z. M. Cui, Q. Liu, W. G. Song, L. J. Wan, *Angew. Chem.* **2006**, *118*, 6662 – 6665; *Angew. Chem. Int. Ed.* **2006**, *45*, 6512 – 6515.
[19] J. A. Martens, J. Perez-Pariente, E. Sastre, A. Corma, P. A. Jacobs, *Appl. Catal.* **1988**, *45*, 85 – 101.
[20] L. A. Clark, M. Sierka, J. Sauer, *J. Am. Chem. Soc.* **2004**, *126*, 936 – 947.
[21] A. M. Vos, X. Rozanska, R. A. Schoonheydt, R. A. van Santen, F. Hutschka, J. Hafner, *J. Am. Chem. Soc.* **2001**, *123*, 2799 – 2809.
[22] B. Arstad, S. Kolboe, O. Swang, *J. Phys. Chem. B* **2002**, *106*, 12722 – 12726.
[23] D. Lesthaeghe, V. Van Speybroeck, G. B. Marin, M. Waroquier, *Chem. Phys. Lett.* **2006**, *417*, 309 – 315.
[24] D. Lesthaeghe, G. Delcour, V. Van Speybroeck, G. B. Marin, M. Waroquier, *Microporous Mesoporous Mater.* **2006**, *96*, 350 – 356.
[25] D. S. Santilli, T. V. Harris, S. I. Zones, *Microporous Mater.* **1993**, *1*, 329 – 341.
[26] M. Schenk, S. Calero, T. L. M. Maesen, L. L. van Benthem, M. G. Verbeek, B. Smit, *Angew. Chem.* **2002**, *114*, 2609 – 2612; *Angew. Chem. Int. Ed.* **2002**, *41*, 2500 – 2502.
[27] A. Sassi, M. A. Wildman, H. J. Ahn, P. Prasad, J. B. Nicholas, J. F. Haw, *J. Phys. Chem. B* **2002**, *106*, 2294 – 2303.
[28] D. Lesthaeghe, V. Van Speybroeck, G. B. Marin, M. Waroquier, *J. Phys. Chem. B* **2005**, *109*, 7952 – 7960.
[29] H. Schulz, M. Wei, *Microporous Mesoporous Mater.* **1999**, *29*, 205 – 218.
[30] S. Svelle, B. Arstad, S. Kolboe, O. Swang, *J. Phys. Chem. B* **2003**, *107*, 9281 – 9289.
[31] S. Svelle, F. Joensen, J. Nerlov, U. Olsbye, K.-P. Lillerud, S. Kolboe, M. Bjorgen, *J. Am. Chem. Soc.* **2006**, *128*, 14770 – 14771
[32] J. F. Haw, D. M. Marcus, *Top. Catal.* **2005**, *34*, 41 – 48.
[33] Gaussian 03 (Revision B.03): M. J. Frisch et al., see the Supporting Information
[34] A. D. Becke, *J. Chem. Phys.* **1993**, *98*, 5648 – 5652.

 © 2007 Wiley-VCH Verlag GmbH & Co. KGaA, Weinheim

3.9

Refinement of the supramolecular concept in methanol-to-olefin catalysis

D. Lesthaeghe, V. Van Speybroeck, G.B. Marin, M. Waroquier
Studies in Surface Science and Catalysis, **2007**, in press.

---

article 3.9

D. Lesthaeghe, V. Van Speybroeck, G.B. Marin, M. Waroquier

Refinement of the supramolecular concept in methanol-to-olefin catalysis

Stud. Surf. Sci. Catal. **2007**, submitted

One plus one equals three: Combining the organic hydrocarbon pool with the inorganic framework unleashes a wide variety of interactions. Based on the results in [art. 3.8], the current supramolecular picture is refined in this review article. An overview of previously defined contributions is extended with the role of transition state shape selectivity and framework electrostatic stabilization on crucial cationic intermediates.

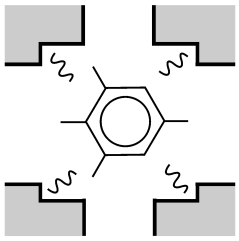

Refinement of the supramolecular concept in methanol-to-olefin catalysis

D. Lesthaeghe,[a] V. Van Speybroeck,[a] G.B. Marin[b] and M. Waroquier[a]

[a] Center for Molecular Modeling, Ghent University, Proeftuinstraat 86, B-9000 Gent, Belgium
[b] Laboratorium voor Petrochemische Techniek, Ghent University, Krijgslaan 281-S5, B-9000 Gent, Belgium

ABSTRACT

The supramolecular character of methanol-to-olefin conversion in acidic zeolites is thoroughly investigated from a theoretical viewpoint. State-of-the-art modeling techniques have not only led to an absolute rejection of the intensively studied direct mechanisms, but have also provided additional insights into the alternative hydrocarbon pool proposal. The role of various external factors such as zeolite topology on the formation of crucial carbenium ions is discussed and the established supramolecular picture is refined.

1. INTRODUCTION

Light olefins are vital components in the petrochemical industry and are traditionally obtained by steam cracking of crude oil fractions. However, because the finite oil reserves will not be able to meet the ever-increasing demand for oil-based chemicals, new developments currently focus on technologies that are based on alternative natural sources. The methanol-to-olefins (MTO) process is a vital step in the conversion of alternative sources to light olefins: methanol can be made from almost any gasifiable carbonaceous material, following which MTO technology converts methanol to crucial petrochemical feedstock like ethene and propene [1,2]. The production of methanol currently occurs mainly through steam reforming of natural gas or through gasification of coal. The conversion of biomass and waste to methanol is, however, on the rise, mainly because these novel technologies form a closed carbon-cycle and do not depend on the declining fossil fuel reserves. By subsequently applying MTO technology to the methanol produced, one could make almost anything out of methanol that can currently be made out of crude oil.

While several different acidic zeolite and zeotype structures, like HZSM-5 and HSAPO-34 respectively, are well-known MTO catalysts, a major target is the design and development of an ideal MTO catalyst. This material should not only exhibit superior catalytic activity towards olefin formation: it should also suppress the secondary reactions that form alkanes and aromatics and lead to deactivation of the catalyst by coke formation. Most importantly, we aim to control product selectivity, e.g. the ethene/propene ratio, to meet the specific market demands at any given time.

In the search for control of product distribution, a detailed understanding of the MTO reaction mechanism is vital. Quite remarkably, however, the actual mechanism of the conversion of methanol to olefins in acidic zeolites has been a hugely challenging problem for more than 30 years. The main question is how initial C-C coupling occurs from C1 species like methanol and dimethylether (DME). This has led to more than 20 distinct mechanistic proposals with all kinds of reactive intermediates, such as ylides, carbenium ions and radicals [1]. Speculation centered mainly on mechanisms based on the 'direct' formation of small olefins from only methanol, dimethylether and other single-carbon derivates. Recently, however, experimental studies by Haw and co-workers provided evidence that extensively purified methanol is unreactive under regular MTO conditions [3,4]. Our own theoretical results confirmed this controversial statement by showing that methanol alone cannot be coupled directly into hydrocarbons at rates relevant to steady-state conversion [5,6]. In this paper we will give a general discussion of recent developments in the alternative 'hydrocarbon pool' (HP) proposal [7,8]. We will focus on the supramolecular picture developed by Haw et al. [9] and further extend it with new contributions that should be considered when charged intermediates are involved.

2. COMPUTATIONAL DETAILS

Density functional theory (DFT) calculations using the B3LYP functional were performed within the Gaussian03 software package [10,11]. Both the small cluster approach and the two-layered QM/QM embedded ONIOM method were employed. This more advanced method allows for inclusion of the zeolite framework at moderate additional computational cost. Inclusion of the framework is vital when studying the HP route, which is space-demanding and based on carbenium-ion intermediates. The ONIOM method is currently widely used in zeolite chemistry [12-17], as it has been shown to be very a robust method [18]. Furthermore, this method gives results as accurate as those of full periodic calculations [19], but at a significantly lower computational cost [20].

Calculations were performed on alumino-silicates with three industrially and/or academically important topologies: MFI, BEA and CHA [21]. HZSM-5 is an industrially important zeolite exhibiting the medium-pore MFI topology and containing two sets of intersecting channels, each composed of 10-membered rings. Durene is the largest polymethylbenzene that can be fed directly along its narrow channels [22]. The HBeta zeolite (BEA), on the other hand is a large pore zeolite with three sets of intersecting 12-membered ring channels, allowing direct introduction of large molecules such as hexamethylbenzene. It is interesting for mechanistic studies, although not as a commercial catalyst for the MTO process because it cokes up too easily. The silico-aluminophosphate HSAPO-34 exhibits the CHA topology, which is a structure with spacious cages, interconnected by small 8-membered ring windows. Because of their higher complexity, we have not yet modeled any silico-aluminophosphates like HSAPO-34. Instead, we have focused on the alumino-silicate chabazite which has the same CHA topology as HSAPO-34. Generally speaking, the zeolite framework can contain parallel or intersecting channels (like the MFI topology of HZSM-5), cages interconnected by small windows (like the CHA topology of HSAPO-34 and chabazite) or a combination of both cages and channels (like the BEA topology in HBeta).

3. RESULTS AND DISCUSSION

3.1. Failure of direct mechanisms from theoretical viewpoint

In previous work, we showed that all combinations of methanol, DME, framework-bound methoxy groups and water could not lead to any C2 species because of excessively high reaction barriers and exotic intermediates preceding the various often-proposed C-C coupling steps. We tackled the vast number of potential direct mechanisms by setting up an extensive reaction scheme, tying together a large variety of possible direct reactions, even including several previously overlooked pathways. Based on reaction rates at MTO-relevant temperatures we demonstrated that no complete direct pathway from methanol leading all the way to ethene (or to any intermediate containing a carbon-carbon bond) exists [6,23]. The only intermediates that could be directly formed are methane, formaldehyde and the trimethyl oxonium ion.

3.2. Alternative hydrocarbon pool proposal

The most likely alternative to the 'direct' mechanisms is provided by the 'hydrocarbon pool' (HP) proposal, in which organic species trapped in the zeolite pores serve as a platform to which C1 species can attach (e.g. through repeated methylation by methanol), following which internal rearrangements and/or additional methylation leads to splitting off of olefins [7,8]. Further methylation steps would then regenerate the original HP and close the catalytic cycle. By using this organic scaffolding to build the C2 species, the high-energy intermediates proposed in the 'direct' mechanisms can be bypassed. The elementary steps governing this HP process are still not well understood, however, mainly because secondary reactions consume and mask the primary products, severely complicating interpretation of experimental data. Theoretical methods provide an ideal tool to unravel this complex network of reactions, as individual reaction steps can easily be modeled separately. Recent calculations are guided by the general consensus on a hydrocarbon pool consisting mainly of polymethylbenzenes, which have been shown to be active for olefin formation independent of the zeotype catalyst chosen [24-26]. There is also strong experimental evidence for cyclic resonance-stabilized tertiary cations as persistent species in the pores, such as cyclopentenyl and pentamethylbenzenium cations in HZSM-5 [27-28] and hexamethylbenzenium and heptamethylbenzenium (7MB+) cations in HBeta [29-30]. *Gem*-dimethylbenzenium cations in particular have been observed by in situ 13C solid-state NMR in alumino-silicates and form the main starting point from which commonly proposed hydrocarbon pool routes (such as the 'paring' and 'side-chain' mechanisms) originate [31]. The heptamethylbenzenium cation (7MB+), for example, is formed from hexamethylbenzene (HMB) through a one-step geminal methylation by methanol.

3.3. Towards a supramolecular catalyst

Due to the complexity of the HP proposal, Haw et al. suggested that the catalyst should not be considered as a typical acid zeolite framework merely containing certain hydrocarbons, but rather that each cage with all included organic and inorganic species should be seen as a supramolecule [9]. The nature and catalytic behavior of various supramolecular sites for MTO conversion is defined by the complex interplay between the inorganic framework, the organic hydrocarbon pool species and several other factors. Figure 1 presents an overview of all the separate contributions, which, when combined, will define the active HP species as well as the reaction mechanism and the products that will consequently be formed.

With respect to the inorganic framework, zeolite composition (F1) is a first important factor. Although traditionally alumino-silicates (like HZSM-5) are most often considered, certain zeotype silico-aluminophosphates (like HSAPO-34) also show excellent MTO activity. Furthermore, the silico-aluminophosphate composition leads to a lower, relatively moderate, acidic strength, which has the great advantage of suppressing the secondary reactions. As the HP mechanism is a space-demanding process, pore architecture and shape selectivity will also play a crucial role. The cage dimensions (F2) will define both the maximum volume and shape allowed for bulky molecules. Channel diameters (F3), on the other hand, will control diffusion: small channels or windows will only allow small molecules like methanol/water and ethene/propene to enter and exit the cages, thus providing a basis for both reactant and product shape selectivity.

The organic reaction center (O1) is essential for an active MTO catalyst, as it acts as a platform upon which C-C bonds can be made and broken. Without this platform, C-C coupling can only occur via the direct mechanisms for which rate coefficients are too low. Different organic components will exhibit different activity and different product selectivity, so establishment and modification of this species is crucial towards understanding and obtaining product control. In the case of polymethylbenzenes as an active HP species, for example, increasing the number of methyl groups is believed to significantly decrease the barrier to olefin synthesis, but at the same time to lead also to higher propene selectivity [32].

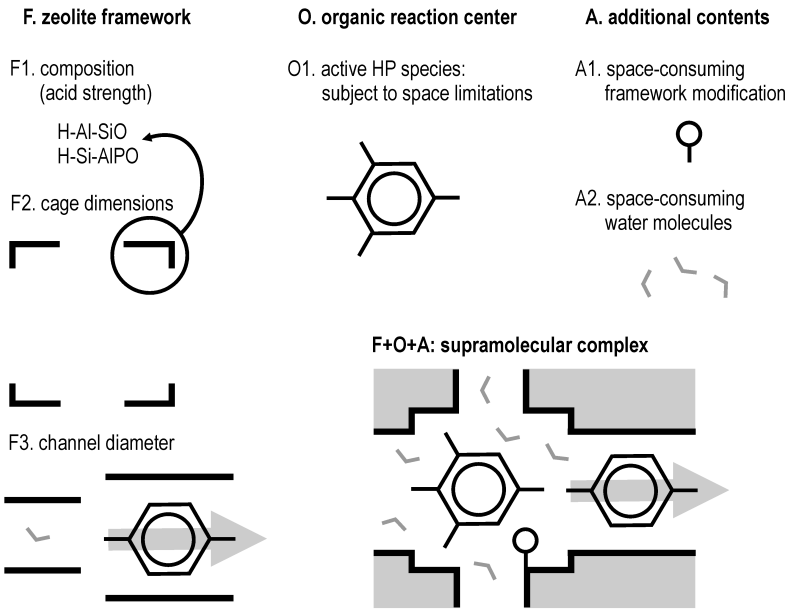

Fig. 1. Separate contributions that create the supramolecular catalyst as suggested by Haw et al. [9]

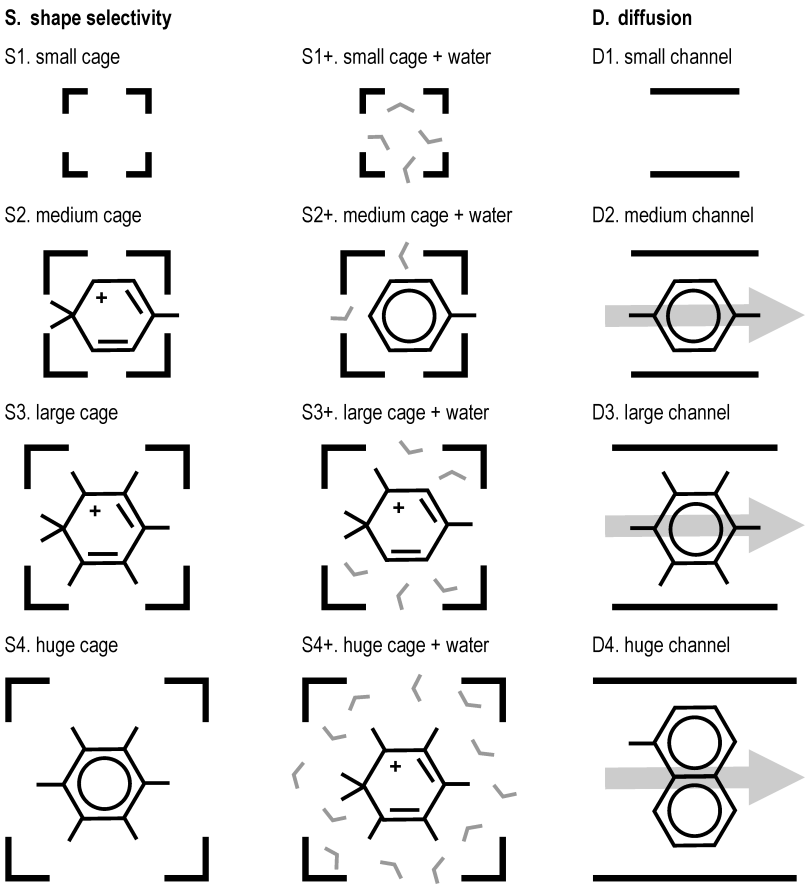

Fig. 2. Most likely intermediates from initiating step depending on zeolite topology.

The number of methyl substitutions on a methylbenzene, and as a consequence also product distribution, will depend on the other contributions shown in Figure 1. The degree of methylation depends mainly on the available volume, which is determined predominantly by the cage dimensions. The cage dimensions can, however, also be tailored by additional space-consuming contents, such as inorganic framework modification or additional adsorbed molecules. Control of the spatial arrangement of cages with diverse functionality is, therefore, one of the ultimate goals in MTO catalysis. Haw et al. succeeded in applying inorganic post-synthesis modification with tetramethylphosphonium cations to occupy cage volume (A1) [33]. They managed to synthesize a material with slightly reduced catalytic activity, but with a significantly increased selectivity towards ethene. Thus, tailoring the organic component by adding additional inorganic material to some cages through ship-in-a-bottle reactions seems to be a first step towards product control. Essential volume can also be occupied by other molecules. For example, Haw et al. also showed that a higher loading of water leads to a

reduction of free volume (A2) [32]. Consequently, only the lower methylbenzenes could act as active HP species and an increase in ethene/propene ratio was observed.

3.4. Failure of direct mechanisms from topological viewpoint

The supramolecular premise of a bulky HP molecule in the zeolite pores shown in Figure 1 implies that zeolites with very small cages (as illustrated in Figure 2: S1 and S1+) that are unable to host this space-demanding process, should not demonstrate any MTO activity whatsoever. Recently, Cui et al. put this hypothesis to the test by performing experiments on systematically selected framework structures with varying pore and channel sizes [34]. Their results confirmed that the MTO reaction only takes place on zeolites that allow the hydrocarbon pool mechanism to work, i.e. zeolites with larger cages or zeolites where channel intersections can also serve as an extended space for reactive intermediates. This important experimental verification of small cages providing an inactive MTO catalyst was attributed to transition state shape selectivity. Experimental claims to transition state shape selectivity are, ideally, verified by theoretical methods, since these are more suited for elucidating the extent to which the local shape of the pore influences local reaction rates [35-36]. For the initiating step forming crucial cationic intermediates, the experimental claim to transition state shape selectivity has indeed been confirmed by our theoretical calculations [37], as will be further explained in the following paragraph.

3.5. Cationic intermediates as part of the supramolecule

For a zeolite with medium sized cages, or in the case of MFI medium sized channel intersections, there is inadequate volume for the higher *gem*-dimethylbenzenium cations to be formed (S2). In a recent communication, we have demonstrated that neither the size of the methylbenzene reactant nor that of the *gem*-dimethylbenzenium cation product is crucial, but that the activity of a HP molecule is governed largely by the size of the transition state leading to the geminal methyl group, and as such will be subject to transition state shape selectivity [37]. This theoretical prediction was confirmed when Svelle et al. demonstrated that even though the higher methylbenzenes are present in MFI, they are virtually unreactive and ethene appears to be formed exclusively from the lower methylbenzenes [38]. It seems to us probable that, even for the lower methylbenzenes, a large number of additional solvent molecules or inorganic framework modification would further take up the much-needed space for the transition state to form and further reaction would become almost impossible (S2+). Most importantly, we stress the novel observation that even if an aromatic HP platform is present, it can only perform as an active species for olefin production if the surrounding conditions allow favorable transition states as well.

For a zeolite with larger cages (like HSAPO-34) there is adequate space, not only for the bulky HP species, but also for the transition state leading to heptamethylbenzenium ion formation (S3). Furthermore, as shown in Figure 3, the encapsulating cage provides ideal electrostatic stabilization of this ion, resulting in a very low barrier to formation of this species [37]. Adding solvent molecules or inorganic features would reduce the amount of methyl substitutions and increase ethene selectivity (S3+), while simultaneously slightly reducing catalytic activity. In a zeolite like HBeta, on the other hand, the cages are too big (S4) to provide the necessary electrostatic stabilization (illustrated in Figure 3). Although there is enough space for the heptamethylbenzenium ion to be formed, it is relatively unstable

with respect to the neutral species. In practice, this will most probably be remedied by solvent molecules like water or methanol (S4+).

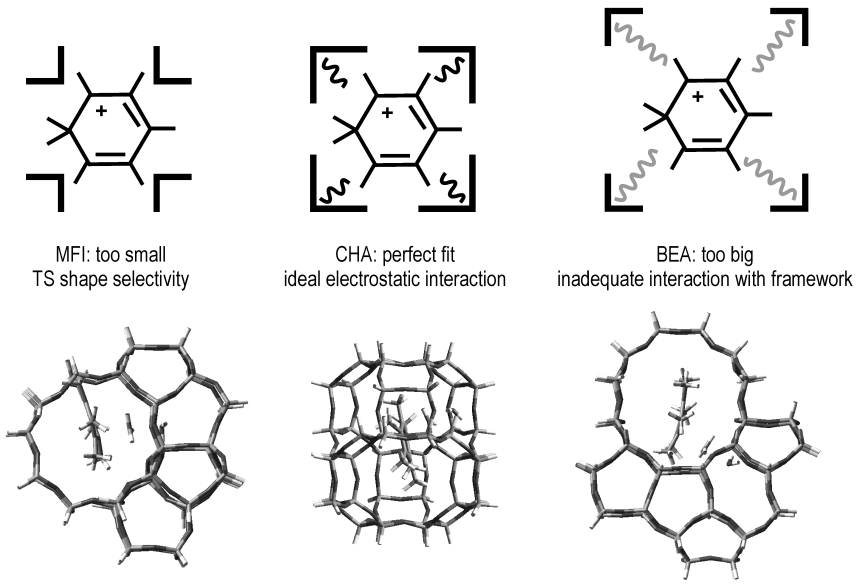

Fig. 3. Refinement of the supramolecular picture: importance of the electrostatic effect of the zeolite topology on the carbenium ion product (top) and transition state shape selectivity (bottom), both for *gem*-methylation of hexamethylbenzene.

3.3. Channel diameter

Not only the cage (or channel intersection) dimensions are important, but also the channel diameters. Very small channels (as in HSAPO-34) in D1 (Figure 2) will not allow diffusion of any HP species. This means that the HP platform needs to be assembled through a ship-in-a-bottle synthesis in the larger cages. Once the methylbenzene is successfully formed, it remains trapped. This guarantees the crucial combination of an acid site and an active HP molecule in one single cage. However, aromatics will age into larger, less active, aromatic species, until the catalyst is filled with coke and must be regenerated by combustion. Medium sized channels (as in ZSM-5) allow for introduction or diffusion from the lower methylbenzenes (D2), while the higher methylbenzenes remain trapped [22]. If we consider only reactant and product shape selectivity, this would seem an interesting topology demonstrating high activity as well as high propene selectivity. But, because of transition state shape selectivity for the initiating step in HZSM-5, the trapped higher methylbenzenes are virtually unreactive.

Large channels (as in HBeta) on the other hand (D3), will not only allow easy entrance but also an easy exit from the catalyst for the active hydrocarbon pool species. Furthermore, there

are no constraints on secondary reactions leading to undesirable larger aromatic species. Methylnaphtalenes, for example, are less reactive HP species than methylbenzenes (D4) and will eventually lead to complete deactivation of the catalyst [9].

4. CONCLUSIONS

In recent developments, both experimental and theoretical work has firmly demonstrated that the frequently suggested direct mechanisms all fail to explain initial C-C coupling in the methanol-to-olefin process. Furthermore, theoretical calculations have clearly illustrated the extent to which the organic hydrocarbon pool species and the inorganic zeolite framework cooperate as a supramolecular catalyst towards alternative pathways. We are currently actively pursuing an entire low-energy pathway linking methanol all the way to ethene.

Both hydrocarbon pool species and zeolite topology play a crucial role in the reaction kiBoth h

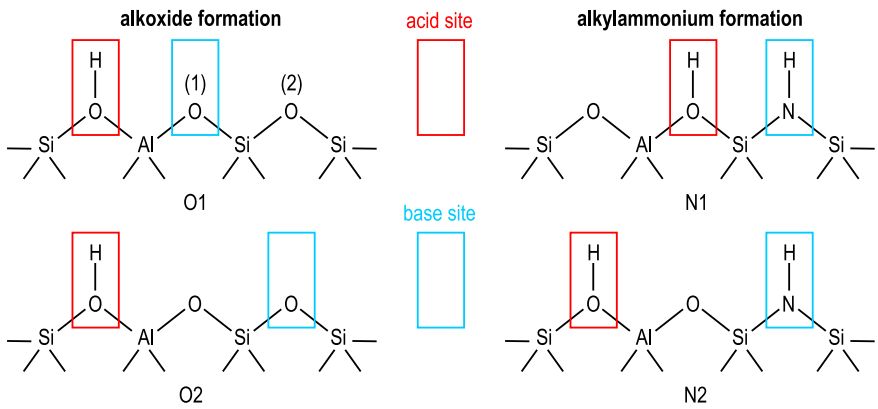

Figure 4.6: Zeolite clusters used to characterize acidic and basic properties.

Si-NH-Si as a measure of basicity for a neutral starting configuration without aluminum defect. Since the reactions studied later in this chapter will all involve the formation of an alkoxide or alkylammonium species, the present definition is more appropriate.

NH substitutions bonded to the aluminum atom (site (1) in Figure 4.5) are thermodynamically prone to protonation, resulting in non-optimal acid-base properties [art. 4.6]. Thus for the amine-modified zeolites, methylammonium formation is always considered at site (2). For traditional zeolites with only oxygen bridges, methoxide species are commonly formed on the more basic oxygen site (1) as shown in Figure 4.6, located next to the aluminum atom. However, for proper comparison with the results on the amine substituted clusters, desorption energies are also calculated for a methoxide species formed at the less basic site (2), referred to as the O2 cluster.

As shown in Table 4.1, the desorption energy $E_{DS} = E[\mathrm{Z}^-]+E[\mathrm{CH}_3^+]-E[\mathrm{Z\text{-}CH}_3]$ for the O2 cluster is substantially lower than for a methoxide species formed on the aluminum tetrahedron (O1 cluster). The energy difference of about 100 kJ mol^{-1} indicates the cost of charge separation due to the positive methoxide group not being located near the negatively charged aluminum defect. Sorption energies for the NH substituted clusters with the methylammonium species also formed at site (2) are about 100 kJ mol^{-1} higher than the O2 cluster, due to the strong basic character of the amine bridge [art. 4.7]. Apparently, two opposing

cluster	deprotonation	CH_3^+ desorption
O1	1231.0	763.4
O2	id. O1	667.4
N1	1226.2	762.1
N2	1234.6	765.7

Table 4.1: Heats of deprotonation and CH_3^+ desorption in kJ mol^{-1} calculated at the B3LYP/6-31g(d) level on 16T clusters [art. 4.7]. Cluster terminology is defined in Figure 4.6.

effects contribute largely to the sorption energy:

- the basicity of the nitrogen or oxygen bridge
- and the energy cost needed for charge separation between the CH_3^+ group and the AlO_4^- tetrahedron.

For the amine-modified zeolites, the two effects seem to simply cancel each other out. Therefore, the sorption energy for CH_3^+ at the oxygen atom located on site (1) is of the same order of magnitude as the corresponding values for nitrogen bridged zeolites at site (2).

In conclusion, we find all clusters to be of similar Brønsted acidity, while the C-O bond formed for the oxygen site (1) is of the same strength as the C-N bonds formed upon site (2). More importantly, based on these results, any lowering of reaction barriers for nitrogen-substituted zeolites cannot solely be ascribed to the Lewis basic properties of the amine group.

4.3.3 Test reaction: alkoxide formation in the MTO process

Having looked at the general properties of the amine-modified catalyst, the remainder of this chapter will focus on chemical reactions in these new materials. Three typical reactions in zeolite chemistry which are also important in the methanol-to-olefin process, and for which the basic NH site might provide improvements, will be discussed: the alkoxide formation from methanol, chloromethane and ethene.

Without any direct evidence, carbenium and carbonium ions were for a long time accepted as intermediate species (analogous to equivalent gas-phase reactions), stabilized in the polar zeolite surroundings by long-range electrostatic interactions. However, solid-state NMR and IR experiments indicate that adsorbed protonated hydrocarbons are not stable [107, 108], with the exception of some cyclic cations with a delocalized positive charge [79, 109], like the heptamethylbenzenium ion in the MTO process. Instead, protonation of adsorbed olefins and alcohols results in the formation of long-lived alkoxide species covalently bonded to the catalyst surface, as evidenced by ^{13}C MAS NMR studies [110, 111]. Theoretical calculations using both the cluster approach and fully periodical techniques indicate that alkoxide species are indeed local minima and thus stable intermediates, while carbenium ions often act as transition states [28, 112–114]. Even so, we must note that the true nature of reactive intermediates in reactions catalyzed by acid zeolites is still a matter of debate, certainly when large hydrocarbons are involved [115]. It can be shown, though, that for important industrial reactions, such as hydrocracking or catalytic cracking of these large hydrocarbons, the corresponding kinetic equations do not depend on the assumed nature of the reaction intermediates, i.e. alkoxides or carbenium ions [116].

As mentioned in Chapter 3, the MTO process involves activation of methanol on the zeolite surface [47, 117]. The Z-CH_3 methoxide intermediate is generated by dissociation of methanol over the acid site. In the light of sustainable energy production, early patents also report the possibility of converting halomethanes [118, 119], circumventing the costly formation of synthesis gas and reducing the number of byproducts. In the hydrocarbon pool proposal, surface methoxide species formed from methanol or halomethanes might also play an important role in the methylation of the aromatic reaction centers [40]. On the other hand, ethylation of a hydrocarbon pool species can occur through a similar stepwise mechanism, starting with the protonation of adsorbed ethene by an acidic zeolite proton, generating a reactive ethoxide species [120, 121].

As demonstrated by our calculations in Table 4.1, the unprotonated oxygen sites in the first coordination sphere of a framework tetrahedral aluminum (O1) show stronger Lewis base properties compared to Si-O-Si bridges (O2), rendering the former the most likely sites for alkoxide species to be formed upon [art. 4.7]. It is believed that chemisorption proceeds in a concerted manner, controlled by a bifunctional (acid-base) mechanism, in which both the Brønsted acid site and the Lewis base properties of an oxygen-atom neighboring the acid site must be carefully balanced [18]. This stresses the importance of the basic centers on the

acid-base pairs, since they play an active role in the stabilization of the charged intermediate species which should be formed in a wide range of reactions catalyzed by proton-exchanged zeolites. While most research focuses on modifying the zeolite's acid properties, the number of Lewis base sites could be drastically enhanced by appropriate iso-electronic substitution. Amine substitution in particular might promote alkylammonium formation instead of alkoxide formation, subsequently influencing corresponding reaction barriers.

4.3.4 Alkoxide vs. alkylammonium formation

Several contributions play an important role when alkoxide formation is compared to alkylammonium formation.

Intrinsic basicity: Under identical conditions, amine groups are intrinsically more basic than oxygen bridges, resulting in a stronger bond to the carbon atom. This aspect will favor alkylammonium formation over alkoxide formation.

Charge separation: Since the NH group cannot be located too close to the aluminum tetrahedron, there will be a larger charge separation between the alkylammonium species and the aluminum site compared to traditional alkoxide groups. This aspect will favor alkoxide formation over alkylammonium formation.

Geometrical changes: When the basic site is not located on the aluminum tetrahedron, this allows for more spread out transition state geometries. For certain reactions, this might noticeably lower reaction barriers.

As demonstrated in the previous section, the first two effects cancel each other out for CH_3^+: Si-NH-Si bridges will be as reactive as Si-O-Al bridges. In this section the role of the third contribution will be discussed for alkoxide and/or alkylammonium formation starting from methanol, chloromethane and ethene.

Methanol

As discussed in Chapter 3, the formation of a methoxide species from methanol occurs through a concerted reaction mechanism [69, 122], illustrated in Figure 4.7a. Initially the methanol molecule is adsorbed to the acid site after which it dissociates while the methyl group is transferred to a zeolite oxygen atom through a carbenium-ion like transition state, leading to the formation of a surface methoxide species and a water molecule. The corresponding transition

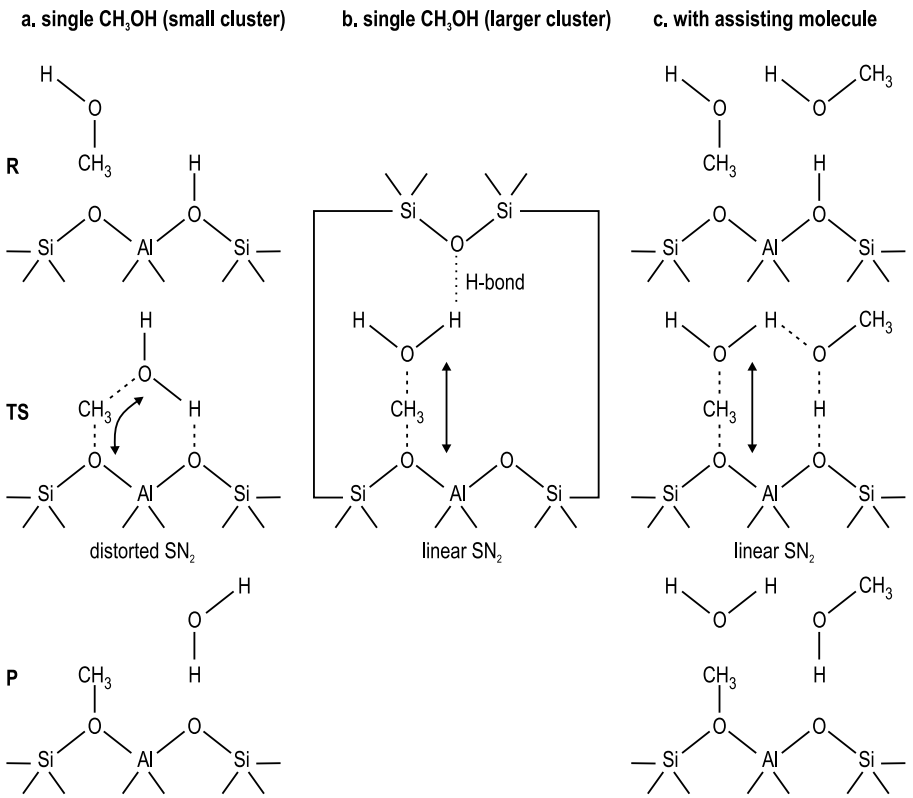

Figure 4.7: Reaction pathways to methoxide formation from methanol, illustrating the importance of assistance by the zeolite framework or an additional molecule.

state is a methoxonium-like ion-pair complex.

However, not all bonds are broken or formed to the same extent in the transition structure. The bond between the acid proton and the hydroxyl group is already formed when the bond breaking of the methyl group and the hydroxyl group and the bond making between methyl group and zeolite are in process. The hydrogen atom that is transferred from zeolite to oxygen forms a hydrogen bond to one of the framework oxygen atoms. This means that in small cluster calculations where only a limited number of framework oxygen atoms are available, the transition state will follow a distorted SN_2 type configuration

(shown in Figure 4.7a). Consequently, the barrier of a single methanol molecule converting to a methoxide group will be too high to proceed [art. 3.6].

For optimal interaction, the methyl-group should be in a planar conformation perpendicular to the axis connecting O, C and the basic site, transferring the methyl-group like a typical SN_2 reaction through an umbrella-like inversion. For small clusters, the transition state structure is considerably distorted in order to interact with both catalyst donor atoms. However, an effective SN_2 intermediate requires a full overlap among the orbitals of the nucleophiles and the active 2p orbital of the carbon atom in the planar methyl group. In practice, the original acid zeolite proton is no longer confined to the zeolite oxygen atom and has the ability to reorient itself in order to form a geometrically favored linear SN_2 like transition structure [art. 4.7]. Therefore the barrier will be lowered by additional framework atoms supplying the necessary hydrogen bond (see Figure 4.7b). Alternatively, methanol or water can also act as an assisting molecule (see Table 3.1 in Chapter 3), providing the optimal transition state as illustrated in Figure 4.7c [art. 3.6].

Because the most optimal transition state structure will be formed automatically, amine modification will not noticeably assist the already geometrically optimal SN_2 transition state [art. 4.7]. The amine groups will only provide more equivalently reactive sites in the zeolite pores.

Chloromethane

Using traditional zeolites, containing only oxygen bridges, this first step follows a concerted reaction mechanism [118], as given in Figure 4.8a [art. 4.6]. Initially chloromethane is adsorbed to the cluster. Next, in a single combined step, it dissociates as the methyl group is transferred to a zeolite oxygen atom through a carbenium-ion like transition state, leading to the formation of a surface methoxide species and hydrochloric acid. Afterwards, this framework-bonded methoxide is available for transfer to a hydrocarbon. Since in the transition state the acid hydrogen atom remains bonded to the basic oxygen, both small and larger cluster calculations give a distorted transition state (Figure 4.8a and 4.8b) with a relatively high energy barrier [art. 4.7].

Compared to the traditional methoxide formation, the nitrogen substitution yields a substantial improvement in catalytic properties, but only for the reaction mechanism spanning two T-sites (N2) [art. 4.6]. As demonstrated in

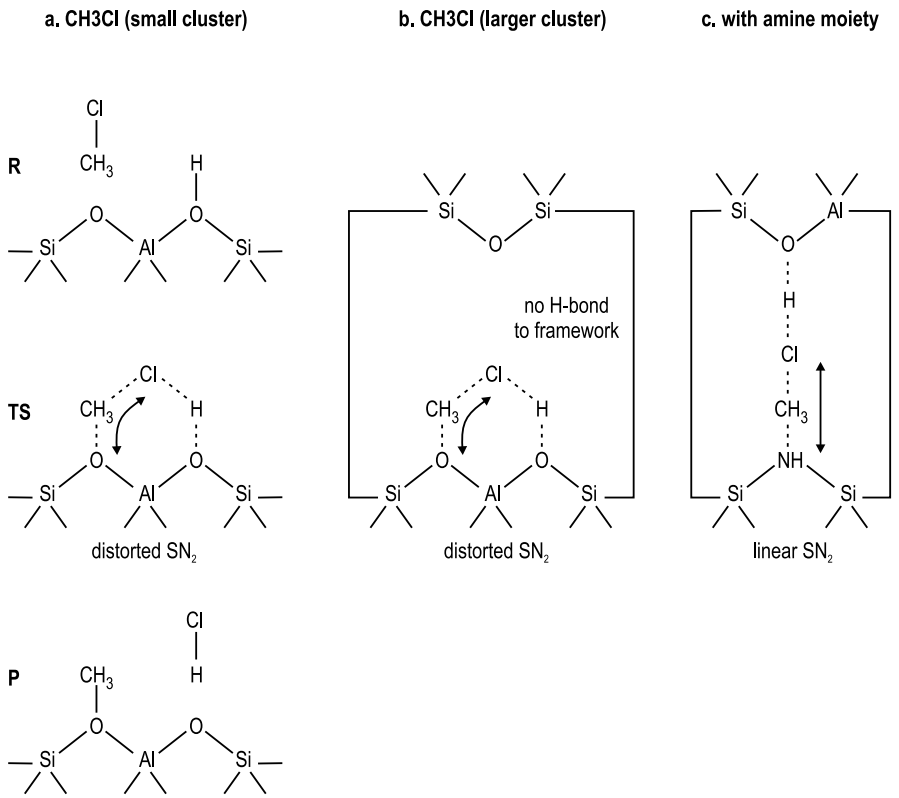

Figure 4.8: Reaction pathways to methoxide or methylammonium formation from chloromethane, illustrating the importance of an additional basic site.

Section 4.3.2, two effects contribute to the stability of the methoxide or methylammonium group: basicity of the basic X site (X=O or NH) and the energy needed for charge separation. These effects cancel each other out for the N2 cluster, and geometrical features lie at the origin of the lower barrier instead.

As can be seen in Figure 4.8, the crucial difference between cluster N2 and cluster O1 (defined in Figure 4.6) lies in the geometry of the transition state: spanning two tetrahedral sites is energetically favorable to constraining the reaction to a single T-site [art. 4.6]. The strong basicity of the nitrogen atom does not directly lower the reaction barrier, but merely provides a more accessible basic site for a

typical SN_2 reaction to occur. Just as in the case of an assisting molecule, the profit of a linear transition state results in a significant lowering of the energy barrier by approximately 30 kJ mol^{-1} [art. 4.7].

Ethene

The protonation of olefins like ethene starts with the formation of a weak π-complex, after which the olefin double bond is attacked by the zeolite acid proton. Upon chemisorption, a covalent C(olefin)-O(zeolite) bond is formed, producing a stable ethoxide σ-complex. The reaction mechanism differs from previously discussed examples like chloromethane and methanol, as it does not occur through a SN_2 mechanism. For this reaction, charge separation dominates reaction kinetics, while the transition state on a single tetrahedron is barely strained [art. 4.7]. As a result, the fully oxygen surrounded zeolite has the lowest activation barriers. Since the main ingredient for activation barrier lowering, i.e. relief of steric hindrance in the transition state, does not occur it is clear that the amine moiety will not improve the catalytic performance.

In conclusion, it seems that the amine moiety can only provide an improvement to the catalyst if it can supply a more favorable transition state geometry for alkylammonium formation compared to alkoxide formation. For the three molecules tested, this is only the case for chloromethane, not for methanol nor for ethene.

4.3.5 Test set for theoretical procedures

In collaboration with other researchers at the Center for Molecular Modeling, the validity of a variety of DFT-based reactivity descriptors [123] and their level-of-theory dependence has been tested on the amine-functionalized zeolites. The results will not be explicitly discussed here, but we refer the interested reader to [art. 4.8] and [art. 4.9], which are included at the end of this chapter.

4.4 Conclusions

This initial study has investigated how methylene and amine units substituting for oxygen atoms in silicates and aluminosilicates alter the fundamental properties on a atomic level. We can summarize our main results as follows:

When methylene functionalization is combined with an aluminum defect, the methylene units do not noticeably influence the proton affinity. However, a proton-hopping study shows that the methylene site is much more prone to protonation than a neighboring basic oxygen site, resulting in cleavage of the framework and creation of terminally bound CH_3 groups. Based on these results it is clear that methylene-aluminosilica will contain not only methylene bridges: several end-standing methyl groups will inevitably be formed as well (in agreement with experimental observations). If the charge is compensated by alkali metal ions, steric obstruction by the methylene moiety weakens the bond between metal ion and aluminum site. Finally, a study on the adsorption of water and ammonia in methylenesilica systems demonstrates how the methylene group is capable of slightly boosting the originally low adsorption energy for both probe molecules, creating regions of somewhat varying adsorption strength.

A study of proton mobility in amine-modified materials revealed that amine substitutions on the aluminum tetrahedron are also easily protonated, resulting in a weakly acidic NH_2 group and a moderately basic oxygen atom. But if the presence of nitrogen-aluminum bridges could be minimized during synthesis, a proton will only sporadically poison the nitrogen sites and the two strong functional groups are able to co-exist. As can be seen from heats of deprotonation, amine modification of the zeolite does not alter the acidic properties of the hydroxyl group. Surprisingly, the effect of charge separation between a positively charged alkylammonium species and the $[AlO_4]^-$ tetrahedron and the effect of a stronger basic nitrogen atom compared to an oxygen atom, simply cancel each other out and the amine site does not necessarily promote alkylammonium formation. Because of the delicate balance between these two effects, geometric features of the transition state will determine whether amine functionalization enhances catalytic performance or not. Lowering of activation barriers is restricted to reactions where transition states centered on the aluminum defect are highly strained. For these type of reactions, the possibility of a multi-center transition state spanning two adjacent T-sites permits an energetically preferable configuration.

In conclusion, it is certainly worth synthesizing both methylene and amine modified zeolites in the light of novel catalytic materials. Organic functionalization of zeolites will provide a huge advance in future modification of catalysts for specific reactions. A combination of theoretical work, experiments and improved synthesis techniques is needed, though, to bring us a step closer to the ultimate goal of organosilicas that are tailored to industrial processes. Ideally, this would

lead finally to the creation of true zeozyme catalysts.

Published papers on organic functionalization

article 4.5

D. Lesthaeghe, G. Delcour,
V. Van Speybroeck, G.B. Marin,
M. Waroquier

Theoretical study on the alteration of fundamental zeolite properties by methylene functionalization

Microporous Mesoporous Mater. 96, **2006**, 350-356

Breaking it up: The effect of organic functionalizations on fundamental properties in organosilicas is probed from a microscopic viewpoint. The simplest functionalization of a bridging methylene unit is modeled in a zeolite framework to serve as a model system for more complex organic moieties and other structures. The combination of a methylene bridge with aluminum impurities is found to cleave the hybrid organic-inorganic lattice.

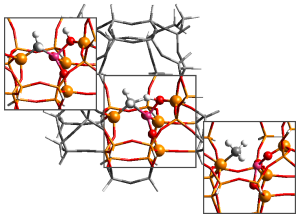

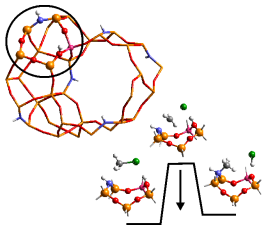

I'm in, and I'm in to win: Amine-substituted zeolites suggest novel reaction pathways to alkylammonium formation that are not centralized solely around the aluminum site. Significant lowering of reaction barriers as opposed to alkoxide formation in full-oxygen zeolites is observed. However, the number of Al-NH-Si bridges needs to be minimized to prevent protonation of the amine group.

article 4.6

D. Lesthaeghe, V. Van Speybroeck,
M. Waroquier

Efficient use of bifunctional acid-base properties for alkylammonium formation in amine-substituted zeolites

J. Am. Chem. Soc. 126, **2004**, 9162-9163

article 4.7

D. Lesthaeghe, V. Van Speybroeck, G.B. Marin, M. Waroquier

DFT investigation of alkoxide vs. alkylammonium formation in amine-substituted zeolites

J. Phys. Chem. B 109, **2005**, 7952-7960

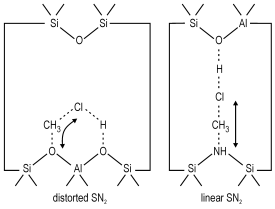

Walk the line: Building on [art. 4.6], alkylammonium and alkoxide formation are also investigated for MTO-related species like methanol and ethene. The amine moiety only lowers barriers for SN2 type reactions with otherwise highly strained transition states, as is the case for chloromethane. By introducing additional basic sites, this enables optimal transition states incorporating various T-sites.

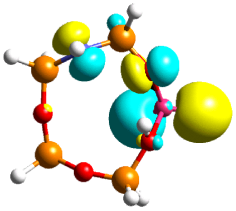

Between a rock and a hard place: Amine-modified zeolites provide an ideal test set to evaluate the overall performance of DFT-based reactivity descriptors. The reactions with CH_3OH, CH_3Cl, C_2H_4 and C_3H_6 are intermediately hard–hard and, therefore, mainly charge-controlled. This is confirmed by the success of the atomic charges and the electrostatic interaction energy at the acid site as descriptors of regio-selectivity.

article 4.8

K. Hemelsoet, D. Lesthaeghe, V. Van Speybroeck, M. Waroquier

Bifunctional acid-base catalyzed reactions in zeolites from the HSAB viewpoint

Chem. Phys. Lett. 419, **2006**, 10-15

article 4.9

K. Hemelsoet, D. Lesthaeghe, V. Van Speybroeck, M. Waroquier

Global DFT-based reactivity indicators: an assessment of theoretical procedures in zeolite catalysis

J. Phys. Chem. C 111, **2007**, published online

To the next level: Building on [art. 4.8], both functional and basis set level-of-theory dependence of global reactivity descriptors are investigated for typical reactions in amine functionalized zeolites. Reactivity sequences, based on global softness differences as well as activation hardness values, are generally found to be independent of the level of theory whenever a DFT functional is used.

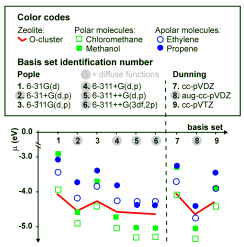

4.5

Theoretical study on the alteration of fundamental zeolite properties by methylene fuctionalization

D. Lesthaeghe, G. Delcour, V. Van Speybroeck, G.B. Marin, M. Waroquier
Microporous and Mesoporous Materials 96, **2006**, 350-356.

---

article 4.5

D. Lesthaeghe, G. Delcour,
V. Van Speybroeck, G.B. Marin,
M. Waroquier

Theoretical study on the alteration of fundamental zeolite properties by methylene functionalization

Microporous Mesoporous Mater. 96,
2006, 350-356

Breaking it up: The effect of organic functionalizations on fundamental properties in organosilicas is probed from a microscopic viewpoint. The simplest functionalization of a bridging methylene unit is modeled in a zeolite framework to serve as a model system for more complex organic moieties and other structures. The combination of a methylene bridge with aluminum impurities is found to cleave the hybrid organic-inorganic lattice.

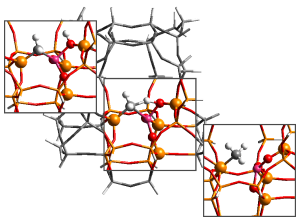

Available online at www.sciencedirect.com
ScienceDirect
Microporous and Mesoporous Materials 96 (2006) 350–356
MICROPOROUS AND MESOPOROUS MATERIALS
www.elsevier.com/locate/micromeso

Theoretical study on the alteration of fundamental zeolite properties by methylene functionalization

David Lesthaeghe [a,*], Gaella Delcour [a,1], Veronique Van Speybroeck [a], Guy B. Marin [b], Michel Waroquier [a,*]

[a] *Center for Molecular Modeling, Ghent University, Proeftuinstraat 86, B-9000 Gent, Belgium*
[b] *Laboratorium voor Petrochemische Techniek, Ghent University, Krijgslaan 281-S5, B-9000 Gent, Belgium*

Received 24 May 2006; received in revised form 13 July 2006; accepted 13 July 2006
Available online 1 September 2006

Abstract

Following the recent boost of papers reporting synthesis of organic functionalized microporous and mesoporous materials, a detailed theoretical study was performed to probe the effect of organic functionalizations on certain fundamental properties in organosilicas from a microscopic viewpoint. The simplest functionalization of a bridging methylene unit was modeled in a zeolite MFI-type framework to serve as a model system for more complex organic moieties and other structures. Calculated adsorption energies for H_2O and NH_3 in methylenesilica reveal that the methylene functionalization increases the strength of the interaction of both probe molecules with the zeolite framework. Investigation of the combination of an ion-exchanged aluminum site containing a CH_2-bridge demonstrates how the methylene moiety creates a steric obstruction for adsorbed alkali metal ions such as Li, Na and K, resulting in a weaker bond between these ions and the aluminum site. Finally, a study of proton mobility from a Brønsted acid site to a neighboring methylene bridge reveals that the acid proton will most likely migrate from the basic oxygen bridge to the methylene substitution. This implies that the combination of methylene moieties with aluminum impurities will lead to terminally bound methyl groups and cleavage of the hybrid organic–inorganic lattice.
© 2006 Elsevier Inc. All rights reserved.

Keywords: Organosilicas; Organic functionalized zeolites; Density functional theory; ONIOM method

1. Introduction

Recent efforts in extending the range of applications for both structured microporous and mesoporous silicas include the incorporation of well-chosen organic functionalizations in the framework [1,2]. Over the last couple of years this field has exploded, culminating in numerous functional mesostructures that have been successfully synthesized [3,4]. However, the number of papers reporting successful synthesis of these novel materials exceeds by far those actually discussing the seemingly promising properties in catalysis, sorption, separation and beyond. A detailed understanding on how these novel materials differ from traditional materials is, however, essential for the next step of putting them to practical use. Theoretical calculations using density functional theory (DFT) can provide additional insights into how the organic groups control fundamental properties over and above the insights provided by experiments. In addition they may even provide guidelines for the design of new materials [5,6]. On a microscopic level, DFT calculations are ideally suited as direct comparison with non-functionalized materials is relatively straightforward.

The simplest organic functionalization is a methylene moiety, which is isoelectronic with oxygen and fits perfectly

* Corresponding authors. Tel.: +32 9 264 65 59; fax: +32 9 264 66 97 (M. Waroquier).
E-mail addresses: david.lesthaeghe@ugent.be (D. Lesthaeghe), michel.waroquier@ugent.be (M. Waroquier).
[1] Present address: Cytec Surface Specialties, N.V., Anderlechtstraat 33, B-1620 Drogenbos, Belgium.

1387-1811/$ - see front matter © 2006 Elsevier Inc. All rights reserved.
doi:10.1016/j.micromeso.2006.07.020

for bridging two silicon atoms to form a functional ≡Si–CH_2–Si≡ group. Just recently, however, have different types of materials containing this functional group, including organosilica cages [7] and periodic mesoporous organosilicas (PMOs) [8,9], been synthesized successfully. Because of the simplicity of this functional group, a Japanese research team has even succeeded in incorporating methylene units into LTA and MFI zeolite frameworks creating zeolites with an organic lattice (ZOLs) [10,11]. Quite spectacularly, up to 30% of the silicon atoms were functionalized with organic bridging methylene or terminal methyl groups, while both pure silicas and aluminosilicas have been prepared. Inspired by the synthesis of methylene-substituted zeolites. Astala et al. provided theoretical evidence through periodic calculations that zeolite frameworks can indeed accommodate both methylene and amine groups at high concentrations with minimal strain [12]. However, their results failed to explain the intrapore ≡Si–CH_3 moieties observed by Yamamoto et al. [10].

Following our previous theoretical work on amine-modified zeolites [5], we will focus here on how these methylene substitutions alter the fundamental adsorption and ion-exchange properties in pure silica and aluminosilica zeolites from a microscopic point of view. In addition, a study of proton mobility in these materials will provide a possible explanation for the experimentally observed terminally bound methyl groups [10]. This initial study may also serve as a springboard to more advanced studies on other organic functionalized microporous and mesoporous materials. Even though the methylene groups under study are assumed to be catalytically inactive, methylenesilica may act as a useful precursor for additional chemical modifications, possibly leading to a whole new class of versatile microporous and mesoporous hybrid materials.

2. Computational details

Geometry optimizations for minimum energy and transition-state structures were performed within the Gaussian03 software package [13]. Zygmunt et al. [14] assessed the applicability of various readily available density functionals for studying molecular adsorption in small zeolite clusters and found that Becke's three-parameter B3LYP exchange-correlation functional [15] yields intermolecular energies and vibrational frequencies similar to those obtained using MP2, concluding that the B3LYP functional is the best choice for DFT treatment of small zeolite clusters.

However, the bulk electrostatic effects induced by the zeolite framework should also be included. Even though in this study small 5T cluster calculations provided a sneak preview into the right qualitative trends, a large cluster model was necessary to calculate correct adsorption energies [16]. Small DFT cluster results were, therefore, used as a starting point for more advanced calculations using the 2-layered ONIOM approach, as developed by Morokuma and co-workers [17]. Recently Solans-Monfort et al. [18] compared adsorption properties of NH_3 and H_2O in acidic chabazite, using both the ONIOM2 scheme and fully periodic ab initio calculations, and found that long-range effects do not extend too far, even when ion pairs are involved. Their major conclusion states that the ONIOM(B3LYP:MNDO) level provides similar geometries to those obtained through periodic calculations, while accurate adsorption energies can be obtained through a single-point energy calculation at the ONIOM(B3LYP:HF) level of theory on the obtained ONIOM(B3LYP:MNDO) geometries. A parallel study by Fermann et al. using the Universal Force Field as low level of theory [19], confirms that the ONIOM scheme provides a computationally attractive alternative to more expensive periodic calculations.

We based our calculations on the scheme developed by Solans-Monfort et al., and used the double ζ level basis set 6-31 + g(d), which includes polarization and diffuse functions, for both the DFT and HF calculations. Using standard notation LOT-E//LOT-G (LOT-E and LOT-G being the electronic levels of theory used for the energetics and geometry optimizations, respectively), all results discussed in this paper were obtained from B3LYP/6-31 + g(d):HF/6-31 + g(d)//B3LYP/6-31 + g(d):MNDO calculations.

For this hybrid high/low-level study the active site was modeled by a 5T cluster (or an extended 8T cluster for the adsorption of water and ammonia), surrounded by the low-level region. Both regions contain a total of 46T-atoms (T = Si or Al). The combined high/low-level zeolite clusters were cut out of the MFI crystallographic structure. This 46T model is considered to be large enough to cover all important framework effects on both the active site and the adsorbate [20]. The pure silica 46T cluster model is shown in Figs. 1 and 2, with low level and high level of theory atoms represented in the cylinder format and the ball + stick format, respectively.

Dangling bonds, which in the authentic zeolite would connect the cluster with the rest of the solid, were saturated with hydrogen atoms in order to preserve electrostatic neutrality and spin multiplicity. These hydrogen atoms were held fixed in crystallographic positions to prevent collapse of the cage formed by the channel intersection, while all other high-level and low-level atoms were left unconstrained. The methylene functionalization was located at the intersection of the main and sinusoidal channels, thus easily accessible to adsorbates. For the combination of a methylene unit with an aluminum defect, the charge-compensating acid proton and alkali ions were also placed near this easily accessible site.

3. Results and discussion

3.1. Adsorption

To our knowledge there exists no previous theoretical work where the adsorption properties of methylene-substituted

zeolites are discussed, as Astala and Auerbach [12] calculated NH_3 and BF_3 adsorption only in amine-modified zeolites. In this paper we investigate and compare the adsorption properties of species like H_2O and NH_3 in methylene functionalized zeolites to non-functionalized zeolites, as both species are considered typical probe molecules in zeolite chemistry [18,21]. As we will demonstrate in a later paragraph, an investigation of proton hopping in methylene-functionalized aluminosilicas reveals that the combination of an acid proton and a methylene moiety near the same active site is unstable with respect to cleavage of the organic–inorganic framework. Because of this, we will limit ourselves to the adsorption of both species in purely siliceous materials.

The adsorption of a single water molecule in pure silicate is visualized in Fig. 1. For the non-functionalized zeolite, the water molecule forms two hydrogen bonds to framework oxygen atoms. The adsorption energy of −21.7 kJ/mol, defined as $E_{ads} = E[ZEO\cdots X] - E[ZEO] - E[X]$ with $X = H_2O$ and NH_3 in Table 1, is in accordance with the hydrophobic nature of purely siliceous zeolites. However, when a neighboring framework oxygen atom is replaced by a methylene bridge, this gives rise to a new hydrogen bond between the H_2O–oxygen atom and one

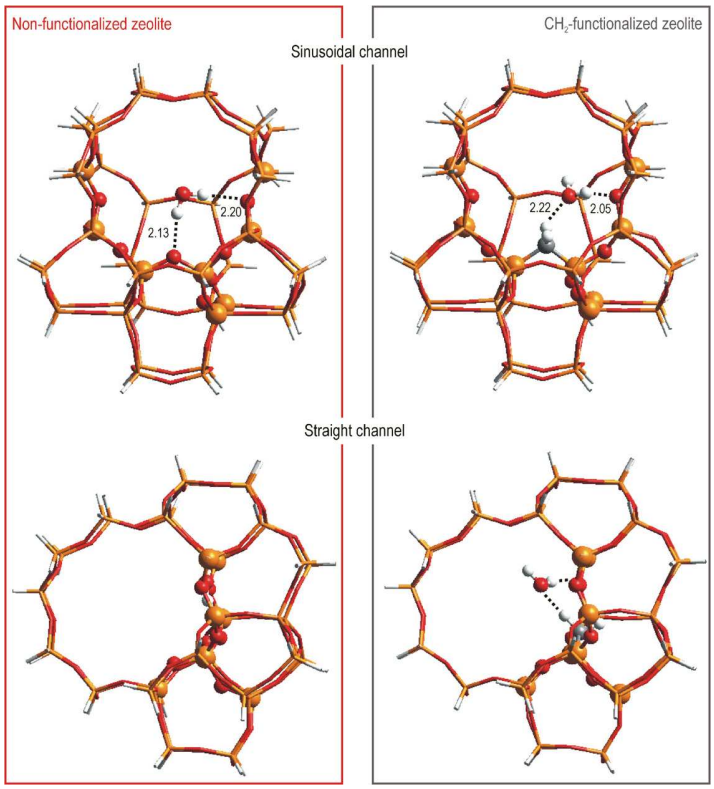

Fig. 1. Optimized structures for the adsorption of water in the silica MFI framework at the B3LYP/6-31 + g(d):HF/6-31 + g(d)//B3LYP/6-31 + g(d):MNDO level of theory. Snapshots from both weak and stronger adsorption complexes, in non-functionalized and methylene-functionalized zeolites, respectively, were taken from different angles (along sinusoidal and straight channels). Low level of theory atoms are represented in the cylinder format, whereas high level of theory atoms are depicted in the ball + stick representation. All distances are in Å.

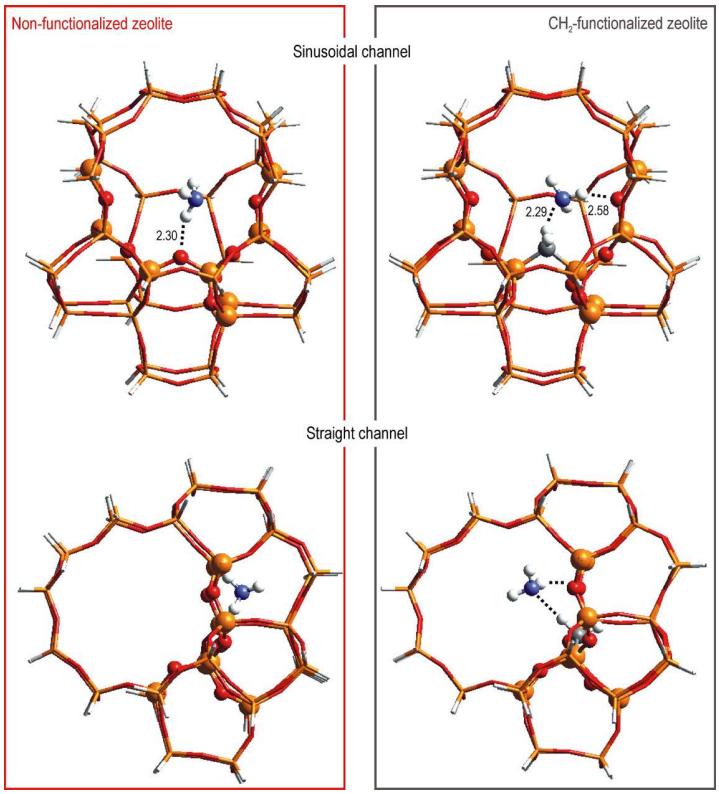

Fig. 2. Optimized structures for the adsorption of ammonia in the silica MFI framework at the B3LYP/6-31 + g(d):HF/6-31 + g(d)//B3LYP/6-31 + g(d):MNDO level of theory. Snapshots from both weak and stronger adsorption complexes, in non-functionalized and methylene-functionalized zeolites respectively, were taken from different angles (along sinusoidal and straight channels). Low level of theory atoms are represented in the cylinder format, whereas high level of theory atoms are depicted in the ball + stick representation. All distances are in Å.

of the CH_2–hydrogen atoms. This results in a substantial increase in adsorption energy from −21.7 to −33.2 kJ/mol. The organic moiety modifies the zeolite to be less hydrophobic, resulting in a new material containing regions with slightly varying degrees of hydrophobicity. The concentration of methylene moieties will be crucial to the properties on bulk level.

Table 1
Calculated adsorption energies (in kJ/mol) of water and ammonia at the B3LYP/6-31 + g(d):HF/6-31 + g(d)//B3LYP/6-31 + g(d):MNDO level of theory

Silica (kJ/mol)	Adsorption energy	
	≡Si–O–Si–O–Si≡	≡Si–CH_2–Si–O–Si≡
H_2O	−21.7	−33.2
NH_3	−15.7	−33.2

Compared to the non-functionalized zeolite (≡Si–O–Si–O–Si≡), adsorption energies are significantly enhanced in the methylene-functionalized zeolite (≡Si–CH_2–Si–O–Si≡).

For the adsorption of a single ammonia molecule, a similar effect is observed (Table 1). As shown in Fig. 2, ammonia in the non-functionalized zeolite forms a weak hydrogen bond with a framework oxygen atom, whereas the nitrogen atom actively participates in a stronger hydrogen bond for the methylene-functionalized zeolite. This results in a more strongly bound adsorption complex from −15.7 kJ/mol to −33.2 kJ/mol. As in the case of water, the methylene-functionalized zeolite will contain different areas

which vary in adsorption properties according to methylene content.

3.2. Charge compensation

The charge induced by the aluminum defect in aluminosilicas can be balanced by a positively charged acid proton, or by extra-framework alkali metal ions like Li^+, Na^+ and K^+. These cations are accessible through the micropores and are crucial to zeolites' large ion-exchange capacity and their utility as size- or shape-selective catalysts. The combination of methylene functionalization with aluminum defects raises new questions: How will the CH_2 group influence zeolite acidity? What effect will the CH_2 group have on cation-exchange? To resolve these issues, we calculated adsorption energies between a negatively charged cluster model containing the ≡Si–CH_2–Al–O–Si≡ active site and the charge-compensating cation or proton as $E_{ads} = E[\text{ZEO-Y}] - E[\text{ZEO}^-] - E[\text{Y}^+]$ with $\text{Y} = \text{H}^+$, Li^+, Na^+ and K^+. Numerical results for the adsorption energies and geometric parameters are shown in Tables 2 and 3, respectively, while close-ups of the stable geometries are shown in Fig. 3. These energies would have been different from a quantitative point of view if solvent effects had been taken into account. However, from our perspective we are mainly interested in qualitative changes induced by the methylene moiety, rather than an accurate reproduction of experimental data.

From Mulliken charge analysis on all optimized structures (including those discussed in the other paragraphs), we systematically observe that the carbon atom is negatively charged by −1.0, both in methylenesilica and methylene-aluminosilica. This result is similar to what has been observed experimentally in small silicon carbide clusters [22]. However, this substantial charge on the carbon atom does not strengthen the interaction with positively charged ions. The adsorption energy of the alkali metals is systematically reduced by a shift of approximately 10–20 kJ/mol. The ions will be less bound through the methylene functionalization, as the steric hindrance of the methyl group obstructs ideal positioning of the alkali ion. This is also clear from the geometric parameters in Table 3, where especially lithium and sodium shift from an O_1–Al–O_2 coordination (sinusoidal channel) to the O_2–Al–O_3 position (straight channel). Nevertheless, ion-exchanged methylene-modified aluminosilicas are perfectly capable of maintaining several stable active sites containing both methylene and alkali ion functionalities.

Table 2
Calculated proton affinity and binding energy (in kJ/mol) of extra-framework alkali metal ions at the B3LYP/6-31 + g(d):HF/6-31 + g(d)//B3LYP/6-31 + g(d):MNDO level of theory

Aluminosilica (kJ/mol)	Adsorption energy	
	[≡Si–O–Al–O–Si≡]$^-$	[≡Si–CH_2–Al–O–Si≡]$^-$
H^+	−1147.7	−1146.6
Li^+	−534.0	−516.3
Na^+	−455.2	−446.1
K^+	−391.7	−377.2

Comparison with the non-functionalized zeolite (≡Si–O–Al–O–Si≡) reveals that steric hindrance weakens the alkali-framework bond for the methylene-functionalized zeolite (≡Si–CH_2–Al–O–Si≡).

Table 3
Geometric parameters for extra-framework alkali metal ions adsorbed in the ZSM-5 cage at the B3LYP/6-31 + g(d):HF/6-31 + g(d)//B3LYP/6-31 + g(d):MNDO level of theory

Aluminosilica	Non-functionalized zeolites		
	O_1–Al–O_2–X dihedral (°)	O_2–Al–O_3–X dihedral (°)	Al–X distance (Å)
Li^+	16.8	48.9	2.57
Na^+	23.8	50.2	2.91
K^+	54.7	49.3	3.09
	Methylene-functionalized zeolites		
	C_1–Al–O_2–X dihedral (°)	O_2–Al–O_3–X dihedral (°)	Al–X distance (Å)
Li^+	47.3	24.2	2.56
Na^+	49.1	35.0	2.84
K^+	50.1	43.7	3.21

3.3. Proton mobility

At first glance, the proton affinity seems to be hardly affected by the neighboring methylene moiety (Table 2). However, in our previous work on amine-modified zeolites, we discovered that the amine moiety plays a major role in the energetics of proton mobility [5,23]. Moreover, we concluded that the amine moiety is systematically protonated if it is located on the aluminum tetrahedron. For acid methylene-substituted aluminosilicas, however, proton hopping is an issue that is yet to be discussed. In Fig. 4, the proton jump between two neighboring basic oxygen atoms on an aluminum site in a non-functionalized zeolite is compared to the equivalent proton jump in a methylene-functionalized zeolite.

For the non-functionalized zeolite, this particular proton jump exhibits a forward barrier of approximately 50 kJ/mol and a reverse barrier of almost 80 kJ/mol. The proton jump considered is clearly exothermic, implying that the proton is bound more strongly to the central oxygen atom. For the methylene-functionalized zeolite, the reaction barrier for proton migration remains almost unaltered (approximately 50 kJ/mol), while the reaction energy is further reduced to −61.2 kJ/mol. Apparently, the proton is much more likely to migrate to the carbon atom, forming an intrapore methyl group and cleaving the carbon–aluminum bond. The negative charge on the carbon atom that we systematically observed explains the preferential movement of the proton. The reaction whereby a terminal methyl group is formed is more favorable than the reverse reaction, which might be an explanation for the methyl end-groups in the

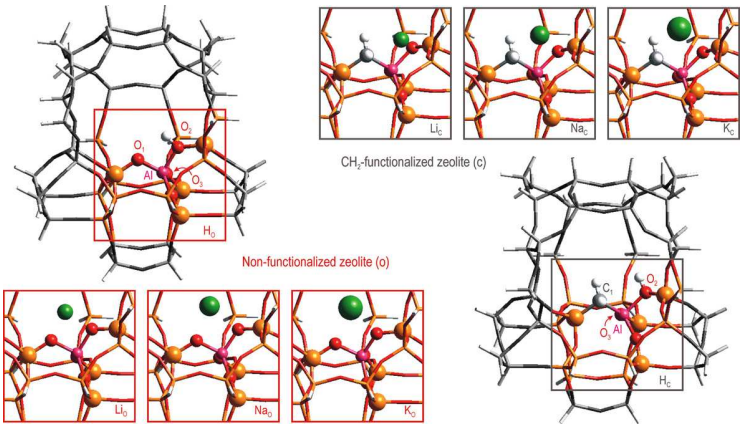

Fig. 3. Optimized structures for different charge-compensating ions (acid proton, lithium, sodium and potassium) near an aluminum defect at the B3LYP/6-31 + g(d):HF/6-31 + g(d)//B3LYP/6-31 + g(d):MNDO level of theory. Low level of theory atoms are represented in the cylinder format, whereas high level of theory atoms are depicted in the ball + stick representation. The methylene moiety slightly distorts the optimal arrangement for the alkali ions, improving their exchangeability.

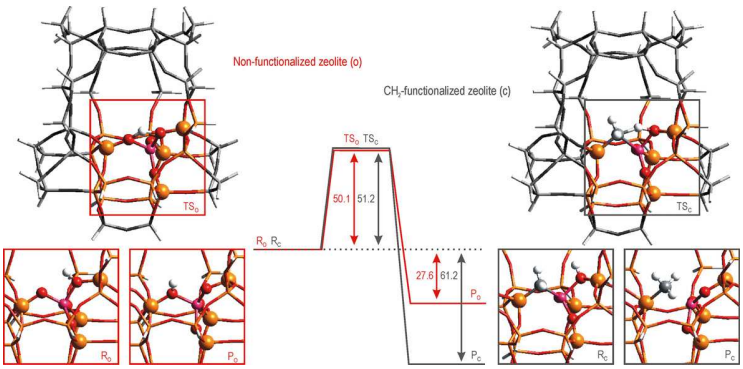

Fig. 4. Stationary points for proton hopping in both non-functionalized zeolite and methylene-functionalized zeolite at the B3LYP/6-31 + g(d):HF/6-31 + g(d)//B3LYP/6-31 + g(d):MNDO level of theory. Low level of theory atoms are represented in the cylinder format, whereas high level of theory atoms are depicted in the ball + stick representation. In the functionalized zeolite, the proton is more likely to create a terminally bound methyl group, resulting in cleavage of the framework.

organo-aluminosilica structures as observed experimentally by Yamamoto et al. [11]. This effect could not be previously explained through framework stability considerations in periodic calculations [12]. Considering proton mobility in methylene-functionalized zeolites, it is obvious that the combination of a methylene moiety with an aluminum defect is likely to result in cleavage of the zeolite lattice.

4. Conclusions

This initial study investigates how methylene units substituting for oxygen atoms in silicas and aluminosilicas alter the fundamental properties on a microscopic level. Density functional theory calculations provide important qualitative insight into how the organic groups control guest molecule adsorption, ion exchange and proton mobility.

Our calculations show that, when methylene functionalization is combined with an aluminum defect, the methylene units do not noticeably influence the proton affinity. However, a proton-hopping study shows that the methylene site is much more prone to protonation than a neighboring basic oxygen site, resulting in cleavage of the framework and creation of terminally bound CH_3 groups. Based on these results it is clear that, independent from specific synthesis details, methylene-aluminosilica will contain not only methylene bridges but inevitably several end-standing methyl groups will be formed as well.

Our study on the adsorption properties of alternative charge-compensating alkali metal ions in methylene-aluminosilica shows that steric obstruction of the methylene moiety weakens the bond between metal ion and aluminum site. This weakening is, however, limited to approximately 10–20 kJ/mol. Finally, a study on the adsorption of water and ammonia in methylenesilica systems demonstrates how the methylene group is capable of slightly boosting the originally low adsorption energy for both probe molecules, creating regions of somewhat varying adsorption strength.

This initial study on the effects of methylene substitutions in organosilicas has aimed at improving insight on a microscopic level. A combination of theoretical work, experiments and improved synthesis techniques is needed, however, to bring us a step closer to the ultimate goal of organosilicas that are tailored to industrial processes.

Acknowledgments

This work is supported by the Fund for Scientific Research – Flanders (FWO) and the Research Board of Ghent University.

References

[1] T. Asefa, M.J. MacLachlan, N. Coombs, G.A. Ozin, Nature 402 (1999) 867.
[2] S. Inagaki, S. Guan, T. Ohsuna, O. Terasaki, Nature 416 (2002) 304.
[3] F. Fajula, A. Galarneau, F. Di Renzo, Micropor. Mesopor. Mater. 82 (2005) 227.
[4] F. Hoffmann, M. Cornelius, J. Morell, M. Fröba, Angew. Chem. 118 (2006) 3290;
Angew. Chem. Int. Ed. 45 (2006) 3216.
[5] D. Lesthaeghe, V. Van Speybroeck, M. Waroquier, J. Am. Chem. Soc. 126 (2004) 9162.
[6] B. Chan, L. Radom, J. Am. Chem. Soc. 128 (2006) 5322.
[7] A. Shimojima, K. Kuroda, Chem. Commun. (2004) 2672.
[8] K. Landskron, B.D. Hatton, D.D. Perovic, G.A. Ozin, Science 302 (2003) 266.
[9] X.Y. Bao, X. Li, X.S. Zhao, J. Phys. Chem. B 110 (2006) 2656.
[10] K. Yamamoto, Y. Sakata, Y. Nohara, Y. Takahashi, T. Tatsumi, Science 300 (2003) 470.
[11] K. Yamamoto, Y. Nohara, Y. Domon, Y. Takahashi, Y. Sakata, J. Plevert, T. Tatsumi, Chem. Mater. 17 (2005) 3913.
[12] R. Astala, S.M. Auerbach, J. Am. Chem. Soc. 126 (2004) 1843.
[13] M.J. Frisch, G.W. Trucks, H.B. Schlegel, G.E. Scuseria, M.A. Robb, J.R. Cheeseman, J.A. Montgomery Jr., T. Vreven, K.N. Kudin, J.C. Burant, J.M. Millam, S.S. Iyengar, J. Tomasi, V. Barone, B. Mennucci, M. Cossi, G. Scalmani, N. Rega, G.A. Petersson, H. Nakatsuji, M. Hada, M. Ehara, K. Toyota, R. Fukuda, J. Hasegawa, M. Ishida, T. Nakajima, Y. Honda, O. Kitao, H. Nakai, M. Klene, X. Li, J.E. Knox, H.P. Hratchian, J.B. Cross, V. Bakken, C. Adamo, J. Jaramillo, R. Gomperts, R.E. Stratmann, O. Yazyev, A.J. Austin, R. Cammi, C. Pomelli, J.W. Ochterski, P.Y. Ayala, K. Morokuma, G.A. Voth, P. Salvador, J.J. Dannenberg, V.G. Zakrzewski, S. Dapprich, A.D. Daniels, M.C. Strain, O. Farkas, D.K. Malick, A.D. Rabuck, K. Raghavachari, J.B. Foresman, J.V. Ortiz, Q. Cui, A.G. Baboul, S. Clifford, J. Cioslowski, B.B. Stefanov, G. Liu, A. Liashenko, P. Piskorz, I. Komaromi, R.L. Martin, D.J. Fox, T. Keith, M.A. Al-Laham, C.Y. Peng, A. Nanayakkara, M. Challacombe, P.M.W. Gill, B. Johnson, W. Chen, M.W. Wong, C. Gonzalez, J.A. Pople, Gaussian 03 Revision C.02, Gaussian, Inc., Wallingford, CT, 2004.
[14] S.A. Zygmunt, R.M. Mueller, L.A. Curtiss, L.E. Iton, J. Mol. Struct. – Theochem. 430 (1998) 9.
[15] A.D. Becke, J. Chem. Phys. 98 (1993) 5648.
[16] D. Lesthaeghe, V. Van Speybroeck, G.B. Marin, M. Waroquier, Chem. Phys. Lett. 417 (2006) 309.
[17] S. Dapprich, I. Komaromi, K.S. Byun, K. Morokuma, M.J. Frisch, J. Mol. Struct. – Theochem 461 (1999) 1.
[18] X. Solans-Monfort, M. Sodupe, V. Branchadell, J. Sauer, R. Orlando, P. Ugliengo, J. Phys. Chem. B 109 (2005) 3539.
[19] J.T. Fermann, T. Moniz, O. Kiowski, T.J. McIntire, S.M. Auerbach, T. Vreven, M.J. Frisch, J. Chem. Theor. Comp. 1 (2005) 1232.
[20] C. Raksakoon, J. Limtrakul, J. Mol. Struct. – Theochem 631 (2003) 147.
[21] D.H. Olson, W.O. Haag, W.S. Borghard, Micropor. Mesopor. Mater. 35–36 (2000) 435.
[22] M.N. Huda, A.K. Ray, Phys. Rev. A 69 (2004). Art. No. 011201.
[23] D. Lesthaeghe, V. Van Speybroeck, G.B. Marin, M. Waroquier, J. Phys. Chem. B 109 (2005) 7952.

4.6

Efficient use of bifunctional acid-base properties for alkylammonium formation in amine-substituted zeolites

D.Lesthaeghe, V. Van Speybroeck, M. Waroquier
Journal of the American Chemical Society 126, **2004**, 9162-9163.

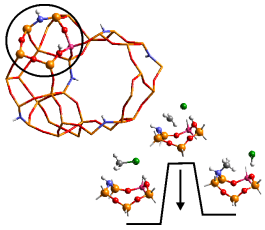

I'm in, and I'm in to win: Amine-substituted zeolites suggest novel reaction pathways to alkylammonium formation that are not centralized solely around the aluminum site. Significant lowering of reaction barriers as opposed to alkoxide formation in full-oxygen zeolites is observed. However, the number of Al-NH-Si bridges needs to be minimized to prevent protonation of the amine group.

article 4.6

D. Lesthaeghe, V. Van Speybroeck, M. Waroquier

Efficient use of bifunctional acid-base properties for alkylammonium formation in amine-substituted zeolites

J. Am. Chem. Soc. 126, **2004**, 9162-9163

J|A|C|S
COMMUNICATIONS

Published on Web 07/13/2004

Efficient Use of Bifunctional Acid−Base Properties for Alkylammonium Formation in Amine-Substituted Zeolites

David Lesthaeghe, Veronique Van Speybroeck, and Michel Waroquier*

Center for Molecular Modeling, Laboratory of Theoretical Physics, Ghent University, Proeftuinstraat 86, B-9000 Ghent, Belgium

Received March 24, 2004; E-mail: michel.waroquier@ugent.be

Zeolites are microporous crystalline aluminosilicates with a wide variety of properties and applications, due mainly to their shape selectivity and Brønsted acid sites. The range of their applications can be extended by a well-chosen organic functionalization,[1] altering the surface properties that control interaction with various guest species. Yamamoto et al. succeeded in synthesizing LTA and MFI frameworks with bridging oxygen atoms replaced by methylene groups.[2] Inspired by these results, Astala and Auerbach provided evidence at the atom and electron levels that zeolites can accommodate methylene and amine groups at high concentrations with minimal strain.[3] Theoretically determined adsorption energies of typical guest molecules such as NH_3 and BF_3 also indicate that Si−NH−Si groups are significantly stronger Lewis bases than the usual Si−O−Si bridges.[3] While only acid or base properties were monitored separately, the chemical behavior of neighboring Brønsted acid−Lewis base sites should be explored thoroughly before actual synthesis of these novel materials.

Many important zeolite-catalyzed reactions in the petrochemical industry include the protonation of olefins and alcohols. In situ spectroscopic studies of the interaction of Brønsted acid sites with adsorbed molecules have demonstrated that carbenium ions are not stable within zeolite cavities[4] but that protonation of adsorbed olefins and alcohols results in the formation of covalent alkoxide species. This was also confirmed by quantum mechanical cluster calculations.[5] It is believed that chemisorption proceeds in a concerted manner, controlled by a bifunctional (acid−base) mechanism, in which both the Brønsted acid site and Lewis base properties of an oxygen atom neighboring the acid site must be carefully balanced. While earlier research focused mainly on the zeolitic acid properties, the basicity of the Lewis base site could be drastically improved by appropriate isoelectronic substitution. Amine substitution in particular might promote alkylammonium formation, subsequently lowering corresponding reaction barriers. Up to now, neither theoretical nor experimental findings have confirmed this hypothesis. This communication provides strong evidence that reaction barriers of important catalytic processes can be significantly lowered by appropriate substitution.

Methanol to hydrocarbon (MTH) and methanol to olefin (MTO) conversions are well-known processes in the production of higher hydrocarbons and other value-added products. In light of sustainable energy production, early patents also report the possibility of converting halomethanes,[6] circumventing the costly formation of synthesis gas and reducing the number of byproducts. As a prototypical reaction step, we studied the first step of the dissociative mechanism in the conversion of chloromethane to hydrocarbons over acidic zeolite catalysts such as H-ZSM-5.[7] Using traditional zeolites, containing only O bridges, this first step leads to the formation of a surface methoxide species and hydrochloric acid, as shown in Figure 1a. Introducing NH bridges into the silicon/aluminum framework leads to the formation of a methylammonium species. The chemical properties and catalytic behavior of these

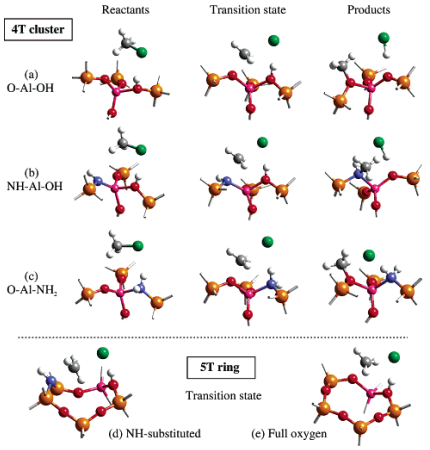

Figure 1. Stationary points for methoxide or methylammonium formation from various initial configurations.

novel materials are explored from a microscopic point of view, simulating the zeolite catalyst by four tetrahedral atoms. Even though these clusters do not fully represent the zeolitic environment, they have been shown to provide an adequate qualitative picture of chemical rearrangements that occur locally on the active site.[8] Full geometry optimizations and frequency calculations were performed within the Gaussian03 software package[9] using DFT, employing Becke's three-parameter B3LYP functional.[10] Activated complexes were validated to be true transition states and to exhibit only one imaginary frequency. Reaction barriers for full-oxygen clusters were calculated for reference purposes (Figure 1a). We stress the fact that we do not aim to perform a detailed study of this particular reaction mechanism; this reaction merely serves to illustrate the effect of amine substitutions on the reaction barrier.

Figure 1b shows a 4T cluster containing a single aluminum substitution with the NH group bridging silicon and aluminum, while a neighboring oxygen site is protonated. The energetic results of the adsorbed species and activated complexes are summarized in Table 1. The adsorption energy increases slightly due to the NH substitution (8.6 kJ/mol), but the main difference can be seen in the activation energy, which is substantially lowered (28.5 kJ/mol). As the process is concerted and the acidity of the OH group is not expected to be significantly altered, the decrease in activation energy must be ascribed to the stronger basic character of the NH group, hereby confirming the preliminary results of Astala and Auerbach.[3] The previous starting configuration is, however, not the energetically

10.1021/ja048305r CCC: $27.50 © 2004 American Chemical Society

Table 1. Energies of Adsorbed Species and Transition States for Methoxide or Methylammonium Formation[a]

B3LYP/6-31G(d)	4T cluster		
+ZPE	(a) O–Al–OH	(b) NH–Al–OH	(c) O–Al–NH_2
adsorbed reactants	−15.9	−24.5	−15.3
transition state	145.5	108.4	164.9
adsorbed products	−7.9	−105.1	60.3
energy barrier	161.4	132.9	180.2

	5T ring	
	(d) NH-substituted	(e) full oxygen
adsorbed reactants	−24.5	−16.6
transition state	93.0	153.4
adsorbed products	0.3	2.5
energy barrier	117.5	170.0

[a] All values are relative to the gas-phase reactants and are in kJ/mol.

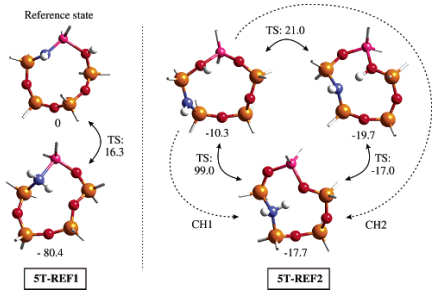

Figure 2. Energy diagram of proton mobility in amine-substituted 5T rings. All energies are in kJ/mol and relative to the reference state (including transition-state energies).

most probable one. Due to the strong basic character of the nitrogen atom, the acidic proton will migrate and create a mildly acidic NH_2 group (Figure 1c). The latter configuration is no longer characterized by optimal acid−base properties and gives rise to an increased energy barrier with respect to the reference material containing only O bridges. This dramatic change finds its origin in the natural neutralization of a zeolite with both strong acid and base sites to a zeolite with weak acid−base properties. Thus, in view of optimizing catalytic performance for typical acid−base reactions, there is no use in synthesizing this type of zeolite in which nitrogen and aluminum substitutions occur on the same T site.

In exploring efficient relative positions for the NH bridge and Al site, proton mobility must be addressed in these new materials. As shown in Figure 2, two 5T rings are considered: a first one with both OH and NH groups located at the same T atom (5T-REF1) and a second cluster with the nitrogen substitution occurring at a neighboring tetrahedral site (5T-REF2). In the 5T-REF1 cluster, amine protonation has a low activation energy and results in a thermodynamically favored configuration, characterized by non-preferable acid−base properties of the zeolite. By ensuring that the nitrogen substitution occurs in a neighboring tetrahedral site, the possibility of amine protonation decreases (5T-REF2). Proton jumps (through a channel indicated by CH1 in Figure 2) between OH- and NH-substituted sites located in the first coordination sphere of a Si atom are now highly activated (109.3 kJ/mol). The only efficient channel (CH2 in Figure 2) for proton mobility leading to a NH_2 substitution is achieved by a two-step process beginning with a common on-site jump between two oxygen atoms followed by a proton jump between an oxygen and nitrogen atom located at the opposite positions of the 5T ring.

From a different perspective, the 5T-REF2 cluster opens the possibility to new reaction pathways, involving two separate T sites. This could lead to more efficient use of the catalyst: larger molecules will not be restricted to a single tetrahedral site, but they will be able to detach the acid proton from the aluminum site while forming alkylammonium groups at nearby silicon sites. The transition state configuration of a possible reaction involving two T atoms is shown in Figure 1d. Due to the strong basic character of the nitrogen atom, the barrier for alkylammonium formation using two T sites is still substantially lower (52.5 kJ/mol) than for alkoxide formation on the Al site in the full-oxygen ring on one T site (Figure 1e). While the preliminary results on small clusters demonstrate the promising nature of these materials, more advanced calculations using larger 16T clusters yield a qualitatively similar effect (a difference in energy barriers of approximately 37 kJ/mol) and will be discussed in detail in a forthcoming publication.

In conclusion, microscopic calculations present strong evidence that amine-modified zeolites can successfully lower energy barriers for reactions in which both a Brønsted acid and a Lewis base site are involved. If the presence of nitrogen−aluminum bridges can be minimized during synthesis, a proton will only sporadically contaminate the nitrogen sites. Combining fullly oxygen-surrounded aluminum sites and nearby Si−NH−Si bridges opens the door to acid−base-catalyzed reactions that are not solely centralized around the aluminum defect but in which two T sites are involved. This unique way of providing more basic sites will improve the chances of an adsorbed molecule undergoing successful reaction, allowing more efficient use of the zeolitic acid site and the surrounding environment.

Acknowledgment. This work was supported by the Fund for Scientific Research−Flanders (FWO) and the Research Board of Ghent University.

References

(1) Jones, C. W. *Science* **2003**, *300*, 439−440.
(2) Yamamoto, K.; Sakata, Y.; Nohara, Y.; Takahashi, Y.; Tatsumi, T. *Science* **2003**, *300*, 470−472.
(3) Astala, R.; Auerbach, S. M. *J. Am. Chem. Soc.* **2004**, *126*, 1843−1848.
(4) (a) Aronson, M. T.; Gorte, R. J.; Farneth, W. E.; White, D. *J. Am. Chem. Soc.* **1989**, *111*, 840−846. (b) Haw, J. F.; Richardson, B. R.; Oshiro, I. S.; Lazo, N. D.; Speed, J. A. *J. Am. Chem. Soc.* **1989**, *111*, 2052−2058.
(5) (a) Kazansky, V. B.; Senchenya, I. N. *J. Catal.* **1989**, *119*, 108−120. (b) Rigby, A. M.; Kramer, G. J.; van Santen, R. A. *J. Catal.* **1997**, *170*, 1−10. (c) Bhan, A.; Joshi, Y. V.; Delgass, W. N.; Thomson K. T. *J. Phys. Chem. B* **2003**, *107*, 10476−10487. (d) Boronat, M.; Viruela, P. M.; Corma, A. *J. Am. Chem. Soc.* **2004**, *126*, 3300−3309.
(6) (a) Butter, A. A.; Jurewicz, A. T.; Kaeding, W. W. U.S. Patent 3,894,-407, July 8, 1975. (b) Kaiser, S. W. International Patent WO 86/04577, Aug 14, 1986.
(7) Svelle, S.; Kolboe, S.; Olsbye U.; Swang, O. *J. Phys. Chem. B* **2003**, *107*, 5251−5260.
(8) (a) Kramer, G. J.; de Man, A. J. M.; van Santen, R. A. *J. Am. Chem. Soc.* **1991**, *113*, 6435−6441. (b) Frasch, M. V.; van Santen, R. A. *Top. Catal.* **1999**, *9*, 191−205.
(9) Frisch, M. J.; Trucks, G. W.; Schlegel, H. B.; Scuseria, G. E.; Robb, M. A.; Cheeseman, J. R.; Montgomery, J. A., Jr.; Vreven, T.; Kudin, K. N.; Burant, J. C.; Millam, J. M.; Iyengar, S. S.; Tomasi, J.; Barone, V.; Mennucci, B.; Cossi, M.; Scalmani, G.; Rega, N.; Petersson, G. A.; Nakatsuji, H.; Hada, M.; Ehara, M.; Toyota, K.; Fukuda, R.; Hasegawa, J.; Ishida, M.; Nakajima, T.; Honda, Y.; Kitao, O.; Nakai, H.; Klene, M.; Li, X.; Knox, J. E.; Hratchian, H. P.; Cross, J. B.; Adamo, C.; Jaramillo, J.; Gomperts, R.; Stratmann, R. E.; Yazyev, O.; Austin, A. J.; Cammi, R.; Pomelli, C.; Ochterski, J. W.; Ayala, P. Y.; Morokuma, K.; Voth, G. A.; Salvador, P.; Dannenburg, J. J.; Zakrzewski, V. G.; Dapprich, S.; Daniels, A. D.; Strain, M. C.; Farkas, O.; Malick, D. K.; Rabuck, A. D.; Raghavachari, K.; Foresman, J. B.; Ortiz, J. V.; Cui, Q.; Baboul, A. G.; Clifford, S.; Cioslowski, J.; Stefanov, B. B.; Liu, G.; Liashenko, A.; Piskorz, P.; Komaromi, I.; Martin, R. L.; Fox, D. J.; Keith, T.; Al-Laham, M. A.; Peng, C. Y.; Nanayakkara, A.; Challacombe, M.; Gill, P. M. W.; Johnson, B.; Chen, W.; Wong, M. W.; Gonzalez, C.; Pople, J. A. *Gaussian 03, revision B.03*; Gaussian, Inc., Pittsburgh, PA, **2003**.
(10) Becke, A. D. *J. Chem. Phys.* **1993**, *98*, 5648−5652.

JA048305R

4.7

DFT investigation of alkoxide vs. alkylammonium formation in amine-substituted zeolites

D. Lesthaeghe, V. Van Speybroeck, G.B. Marin, M. Waroquier
Journal of Physical Chemistry B 109, **2005**, 7952-7960.

---

article 4.7

D. Lesthaeghe, V. Van Speybroeck, G.B. Marin, M. Waroquier

DFT investigation of alkoxide vs. alkylammonium formation in amine-substituted zeolites

J. Phys. Chem. B 109, **2005**, 7952-7960

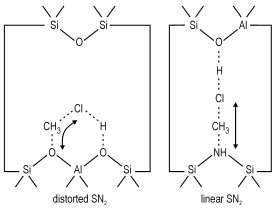

Walk the line: Building on [art. 4.6], alkylammonium and alkoxide formation are also investigated for MTO-related species like methanol and ethene. The amine moiety only lowers barriers for SN2 type reactions with otherwise highly strained transition states, as is the case for chloromethane. By introducing additional basic sites, this enables optimal transition states incorporating various T-sites.

7952 *J. Phys. Chem. B* **2005,** *109,* 7952−7960

DFT Investigation of Alkoxide vs Alkylammonium Formation in Amine-Substituted Zeolites

David Lesthaeghe,[†] Veronique Van Speybroeck,[†] Guy B. Marin,[‡] and Michel Waroquier*,[†]

Center for Molecular Modeling, Laboratory of Theoretical Physics, Ghent University, Proeftuinstraat 86, B-9000 Gent, Belgium, and Laboratorium voor Petrochemische Techniek, Ghent University, Krijgslaan 281-S5, B-9000 Gent, Belgium

Received: January 4, 2005; In Final Form: February 4, 2005

Density functional theory (DFT) cluster calculations were used to describe bifunctional acid−base properties of amine-substituted zeolites containing a Brønsted acid site. Preliminary results (*J. Am. Chem. Soc.* **2004**, *126*, 9162) indicated that efficient use of both functional groups might lead to a substantial lowering of activation barriers. In this paper, comparison is made between the alkoxide formation in zeolites containing only oxygen bridges and alkylammonium formation on the bridging NH groups in amine-functionalized zeolites for various guest species, such as methanol, ethene, and chloromethane. The amine functionalization only lowers barriers for SN_2 type reactions with otherwise highly strained transition states, as is the case for chloromethane. In these new materials more basic sites are introduced into the zeolite framework, enabling optimal linear SN_2 type transition states incorporating various T sites.

1. Introduction

Zeolites are microporous crystalline aluminosilicates, built from corner-sharing SiO_4 and AlO_4 tetrahedra interlinked through common oxygen atoms, giving rise to complex three-dimensional networks of channels, cages, and rings. These solid-state catalysts portray a wide variety of properties and applications (ranging from petroleum cracking to fine chemical synthesis), due mainly to their shape-selectivity and Brønsted acid sites that have the form ≡Si−OH−Al≡.[1]

Recent research has focused on extending the range of their applications by a well-chosen organic functionalization, altering the surface properties that control interaction with various guest species.[2] Manipulating these properties by replacing small parts of the zeolite structure by selected organic groups could create new catalytically active sites, allowing these novel materials to promote a broad range of reactions with potentially improved selectivity. Efforts in incorporating organic sites into the structure of microporous zeolites have not been straightforward. While first attempts using organosilanes with pendant organic groups succeeded in attaching, e.g., phenethyl groups into zeolite structures covalently bonded to framework silicon atoms,[3,4] the process was limited to certain zeolite structures. More importantly, even though a significant advance in widening the range of possible applications was made, the rather large organic groups tended to stick out of the framework, consequently blocking the molecular-sized pores. Increasing the density of organic groups in these organic-functionalized molecular sieves (OFMSs) led to two competing effects: not only a beneficial increase in amount of active centers but also a detrimental increase in diffusional limitations.

The problem of micropore clogging was eliminated when Yamamoto et al. succeeded in synthesizing LTA and MFI frameworks incorporating organic groups directly into the zeolite structure by partially superseding a lattice oxygen atom by a methylene group.[5] These organic−inorganic hybrid zeolites containing organic groups as lattice, or ZOLs, were synthesized from bis(triethoxysilyl)methane (BTESM). While the organic CH_2 groups significantly altered the adsorption properties of the zeolite, the methylene groups were not catalytically active, and chemically interesting materials are probably at least a generation off. Furthermore, the CH_2-substituted zeolites contained intrapore ≡Si−CH_3 moieties in addition to the bridging ≡Si−CH_2−Si≡ groups. This raised the question of whether these end groups were necessary to relieve induced strain due to the substitution or whether they were merely impurities, subject to synthesis conditions. Inspired by these results, Astala and Auerbach provided evidence through periodic DFT calculations that zeolites can accommodate not only methylene, but also amine groups at high concentrations with minimal strain.[6] They concluded that neighboring oxygen bridges easily absorbed the strain induced by the isoelectronic substitution. As opposed to methylene-functionalized zeolites, these amine-functionalized zeolites might possess chemically interesting properties. Theoretically determined adsorption energies of typical guest molecules such as NH_3 and BF_3 indicate that ≡Si−NH−Si≡ groups are significantly stronger Lewis bases than the usual ≡Si−O−Si≡ bridges, while ≡Al−NH_2−Si≡ groups show weaker Brønsted acid properties compared to ≡Al−OH−Si≡.[6] Though recently several research groups have succeeded in post-synthesizing nitrogen-containing mesoporous and microporous materials,[7−10] the crystallographic structure and true nature of the basic behavior of these novel materials is still under debate. Conclusive evidence of pure ZOL materials containing NH bridges directly incorporated into the zeolite framework remains to be reported.

The Lewis base properties of amine-modified zeolites are catalytically interesting in their own right; even more intriguing is the combination with well-known Brønsted acid sites due to aluminum impurities, which might lead to a dramatic increase in bifunctional acid−base properties. The zeolite framework would act as a unique host, providing both strong acid and base groups near a single active site. The prospective of improving

* To whom all correspondence should be addressed. Fax: 32 (0) 9 264 65 60. Email: michel.waroquier@UGent.be.
[†] Center for Molecular Modeling.
[‡] Laboratorium voor PetrochemischeTechniek.

10.1021/jp050032e CCC: $30.25 © 2005 American Chemical Society
Published on Web 03/25/2005

both functional sites simultaneously demonstrates the necessity of a detailed theoretical study of the chemical behavior of neighboring Brønsted acid and Lewis base sites, providing useful guidelines for actual synthesis of these novel materials. First results of the interaction of chloromethane with small 4T and 5T clusters, as published in a previous communication,[11] show that amine modification of zeolites is capable of drastically lowering energy barriers for reactions in which both a Brønsted acid and a Lewis base site play a decisive role (e.g., for the formation of an intermediate alkoxide species). In the same paper, a study of proton mobility in these small clusters reveals that both strong acid and base sites will be present, providing the amine moiety is not located on the aluminum site. The combination of fully oxygen-surrounded aluminum sites and nearby ≡Si−NH−Si≡ bridges opens up the possibility of acid−base catalyzed reactions that are not solely centralized around the aluminum defect, but in which two T sites are involved. In this follow-up paper we will extend the brief results of our previous communication and discuss the interaction of amine-modified zeolites with several typical guest molecules such as methanol, chloromethane, and ethene. The zeolite environment is also modeled by larger 16T clusters and results will be discussed in more detail, providing conclusive information on possible use of these materials.

2. Alkoxide Formation in Zeolites

Many important zeolite-catalyzed reactions in the petrochemical industry make use of the acidic properties of protonated zeolites; most of these involve proton-transfer reactions as elementary steps (e.g., protonation of olefins and alcohols). Without any direct evidence, carbenium and carbonium ions were for a long time accepted as intermediate species stabilized in the polar zeolite surroundings by long-range electrostatic interactions (analogous to equivalent gas-phase reactions). Solid-state NMR and IR experiments indicate that adsorbed protonated hydrocarbons are not stable,[12,13] with exception of some cyclic cations with a delocalized positive charge and sterically inaccessible to framework oxygens.[14,15] Instead, protonation of adsorbed olefins and alcohols results in the formation of long-lived intermediate alkoxide species covalently bonded to the catalyst surface. Further arguments for the existence of such an alkoxide species inside zeolites can be found in ^{13}C MAS NMR studies.[16,17] Theoretical calculations using both the cluster approach and fully periodical techniques indicate that alkoxy species are local minima and thus stable intermediates, while carbenium ions act as transition states.[18−21] Actually, we must note that the true nature of reactive intermediates in reactions catalyzed by acid zeolites is still a matter of debate, certainly when large hydrocarbons are involved.[22] It can, however, be shown that for important industrial reactions, such as hydrocracking or catalytic cracking of these large hydrocarbons, the corresponding kinetic equations do not depend on the assumed nature of the reaction intermediates, i.e., alkoxides or carbenium ions.[23]

Methanol-to-gasoline (MTG) and methanol-to-olefin (MTO) processes are well-known in the production of higher hydrocarbons and other value-added products[24,25] and involve activation of the alcohol on the zeolite surface.[26−28] The methoxy intermediate is generated by dissociation of methanol over the acid site, resulting in a water molecule and a methyl group bound to a lattice oxygen atom. In light of sustainable energy production, early patents also report the possibility of converting halomethanes,[29] circumventing the costly formation of synthesis gas and reducing the number of byproducts. While the dissociative reaction mechanism involving an intermediate methoxy group is believed to be similar to the dissociation of methanol, subtle differences in the location of the acid proton in the transition state structure will have their consequences regarding catalytic properties of amine-modified zeolites, as will be demonstrated further on. Surface methoxy species formed from methanol or halomethanes also play an important role in the methylation of aromatics. On the other hand, ethylation of benzene can occur through a similar stepwise mechanism, starting with the protonation of adsorbed ethene by an acidic zeolite proton, generating a reactive ethoxide species.[30,31] The catalytic protonation of ethene and other olefins is often used to characterize the formation and reactivity of alkoxide species.

The unprotonated oxygen sites in the first coordination sphere of a framework tetrahedral aluminum show stronger Lewis base properties compared to ≡Si−O−Si≡ bridges, rendering the former the most likely sites for alkoxide species to be formed upon. It is believed that chemisorption proceeds in a concerted manner, controlled by a bifunctional (acid−base) mechanism, in which both the Brønsted acid site and the Lewis base properties of an oxygen-atom neighboring the acid site must be carefully balanced.[32] This stresses the importance of the basic centers on the acid−base pairs, since they play an active role in the stabilization of the charged intermediate species which should be formed in a wide range of reactions catalyzed by proton-exchanged zeolites. While earlier research focused mainly on improving the zeolite's acid properties, the basicity of the Lewis base site could be drastically enhanced by appropriate isoelectronic substitution. Amine substitution in particular might promote alkylammonium formation instead of alkoxide formation, subsequently influencing corresponding reaction barriers. In this paper, we report a theoretical study on the formation of an alkylammonium species starting from methanol, chloromethane, and ethene, and we will provide strong evidence that certain reaction barriers of important catalytic processes can be significantly lowered by appropriate substitution.

3. Method

3.1. Computational Details. Full geometry optimizations and frequency calculations for minimum energy and transition-state structures were performed within the Gaussian03 software package[33] using density functional theory (DFT). Zygmunt et al.[34] assessed the applicability of various readily available functionals for studying molecular adsorption in zeolite clusters and found that Becke's three-parameter B3LYP exchange-correlation functional[35] gives intermolecular energies and vibrational frequencies similar to those obtained using MP2. Their final conclusion stated that the B3LYP functional was the best choice for DFT treatment of zeolite clusters. Double ζ level basis sets at the 6-31g(d) level were used, and zero point energy corrections were included for all calculated energies. Activated complexes were validated to be true transition states and to exhibit only one imaginary frequency, whose normal mode corresponds with the reaction coordinate, while reactants and products were verified to contain no imaginary frequencies. For calculations using constraints, unavoidable additional imaginary frequencies (all with a magnitude smaller than 100 cm^{-1}) were checked to correspond with the motion of constrained atoms.

3.2. Cluster selection. The catalytic behavior of these novel materials is explored from a microscopic point of view, simulating the zeolite catalyst using the molecular cluster approach. We will refer to clusters as nT clusters, depending

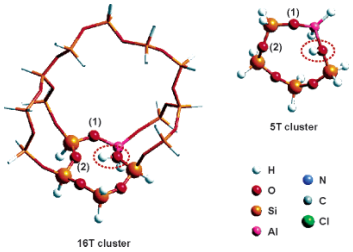

Figure 1. Full oxygen 5T cluster (21 atoms) and 16T cluster (62 atoms) with a single Brønsted acid site, used for ab initio calculations. (1) Oxygen site on aluminum tetrahedron. (2) Oxygen site opposite hydroxyl group. Red dotted line encircles acidic hydroxyl group. Color coding for different atoms is shown as well, including atoms occurring in following figures.

on the number *n* of tetrahedral Si or Al atoms incorporated in the cluster. The calculations were performed on a single ring of five tetrahedral atoms (5T cluster) and a larger 16T extension of this same ring to test the influence of a larger environment on the results. Both cluster types contain a Brønsted acid site, as shown in Figure 1. Even though these models do not fully represent the zeolitic environment, small clusters have shown to provide an adequate qualitative picture of chemical rearrangements that occur locally on the active site.[36−38] Cluster size has a distinct effect on quantitative properties, such as proton affinity and OH stretching frequencies,[39] but for a qualitative description of acid zeolite catalyzed reactions, 5T clusters or even smaller 4T clusters have proven to be sufficient. For example, Rozanska et al.[40] studied the isomerization and transalkylation of toluene and xylenes and found that the relative order of the activation energies is conserved when comparing results obtained using small 4T clusters and fully periodic calculations.

On the other hand, small clusters may correctly model the active site, but they do not fully incorporate structurally distinguishable properties of particular zeolites, and larger clusters are needed to capture pertinent features of specific zeolite structures. More representative 16T clusters, containing the initial 5T ring surrounded by a larger part of the zeolite framework, were used for more advanced calculations in order to check the validity of the 5T results. For the calculations on the 5T cluster no geometric constraints were imposed to verify the true nature of stationary points, i.e., absolute minima or saddle points. At this level of approximation we obtain molecular-type systems with atoms having a larger degree of freedom compared to the real active sites that are embedded in a solid framework. As a result, artificial deformations of the model occur in the smaller 5T cluster. The larger 16T cluster does not suffer from these shortcomings since the fixed volume approach (by constraining the 11 exterior Si atoms to crystallographic positions) was employed to preserve geometric integrity of the zeolite, thereby reducing the artificial deformation of the incorporated 5T ring. Dangling bonds, which in the authentic zeolite would connect the cluster with the rest of the solid, were saturated with hydrogen atoms in order to preserve electrostatic neutrality and spin multiplicity.

In reality, the entire zeolite framework stabilizes charged species, while neutral species are less affected. The calculated activation energies can be expected to decrease by a further 10−50% when the zeolite lattice is properly taken into account.[40−43] For the course of this paper, in which we are

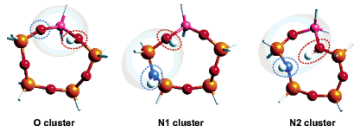

Figure 2. 5T clusters with terminating hydrogens displayed as cylinders. Red dotted line shows acid site, blue dotted line denotes basic site, while reactive area is visualized by gray background.

interested in a qualitative description of a material for which no experimental data are available, the two suggested clusters provide a reasonable compromise between realistic and computationally feasible models. The current investigation concentrates on protonated and amine-substituted ZSM-5, since this structure type can be synthesized over a wide range of Si/Al ratios. Moreover, Yamamoto et al.[5] already succeeded in synthesizing methylene-substituted MFI frameworks. The ZSM-5 (MFI) framework consists of two-dimensional intercrossing straight 10-ring channels in the [010] direction and sinusoidal channels in the [100] direction,[44] exhibiting crucial shape selective characteristics. The suggested cluster models do not incorporate the steric constraints needed for shape selectivity, but this is of minor importance as we only study the interaction with relatively small molecules.

Following our previous communication,[11] we will compare three different acid−base combinations, as shown in Figure 2. As a reference to zeolites containing only oxygen bridges, we studied the O cluster with both the acid hydroxyl group and the basic oxygen atom located on the aluminum tetrahedron. Reactions based on bifunctional acid−base properties will be centralized around this single T-site. Direct comparison can be made with the N1 cluster, where the nitrogen substitution is one tetrahedral site removed from the aluminum defect, but the hydroxyl group and amine group are still located on the same T-site, albeit a silicon tetrahedron. The N2 cluster has a hydroxyl group located in the same position as the O cluster. Similar to the N1 cluster, the amine moiety is one oxygen bridge removed from the aluminum substitution. The main difference between N2 and O/N1 lies in the fact that the acid proton is now located opposite the hydroxyl group. Consequently, reactions incorporating both functional groups will span two separate T-sites instead of one, which has a major influence on transition state geometries.

4. Results and Discussion

4.1. Proton mobility. The fact that protonated zeolites such as H−Y and H−ZSM-5 exhibit strong acidic properties, suggests that protons may be able to jump among oxygens in an AlO_4 tetrahedron. This is confirmed by experimental studies suggesting that acidic protons are not fixed to a specific framework oxygen atom, but are quite mobile at elevated temperatures: NMR measurements on acidic zeolites reveal significant proton mobility with surprisingly low activation energies, depending on the zeolite and Si/Al ratio studied. For example, through variable temperature ^{1}H magic-angle spinning NMR studies of H−ZSM-5, Sarv et al. report an activation energy of 45 kJ/mol,[45] while Baba et al. report 17−20 kJ/mol.[46] For hydrated zeolites, proton mobility is known to be greatly enhanced by trace amounts of water in the micropores,[47] acting as proton vehicle molecules.

Two different types of proton motion must be distinguished: local on-site jumps between four atoms in the first coordination sphere of an aluminum atom and translational intersite motion

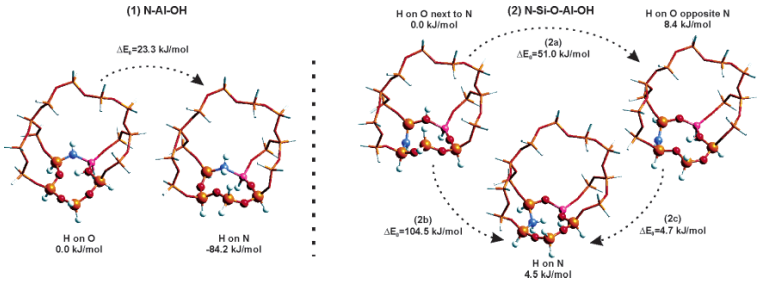

Figure 3. Geometry and energy (in kJ/mol) relative to a chosen reference state for different proton locations in amine-substituted 16T clusters. The (1) cluster has the nitrogen substitution located on the aluminum tetrahedron, while for the (2) cluster the amine moiety is located opposite the hydroxyl group.

between two different aluminum sites. In traditional zeolites, the on-site jumps are much more probable than translational jumps,[48] as in the latter case the protons would have to leave the AlO_4^- site and move to less basic bridging ≡Si−O−Si≡ sites. The presence of NH bridges in organic functionalized materials significantly alters these proton mobility properties. Additionally, the proton location is essential in exploring efficient relative positions for the NH bridge and Al site. Two distinct configurations are considered (Figure 3): a first cluster (1) with both OH and NH groups located at the same T atom, and a second cluster (2) with the nitrogen substitution occurring at a neighboring tetrahedral site. As indicated in Figure 3, all energies are relative to a chosen reference state.

Even though a much larger part of the zeolite was incorporated for the 16T cluster, qualitative results are identical to the 5T cluster.[11] For the cluster (1), in which the NH and OH functional groups are located in the first coordination sphere of the aluminum atom, amine protonation has a low activation energy of 23.3 kJ/mol and results in a thermodynamically favored configuration (−84.2 kJ/mol). This latter configuration, containing a mildly acidic NH_2 group exhibits nonoptimal acid−base properties.

To obtain combined optimal acid and base properties for a thermodynamically favored zeolite, it is essential to separate the amine moiety from the aluminum site, e.g., to have the configuration (2) as shown in Figure 3. The on-site proton hopping barrier between two basic oxygens (2a) is hardly influenced by the amine substitution, with an energy barrier of 51 kJ/mol.[49] Proton jumps between OH and NH substituted sites located in the first coordination sphere of a silicon atom (path 2b) are highly activated by 104.5 kJ/mol, comparable to equivalent intersite proton jumps in full oxygen zeolites.[48] A much more efficient channel leading to a NH_2 substitution is characterized by an almost barrierless proton jump of 4.7 kJ/mol crossing the 5T ring (2c). This last jump to a "free" proton, in the sense that it is no longer located on the aluminum T-site, is easily made because the proton bound to the oxygen atom forms a hydrogen bond with the opposite nitrogen atom and vice versa. Whereas in traditional zeolites jumps to non-aluminum oxygen bridges are less probable,[48] this is not the case for amine-substituted zeolites. All three possible configurations as shown in (2) have comparable binding energies and will be equally likely to occur. As opposed to the ≡Al−NH−Si≡ cluster (1) in Figure 3, there is a reasonable probability of the nitrogen site not being protonated. It is exactly this

SCHEME 1

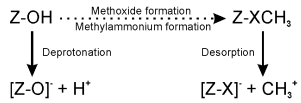

TABLE 1: Heats of Deprotonation and CH_3^+ Desorption for 5T and 16T Clusters (cluster terminology defined in Figure 2)

B3LYP/6-31g(d) (kJ/mol)	deprotonation		CH_3^+ desorption	
	5T	16T	5T	16T
O	1259.8	1231.0	791.7	763.4
O2			689.7	667.4
N1	1265.4	1226.2	775.7	762.1
N2	1263.3	1234.6	775.7	765.7

coexistence of the hydroxyl group with the amine group that allows for a drastic improvement in bifunctional acid−base properties.

4.2. Characterization of Acidic and Basic Properties. All reactions studied in this paper proceed through a bifunctional (acid−base) mechanism and a careful balancing of acid and base properties is crucial. In this section, we will quantify these specific aspects of the various sites for our different cluster models. The acid properties can be quantified by calculating the enthalpy of deprotonation or by calculating the adsorption heat of ammonia.[39,50,51] In this paper, we will use the former scale of acidity, as illustrated in Scheme 1. Since the calculations are performed on a finite model of the active site, the results will contribute substantially to our knowledge of Brønsted acidity of organic functionalized materials but will not differentiate between the acidities of Brønsted acid sites in different crystallographic environments.[42] It is solely our intention to obtain insight into the factors contributing to acidity caused by changes in the local environment, i.e., the difference between traditional zeolites with only oxygen bridges and new materials with amine substitutions.

The results for deprotonation energies defined as $E_{DP} = E_0([Z-O]^-) + E_0(H^+) - E_0(Z-OH)$ are summarized in Table 1. The absolute values obtained in the larger 16T cluster are approximately 20−30 kJ/mol lower than for the smaller 5T cluster, illustrating the stabilizing effect of the larger environment on the positive charge. No clear distinction can be made between the acidity of oxygen sites in traditional zeolites or NH-substituted clusters. Only variations of the order of 5 kJ/

mol can be noted, and finite cluster calculations are not accurate enough to distinguish between such small energy differences.

To characterize the Lewis base properties of these materials, i.e., the ability of donating an electron pair, we calculate the sorption energies of CH_3^+ according to Scheme 1. Note that the starting configuration is negatively charged due to the presence of an unsaturated aluminum substitution. The definition of basicity we use is slightly different from the basicity scale employed by Astala and Auerbach,[6] who used the sorption energy of BF_3 on ≡Si−X−Si≡ as a measure of basicity for a neutral starting configuration without aluminum defect. As the studied reactions all involve the formation of an alkoxide species, the present definition is more appropriate for our cause and results are given in Table 1. A stronger binding of the methyl group to the basic group might have a significant lowering effect on reaction barriers. On the other hand, the formation of an intermediate methoxide species is usually the first step in the multiple-step reaction process. If the methyl group is too strongly bound it might not be reactive enough for these following steps to occur.

It was shown above that NH substitutions bonded to the aluminum atom (site (1) in Figure 3) are thermodynamically prone to protonation, resulting in nonoptimal acid−base properties. Thus, for the amine-modified zeolites, methylammonium formation was always considered at site (2). For traditional zeolites with only oxygen bridges, it is commonly accepted that a methoxide species is formed on the more basic oxygen site (1) as shown in Figure 1, located next to the aluminum atom. However, for proper comparison with the results on the amine-substituted clusters, we also calculated desorption energies for a methoxide species formed at site (2), from now on referred to as the O2 cluster. As shown in Table 1, the desorption energy $E_{DS} = E_0([Z-X]^-) + E_0([CH_3]^+) - E_0([Z-XCH_3])$ (where X equals O or NH depending on the zeolite functionalization) for the O2 cluster is substantially lower than for a methoxide species formed on the aluminum tetrahedron. The energy difference of about 100 kJ/mol indicates the cost of charge separation due to the positive methoxy group not being located near the negatively charged aluminum defect. Sorption energies for the NH-substituted clusters with the methylammonium species also formed at site (2) are about 100 kJ/mol higher compared to the O2 cluster, due to the strong basic character of the amine bridge. The sorption energy for CH_3^+ at the oxygen atom located on site (1) is of the same order of magnitude as the corresponding values for nitrogen-bridged zeolites. Apparently, two effects largely contribute to the sorption energy: (i) the basicity of the nitrogen or oxygen bridge and (ii) the energy cost needed for charge separation between the CH_3^+ group and the AlO_4^- tetrahedron. For the amine-modified zeolites, these effects seem to simply cancel each other out. Also note that due to the charge separation effects, the methylammonium group is just as readily available for succeeding reaction steps as the methoxide species is.

In conclusion, we find all clusters to be of similar Brønsted acidity, while the formed C−O bond for the oxygen site (1) is of equal strength as the C−N bonds formed upon site (2). More importantly, based on these results, any lowering of reaction barriers for nitrogen-substituted zeolites cannot solely be ascribed to the strong Lewis basic properties of the nitrogen group.

4.3. Interaction with Chloromethane. We studied the first step of the dissociative mechanism in the conversion of chloromethane to hydrocarbons over acidic zeolite catalysts such as H−ZSM-5. Using traditional zeolites, containing only oxygen bridges, this first step follows a concerted reaction mechanism.[52] Initially the halomethane is adsorbed to the cluster. Next, in a single combined step, the halomethane dissociates as the methyl group is transferred to a zeolite oxygen atom through a carbenium-ion like transition state, leading to the formation of a surface methoxide species and hydrochloric acid. Afterward, this framework-bonded methoxide is available for transfer to a hydrocarbon. No stable charged intermediates were found during the reaction. Introducing NH bridges into the silicon/aluminum framework does not severely alter the reaction mechanism, except for the formation of a methylammonium species instead of a methoxide species. The reactions were studied on the three clusters shown in Figure 2: the traditional formation of a methoxide species in an exclusively oxygen-bridged zeolite, with the transition state localized around one tetrahedral site (Al), the formation of a methylammonium group, also centered around a single T-site (Si), and the formation of a methylammonium group spanning two neighboring tetrahedral sites (Al+Si). Stationary points are shown in Figure 4 and energetic results of the adsorbed species and activated complexes are summarized in Table 2. Energies are always referred to the ground-state energy of the adsorbed reactants.

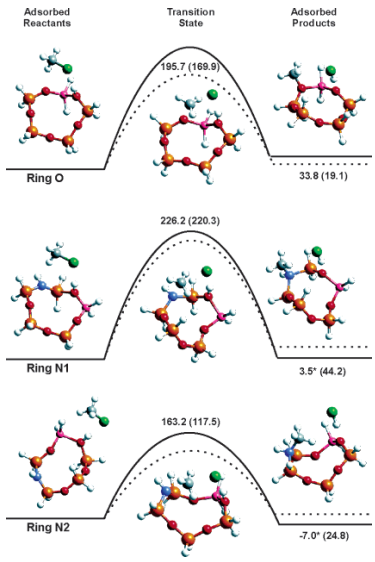

Figure 4. Stationary points for methoxide or methylammonium formation from chloromethane for various initial configurations. Energies are given in kJ/mol and are relative to the energy of the adsorbed reactants. 16T cluster results are shown with a solid line, while the dotted line represents the 5T cluster results (value between brackets). 16T energies marked with an asterisk are the result of a hydrogen bond with a framework oxygen atom not present in the 5T cluster.

As expected, while they substantially differ quantitatively speaking, the 5T and 16T clusters reveal similar qualitative information. The main difference among the three clusters can be seen in the energy barrier, large enough to conclude following order: $\Delta E_0(N2) < \Delta E_0(O) < \Delta E_0(N1)$. Compared to the traditional methoxide formation (cluster O; 5T: 169.9 kJ/mol; 16T: 195.7 kJ/mol), the nitrogen substitution yields a substantial improvement in catalytic properties, but only for the reaction

TABLE 2: Calculated DFT Energies + ZPE for Stationary Points in Reference to Corresponding Energy of Adsorbed Reactants[a]

B3LYP/6-31g(d) (kJ/mol)		CH_3Cl		CH_3OH		C_2H_4	
		5T	16T	5T	16T	5T	16T
O	R	16.6	13.7	68.3	57.4	13.4	17.0
	AR	0.0	0.0	0.0	0.0	0.0	0.0
	TS	169.9	195.7	199.8	*146.7	96.6	96.4
	AP	19.1	33.8	37.0	38.6	−52.7	−49.0
	P	45.2	41.9	80.5	69.1		
N1	R	29.2	11.8	54.3	68.9	11.9	18.4
	AR	0.0	0.0	0.0	0.0	0.0	0.0
	TS	220.3	226.2	165.8	*147.4	141.0	125.3
	AP	44.2	*3.5	42.3	*40.9	−11.7	−26.4
	P	62.6	36.4	88.1	77.1		
N2	R	11.0	9.8	40.9	81.0	6.5	22.5
	AR	0.0	0.0	0.0	0.0	0.0	0.0
	TS	117.5	163.2	150.3	181.4	124.3	125.7
	AP	24.8	*−7.0	26.8	*35.9	−19.2	−49.6
	P	59.1	23.2	72.6	78.1		

[a] 16T energies marked with an asterisk are the result of a hydrogen bond between the adsorbed species and a framework oxygen atom not present in the 5T cluster.

TABLE 3: Geometric Parameters of CH_3Cl Transition States Compared to Ideal SN_2 Values (basic site denoted by X: X=O or NH)

transition state	O		N1		N2		ideal
CH_3Cl (°)	5T	16T	5T	16T	5T	16T	SN_2
$C-H_a-H_b-H_c$ dihedral	7.5	10.3	9.1	11.5	5.4	7.9	0.0
Cl−C−X angle	145.0	144.7	140.3	144.2	172.6	168.0	180.0
$Cl-C-H_a$ angle	109.1	108.0	112.6	108.0	91.1	93.0	90.0
$Cl-C-H_b$ angle	75.9	72.2	75.4	72.7	84.9	82.3	90.0
$Cl-C-H_c$ angle	76.2	76.8	71.7	74.6	86.0	83.0	90.0
$X-C-H_a$ angle	105.9	107.2	107.0	107.7	95.8	98.5	90.0
$X-C-H_b$ angle	88.4	89.8	89.1	89.5	90.0	89.1	90.0
$X-C-H_c$ angle	88.3	90.1	89.1	91.7	92.7	94.5	90.0

mechanism spanning two T-sites (cluster N2; 5T: 117.5 kJ/mol; 16T: 163.2 kJ/mol). As the process is concerted and the acidity of the OH group is not significantly altered (Table 1), one would at first sight ascribe the decrease in activation energy to the stronger basic character of the NH group. If basicity of the nitrogen group were the only determining factor, the N1 cluster would also show a lowering in activation energy. On the contrary, the opposite is observed (cluster N1; 5T: 220.3 kJ/mol; 16T: 226.2 kJ/mol). As demonstrated earlier, two effects contribute to the stability of the methoxide or methylammonium group: basicity of the basic X site (X = O or NH) and the energy needed for charge separation. These effects cancel each other out for the N2 cluster and lead to an equally stable N-C bond for the N1 site. To explain the decrease in activation energy, we must look at geometrical features instead.

As can be seen in Figure 4, the crucial difference between cluster N2 and clusters N1 and O lies in the geometry of the transition state: spanning two tetrahedral sites is energetically favorable to constraining the reaction to a single T-site. For optimal interaction, the methyl group should be in a planar conformation perpendicular to the axis connecting Cl, C and the basic site X (X=O or NH), transferring the methyl-group like a typical SN_2 reaction through an umbrella-like inversion. For the fully oxygen-surrounded clusters, the transition state structure is largely distorted in order to interact with both catalyst donor atoms. However, an effective SN_2 intermediate requires a full overlap among the orbitals of the nucleophiles and the active 2p orbital of the carbon atom in the planar methyl group. For O and N1, this requirement is not fulfilled, as shown in

TABLE 4: Geometric Parameters of CH_3OH Transition States Compared to Ideal SN_2 Values (basic site denoted by X: X=O or NH)

transition state	O		N1		N2		ideal
CH_3OH (°)	5T	16T	5T	16T	5T	16T	SN_2
$C-H_a-H_b-H_c$ dihedral	−12.1	−4.0	−3.0	−2.8	−3.0	−3.4	0.0
O−C−X angle	175.2	167.8	172.0	171.4	172.0	164.6	180.0
$O-C-H_a$ angle	97.2	96.0	95.5	95.2	95.5	96.6	90.0
$O-C-H_b$ angle	94.5	88.5	90.6	88.0	90.6	93.2	90.0
$O-C-H_c$ angle	96.8	91.7	88.3	91.0	88.3	85.4	90.0
$X-C-H_a$ angle	86.1	96.2	92.4	93.4	92.4	96.5	90.0
$X-C-H_b$ angle	86.9	84.7	84.6	87.2	84.6	81.1	90.0
$X-C-H_c$ angle	78.6	83.3	88.6	85.2	88.6	87.5	90.0

Table 3, and the transition state structure is rather unstable. For the N2 cluster, the situation is completely different: the methyl group is indeed in a planar configuration as in typical SN_2 reactions, but more importantly the Cl, C, and N atoms are almost collinear. This proves that the strong basicity of the nitrogen atom does not directly lower the reaction barrier, but merely provides a more accessible basic site for a typical SN_2 reaction to occur. Apparently, the profit of a linear transition state outweighs the cost of charge separation. The N1 cluster on the other hand suffers from both disadvantages: a strained transition state combined with charge separation, resulting in the highest energy barrier for this reaction.

4.4. Interaction with Methanol. A similar concerted reaction path can be calculated for zeolite acid−base interaction with methanol.[53,54] Initially the methanol molecule is adsorbed to the cluster, after which it dissociates as the methyl group is transferred to a zeolite oxygen atom through a carbenium-ion-like transition state, leading to the formation of a surface methoxide species and a water molecule. The corresponding transition state is a methoxonium-like ion-pair complex. However, compared to chloromethane, the equivalent reaction with methanol shows several distinct differences, as not all bonds are broken or formed to the same extent in the transition structure. The bond between the acid proton and the hydroxyl group is already formed, while bond breaking of the methyl group and the hydroxyl group and bond making between methyl group and zeolite are simultaneously in process. This specific detail is crucial for the geometric features of the transition state. As opposed to chloromethane, the original acid zeolite proton is no longer confined to the zeolite oxygen atom and has the ability to reorient itself in order to form a geometrically favored linear SN_2-like transition structure (Table 4). The methyl umbrella is already slightly inverted, visible through a negative $C-H_a-H_b-H_c$ dihedral. This asynchronous pathway does not result in the formation of stable charged intermediates. Reaction schemes are shown in Figure 5 and the energies for all stationary points are given in Table 2. This linear transition state differs from previously reported small cluster calculations[53,54] where only the aluminum tetrahedron was modeled. In these models, the only available basic groups were located next to the acidic hydroxyl group and only a highly strained transition state could be found. Zicovich-Wilson et al.[55] mentioned this limitation of small cluster models and reported an unstrained multicenter transition state, similar to the transition states we obtained, with a methoxide species formed on a less basic ≡Si−O−Si≡ bridge. Recently, Vos et al.[56] also reported an almost linear methoxonium-like SN_2 transition state for calculations on a 4T cluster, similar to the one we obtained.

From a geometrical point of view it makes no difference whether the reactions occur at one or two T sites (all active sites show nearly identical features), and thus similar reaction

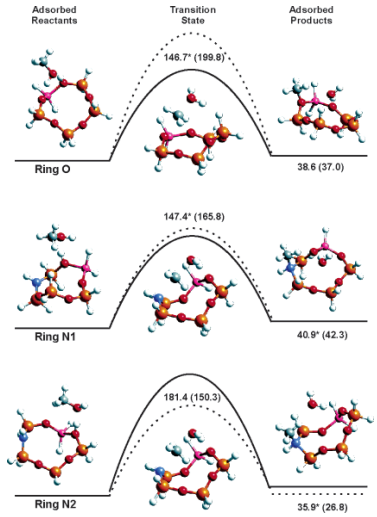

Figure 5. Stationary points for methoxide or methylammonium formation from methanol for various initial configurations. Energies (in kJ/mol) are relative to the energy of the adsorbed reactants. 16T cluster results are shown with a solid line, while the dotted line represents the 5T cluster results (value between brackets). 16T energies marked with an asterisk are the result of a hydrogen bond with a framework oxygen atom not present in the 5T cluster.

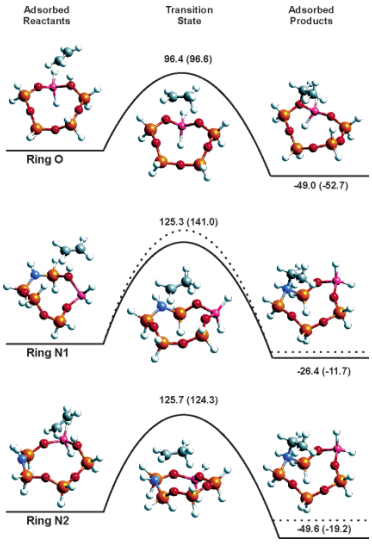

Figure 6. Stationary points for ethoxide or ethylammonium formation from ethene for various initial configurations. Energies (in kJ/mol) are relative to the energy of the adsorbed reactants. 16T cluster results are shown with a solid line, while the dotted line represents the 5T cluster results (value between brackets).

barriers are expected for O, N1, and N2 clusters. This is not the case due to the appearance of hydrogen bonds that stabilize the transition structures and adsorbed species. For the 5T cluster, the oxygen ring shows a highly energetic transition state (199.8 kJ/mol), whereas the N1 and N2 transition states are much lower in energy. For the N-substituted clusters, the water molecule always forms a hydrogen bond with the opposite basic oxygen atom at the aluminum T site. This is not the case for the oxygen bridged zeolite, and no hydrogen bonds were formed. By incorporating a larger part of the zeolite environment (16T), the water molecule in the O cluster also stabilizes in the transition state by formation of a hydrogen bond with one of the framework oxygen atoms that was nonexistent in the 5T cluster. The differences in activation energies between N1 and N2 clusters must be mainly ascribed to variations in adsorption energies of the reactants and slight deformations in ideal SN_2 parameters. One must, however, be extremely cautious with the energetics of clusters containing weak hydrogen bonds with framework oxygen atoms, as it is commonly known that accurate values of these energies require incorporation of large extents of the zeolite cluster. Furthermore, density functional theory is known for its severe limitations in correctly describing these weak interactions.

For the interaction with methanol, we can conclude that the system will automatically take on the optimal SN_2-type transition state, with the water molecule hydrogen bonded to a framework oxygen atom. Even though reaction barriers are not reduced, amine functionalization of the catalyst is far from pointless. The amine groups will provide more basic sites and will facilitate the formation of multicenter transition states in the zeolite micropores.

4.5. Interaction with Ethene. We will now discuss the zeolite-catalyzed protonation of a doubly bonded system such as ethene, which has been the subject of numerous theoretical studies.[57−62] The protonation of olefins such as ethene starts with the formation of a weak π-complex, after which the olefin double bond is attacked by the zeolite acid proton. Upon chemisorption, a covalent C(olefin)−O(zeolite) bond is formed, producing a stable alkoxide σ-complex. The chemisorption reaction is strongly exothermic. The reaction profiles, which are similar for various clusters, are shown in Figure 6, whereas energies for stationary points are given in Table 2.

The reaction mechanism differs from previously discussed examples such as chloromethane and methanol, as it does not occur through a SN_2 mechanism. For this reaction, charge separation dominates reaction kinetics, while the 1T transition state is hardly strained. As a result, the fully oxygen surrounded zeolite has the lowest activation barriers: for the amine substituted clusters there is still the effect of charge separation between the aluminum atom and the positively charged $[CH_3-CH_2]^+$ species, resulting in higher activation energies. As the main ingredient for activation barrier lowering, i.e., relief of steric hindrance in the transition state, does not occur, it is clear that the amine moiety will not improve the catalytic performance.

5. Conclusions

We performed a series of both 5T and 16T cluster calculations using density functional theory to describe the interaction between amine-modified zeolites and various guest species. We especially focused on combining a strong Lewis base amine site with a Brønsted acid proton near an aluminum substitution,

to explore whether this specific combination would substantially improve bifunctional acid−base properties of the catalyst. As the formation of an intermediate alkoxy species is a typical reaction step in the conversion of small alcohols and olefins on protonated zeolites, we compared the alkoxide formation in traditional zeolites (containing only oxygen bridges) to alkylammonium formation on the bridging NH groups in amine-functionalized zeolites. Furthermore, these specific reactions are characterized not only by the acidity of the hydroxyl group but also by the Lewis base properties of the neighboring site responsible for the crucial zeolite−carbon bond.

A study of proton mobility in these novel materials revealed that amine substitutions on the aluminum tetrahedron are easily protonated, resulting in a weakly acidic NH_2 group and a moderately basic oxygen atom. However, if the presence of nitrogen−aluminum bridges could be minimized during synthesis, a proton will only sporadically contaminate the nitrogen sites and the two strong functional groups are able to coexist. By calculating heats of deprotonation, we found that amine modification of the zeolite does not alter the acidic properties of the hydroxyl group. Surprisingly, we also found that the effect of charge separation between the positively charged alkylammonium species and the $[AlO_4]^-$ tetrahedron and the effect of a stronger basic nitrogen atom compared to an oxygen atom simply cancel each other out. This means that the N−C bond in amine-modified zeolites is no stronger than the O−C bond in fully oxygen-bridged zeolites. Consequently, due to the fact that the amine moiety cannot be located on the aluminum tetrahedron to prevent protonation, the amine site does not necessarily promote alkylammonium formation. Because of the delicate balance between these two effects, geometric features of the transition state will determine whether amine functionalization enhances catalytic performance or not.

In the case of chloromethane, our microscopic calculations present strong evidence that amine-modified zeolites are capable of drastically lowering energy barriers. However, this lowering of activation barriers is restricted to reactions where transition states centered on the aluminum defect are highly strained. For these SN_2 type reactions, the possibility of a multicenter transition state spanning two adjacent T-sites allows for an energetically preferable configuration. Methanol, on the other hand, will always try to take on the optimal linear SN_2 transition state. Therefore, supplying additional amine sites will not lower the reaction barriers as in the case of chloromethane. Nevertheless, amine functionalization will still lead to a significant progress in catalytic performance, as this unique way of providing more basic sites will also improve the chances of an adsorbed molecule undergoing successful reaction, allowing more efficient use of the zeolite acid site and the surrounding environment. However, it remains uncertain whether the gain in catalytic properties would outweigh the expensive cost of actual synthesis. Finally, we found that for reactions such as the protonation of ethene, which do not exhibit any strain in the 1T transition state structure, amine-modified zeolites are only capable of providing more basic sites. Without the gain of a more preferable transition state geometry, activation barriers for reaction mechanisms that are not centered around the aluminum atom will be slightly higher.

In conclusion, we state that it is certainly worth synthesizing Al-containing amine-modified zeolites in the light of novel catalytic materials, and we believe that organic functionalization of zeolites will mean a huge advance in future tailoring of catalysts for specific reactions.

Acknowledgment. This work is supported by the Fund for Scientific Research − Flanders (FWO) and the Research Board of Ghent University.

Supporting Information Available: Cartesian coordinates of all adsorbed species and transition states (5T). This material is available free of charge via the Internet at http://pubs.acs.org.

References and Notes

(1) Corma, A. *Chem. Rev.* **1995**, *95*, 559−614.
(2) Jones, C. W. *Science* **2003**, *300*, 439−440.
(3) Jones, C. W.; Tsuji, K.; Davis, M. E. *Nature* **1998**, *393*, 52−54.
(4) Jones, C. W.; Tsapatsis, M.; Okubo, T.; Davis, M. E. *Microporous Mesoporous Mater.* **2001**, *42*, 21−35.
(5) Yamamoto, K.; Sakata, Y.; Nohara, Y.; Takahashi, Y.; Tatsumi, T. *Science* **2003**, *300*, 470−472.
(6) Astala, R.; Auerbach, S. M. *J. Am. Chem. Soc.* **2004**, *126*, 1843−1848.
(7) Ernst, S.; Hartmann, M.; Sauerbeck, S.; Bongers, T. *Appl. Catal. A: General* **2000**, *200*, 117−123.
(8) Xia, Y.; Mokaya, R *Angew. Chem., Int. Ed.* **2003**, *42*, 2639−2644.
(9) Xiong, J.; Ding, Y.; Zhu, H.; Yan, L.; Liu, X.; Lin, L. *J. Phys. Chem. B* **2003**, *107*, 1366−1369.
(10) Zhang, C.; Xu, Z.; Wan, K.; Liu, Q. *Appl. Catal. A: General* **2004**, *258*, 55−61.
(11) Lesthaeghe, D.; Van Speybroeck, V.; Waroquier, M. *J. Am. Chem. Soc.* **2004**, *126*, 9162−9163.
(12) Aronson, M. T.; Gorte, R. J.; Farneth, W. E.; White, D. *J. Am. Chem. Soc.* **1989**, *111*, 840−846.
(13) Haw, J. F.; Richardson, B. R.; Oshiro, I. S.; Lazo, N. D.; Speed, J. A. *J. Am. Chem. Soc.* **1989**, *111*, 2052−2058.
(14) Haw, J. F. *Phys. Chem. Chem. Phys.* **2002**, *4*, 5431−5441.
(15) Bjørgen, M.; Bonino, F.; Kolboe, S.; Lillerud, K. P.; Zecchina, A.; Bordiga S. *J. Am. Chem. Soc.* **2003**, *125*, 15863−15868.
(16) Bosacek, V. *J. Phys. Chem.* **1993**, *97*, 10732−10737.
(17) Philippou, A.; Salehirad, F.; Luigi, D. P.; Anderson, M. W. *J. Chem. Soc., Faraday Trans.* **1998**, *94*, 2851−2856.
(18) Kazansky, V. B. *Catal. Today* **1999**, *51*, 419−434.
(19) Benco, L.; Hafner, J.; Hutschka, F.; Toulhoat, H. *J. Phys. Chem. B* **2003**, *107*, 9756−9762.
(20) Bhan, A.; Joshi, Y. V.; Delgass, W. N.; Thomson, K. T. *J. Phys. Chem. B* **2003**, *107*, 10476−10487.
(21) Boronat, M.; Viruela, P. M.; Corma, A. *J. Am. Chem. Soc.* **2004**, *126*, 3300−3309.
(22) Thybaut, J. W.; Narasimhan, C. S. L.; Marin, G. B.; Denayer, J. F. M.; Baron, G. V.; Jacobs, P. A.; Martens, J. A. *Catal. Lett.* **2004**, *94*, 81−88.
(23) Yaluris, G.; Madon, R.; Dumesic, J. *J. Catal.* **1999**, *186*, 134−146.
(24) Meisel, S. L.; McCullough, J. P.; Lechthaler, C. H.; Weisz, P. B. *Chemtech* **1976**, *6*, 86−89.
(25) Chang, C. D. *Hydrocarbons from methanol*; Marcel Dekker: New York, 1983.
(26) Wang, W.; Seiler, M.; Hunger, M. *J. Phys. Chem. B* **2001**, *105*, 12553−12558.
(27) Wang, W.; Buchholz, A.; Seiler, M.; Hunger, M. *J. Am. Chem. Soc.* **2003**, *125*, 15260−15267.
(28) Dewaele, O.; Geers, V. L.; Froment, G. F.; Marin, G. B. *Chem. Eng. Sci.* **1999**, *54*, 4385−4395.
(29) (a) Butter, A. A.; Jurewicz, A. T.; Kaeding, W. W. U.S. Patent 3,894,407, July 8, 1975. (b) Kaiser S. W. International Patent WO 86/045777, Aug. 14, 1986.
(30) Degnan, T. F., Jr.; Smith, C. M.; Venkat, C. R. *Appl. Catal. A: General* **2001**, *221*, 283−294.
(31) Namuangruk, S.; Pantu, P.; Limtrakul, J. *J. Catal.* **2004**, *225*, 523−530.
(32) van Santen, R. A.; Kramer, G. J. *Chem. Rev.* **1995**, *95*, 637−660.
(33) Frisch, M. J.; Trucks, G. W.; Schlegel, H. B.; Scuseria, G. E.; Robb, M. A.; Cheeseman, J. R.; Montgomery, J. A., Jr.; Vreven, T.; Kudin, K. N.; Burant, J. C.; Millam, J. M.; Iyengar, S. S.; Tomasi, J.; Barone, V.; Mennucci, B.; Cossi, M.; Scalmani, G.; Rega, N.; Petersson, G. A.; Nakatsuji, H.; Hada, M.; Ehara, M.; Toyota, K.; Fukuda, R.; Hasegawa, J.; Ishida, M.; Nakajima, T.; Honda, Y.; Kitao, O.; Nakai, H.; Klene, M.; Li, X.; Knox, J. E.; Hratchian, H. P.; Cross, J. B.; Adamo, C.; Jaramillo, J.; Gomperts, R.; Stratmann, R. E.; Yazyev, O.; Austin, A. J.; Cammi, R.; Pomelli, C.; Ochterski, J. W.; Ayala, P. Y.; Morokuma, K.; Voth, G. A.; Salvador, P.; Dannenberg, J. J.; Zakrzewski, V. G.; Dapprich, S.; Daniels, A. D.; Strain, M. C.; Farkas, O.; Malick, D. K.; Rabuck, A. D.; Raghavachari, K.; Foresman, J. B.; Ortiz, J. V.; Cui, Q.; Baboul, A. G.; Clifford, S.; Cioslowski, J.; Stefanov, B. B.; Liu, G.; Liashenko, A.; Piskorz,

P.; Komaromi, I.; Martin, R. L.; Fox, D. J.; Keith, T.; Al-Laham, M. A.; Peng, C. Y.; Nanayakkara, A.; Challacombe, M.; Gill, P. M. W.; Johnson, B.; Chen, W.; Wong, M. W.; Gonzalez, C.; and Pople, J. A.; *Gaussian 03*, Revision B.03; Gaussian, Inc.: Pittsburgh, PA, 2003.

(34) Zygmunt, S. A.; Mueller, R. M.; Curtiss, L. A.; Iton, L. E. *J. Mol. Struct. (THEOCHEM)* **1998**, *430*, 9−16.

(35) Becke, A. D. *J. Chem. Phys.* **1993**, *98*, 5648−5652.

(36) Sauer, J. *Chem. Rev.* **1989**, *89*, 199−255.

(37) Kramer, G. J.; de Man, A. J. M.; van Santen, R. A. *J. Am. Chem. Soc.* **1991**, *113*, 6435−6441.

(38) Kramer, G. J.; van Santen, R. A.; Emeïs, C. A.; Nowak, A. K. *Nature* **1993**, *363*, 529−531.

(39) Brand, H. V.; Curtiss, L. A.; Iton, L. E. *J. Phys. Chem.* **1992**, *96*, 7725−7732.

(40) Rozanska, X.; van Santen, R. A.; Hutschka, F.; Hafner, J. *J. Am. Chem. Soc.* **2001**, *123*, 7655−7667.

(41) Vollmer, J. M.; Truong T. N. *J. Phys. Chem. B* **2000**, *104*, 6308−6312.

(42) Sierka, M.; Sauer, J. *J. Phys. Chem. B* **2001**, *105*, 1603−1613.

(43) Vos, A. M.; Rozanska, X.; Schoonheydt, R. A.; van Santen, R. A.; Hutschka, F.; Hafner, J. *J. Am. Chem. Soc.* **2001**, *123*, 2799−2809.

(44) Meier, W. M.; Olson, D. H. *Atlas of Zeolite Structure Types*, 2nd rev. ed.; Butterworths: London, 1987.

(45) Sarv, P.; Tuherm, T.; Lippmaa, E.; Keskinen, K.; Root, A. *J. Phys. Chem.* **1995**, *99*, 13763−13768.

(46) Baba, T.; Komatsu, N.; Ono, Y.; Sugisawa, H.; *J. Phys. Chem. B* **1998**, *102*, 804−808.

(47) Ryder, J. A.; Chakraborty, A. K.; Bell, A. T. *J. Phys. Chem. B* **2000**, *104*, 6998−7011.

(48) Franke, M. E.; Sierka, M.; Simon, U.; Sauer, J. *Phys. Chem. Chem. Phys.* **2002**, *4*, 5207−5216.

(49) Fermann, J. T.; Blanco, C.; Auerbach, S. *J. Chem. Phys.* **2000**, *112*, 6779−6786.

(50) Brändle, M.; Sauer, J. *J. Am. Chem. Soc.* **1998**, *120*, 1556−1570.

(51) Lo, C.; Trout, B. L. *J. Catal.* **2004**, *227*, 77−89.

(52) Svelle, S.; Kolboe, S.; Olsbye U.; Swang, O. *J. Phys. Chem. B* **2003**, *107*, 5251−5260.

(53) Blaszkowski, S. R.; van Santen, R. A. *J. Phys. Chem.* **1995**, *99*, 11728−11738.

(54) Sinclair, P. E.; Catlow, C. R. A. *J. Chem. Soc., Faraday Trans.* **1997**, *93*, 333−345.

(55) Zicovich-Wilson, C. M.; Viruela, P.; Corma, A. *J. Phys. Chem.* **1995**, *99*, 13224−13231.

(56) Vos, A. M.; Nulens, K. H. L.; De Proft, F.; Schoonheydt, R. A.; Geerlings, P. *J. Phys. Chem. B* **2002**, *106*, 2026−2034.

(57) Viruela-Martin, P.; Zicovich-Wilson, C. M.; Corma, A. *J. Phys. Chem.* **1993**, *97*, 13713−13719.

(58) Rigby, A. M.; Kramer, G. J.; van Santen, R. A. *J. Catal.* **1997**, *170*, 1−10.

(59) Boronat, M.; Viruela, P.; Corma, A. *J. Phys. Chem. A* **1998**, *102*, 982−989.

(60) Sinclair, P. E.; de Vries, A.; Sherwood, P.; Catlow, C. R. A.; van Santen, R. A. *J. Chem. Soc., Faraday Trans.* **1998**, *94*, 3401−3408.

(61) Senger, S.; Radom, L. *J. Am. Chem. Soc.* **2000**, *122*, 2613−2620.

(62) Svelle, S.; Kolboe, S.; Swang, O. *J. Phys. Chem. B* **2004**, *108*, 2953−2962.

4.8

Bifunctional acid-base catalyzed reactions in zeolites from the HSAB viewpoint

K. Hemelsoet, D. Lesthaeghe, V. Van Speybroeck, M. Waroquier
Chemical Physics Letters 419, **2006**, 10-15.

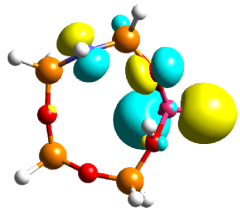

Between a rock and a hard place: Amine-modified zeolites provide an ideal test set to evaluate the overall performance of DFT-based reactivity descriptors. The reactions with CH_3OH, CH_3Cl, C_2H_4 and C_3H_6 are intermediately hard–hard and, therefore, mainly charge-controlled. This is confirmed by the success of the atomic charges and the electrostatic interaction energy at the acid site as descriptors of regio-selectivity.

article 4.8

K. Hemelsoet, D. Lesthaeghe, V. Van Speybroeck, M. Waroquier

Bifunctional acid-base catalyzed reactions in zeolites from the HSAB viewpoint

Chem. Phys. Lett. 419, **2006**, 10-15

Available online at www.sciencedirect.com
SCIENCE DIRECT®
Chemical Physics Letters 419 (2005) 10–15
CHEMICAL PHYSICS LETTERS
www.elsevier.com/locate/cplett

Bifunctional acid–base catalyzed reactions in zeolites from the HSAB viewpoint

K. Hemelsoet, D. Lesthaeghe, V. Van Speybroeck, M. Waroquier *

Center for Molecular Modeling, Laboratory of Theoretical Physics, Ghent University, Proeftuinstraat 86, 9000 Gent, Belgium

Received 7 October 2005

Abstract

The applicability of the hard and soft acids and bases principle is investigated for the interaction of 5T zeolite clusters with probe molecules such as chloromethane, methanol and olefins. The reactions are intermediately hard–hard and, therefore, mainly charge-controlled. This is confirmed by the success of the atomic charges and the electrostatic interaction energy at the acid site as correct descriptors of regio-selectivity and reactivity sequences. Both acid and basic reactive sites can be clearly indicated using frontier orbitals. Moreover, an excellent correlation is found between the activation hardnesses and the energy barriers at the absolute zero.
© 2005 Elsevier B.V. All rights reserved.

1. Introduction

Zeolites are microporous crystalline aluminosilicates, built from corner-sharing SiO_4 and AlO_4 tetrahedra. These solid-state catalysts portray a wide variety of properties and applications, due mainly to their shape-selectivity and Brønsted acid sites ≡Si–OH–Al≡, in combination with neighboring Lewis base ≡Si–O–Si≡ sites [1]. To extend the range of possible applications, Astala and Auerbach [2] provided evidence through periodic DFT calculations that zeolites are capable of accommodating both methylene and amine groups at high concentrations. Theoretically determined sorption energies of typical guest molecules like NH_3 and BF_3 in amine-modified zeolites indicate that ≡Si–NH–Si≡ groups form significantly stronger Lewis bases than the usual ≡Si–O–Si≡ bridges. The combination of these Lewis basic sites with the well-known Brønsted acid sites due to aluminum impurities might lead to a substantial increase in bifunctional acid–base properties, as published in a previous communication [3]. In this Letter, we will study the formation of an alkoxide or an equivalent alkylammonium species, an archetypal step in zeolite chemistry for which both acid and basic site play a crucial role. In a traditional zeolite with only oxygen bridges, both sites are located near the aluminum defect. Amine moieties on the other hand cannot be located next to this aluminum, in order to prevent protonation of the ≡Si–NH–Al–OH–Si≡ bridge to a lesser reactive ≡Si–NH_2–Al–O–Si≡ connection. As previously shown, amine substituted zeolites have noticeably lower reaction barriers for SN_2 type reactions [3]. Recent work also shows that the stronger basic character of the amine bridge is compensated by undesired energetic effects caused by a larger charge separation between the positively charged intermediate and the negative aluminum [4]. The nitrogen site serves as an equivalently reactive site (compared to O) but located in a geometrically more favorable position.

In this Letter, we assess whether DFT-based reactivity descriptors, such as global hardness, Fukui function and local softness are capable of providing reliable information about typical reactions between small molecules and different zeolite frameworks. Generally speaking, several of these reactivity indicators have proven successful for various soft–soft reactions occurring in the gas phase [5–7]. In the specific field of zeolites, some relevant works have already been published. The influence of isomorphous substitution of Al (by B and Ga) and Si (by Ge) on the catalytic activity of zeolite systems has been investigated using a range of reactivity indicators [8,9]. Beside local

* Corresponding author.
E-mail address: michel.waroquier@ugent.be (M. Waroquier).

0009-2614/$ - see front matter © 2005 Elsevier B.V. All rights reserved.
doi:10.1016/j.cplett.2005.10.145

softness values, relative electrophilicity and relative nucleophilicity, defined as the ratio of electrophilic and nucleophilic local softness values and their inverse, were found to be suitable descriptors for the acidity and basicity, respectively. The descriptors were also successful in describing the acidity and basicity of cation-exchanged zeolites [10–14], where cations act as Lewis acid sites while framework oxygen atoms show basic character. The applicability of a hard soft acid base approach was tested for the interaction of small probe molecules with clusters representing the active sites [15–17]. The systems studied in this paper are bifunctional in the sense that the acid and basic sites are both located on framework atoms, either being oxygen bridges or an oxygen and a nitrogen bridge in case of an amine substituted zeolite. To the best of our knowledge only Vos et al. [18,19] studied reactivity indicators on similar systems limited to solely oxygen bridges to predict reaction preference for the alkylation of toluene and benzene.

2. Theoretical background

DFT-based reactivity indicators are defined as derivatives of the electronic energy $E[N, v(\mathbf{r})]$ with N the total number of electrons and $v(\mathbf{r})$ the external potential [5,20]. Using the finite difference approach, the global hardness η and global softness S can be computed from the vertical ionization potential (IP) and electron affinity (EA):

$$\eta = \frac{IP - EA}{2}, \quad S = \frac{1}{2\eta}. \tag{1}$$

The hardness equals the Kohn–Sham HOMO–LUMO gap:

$$\eta = \frac{\epsilon_{\mathrm{LUMO}} - \epsilon_{\mathrm{HOMO}}}{2}. \tag{2}$$

According to the hard soft acid base (HSAB) principle, a reaction between systems A and B will be favored when the global softness difference $\Delta S = S_{\mathrm{A}} - S_{\mathrm{B}}$ is minimal. This rule was obtained through optimization of the covalent contribution of the interaction energy, consequently neglecting other effects such as polarization.

Site-selectivity can be described using local indicators. The Fukui function $f(\mathbf{r})$ and local softness $s(\mathbf{r}) = S\ f(\mathbf{r})$ mainly describe orbital-controlled effects, whereas the local hardness $\eta(\mathbf{r})$ is dominantly charge-controlled. The condensed form of $f(\mathbf{r})$ gives an approximate value at the position of an atomic center [21]:

$$f_k^+ = \tilde{q}_k(N+1) - \tilde{q}_k(N) \text{ (nucleophilic attack)},$$
$$f_k^- = \tilde{q}_k(N) - \tilde{q}_k(N-1) \text{ (electrophilic attack)},$$

with $\tilde{q}_k(N)$ the electron population on the kth atom of the molecule with N electrons. Within frontier orbital theory (FOT), the following approximation can be obtained:

$$f_k^+ = \rho_{\mathrm{LUMO}}(\mathbf{r}) \quad \text{and} \quad f_k^- = \rho_{\mathrm{HOMO}}(\mathbf{r}).$$

Reactivity sequences can also be obtained using the local HSAB principle.

The electrostatic energy between two atoms is also used to describe charge effects:

$$\Delta E_{\mathrm{el}} \propto \frac{q_i q_j}{R_{ij}}, \tag{3}$$

with R_{ij} being the distance between atom i and atom j and q_i and q_j the atomic charges.

According to the principle of maximal hardness (PMH), molecules will rearrange themselves to achieve maximal hardness. Consequently, the transition state of a reaction should exhibit minimal hardness [22]. The activation hardness $\Delta\eta_{\mathrm{act}} = \eta_{\mathrm{adsorbed\ reactant}} - \eta_{\mathrm{transition\ state}}$ describes hardness variations along the reaction path [23]. The smaller the activation hardness, the easier a reaction should occur.

In this Letter, we will verify whether a correlation exists between HSAB results, the electrostatic interaction energy term and the activation hardness on one hand and the reaction barrier at 0 K on the other hand. We will also investigate the applicability of the frontier orbitals and Fukui functions on indicating the preferred interaction sites. We will study both orbital- and charge-controlled effects.

3. Computational details

A similar approach was adopted as in [3], simulating the zeolite catalyst by a cluster built from 5 tetrahedral atoms (5T), which is capable of providing an adequate qualitative picture of chemical rearrangements that occur locally on the active site [24,25]. As shown in Fig. 1, three cases were studied: a fully oxygen surrounded cluster (O) and two amine substituted clusters (N1 and N2), with different proton locations. Full geometry optimizations and frequency calculations for minimum energy and transition-state structures were performed within the GAUSSIAN03 software package [26] using density functional theory (DFT) with the hybrid B3LYP functional [27] and 6-31g(d) basis set. The atomic charges were systematically calculated using the Merz–Singh–Kollman (MK) analysis scheme, which is derived from the electrostatic potential [28,29].

4. Results and discussion

We studied the interaction of chloromethane, methanol, ethylene and propene with 3 zeolite model clusters O, N1 and N2, depicted in Fig. 1. The acid and basic sites where the reactions occur are also indicated. The global hardness values in Table 1 immediately show that the HOMO–LUMO method (Eq. (2)) results in smaller values than obtained using the finite difference approach (Eq. (1)). This underestimation is due to derivative discontinuities of the exchange-correlation energy as elaborated by Perdew et al. [30]. Closer inspection of the computed values indicates an intermediately hard character for all three clusters. Substitution of an oxygen by a nitrogen atom lowers the hardness, increasing the reactivity of the amine-modified

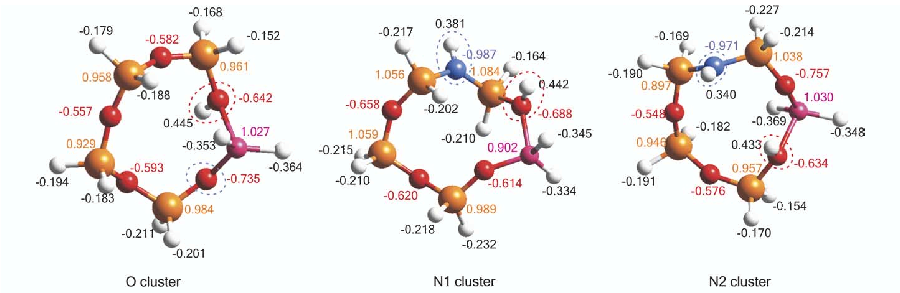

Fig. 1. Optimized cluster geometries, with acid site (red dotted line) and basic site (blue dotted line). MK charges at B3LYP/6-31g(d) level. (For interpretation of the references to colour in this figure legend, the reader is referred to the web version of this article.)

Table 1
Absolute hardness (eV) of isolated reactants, using the finite difference (FD) and HOMO–LUMO method

B3LYP/6-31g(d)	FD	HOMO–LUMO
O cluster	5.413	3.505
N_1 cluster	5.165	3.366
N_2 cluster	5.217	3.467
CH_3Cl	7.311	4.384
CH_3OH	7.574	4.623
C_2H_4	6.850	3.883
C_3H_6	6.496	3.805

cluster. The smaller guest molecules are all found to be hard. The two polar species exhibit the largest hardness values due to the occurrence of hetero atoms which are electronegative. The reactions can be described as intermediately hard–hard and we, therefore, expect electrostatic effects to be dominant.

The reactions of interest are all concerted, making use of both acid and base properties of the zeolite. The first step is the protonation of the adsorbed molecules in order to form a covalent alkoxide or alkylammonium species. The energetic results were already studied in detail in [4]: the amine substitution drastically lowers energies of transition states that occur typically through an SN_2-like activated complex which is highly strained in traditional oxygen bridged zeolites. In these cases, the nitrogen substitution introduces more basic sites, allowing reactions spanning two tetrahedral sites, for the case of cluster N2. The normally strained SN_2-type transition states are then more easily accessible through a linear transfer. The interaction of chloromethane is a typical example of such a reaction and the barriers correspondingly predict that reaction at the N2 cluster is substantially lower activated. For the N1 cluster the same reaction is less favored due to a strained 1T-transition state, which is combined with charge separation effects between the carbenium-like transition state and the negatively charged aluminum. The situation differs for methanol, where an optimal SN_2-type transition state automatically occurs. The reactions with the apolar guest molecules ethylene and propene are dominated by charge separation and nitrogen substitution does not improve catalytic performance.

In the following discussion, we will systematically use the reaction barriers at 0 K (ΔE_0) obtained from transition state theory as reference for the validation of the HSAB principle. Since all studied interactions are (intermediately) hard–hard, it is interesting to investigate whether a correlation can be established between the energy barriers and the HSAB results, keeping in mind that the HSAB principle is based upon a simple electron transfer effect [31]. The computed properties ΔE_0 and ΔS are listed in Table 2. We find that no correlation exists between ΔS and ΔE_0 for the reac-

Table 2
ΔE_0 values (kJ/mol), ZPE included, ΔS (1/au), ΔE_{act} (eV), ΔE^a_{el} at acid site and ΔE^b_{el} at basic site ($10^3 \times$ au)

B3LYP/6-31g(d)	ΔE_0	ΔS	$\Delta\eta_{act}$	ΔE^a_{el}	ΔE^b_{el}	ΔE_0	ΔS	$\Delta\eta_{act}$	ΔE^a_{el}	ΔE^b_{el}
	CH_3Cl					CH_3OH				
O	169.9	0.653	0.635	−16.1	−20.0	199.8	0.717	1.094	−20.6	−20.3
N1	220.3	0.773	1.080	−12.1	−13.5	165.8	0.838	0.720	−28.6	−16.5
N2	117.5	0.747	0.458	−13.3	−7.5	150.3	0.811	0.556	−27.5	−13.6
	C_2H_4					C_3H_6				
O	96.6	0.528	1.096	−31.5	11.2	86.0	0.419	1.454	−53.8	−22.3
N1	141.0	0.648	1.494	−24.0	12.0	117.6	0.540	1.880	−40.9	−12.6
N2	124.3	0.622	1.354	−26.0	9.0	119.6	0.513	1.840	−42.0	−12.1

tion with the polar molecules chloromethane and methanol. However, for the reactions with the apolar guest molecules ethylene and propene, we see that the softness matching criterion yields the same reactivity sequence as shown by the energy barriers. These results are a manifestation of the importance of polarization effects, which are only partially included within the HSAB principle.

The PMH principle is also based on global descriptors, but additionally takes into account the hardness values along the reaction path, including information from transition structures. The values for the activation hardness $\Delta\eta_{act}$ for the various reactions are given in Table 2 and the PMH is also schematically shown in Fig. 2, where calculations were performed on the three stationary points (adsorbed reactants, transition states, products). We find an excellent correlation between the activation hardness and the activation barriers at the absolute zero for all studied reactions. For the reaction with chloromethane, it is clear that including information from the transition structure leads to a correct reactivity description. On other zeolite systems, Vos et al. [18,19] also found a similar correlation for the methylation of benzene and toluene but not for the ethylation and isopropylation of benzene.

While global properties may explain reactivity, site selectivity is described by local quantities such as the Fukui function and the HOMO and LUMO frontier orbitals. Fig. 3 shows the 3-dimensional iso-surfaces of the frontier orbitals and the Fukui function governing electrophilic attack. Inspection of the HOMO for all three clusters shows that a suitable site for electrophilic attack (basic site) can be identified. However, in the case of the N1 cluster, the nitrogen site is not recognized as a basic site. The Fukui function $f^{-}(\mathbf{r})$ contains more detailed information, taking also orbital relaxation effects into account. Nevertheless, the Fukui function iso-surface of the O cluster is not concentrated on a specific region and, therefore, does not succeed in predicting the basic site for this cluster. For the N1 and N2 clusters, the basic oxygen can be identified, but the nitrogen site only shows significant basic character for the N2 cluster. The acid site of the zeolite cluster (the protonated oxygen) can be determined, as illustrated by the LUMO surfaces.

Studying local softness differences within an HSAB viewpoint on the other hand is not straightforward, as we are dealing with multiple site interactions. Ponti [32] suggested a definition for the softness differences, for which we generally found no agreement with the energy barriers

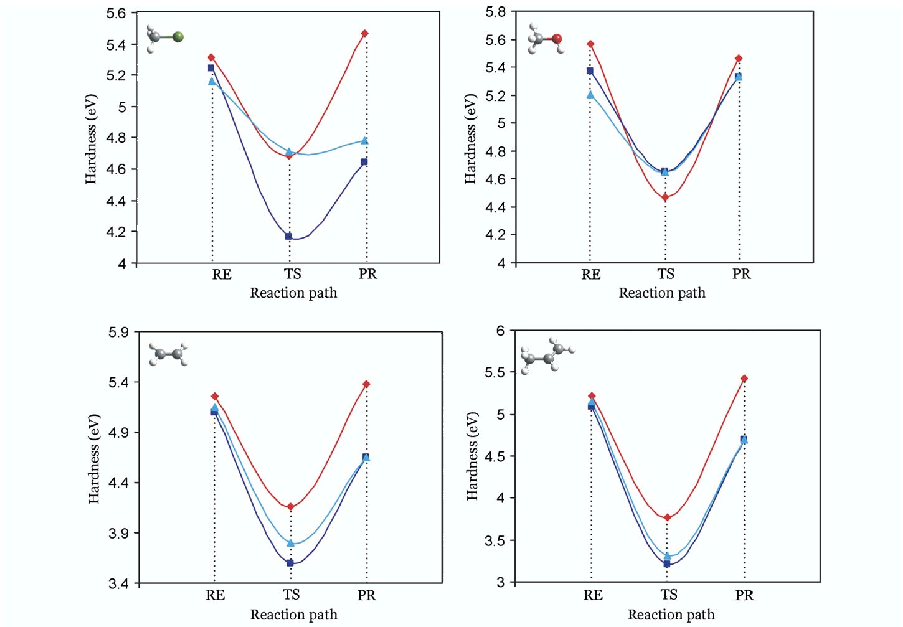

Fig. 2. Illustration of PMH, for O (♦ red line), N1 (■ dark blue line) and N2 cluster (▲ light blue line). (For interpretation of the references to colour in this figure legend, the reader is referred to the web version of this article.)

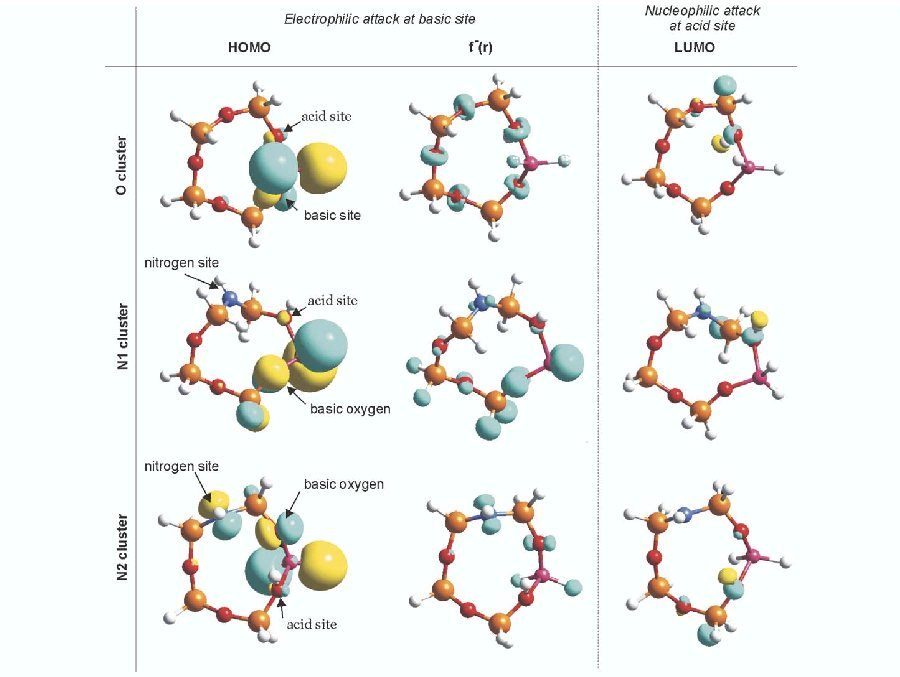

Fig. 3. Iso-surfaces (value 0.2) of the highest occupied orbital (HOMO), the Fukui function ($f^-(\mathbf{r})$) for electrophilic attack and the lowest unoccupied orbital (LUMO).

at 0 K. It has been found by other researchers that the Fukui function, as well as the local softness, are less suitable reactivity descriptors for reactions between (intermediate) hard species [33–35].

Atomic charges are useful indicators to alternatively identify the preferred site when charge effects are important and we investigate their applicability on the studied reactions. Fig. 1 shows the isolated zeolite frameworks with the charges on all atoms, according to the MK population analysis scheme. For all three clusters, the basic site is identified by the largest negative atomic charge, leading to the correct oxygen or nitrogen atom for the purely oxygen or

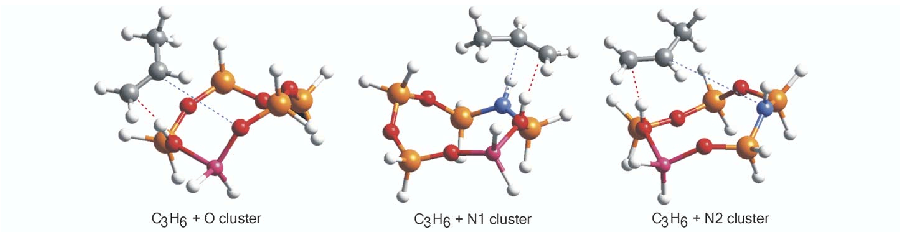

Fig. 4. Adsorbed reactants for reactions with propene, interaction at acid site (red line) and basic site (blue line). (For interpretation of the references to colour in this figure legend, the reader is referred to the web version of this article.)

amine-substituted zeolite clusters, respectively. The acid site is also correctly identified by the largest positive atomic charge on a hydrogen atom.

We computed the electrostatic energy (eq. (3)) of the interacting functional groups, using atomic charges and distances calculated on the stable adsorbed structures (illustrated for propene in Fig. 4). The obtained values for the concerted reaction occurring both at the acid and basic site are given in Table 2. For the reactions taking place at the acid site, we find a good agreement between ΔE^{a}_{el} and ΔE_0 for methanol, ethylene and propene, confirming the importance of charge effects. For chloromethane, no correlation could be expected since the values for the reaction barriers are governed by geometric strain in the transition states and the reactivity indicators are based solely on the reactants. The situation is less straightforward for the reactions occurring at the basic sites and differs for all studied examples. Only in the case of propene, an agreement between ΔE^{b}_{el} and ΔE_0 is noticed. The repulsive terms obtained for ethylene are due to the fact that the reaction occurring at the acid site (interaction of the protonated hydrogen with the π bond of ethylene) is dominant, as can be seen in the transition structure.

5. Conclusion

We have critically analyzed different DFT-based reactivity descriptors for the interaction of zeolites containing both oxygen and amine bridges with different probe molecules such as chloromethane, methanol, ethylene and propene. We performed a series of 5T cluster calculations to obtain reactivity sequences which were compared with energy barriers at the absolute zero. All the studied reactions are characterized as (intermediately) hard–hard, which is confirmed by the success of the atomic charges and the electrostatic energy term at the acid site to describe both the correct regio-selectivity and reactivity sequences. Within a global hard and soft viewpoint, a correlation could be established between the global softness differences and the reaction barriers for apolar molecules. For polar molecules no such correspondence was found. These results clearly illustrate the influence of only taking into account the covalent contribution towards the interaction energy in the theoretical backbone of the HSAB principle, hereby neglecting electrostatic and polarization effects. The excellent agreement between the activation hardness and energy barriers for all studied reactions is also remarkable, indicating the necessity of taking into account transition state effects for the interaction with polar molecules.

References

[1] A. Corma, Chem. Rev. 95 (1995) 559.
[2] R. Astala, S.M. Auerbach, J. Am. Chem. Soc. 126 (2004) 1843.
[3] D. Lesthaeghe, V. Van Speybroeck, M. Waroquier, J. Am. Chem. Soc. 126 (2004) 9162.
[4] D. Lesthaeghe, V. Van Speybroeck, G.B. Marin, M. Waroquier, J. Phys. Chem. B 109 (2005) 7952.
[5] P. Geerlings, F. De Proft, W. Langenaeker, Chem. Rev. 103 (2003) 1793.
[6] K. Hemelsoet, V. Van Speybroeck, G.B. Marin, F. De Proft, P. Geerlings, M. Waroquier, J. Phys. Chem. A 108 (2004) 7281.
[7] K. Van Cauter, K. Hemelsoet, V. Van Speybroeck, M.F. Reyniers, M. Waroquier, Int. J. Quant. Chem. 102 (2005) 454.
[8] W. Langenaeker, N. Coussement, F. De Proft, P. Geerlings, J. Phys. Chem. 98 (1994) 3010.
[9] R.C. Deka, R. Vetrivel, S. Pal, J. Phys. Chem. A 103 (1999) 5978.
[10] R.C. Deka, R.K. Roy, K. Hirao, Chem. Phys. Lett. 332 (2000) 576.
[11] R.C. Deka, K. Hirao, J. Mol. Catal. A 181 (2002) 275.
[12] R.C. Deka, R.K. Roy, K. Hirao, Chem. Phys. Lett. 389 (2004) 186.
[13] J.C. Santos, R. Contreras, E. Chamorro, P. Fuentealba, J. Chem. Phys. 116 (2002) 4311.
[14] A. Chatterjee, F. Mizukami, Chem. Phys. Lett. 385 (2004) 20.
[15] S. Pal, K.R.S. Chandrakumar, J. Am. Chem. Soc. 122 (2000) 4145.
[16] S. Krishnamurthy, R.K. Roy, R. Vetrivel, S. Iwata, S. Pal, J. Phys. Chem. A 101 (1997) 7253.
[17] R.C. Deka, D. Ajitha, K. Hirao, J. Phys. Chem. B 107 (2003) 8574.
[18] A.M. Vos, K.H.L. Nulens, F. De Proft, R.A. Schoonheydt, P. Geerlings, J. Phys. Chem. B 106 (2002) 2026.
[19] A.M. Vos, R.A. Schoonheydt, F. De Proft, P. Geerlings, J. Phys. Chem. B 107 (2003) 2001.
[20] R.G. Parr, W. Yang, Density-Functional Theory of Atoms and Molecules, Oxford Science Publications, 1988.
[21] W. Yang, W.J. Mortier, J. Am. Chem. Soc. 108 (1986) 5708.
[22] D. Datta, J. Phys. Chem. 96 (1992) 2409.
[23] Z. Zhou, R.G. Parr, J. Am. Chem. Soc. 112 (1990) 5720.
[24] J. Sauer, Chem. Rev. 89 (1989) 199.
[25] R.A. van Santen, G.J. Kramer, Chem. Rev. 95 (1995) 637.
[26] M.J. Frisch et al., Gaussian03, Revision B.03, Gaussian, Inc., Wallingford, CT, 2004.
[27] A.D. Becke, J. Chem. Phys. 98 (1993) 5648.
[28] U.C. Singh, P.A. Kollman, J. Comput. Chem. 5 (1984) 129.
[29] B.H. Besler, K.M. Merz Jr., P.A. Kollman, J. Comput. Chem. 11 (1990) 431.
[30] J.P. Perdew, M. Levy, Phys. Rev. Lett. 51 (1983) 1884.
[31] P.W. Ayers, J. Chem. Phys. 122 (2005) 141102.
[32] A. Ponti, J. Phys. Chem. A 104 (2000) 8843.
[33] P.K. Chattaraj, J. Phys. Chem. A 105 (2001) 511.
[34] J. Melin, F. Aparicio, V. Subramanian, M. Galvan, P.K. Chattaraj, J. Phys. Chem. A 108 (2004) 2487.
[35] P. Thanikaivelan, J. Padmanabhan, V. Subramanian, T. Ramasami, Theor. Chem. Acc. 107 (2002) 326.

4.9

Global DFT-based reactivity indicators: an assessment of theoretical procedures in zeolite catalysis

K. Hemelsoet, D. Lesthaeghe, V. Van Speybroeck, M. Waroquier
Journal of Physical Chemistry C 111, **2007**, 3028-3037.

---

article 4.9

K. Hemelsoet, D. Lesthaeghe,
V. Van Speybroeck, M. Waroquier

Global DFT-based reactivity indicators: an assessment of theoretical procedures in zeolite catalysis

J. Phys. Chem. C 111, **2007**,
published online

To the next level: Building on [art. 4.8], both functional and basis set level-of-theory dependence of global reactivity descriptors are investigated for typical reactions in amine functionalized zeolites. Reactivity sequences, based on global softness differences as well as activation hardness values, are generally found to be independent of the level of theory whenever a DFT functional is used.

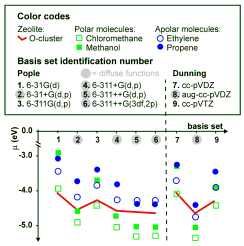

3028 *J. Phys. Chem. C* **2007,** *111,* 3028−3037

Global DFT-Based Reactivity Indicators: An Assessment of Theoretical Procedures in Zeolite Catalysis

Karen Hemelsoet,* David Lesthaeghe, Veronique Van Speybroeck, and Michel Waroquier*

Center for Molecular Modeling, Ghent University, Proeftuinstraat 86, B-9000 Ghent, Belgium

Received: August 30, 2006; In Final Form: November 23, 2006

The dependence of global reactivity descriptors on electronic structure method as well as basis set is investigated for typical reactions in zeolite catalysis. This research is especially focused on hard−hard interactions between small probe molecules (such as chloromethane, methanol, ethylene, and propene) and different zeolite clusters containing both oxygen and amine functionalities. The performance of novel hybrid metafunctionals (such as BMK and MPWB1K) on crucial reactivity predictors is assessed through comparison with both Hartree−Fock and B3-LYP results. For the complex bifunctional zeolite systems, we find accurate results using any of the DFT functionals, in conjunction with a basis set of at least double-ζ quality further augmented with both polarization and diffuse functions. Reactivity sequences, based on global softness differences as well as activation hardness values, are generally found to be independent of the level of theory whenever a DFT functional is used.

1. Introduction

Ab initio quantum mechanical calculations are nowadays widely used to rationalize all kinds of chemical problems. The standard wave function based Hartree−Fock (HF) method has proven successful, even though computational bond lengths and reaction barriers often overestimate experimental values. Although later refinements (called post-HF methods) lead to more accurate and reliable results, this is at the expense of computational efficiency, which becomes especially problematic when systems of medium or large molecular size are studied. Density functional theory (DFT), on the other hand, has gained a lot of attention over the years, based on an excellent cost-to-performance ratio.[1] Additionally, DFT provides important advantages as a conceptual theory,[2,3] enabling a precise definition for many commonly used chemical concepts such as electronegativity[4] and hardness.[5] These properties, currently referred to as DFT-based reactivity indicators, are defined as functional derivatives of the total electronic energy to the total number of electrons or the external potential.[2,6] In this paper, we will only focus on the so-called "global" indicators (as opposed to "local" indicators), which are used to describe the overall reactivity of a chemical system. These have been commonly applied to a broad variety of organic and inorganic chemical systems, discussing the reactive behavior of one single molecule or a set of related systems, occasionally even providing reactivity sequences for the latter (for a comprehensive review, see ref 3). Compared to traditional reaction rate theories such as transition state theory, calculations based on reactivity indicators are computationally less intensive (but in the same time less detailed) because all information is obtained through study of the reactants only.

Most studies in the field of DFT-based reactivity descriptors focus on their applicability and interpretative use, whereas little attention is generally given to the level of theory at which the indicators are computed. As a standard procedure, they are calculated by simply using the level as was used for the geometry optimization. The choice of basis set and the selection of a quantum mechanical Hamiltonian are nevertheless two essential points which can hardly be neglected, as the main advantage of the indicators is precisely their low computational cost. Furthermore, a strong level-of-theory dependence of the reactivity descriptors would almost certainly undermine their reliability. Relevant works investigating the performance of different theoretical procedures for describing reactivity-related properties are, however, rather scarce, and we will give a brief overview of the literature in the remainder of this paragraph. Most studies primarily assess the influence of the level of theory on local reactivity descriptors.[7] For the global indicators, however, only De Proft and Geerlings previously studied the effect of different theoretical methods on the electronegativity and hardness.[8] They concluded that all DFT methods perform better than the high-level coupled cluster method. A superior behavior was demonstrated for the B3-LYP and B3-PW91 functionals in particular. Additionally, Jalbout et al.[9] reported the excellent performance of the CBS-QB3 and G3B3 methods for a set of heteronuclear and homonuclear diatomic molecules. In an early work by Chattaraj and Schleyer, comparing HF and MP2 results, the effect of correlation was found to be important for the validity of the HSAB principle in the case of soft−soft interactions, whereas interactions involving the hard Ag^+ acid could be sufficiently described using the far less time-consuming HF level.[10] To our knowledge, all research presenting level-of-theory studies on global reactivity indicators is limited to this handful of papers.

For the practical computation of global reactivity descriptors, the finite difference method is by far the most popular. In this approach, the functional derivatives are written as appropriate combinations of the vertical ionization potential and electron affinity. These quantities are absolutely crucial in both experimental and computational chemistry and have consequently gained widespread attention. The computation of these energy differences is, however, not always straightforward: they are

* Authors to whom all correspondence should be addressed. E-mail: Karen.Hemelsoet@UGent.be (K.H.); Michel.Waroquier@UGent.be (M.W.).

10.1021/jp0656227 CCC: $37.00 © 2007 American Chemical Society
Published on Web 01/26/2007

largely influenced by the incorporation of electron correlation in the calculation method and require the use of large basis sets, which becomes prohibitive for larger molecular systems.[11] Therefore, almost all studies so far have focused on testing a subset of two data sets developed by Pople and co-workers, denoted as G2−1[12] and G2−2.[13] These sets cover 148 neutral and 146 ionic species and contain extremely accurate experimental data. Whereas the G2−1 test set contains smaller molecules, the G2−2 test set also includes several larger systems such as substituted benzenes. For a recent overview on the electron affinities, we refer to the work of Schaefer and co-workers.[14] In addition to a detailed overview of experimental techniques, several DFT methods were also tested, demonstrating a satisfactory accuracy (within 0.2 eV) for larger molecules of the B3-LYP, BLYP, and BP86 functionals. This accuracy can be spectacularly improved when composite methods are used, e.g., G2 theory has average deviations of 0.06 eV for both ionization energies and electron affinities.[13] The computationally extremely demanding Wn procedures[15−17] show an absolute superior behavior, as W1 is characterized by a mean absolute deviation of 0.013 eV for the G2−1 set and 0.018 eV for the G2−2 set (minus 5 molecules, due to the size of the systems concerned).[16] These methods were, of course, specifically developed and parametrized on relatively small systems. Nevertheless, these studies emphasize how quantum mechanical methods have been developed beyond the level of just reproducing experimental data and are now capable of making accurate predictions where the experimental results are unknown or uncertain. It should also be noted that the electron affinity is typically only a fraction of the size of the ionization potential. Moreover, although every atom and molecule has an ionization potential, they need not necessarily have an electron affinity: there are quite some atomic and molecular negative ions that are simply not stable. Within this respect, density functional methods have been suggested to be fundamentally in error for the computation of anionic systems.[18] However, no convincing evidence was found to support this concern.[19] Moreover, a recent discussion has shown that DFT-based reactivity indicators, and the hardness in particular, can contribute to an improved understanding of this problem.[20]

In this paper, the influence of the level of theory on global DFT-based reactivity indicators is studied. More specifically, the effect of both basis set size and electronic structure method is thoroughly discussed. In order to probe the latter effect, HF (representing a wave function-based method) as well as three density-functional-based techniques are tested. The performance of the MPWB1K[21] and BMK functionals,[22] representing the latest class of hybrid metafunctionals, are assessed for the first time. These metafunctionals are primarily known for their successful description of kinetic properties. Even though the BMK functional is brand new, it has already shown promising results for various properties such as geometries and reaction barriers.[22,23] Overall, our main interest is to qualitatively investigate whether reactivity sequences remain unchanged when different levels of theory are used. This would also be the first time that large inorganic molecules such as zeolites are considered as a test set for an expanded assessment, as these molecules of considerable size are, quite logically, not included in the aforementioned G2−1 and G2−2 test sets.

As just mentioned, the present level-of-theory study on global reactivity indicators is performed on typical zeolite systems. Zeolites are microporous crystalline aluminosilicates, built from corner-sharing SiO_4 and AlO_4 tetrahedra. These solid-state catalysts portray a wide variety of properties and applications,

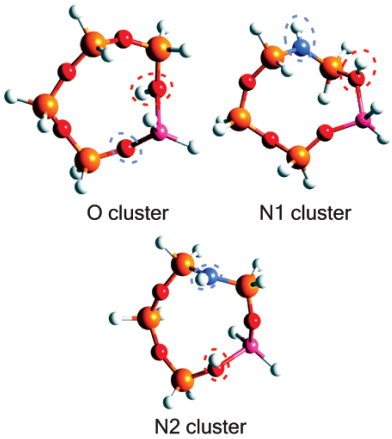

Figure 1. Optimized cluster geometries at B3-LYP/6-31G(d) level of theory, with acid site (red dotted line) and basic site (blue dotted line). For the O and N1 clusters both active sites are located on the same tetrahedron, whereas for the N2 cluster, the acid and base sites are further separated.

due mainly to their shape-selectivity and Brönsted acid sites ≡Si−OH−Al≡, in combination with neighboring Lewis base ≡Si−O−Al≡ sites. The size of the zeolite clusters needed for an adequate description of the chemically active part, combined with the presence of different elements which all play a crucial role in defining the chemical properties, add to the challenge of describing these systems through global reactivity descriptors. This explains why the zeolite systems under study form an ideal test set for both absolute and relative values of these descriptors, outside the scope of G2−1 and G2−2. In addition to a traditional acidic zeolite cluster, we will also compare results with amine substituted zeolites,[24] allowing us to validate whether reactivity sequences in zeolites remain unaltered for different levels of theory. The appeal of nitrogen-substituted zeolites is mainly based on the minor change on the molecular level (substituting a single oxygen bridge by a N−H bridge), yet which leads to completely different reactivity profiles. By applying detailed theoretical calculations on reactions in both zeolite types using classical transition state theory, amine-based zeolites have shown to be catalytically more active than the conventional analogue with O linkages.[25,26] Therefore, these catalysts represent a new class of highly promising materials. In previous work, we specifically studied the interactions of chloromethane, methanol, ethylene, and propene with three zeolite model clusters (O, N1, and N2),[27] which are depicted in Figure 1. In addition to a kinetic description of these reactions, we also investigated their reactive behavior from the viewpoint of DFT-based reactivity descriptors.[28] Using both local and global descriptors, calculated at the B3-LYP/6-31G(d)//B3-LYP/6-31G(d) level of theory, we demonstrated that the interaction can be characterized as hard−hard, and that certain quantities are fully capable of predicting the reactivity sequences as a result of the amine-substitution. In general, the descriptors were found to provide valuable information on the catalytic abilities of the various clusters.[28]

Summarizing, in this paper, we will validate whether the absolute values of global descriptors, which we previously calculated for some small molecules and a typical zeolite

containing only oxygen bridges on one specific level of theory, remain unchanged when different levels of theory are employed. We will investigate the low-cost HF method as well as three different DFT functionals, more precisely: B3-LYP, BMK, and MPWB1K. Although B3-LYP is the traditional functional of choice for calculations on zeolite systems, this is, to our knowledge, the first application of the hybrid metafunctionals MPWB1K and BMK in zeolite catalysis. In a next step, we will use the amine substituted zeolites to verify whether the choice in level of theory might influence reactivity sequences.

2. Global Reactivity Descriptors

The DFT-based reactivity indicators are defined as derivatives of the electronic energy $E[N,v(\mathbf{r})]$ with N the total number of electrons and $v(\mathrm{r})$ the external potential.[2,3,6] Global reactivity indicators provide information on the overall reactivity of a chemical system and are used to discuss reactivity sequences. The chemical potential (μ) equals the negative of the electronegativity, expressing the initial attraction toward electronic charge:

$$\mu = -\chi = \left(\frac{\partial E}{\partial N}\right)_v$$

The second derivative or hardness (η) measures the resistance to charge transfer, and the reciprocal is identified with the global softness (S)

$$\eta = \frac{1}{2S} = \left(\frac{\partial^2 E}{\partial^2 N}\right)_v$$

Using the finite difference approach, μ, η, and S can be computed from the vertical ionization potential (IP) and electron affinity (EA)

$$\mu = -\frac{\mathrm{IP} + \mathrm{EA}}{2}$$

$$\eta = \frac{\mathrm{IP} - \mathrm{EA}}{2}$$

$$S = \frac{1}{\mathrm{IP} - \mathrm{EA}}$$

The computation of these descriptors requires three single-point energy calculations. Nevertheless, as these calculations must be performed at a fixed geometry (the optimized geometry of the N-electron system), the computational effort in order to follow this procedure remains limited. The quantities are implemented in empirically well-known chemical principles. The hard soft acid base (HSAB) principle was originally discussed by Pearson[29] and states that a reaction between systems A and B will be favored when the global softness difference $\Delta S = S_A - S_B$ is minimal.[30] This rule was obtained through optimization of the covalent contribution of the interaction energy, consequently neglecting other effects such as polarization. According to the principle of maximal hardness (PMH),[31] molecules will rearrange themselves to achieve maximal hardness. Consequently, the transition state of a reaction should exhibit minimal hardness.[32] The activation hardness $\Delta\eta_{\mathrm{act}} = \eta_{\mathrm{adsorbed\ reactant}} - \eta_{\mathrm{transition\ state}}$ describes hardness variations along the reaction path.[33] The smaller the activation hardness, the easier a reaction should occur.

3. Computational Methods

All calculations were performed using the Gaussian 03 software package.[34] The zeolite catalysts were simulated by a cluster built from 5 tetrahedral atoms (5T, T-atoms = Al or Si), which is capable of providing an adequate qualitative picture of chemical rearrangements that occur locally on the active site.[35,36] For the three zeolite clusters, the four probe molecules, as well as the adsorbed complexes, full geometry optimizations and frequency calculations using the hybrid B3-LYP functional[37,38] and 6-31G(d) basis set were performed as obtained in ref 25. The B3-LYP functional is known to provide accurate geometries within zeolite catalysis: Zygmunt et al. assessed the applicability of various readily available functionals for studying molecular adsorption in zeolite clusters and found that the B3-LYP functional gives intermolecular energies and vibrational frequencies similar to those obtained using MP2. Their final conclusion stated that the B3-LYP functional was the best choice for DFT treatment of zeolite clusters.[39] Nevertheless, we will also verify the suitability of the B3-LYP geometries by investigating the influence of the level of theory used for the geometry optimization. First, the performance of other functionals for geometry optimization, in particular BMK and MPWB1K, will be assessed. Second, we will upgrade the small basis set 6-31G(d) to 6-31+G(d,p), testing the influence of additional diffuse and polarization functions on the final geometry.

For the single-point energy calculations, four theoretical procedures were assessed. First of all, the standard Hartree−Fock (HF) method, in which correlation energy is completely neglected, was selected, due to the low computational cost. Note that the "DFT-based reactivity descriptors" are not rigorously defined within the HF scheme. However, we have used the finite difference approach to calculate these descriptors from the ionization potential and electron affinity obtained at the HF level. Furthermore, the popular B3-LYP hybrid functional[37,38] was applied. This functional is the standard choice to perform calculations within zeolite catalysis. In addition, two recently developed up-and-coming meta-gradient corrected functionals (BMK[22] and MPWB1K[21]) were also chosen, as their performance within the theory of conceptual DFT, as well as within zeolite catalysis, has not been investigated earlier.

Since the electron affinity values are very sensitive to the basis set,[40] as the addition of the electron entails a profound change in the spatial extent of the wave function of the anion, many Gaussian Pople basis sets were tested,[41] including 6-31G(d) (**1**), 6-31+G(d,p) (**2**), 6-311G(d,p) (**3**), 6-311+G(d,p) (**4**), 6-311++G(d,p) (**5**), and 6-311++G(3df,2p) (**6**). The performance of a selection of Dunning's correlation consistent basis sets,[42] cc-pVDZ (**7**), aug-cc-pVDZ (**8**), cc-pVTZ (**9**), and aug-cc-pVTZ (**10**) was also studied. The augmented basis sets **8** and **10** include one set of diffuse functions for each value of the angular momentum ∠

Additionally, for the smaller probe molecules (methanol, chloromethane, ethylene, and propene) high-level single-point energy calculations were performed, using the QCISD(T)[43] and CCSD(T)[44] post-HF methods in conjunction with the 6-311+G(d,p) and/or 6-311+G(3df,2p) basis sets. For these computations, the optimized B3-LYP/6-31G(d) geometries were used.

4. Results and Discussion

4.1. Comparison with Experiment: Small Probe Molecules. Resulting IP and EA values as well as their derived properties μ and η were calculated for four small probe molecules: chloromethane, methanol, ethylene, and propene. The calculated IP values were compared with available experimental data and mean absolute deviations (MADs) are reported in Table 1. The experimental IP values were obtained using

TABLE 1: Performance of Different Functional Methods[a]

	IP				μ and η			
	HF	B3-LYP	BMK	MPWB1K	HF	B3-LYP	BMK	MPWB1K
1. 6-31G(d)	1.43	0.25	0.25	0.25	1.62	1.21	1.31	1.28
2. 6-31+G(d,p)	1.36	0.11	0.14	0.16	0.72	0.21	0.34	0.31
3. 6-311G(d,p)	1.39	0.15	0.15	0.20	1.23	0.76	0.87	0.87
4. 6-311+G(d,p)	1.36	0.08	0.11	0.14	0.69	0.16	0.28	0.25
5. 6-311++G(d,p)	1.36	0.08	0.11	0.14	0.69	0.25	0.20	0.21
6. 6-311++G(3df,2p)	1.40	0.07	0.11	0.14	0.71	0.26	0.19	0.21
7. cc-pVDZ	1.42	0.20	0.20	0.21	1.43	0.97	1.10	1.07
8. aug-cc-pVDZ	1.38	0.09	0.12	0.15	0.70	0.31	0.20	0.16
9. cc-pVTZ	1.42	0.11	0.14	0.16	1.11	0.65	0.77	0.76
10. aug-cc-pVTZ	1.41	0.08	0.13	0.14	0.72	0.35	0.25	0.26
average values:								
over all basis sets	1.39	0.12	0.15	0.17	0.96	0.51	0.55	0.54
without diffuse functions	1.42	0.18	0.19	0.21	1.34	0.90	1.01	1.00
with diffuse functions	1.38	0.08	0.12	0.14	0.70	0.26	0.24	0.23

[a] Mean average deviations (MADs) in eV for the set of small probe molecules CH_3Cl, CH_3OH, C_2H_4, and C_3H_6. For the IPs the MADs are referred with respect to experiment, whereas for the global indicators μ and η the reference is the high level of theory QCISD(T)/6-311++G(3df,2p)//B3-LYP/6-31G(d).

photoelectron spectroscopy, amounting to 11.29 eV for chloromethane,[45] 10.96 eV for methanol,[46] 10.68 eV for ethylene,[47] and 9.91 eV for propene.[48]

From Table 1, it is immediately clear that the performance of the HF method is well below standard, showing deviations between 1.36 and 1.43 eV. In large contrast, the computed MAD values for the DFT functionals all indicate an excellent correlation with experiment, as the maximum MAD amounts to 0.25 eV, which corresponds to the smallest basis set 6-31G-(d) taken into consideration. It is furthermore difficult to differentiate between the three DFT methods, as all of them succeed in an almost exact reproduction of the experimental data. The influence of the basis set is rather limited: the effect of adding extra polarization functions to a triple-ζ basis set (transition from basis set **5** to **6**) is, for instance, negligible. However, inclusion of diffuse functions leads to a substantial improvement of the results. This is a general observation, valid for both double- and triple-ζ basis sets. Furthermore, the Pople (**1**−**6**) and Dunning (**7**−**10**) basis set series perform very similarly, but because of the computational cost of the augmented basis sets, the latter series are not recommended for systems of considerable size. Overall, usage of 6-31G(d) and cc-pVDZ basis sets is discouraged.

As the global properties μ and η are not directly experimentally accessible and reliable experimental electron affinity data were not found, additional single-point energy calculations using the QCISD(T) and CCSD(T) levels, and using the B3-LYP/6-31G(d) optimized geometries, were performed (not included in Table 1). Among these, the QCISD(T)/6-311++G(3df,2p) level was chosen for benchmarking purposes as the MAD for the ionization potential with respect to the experimental values turned out to be the lowest (0.04 eV). MAD values for μ and η, resulting from comparison with the benchmark QCISD(T)/6-311++G(3df,2p) method, are given in Table 1. Closer inspection demonstrates how the three DFT functionals perform very similarly, whereas the HF MAD values are again substantially higher. All basis sets without diffuse functions perform poorly, irrespective of their double or triple-ζ character.

We conclude that for the computation of global descriptors, in the case of the four small probe molecules, accurate results can be obtained using either one of B3-LYP, BMK, or MPWB1K DFT functionals, in combination with a basis set of double-ζ or triple-ζ quality, augmented with both diffuse and polarization functions.

4.2. Reactivity Indicators: Purely Oxygen-Bridged Zeolites. Resulting IP, EA, μ and η values were calculated for the isolated, purely oxygen-bridged zeolite reactant (O cluster in Figure 1). Four electronic structure methods and nine basis sets were tested (in the remainder of the article the aug-cc-pVTZ basis set **10** is omitted, due to the large computational cost), and the results are reported in Table 2. Using the same extended set of various computational methods, global softness differences ΔS for the interactions between the O cluster and the small probe molecules were computed and consequently listed in Table 3. Finally, activation hardnesses $\Delta\eta_{act}$ were also calculated, using the optimized geometries of the adsorbed reactants and transition structures, and these values are given in Table 4.

4.2.1. Ionization Potential, Electron Affinity, Chemical Potential, and Hardness. The calculated IP values for this inorganic species (Table 2) show only a minor dependence on the level of theory, as they all lie in the narrow range between 9.35 and 9.90 eV. Inclusion of diffuse functions does not significantly alter the results. The EA values, on the other hand, vary more substantially, ranging from −0.19 to −2.81 eV. This effect is mostly attributed to the inclusion of diffuse functions, which are necessary for an accurate description of the more diffuse electron distribution of the anion state.

The influence of level of theory on the final geometry optimization was assessed for the purely oxygen-bridged zeolite cluster. The BMK/6-31G(d) and MPWB1K/6-31G(d) levels were used to assess the influence of a different functional and the B3-LYP/6-31+G(d,p) level was used to define the influence of a different basis set on the optimization. The sensitivity to geometry optimization is found to be extremely limited: Figure S1 in the Supporting Information depicts the global hardness of the zeolite catalyst which coincides for all levels of theory. The sole exception is formed by the low-cost HF single-point calculation on the MPWB1K optimized geometry, but the general trend is maintained nonetheless. Therefore, only the B3-LYP/6-31G(d) optimized geometries were retained in the remainder of this work.

The calculated μ varies between −3.40 and −4.69 eV, whereas η values range between 4.81 and 6.22 eV, indicating a relatively hard character of the investigated zeolite. The role of basis set is again restricted to the presence of diffuse functions, giving rise to a decrease of the hard character of the species with approximately 0.40 eV. We note that for all functionals under consideration, the 6-31+G(d,p), 6-311+G-(d,p), 6-311++G(d,p), 6-311++G(3df,2p) and aug-cc-pVDZ results are extremely similar to one another. Based on these results, a double-ζ basis set, augmented with one set of diffuse

TABLE 2: Ionization Potentials, IP, Electron Affinities, EA, Chemical Potential, μ, and Global Hardness, η, for the Purely Oxygen-Bridged Zeolite[a]

	IP				EA			
	HF	B3-LYP	BMK	MPWB1K	HF	B3-LYP	BMK	MPWB1K
1. 6-31G(d)	9.65	9.37	9.77	9.78	−2.80	−1.35	−1.69	−1.59
2. 6-31+G(d,p)	9.68	9.48	9.86	9.86	−1.25	−0.41	−0.79	−0.67
3. 6-311G(d,p)	9.64	9.47	9.86	9.83	−2.27	−0.94	−1.32	−1.22
4. 6-311+G(d,p)	9.65	9.50	9.90	9.86	−1.20	−0.38	−0.76	−0.64
5. 6-311++G(d,p)	9.65	9.50	9.88	9.86	−1.03	−0.35	−0.68	−0.58
6. 6-311++G(3df,2p)	9.61	9.50	9.90	9.84	−0.96	−0.30	−0.61	−0.54
7. cc-pVDZ	9.62	9.35	9.74	9.75	−2.81	−1.33	−1.67	−1.58
8. aug-cc-pVDZ	9.57	9.43	9.77	9.77	−0.68	−0.19	−0.48	−0.39
9. cc-pVTZ	9.60	9.47	9.86	9.82	−2.36	−0.97	−1.32	−1.24
average values:								
over all basis sets	9.63	9.45	9.84	9.82	−1.70	−0.69	−1.04	−0.94
without diffuse functions	9.63	9.41	9.81	9.79	−2.56	−1.15	−1.50	−1.41
with diffuse functions	9.63	9.48	9.86	9.84	−1.02	−0.32	−0.66	−0.56

	μ				η			
	HF	B3-LYP	BMK	MPWB1K	HF	B3-LYP	BMK	MPWB1K
1. 6-31G(d)	−3.43	−4.01	−4.04	−4.09	6.22	5.36	5.73	5.68
2. 6-31+G(d,p)	−4.21	−4.54	−4.54	−4.60	5.47	4.95	5.32	5.26
3. 6-311G(d,p)	−3.69	−4.27	−4.27	−4.31	5.96	5.20	5.59	5.53
4. 6-311+G(d,p)	−4.22	−4.56	−4.57	−4.61	5.43	4.94	5.33	5.25
5. 6-311++G(d,p)	−4.31	−4.58	−4.60	−4.64	5.34	4.92	5.28	5.22
6. 6-311++G(3df,2p)	−4.33	−4.60	−4.65	−4.65	5.28	4.90	5.26	5.19
7. cc-pVDZ	−3.40	−4.01	−4.04	−4.09	6.21	5.34	5.70	5.66
8. aug-cc-pVDZ	−4.45	−4.62	−4.65	−4.69	5.13	4.81	5.12	5.08
9. cc-pVTZ	−3.63	−4.25	−4.27	−4.29	5.98	5.22	5.59	5.53
average values:								
over all basis sets	−3.96	−4.38	−4.40	−4.44	5.67	5.07	5.44	5.38
without diffuse functions	−3.54	−4.13	−4.15	−4.19	6.09	5.28	5.65	5.60
with diffuse functions	−4.30	−4.58	−4.60	−4.64	5.33	4.90	5.26	5.20

[a] All values are given in eV.

TABLE 3: ΔS Results in Absolute Values (au^{-1}) for the Reactions between the Probe Molecules and the Purely Oxygen-Bridged Zeolite

	zeolite O + CH_3Cl				zeolite O + CH_3OH			
	HF	B3-LYP	BMK	MPWB1K	HF	B3-LYP	BMK	MPWB1K
1. 6-31G(d)	0.321	0.677	0.556	0.557	0.399	0.741	0.635	0.641
2. 6-31+G(d,p)	0.274	0.594	0.467	0.478	0.185	0.546	0.406	0.414
3. 6-311G(d,p)	0.325	0.639	0.506	0.530	0.288	0.633	0.514	0.525
4. 6-311+G(d,p)	0.246	0.576	0.427	0.448	0.158	0.524	0.384	0.388
5. 6-311++G(d,p)	0.148	0.483	0.354	0.360	0.025	0.409	0.285	0.277
6. 6-311++G(3df,2p)	0.158	0.490	0.359	0.368	0.047	0.424	0.297	0.293
7. cc-pVDZ	0.303	0.640	0.534	0.537	0.295	0.639	0.544	0.547
8. aug-cc-pVDZ	0.226	0.533	0.417	0.410	0.097	0.454	0.337	0.322
9. cc-pVTZ	0.272	0.600	0.485	0.502	0.226	0.587	0.471	0.484
average values:								
over all basis sets	0.252	0.581	0.456	0.466	0.191	0.551	0.430	0.432
without diffuse functions	0.305	0.639	0.520	0.531	0.302	0.650	0.541	0.549
with diffuse functions	0.211	0.535	0.405	0.413	0.102	0.471	0.342	0.339

	zeolite O + C_2H_4				zeolite O + C_3H_6			
	HF	B3-LYP	BMK	MPWB1K	HF	B3-LYP	BMK	MPWB1K
1. 6-31G(d)	0.058	0.552	0.401	0.405	0.023	0.435	0.297	0.300
2. 6-31+G(d,p)	0.144	0.532	0.378	0.396	0.066	0.406	0.274	0.287
3. 6-311G(d,p)	0.095	0.567	0.403	0.412	0.017	0.448	0.301	0.308
4. 6-311+G(d,p)	0.166	0.543	0.385	0.405	0.125	0.411	0.276	0.289
5. 6-311++G(d,p)	0.011	0.392	0.408	0.419	0.139	0.168	0.056	0.031
6. 6-311++G(3df,2p)	0.003	0.401	0.413	0.429	0.059	0.178	0.062	0.041
7. cc-pVDZ	0.020	0.522	0.376	0.376	0.059	0.403	0.273	0.270
8. aug-cc-pVDZ	0.012	0.419	0.283	0.476	0.212	0.208	0.099	0.209
9. cc-pVTZ	0.043	0.521	0.360	0.375	0.032	0.404	0.261	0.272
average values:								
over all basis sets	0.061	0.494	0.379	0.410	0.081	0.340	0.211	0.223
without diffuse functions	0.054	0.540	0.385	0.392	0.033	0.422	0.283	0.288
with diffuse functions	0.067	0.458	0.373	0.425	0.120	0.274	0.153	0.171

functions and polarization functions (e.g., basis set **2**), seems sufficient for a reliable calculation of the global reactivity descriptors.

From a more interpretative point of view, μ can be applied to characterize the relative electrophilic or nucleophilic behavior of the involved molecules.[49] The chemical potentials for the

TABLE 4: $\Delta\eta_{act}$ Values (eV) for the Reactions between the Probe Molecules and the Purely Oxygen-Bridged Zeolite

	zeolite O + CH_3Cl				zeolite O + CH_3OH			
	HF	B3-LYP	BMK	MPWB1K	HF	B3-LYP	BMK	MPWB1K
1. 6-31G(d)	1.902	0.601	0.854	0.892	1.274	1.093	1.201	1.185
2. 6-31+G(d,p)	1.108	0.226	0.591	0.607	0.909	1.024	1.174	1.086
3. 6-311G(d,p)	2.155	0.501	0.731	0.784	1.075	1.085	1.232	1.159
4. 6-311+G(d,p)	1.044	0.387	0.591	0.600	0.871	1.006	1.159	1.041
5. 6-311++G(d,p)	0.949	0.347	0.528	0.526	0.888	0.948	1.054	0.988
6. 6-311++G(3df,2p)	1.507	0.311	0.607	0.514	0.890	0.955	1.063	0.983
7. cc-pVDZ	1.845	0.607	0.842	0.893	1.306	1.167	1.252	1.246
8. aug-cc-pVDZ	1.316	0.283	0.418	0.324	0.820	0.894	1.012	0.908
9. cc-pVTZ	2.319	0.419	0.798	0.829	1.267	1.165	1.294	1.249
average values:								
over all basis sets	1.572	0.409	0.662	0.663	1.033	1.037	1.160	1.094
without diffuse functions	2.055	0.532	0.806	0.850	1.230	1.127	1.245	1.210
with diffuse functions	1.185	0.311	0.547	0.514	0.876	0.965	1.092	1.001

	zeolite O + C_2H_4				zeolite O + C_3H_6			
	HF	B3-LYP	BMK	MPWB1K	HF	B3-LYP	BMK	MPWB1K
1. 6-31G(d)	1.616	1.092	1.275	1.304	2.151	1.452	1.722	1.730
2. 6-31+G(d,p)	1.089	0.852	1.015	1.024	1.526	1.509	1.436	1.408
3. 6-311G(d,p)	1.611	0.980	1.143	1.169	2.057	1.371	1.588	1.583
4. 6-311+G(d,p)	1.011	0.845	1.002	0.982	1.437	1.171	1.409	1.361
5. 6-311++G(d,p)	0.868	0.819	1.024	0.894	1.283	1.093	1.306	1.254
6. 6-311++G(3df,2p)	0.883	0.821	1.000	0.908	1.312	1.122	1.428	1.286
7. cc-pVDZ	1.531	1.096	1.255	1.282	2.058	1.454	1.678	1.697
8. aug-cc-pVDZ	1.285	0.743	0.964	0.795	1.206	1.049	1.368	1.184
9. cc-pVTZ	1.442	1.014	1.196	1.204	1.983	1.407	1.605	1.622
average values:								
over all basis sets	1.259	0.918	1.097	1.063	1.668	1.292	1.504	1.458
without diffuse functions	1.550	1.046	1.217	1.240	2.062	1.421	1.648	1.658
with diffuse functions	1.027	0.816	1.001	0.921	1.353	1.189	1.389	1.298

four probe molecules are tabulated in Table S2 of the Supporting Information. All Pople basis sets including diffuse functions succeed in a correct prediction of the stronger electrophilic behavior of the polar molecules (methanol and chloromethane) and a more nucleophilic behavior for the apolar molecules (ethene and propene). This is clearly illustrated in Figure 2, where the variation of the chemical potential depending on basis set size is depicted. As functional sensitivity was found to be small, only BMK results are included in Figure 2. The basis sets without diffuse functions, on the other hand, do not show a clear separation between molecules with polar and apolar character. Large deviations are clear for methanol in particular.

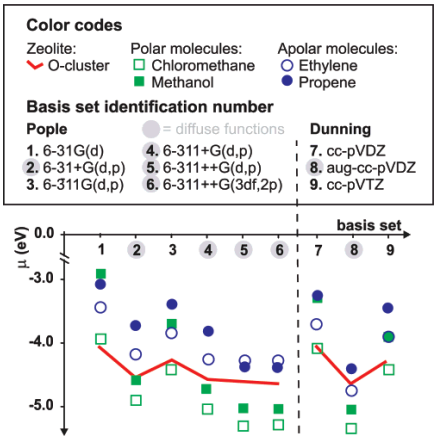

Figure 2. μ values for the O cluster (red line) and the four probe molecules chloromethane, methanol, ethylene and propene, calculated using the BMK functional (polar molecules: green; apolar molecules: blue).

4.2.2. Softness Differences. In Table 3, we list ΔS for the interaction between the four small probe molecules and the purely oxygen-bridged zeolite cluster. Large variations occur depending on both basis set and electronic structure method, but the overall predictions for ΔS are systematically larger for the two polar molecules compared to the apolar systems. Closer inspection of Table 3 reveals that the BMK and MPWB1K functionals predict almost identical values, whereas the HF predictions show large deviations from the DFT results. Concerning basis set dependence, the lack of diffuse functions will most often lead to higher ΔS values. At any rate, caution is absolutely necessary when applying the softness matching criterion to predict reaction preferences, as conclusions may depend on the applied level of theory. For sake of completeness, Table S1 of the Supporting Information tabulates the influence of the level of theory used for the geometry optimization on the average ΔS values. Yet again, this influence is negligible and our choice for B3-LYP/6-31G(d) geometries is warranted.

4.2.3. Activation Hardnesses. The $\Delta\eta_{act}$ values (Table 4) use information from the adsorbed reactants as well as from transition state structures. The smaller the $\Delta\eta_{act}$ value, the easier the reaction should proceed and the lower the reaction barrier should be. In ref 28, we compared $\Delta\eta_{act}$ values with energy barriers at 0 Kelvin (ΔE_0, Table 5; all properties were calculated using the B3-LYP/6-31G(d)//B3-LYP/6-31G(d) level of theory). Based on the ΔE_0 values, the following reactivity sequence corresponding to the interactions between the various small probe molecules and the purely oxygen-bridged cluster was obtained: propene < ethylene < chloromethane < methanol. No correlation exists between ΔE_0 and $\Delta\eta_{act}$, leading to the

TABLE 5: ΔE_0 Values (kJ/mol) for Chemisorption Reactions, ZPE Included, Taken from ref 28

	ΔE_0			
B3-LYP/6-31G(d)	CH_3Cl	CH_3OH	C_2H_4	C_3H_6
O	169.9	199.8	96.6	86.0
N1	220.3	165.8	141.0	117.6
N2	117.5	150.3	124.3	119.6

conclusion that the reactivity descriptor $\Delta\eta_{act}$ is inadequate in differentiating between the reactivities of the various probe molecules. The present study strongly confirms this conclusion: no correlation is obtained between the ΔE_0 and $\Delta\eta_{act}$ values, regardless of the level of theory used (see Table 4). We readily see that the overall $\Delta\eta_{act}$ value is smallest in the case of adsorption of chloromethane, while slight deviations can be noticed in the estimates predicted for methanol and ethylene. The largest values are found for propene. We note that for the current study the energy barriers were recalculated using the various levels of theory (included in Table S3 in the Supporting Information), but they do not differ qualitatively from the values at the B3-LYP/6-31G(d) level (displayed in Table 5). Finally, we report that the absolute values of HF differ substantially from the DFT results. The various $\Delta\eta_{act}$ predictions can again be classified in two categories, depending on the inclusion or exclusion of diffuse functions in the basis set.

4.3. Reactivity Sequences: Amine-Modified Zeolites. Comparison with kinetic data, such as ΔE_0 (Table 5), becomes more challenging when various zeolite clusters are compared. As in previous works of the authors, amine-substituted zeolite clusters (Figure 1) have been intensively investigated.[25,27] They form a suitable set of zeolite clusters to further validate the various rules on global reactivity descriptors. In particular, we will investigate whether the reactivity sequences between the three zeolite model clusters, as predicted in ref 28 using B3-LYP/6-31G(d), are maintained throughout the various levels of theory.

4.3.1. Hardness Sequence. In Tables S4 and S5 of the Supporting Information, the calculated IP and EA values as well as their derived global properties are given for the isolated amine-substituted zeolite models N1 and N2. It was earlier reported that all three investigated clusters are considered intermediately hard and that substitution of an oxygen by a nitrogen atom lowers the hardness, increasing the reactivity of the amine-modified cluster.[28] These conclusions were based on B3-LYP/6-31G(d) results, we now demonstrate that the hardness sequence $\eta(O) > \eta(N2) > \eta(N1)$ is retained for all investigated levels. The average difference between the $\eta(O)$ and $\eta(N2)$ values is 0.14 eV, whereas the average difference between the amine-substituted hardness values N2 and N1 is much smaller (0.07 eV). The reported hardness sequence indicates that substitution of an oxygen by a nitrogen atom lowers the hardness, increasing the reactivity of the amine-modified cluster.

4.3.2. Softness Differences. Global softness differences are calculated for the interactions between the three zeolite clusters and the probe molecules. Chloromethane and ethylene were chosen as the case study polar and apolar system, respectively. It was previously observed, using the B3-LYP/6-31G(d) level of theory, that for the interactions with the polar molecules, the HSAB principle fails due to a lack of any correlation between ΔS and ΔE_0.[28] This failure illustrates the limitations of the HSAB principle, where polarization effects are only partially included. For the apolar molecules however, the HSAB was shown to be successful.[28] In Figures 3 and 4 results for chloromethane and ethylene are illustrated. The following conclusions can be made.

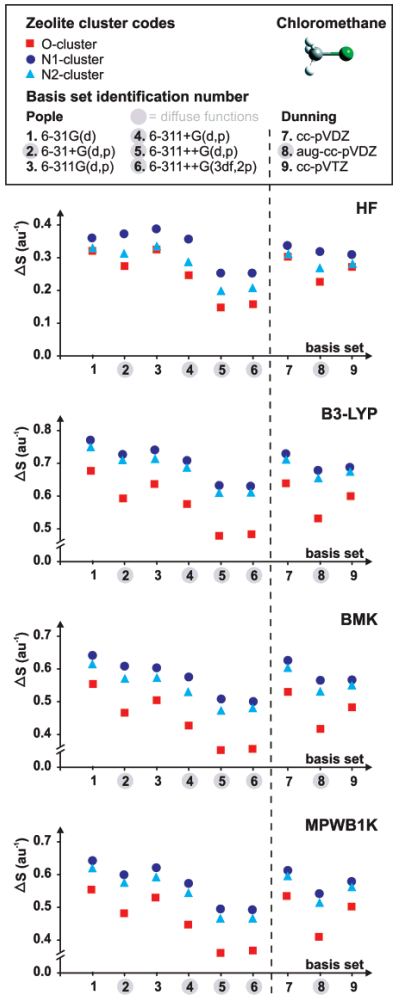

Figure 3. ΔS values for the interactions with chloromethane. Red squares correspond to the O cluster, dark blue circles to the N1 cluster, and light blue triangles to the N2 cluster.

First, we find that the overall qualitative basis set dependence of the various DFT functionals is extremely similar. A striking exception is noticed for the interaction with C_2H_4, where augmentation from the Dunning cc-pVDZ basis set leads to a largely deviating behavior for the MPWB1K functional.

Second, for ethylene the basis set dependence is largest in HF. From a quantitative perspective, the HF values are systematically smaller than the DFT results.

Third, the reactivity sequence $\Delta S(O) < \Delta S(N2) < \Delta S(N1)$ is found throughout, for both ethylene and chloromethane. Only

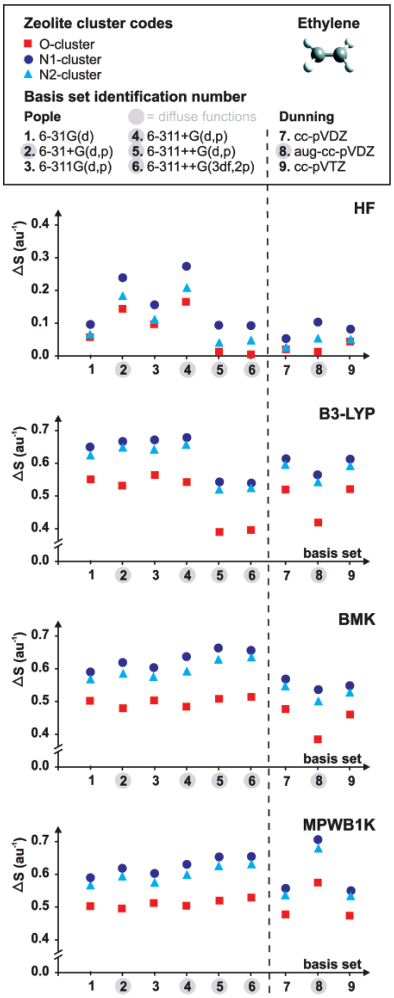

Figure 4. ΔS values for the interactions with ethylene. Red squares correspond to the O cluster, dark blue circles to the N1 cluster, and light blue triangles to the N2 cluster.

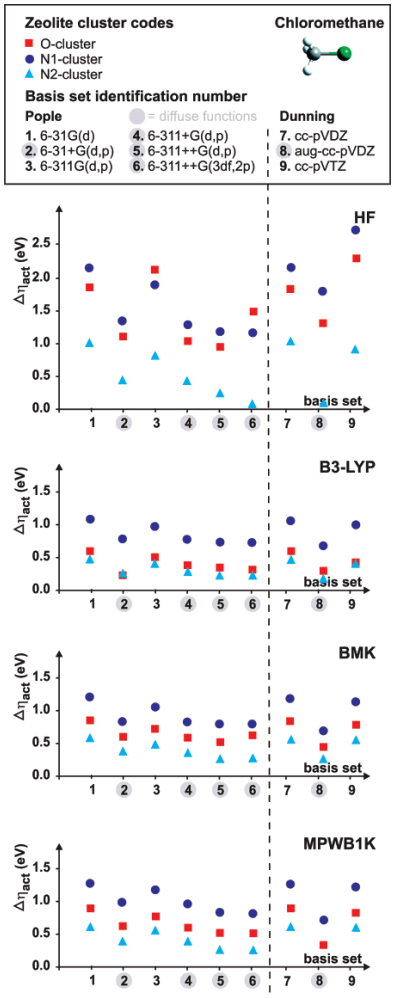

Figure 5. $\Delta\eta_{act}$ values or the interactions with chloromethane. Red squares correspond to the O cluster, dark blue circles to the N1 cluster, and light blue triangles to the N2 cluster.

in the case of ethylene this sequence matches the kinetic results in Table 5. For the studied hard−hard interactions within zeolite catalysis, reactivity sequences based on ΔS values are entirely independent of the computational method used for the calculation of the global reactivity descriptors. This is no guarantee, however, for sequences based on the HSAB principle to coincide with sequences obtained from kinetic data.

4.3.3. Activation Hardnesses. Activation hardnesses were calculated for the interactions between the three zeolite clusters and the probe molecules. Computations on both the optimized structures of the adsorbed reactants and transition structures were performed. Application of the B3-LYP/6-31G(d) level of theory on these systems has already been performed,[28] and an excellent correlation between the $\Delta\eta_{act}$ and ΔE_0 values for all studied reactions was observed. However, does this agreement still hold when the level of theory, used for the single-point energy calculations, is altered? Chloromethane and ethylene (optimized at B3-LYP/6-31G(d)) were again chosen as reference polar and apolar systems, respectively. The results are illustrated in Figures 5 and 6.

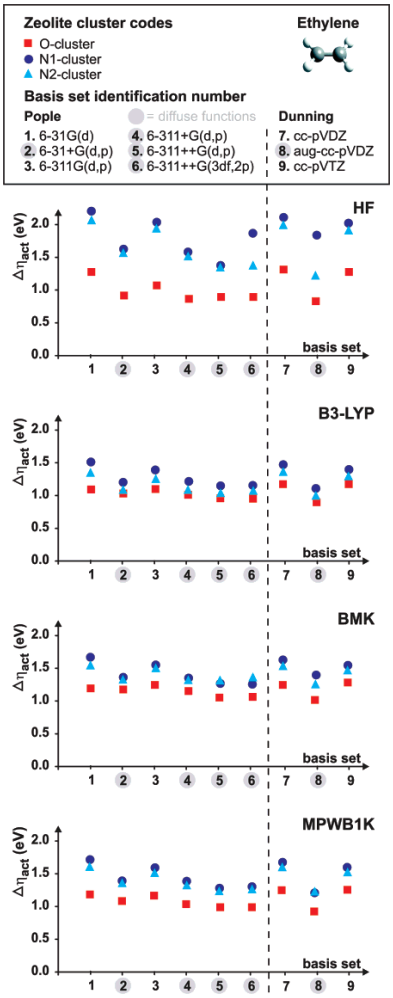

Figure 6. $\Delta\eta_{act}$ values for the interactions with ethylene. Red squares correspond to the O cluster, dark blue circles to the N1 cluster, and light blue triangles to the N2 cluster.

The conclusions about basis set and functional dependence are quite similar to those obtained in the previous section for the ΔS values. The basis set sensitivity of the four methods follows a similar pattern. The HF results show again a larger scattering from the DFT results, the latter which are closer to each other.

For the interaction with chloromethane, the sequence based on reaction barriers is the following: $\Delta E_0(N1) > \Delta E_0(O) > \Delta E_0(N2)$ and this trend is correctly reproduced by all three DFT methods using the $\Delta\eta_{act}$ descriptor. The MPWB1K/aug-cc-pVDZ result for the N2 cluster has been omitted due to spin-contamination in the calculation of the cation. The HF results show occasional deviations from this sequence, more precisely when the 6-311G(d,p) (**3**), 6-311++G(3df,2p) (**6**) basis sets are used. As mentioned earlier, HF performs poorly for the computation of $\Delta\eta_{act}$ values, underlying the importance of including correlation effects for an accurate energy calculation of the adsorbed reactants and transition structures.

For the interaction with ethylene, the correct sequence is different: $\Delta\eta_{act}(N1) > \Delta\eta_{act}(N2) > \Delta\eta_{act}(O)$. Here all levels of theory succeed in reproducing correctly this sequence. Only the BMK functional predicts an occasional reversed sequence between the N1 and N2 clusters, albeit based on very small differences.

5. Conclusions

We have thoroughly assessed the level-of-theory dependence of important molecular properties, such as the ionization potential and electron affinity, as well as global reactivity descriptors, such as the chemical potential and global hardness. This investigation was concentrated on typical interactions within zeolite catalysis between small probe molecules (chloromethane, methanol, ethylene, and propene) and three model zeolite clusters. All calculations were submitted to an extended set of computational methods. First of all, the dependence on electronic structure method was investigated by testing the HF and three DFT methods, in particular B3-LYP, BMK, and MPWB1K. The performance of the latter two hybrid meta-DFT functionals for the computation of reactivity descriptors was hereby addressed for the first time. The basis set dependence on the other hand was also intensively studied, using a broad set of both Pople and Dunning basis sets.

Comparison with available experimental data and high-level post-HF calculations shows that, at least for the small molecules, quantitatively accurate and reliable results can be obtained using any of the aforementioned DFT functionals in conjunction with a basis set of at least double-ζ quality, further augmented with a set of polarization and diffuse functions. The interactions between the oxygen-cluster and the probe molecules are addressed by investigating the global softness differences and activation hardnesses. We generally find similar performance for the three investigated DFT functionals, with the BMK and MPWB1K results particularly close to each other. The HF results, on the other hand, are more scattered and sensitive to the applied basis set.

As the reactivity descriptors are often applied to investigate intermolecular reactivity sequences, we found it crucial to investigate whether these sequences depend on a particular choice of computational method. In this view, three model clusters containing both oxygen and amine bridges were studied in detail. The ordering of the global hardness values is retained, no matter what electronic structure method or basis set is used. The same conclusion holds for the global softness differences, for interactions with both polar and apolar probe molecules. The reactivity ordering, based on activation hardnesses, turns out to show a minor dependence on the level of theory used. Comparison between the DFT functionals demonstrates an extreme similarity between BMK and MPWB1K results, while they both deviate substantially from the B3-LYP results. However, this deviation is only manifested from a quantitative, but not from a qualitative perspective. We gladly report that, for the studied hard−hard interactions, reactivity sequences are mainly independent of DFT functional and/or basis set used. In particular, the previously mentioned necessity to include

diffuse functions is not as strict when focus solely lies on obtaining reliable qualitative reactivity trends. Furthermore, the reactivity sequences obtained using the reactivity descriptors are overall in agreement with sequences based on ab initio reaction energies. An exception is found for the interactions between the oxygen-bridged zeolite cluster and the polar molecules, where the reactivity ordering is not in accordance with the HSAB principle.

Acknowledgment. This work is supported by the Fund for Scientific Research—Flanders (FWO), the Research Board of Ghent University, and the Institute for Science and Technology (I.W.T.).

Supporting Information Available: Global hardness of the purely oxygen-bridged cluster using various levels for the geometry optimization (Figure S1); average softness differences between the purely oxygen-bridged cluster and the probe molecules using various levels for the geometry optimization (Table S1); chemical potential for the probe molecules (Table S2); reaction barriers using various levels for the single-point energies (Table S3); ionization potentials, electron affinities, chemical potentials and global hardnesses for the amine-substituted zeolites N1 (Table S4) and N2 (Table S5). This material is available free of charge via the Internet at http://pubs.acs.org.

References and Notes

(1) Kohn, W.; Becke, A. D.; Parr, R. G. *J. Phys. Chem.* **1996**, *100*, 12974.
(2) Parr, R. G.; Yang, W. *Density-Functional Theory of Atomsand Molecules*; Oxford Science Publications, New York, 1988.
(3) Geerlings, P.; De Proft, F.; Langenaeker, W. *Chem. Rev.* **2003**, *103*, 1793.
(4) Parr, R. G.; Donnelly, R. A.; Levy, M.; Palke, W. E. *J. Chem. Phys.* **1978**, *68*, 3801.
(5) Parr, R. G.; Pearson, R. G. *J. Am. Chem. Soc.* **1983**, *105*, 7512.
(6) Chermette, H. *J. Comput. Chem.* **1999**, *20*, 129.
(7) (a) De, Proft, F.; Martin, J. M. L.; Geerlings, P. *Chem. Phys. Lett.* **1996**, *256*, 400. (b) De Proft, F.; Martin, J. M. L.; Geerlings, P. *Chem. Phys. Lett.* **1996**, *250*, 393. (c) Langenaeker, W.; De Proft, F.; Geerlings, P. *J. Mol. Struct. (THEOCHEM)* **1996**, *362*, 175. (d) Arulmozhiraja, S.; Kolandaivel, P. *Mol. Phys.* **1997**, *90*, 55. (e) Thanikaivelan, P.; Padmanabhan, J.; Subramanian, V.; Ramasami, T. *Theor. Chem. Acc.* **2002**, *107*, 326. (f) Martin, F.; Zipse, H. *J. Comp. Chem.* **2005**, *26*, 97. (g) Cioslowski, J.; Martinov, M.; Mixon, S. T. *J. Phys. Chem.* **1993**, *97*, 10948. (h) Gilardoni F.; Weber, J.; Chermette, H.; Ward, T. R. *J. Phys. Chem. A* **1998**, *102*, 3607.
(8) De Proft, F.; Geerlings, P. *J. Chem. Phys.* **1997**, *106*, 3270.
(9) (a) Jalbout, A. F.; Darwish, A. M.; Alkahby, H. Y. *J. Mol. Struct. (THEOCHEM)* **2002**, *585*, 205. (b) Jalbout, A. F.; Jalbout, F. N.; Alkahby, H. Y. *J. Mol. Struct. (THEOCHEM)* **2001**, *574*, 141.
(10) Chattaraj, P. K.; Schleyer, P. v. R. *J. Am. Chem. Soc.* **1994**, *116*, 1067.
(11) Simons, J.; Jordan, K. D. *Chem. Rev.* **1987**, *87*, 535.
(12) Curtiss, L. A.; Raghavachari, K.; Trucks, G. W.; Pople J. A. *J. Chem. Phys.* **1991**, *94*, 7221.
(13) Curtiss, L. A.; Redfern, P. C.; Raghavachari, K.; Pople J. A. *J. Chem. Phys.* **1998**, *109*, 42.
(14) Rienstra-Kiracofe, J. C.; Tschumper, G. S.; Schaefer, H. F.; Nandi, S.; Ellison, G. B. *Chem. Rev.* **2002**, *102*, 231.
(15) Martin, J. M. L.; de Oliveira, G. *J. Chem. Phys.* **1999**, *111*, 1843.
(16) Parthiban, S.; Martin, J. M. L. *J. Chem. Phys.* **2001**, *114*, 6014.
(17) Boese, A. D.; Oren, M.; Atasoylu, O.; Martin, J. M. L.; Kallay, M.; Gauss, J. *J. Chem. Phys.* **2004**, *120*, 4129.
(18) (a) Shore, H. B.; Rose, J. H.; Zaremba, E. *Phys. Rev. B* **1977**, *15*, 2858. (b) Schwarz, K. *Chem. Phys. Lett.* **1978**, *57*, 605.
(19) Galbraith, J. M.; Schaefer, H. F. *J. Chem. Phys.* **1996**, *105*, 862.
(20) Tozer, D. J.; De Proft, F. *J. Phys. Chem. A* **2005**, *109*, 8923.
(21) Zhao, Y.; Truhlar, D. G. *J. Phys. Chem. A* **2004**, *108*, 6908.
(22) Boese, A. D.; Martin, J. M. L. *J. Chem. Phys.* **2004**, *121*, 3405.
(23) Hemelsoet, K.; Moran, D.; Van Speybroeck, V.; Waroquier, M.; Radom, L. *J. Phys. Chem. A* **2006**, *110*, 8942.
(24) Astala, R.; Auerbach, S. M. *J. Am. Chem. Soc.* **2004**, *126*, 1843.
(25) Lesthaeghe, D.; Van Speybroeck, V.; Waroquier, M. *J. Am. Chem. Soc.* **2004**, *126*, 9162.
(26) Chan, B.; Radom, L. *J. Am. Chem. Soc.* **2006**, *128*, 5322.
(27) Lesthaeghe, D.; Van, Speybroeck, V.; Marin, G. B.; Waroquier, M. *J. Phys. Chem. B* **2005**, *109*, 7952.
(28) Hemelsoet, K.; Lesthaeghe, D.; Van Speybroeck, V.; Waroquier M. *Chem. Phys. Lett.* **2006**, *419*, 10.
(29) Pearson, R. G. *J. Am. Chem. Soc.* **1963**, *85*, 3533.
(30) (a) Chattaraj, P. K.; Lee, H.; Parr, R. G. *J. Am. Chem. Soc.* **1991**, *113*, 1855. (b) Damoun, S.; Van de Woude, G.; Mendez, F.; Geerlings, P. *J. Phys. Chem. A* **1997**, *101*, 886.
(31) (a) Pearson, R. G. *Acc. Chem. Res.* **1993**, *26*, 250. (b) Parr, R. G.; Chattaraj, P. K. *J. Am. Chem. Soc.* **1991**, *113*, 1854. (c) Chattaraj, P. K.; Ayers, P. W. *J. Chem. Phys.* **2005**, *123*, 086101.
(32) Datta, D. *J. Phys. Chem.* **1992**, *96*, 2409.
(33) Zhou, Z.; Parr, R. G. *J. Am. Chem. Soc.* **1990**, *112*, 5720.
(34) Frisch, M. J.; Trucks, G. W.; Schlegel, H. B.; Scuseria, G. E.; Robb, M. A.; Cheeseman, J. R.; Montgomery, J. A., Jr.; Vreven, T.; Kudin, K. N.; Burant, J. C.; Millam, J. M.; Iyengar, S. S.; Tomasi, J.; Barone, V.; Mennucci, B.; Cossi, M.; Scalmani, G.; Rega, N.; Petersson, G. A.; Nakatsuji, H.; Hada, M.; Ehara, M.; Toyota, K.; Fukuda, R.; Hasegawa, J.; Ishida, M.; Nakajima, T.; Honda, Y.; Kitao, O.; Nakai, H.; Klene, M.; Li, X.; Knox, J. E.; Hratchian, H. P.; Cross, J. B.; Bakken, V.; Adamo, C.; Jaramillo, J.; Gomperts, R.; Stratmann, R. E.; Yazyev, O.; Austin, A. J.; Cammi, R.; Pomelli, C.; Ochterski, J. W.; Ayala, P. Y.; Morokuma, K.; Voth, G. A.; Salvador, P.; Dannenberg, J. J.; Zakrzewski, V. G.; Dapprich, S.; Daniels, A. D.; Strain, M. C.; Farkas, O.; Malick, D. K.; Rabuck, A. D.; Raghavachari, K.; Foresman, J. B.; Ortiz, J. V.; Cui, Q.; Baboul, A. G.; Clifford, S.; Cioslowski, J.; Stefanov, B. B.; Liu, G.; Liashenko, A.; Piskorz, P.; Komaromi, I.; Martin, R. L.; Fox, D. J.; Keith, T.; Al-Laham, M. A.; Peng, C. Y.; Nanayakkara, A.; Challacombe, M.; Gill, P. M. W.; Johnson, B.; Chen, W.; Wong, M. W.; Gonzalez, C.; Pople, J. A. *Gaussian 03*, revision B.03; Gaussian, Inc.: Wallingford, CT, 2004.
(35) Sauer, J. *Chem. Rev.* **1989**, *89*, 199.
(36) van Santen, R. A.; Kramer, G. J. *Chem. Rev.* **1995**, *95*, 637.
(37) Becke, A. D. *J. Chem. Phys.* **1993**, *98*, 5648.
(38) Lee, C.; Yang, W. T.; Parr, R. G. *Phys. Rev. B* **1988**, *37*, 785. (b) Miehlich, B.; Savin, A.; Stoll, H.; Preuss H. *Chem. Phys. Lett.* **1989**, *157*, 200.
(39) Zygmunt, S. A.; Mueller, R. M.; Curtiss, L. A.; Iton, L. E. *J. Mol. Struct. (THEOCHEM)* **1998**, *430*, 9.
(40) Dunning, T. H., Jr.; Peterson, K. A.; Woon, D. E. Basis Sets: Correlation Consistent Sets. In *The Encyclopedia of Computational Chemistry*; Schleyer, P. v. R., Ed; John Wiley: Chichester, U.K., 1998.
(41) Frisch, M. J.; Pople, J. A.; Binkley, J. S. *J. Chem. Phys.* **1984**, *80*, 3265 and references therein.
(42) (a) Woon, D. E.; Dunning, T. H. *J. Chem. Phys.* **1993**, *98*, 1358. (b) Kendall, R. A.; Dunning, T. H.; Harrison, R. *J. Chem. Phys.* **1992**, *96*, 6796. (c) Dunning, T. H. *J. Chem. Phys.* **1989**, *90*, 1007. (d) Peterson, K. A.; Woon, D. E.; Dunning, T. H. *J. Chem. Phys.* **1994**, *100*, 7410. (e) Wilson, A. K.; van Mourik, T.; Dunning, T. H., Jr. *J. Mol. Struct. (THEOCHEM)* **1996**, *388*, 339.
(43) (a) Pople, J. A.; Head-Gordon, M.; Raghavachari, K. *J. Chem. Phys.* **1987**, *87*, 5968. (b) Gauss, J.; Cremer, D. *Chem. Phys. Lett.* **1988**, *150*, 280. (c) Salter, E. A.; Trucks, G. W.; Bartlett, R. J. *J. Chem. Phys.* **1989**, *90*, 1752.
(44) (a) Purvis, G. D.; Bartlett, R. J. *J. Chem. Phys.* **1982**, *76*, 1910. (b) Raghavachari, K.; Trucks, G. W.; Pople, J. A.; Head-Gordon, M. *Chem. Phys. Lett.* **1989**, *157*, 479.
(45) Kimura, K.; Katsumata, S.; Achiba, Y.; Yamazaki, T.; Iwata, S. *Ionization energies, Ab initio assignments, and valence electronic structure for 200 molecules in Handbook of HeI Photoelectron Spectra of Fundamental Organic Compounds*; JapanScientific Soc. Press: Tokyo, 1981.
(46) Vorob'ev, A. S.; Furlei, I. I.; Sultanov, A. S.; Khvostenko, V. I.; Leplyanin, G. V.; Derzhinskii, A. R.; Tolstikov, G. A. *Bull. Acad. Sci. USSR, Div. Chem. Sci.* **1989**, *38*, 1388.
(47) Bieri, G.; Asbrink, L. *J. Electron Spectrosc. Relat. Phenom.* **1980**, *20*, 149.
(48) Krause, D. A.; Taylor, J. W.; Fenske, R. F. *J. Am. Chem. Soc.* **1978**, *100*, 718.
(49) Chandra, A. K.; Uchimaru, T.; Sugie, M.; Sekiya, A. *Chem. Phys. Lett.* **2000**, *318*, 69.

5 Conclusions and perspectives

This thesis has demonstrated quite clearly how theoretical methods, serving as a molecular microscope, are able both to solve complex problems in heterogeneous catalysis and to suggest and test appropriate modifications to the catalyst.

We have indeed partially resolved one of the most controversial issues in heterogeneous catalysis: the reaction mechanism of the industrially important methanol-to-olefin process. For a long time, this process was believed to be governed by a direct C-C coupling from two C1 species, even though the most recent experimental observations seem to completely contradict this fact. The two major opposing proposals for C-C coupling in the methanol-to-olefin process were extensively investigated. Firstly, the vast number of possible direct mechanisms was tackled by setting up an extensive and consistent reaction scheme, tying together a large variety of possible direct reactions, even including several previously overlooked pathways. By looking at the calculated rate coefficients - rather than just the less-informative energy barriers - in this scheme, we have been able to show clearly how all direct mechanisms fail at one point or another and to identify the three main bottlenecks responsible: the high instability of carbene-based intermediates, the slow co-reaction of methane and formaldehyde and the high energy barrier for a general concerted C-C coupling mechanism. No complete direct pathway from methanol leading all the way to ethene (nor to any C2 intermediate) exists. Because this result completely defies conventional wisdom, this can be considered, without a doubt, the greatest accomplishment of the research presented here.

The hydrocarbon pool alternative, on the other hand, seems to offer an even more complex challenge, not only because of the immense number of reactions which form a complicated and tangled network, but also because the organic hydrocarbon pool species and the inorganic zeolite framework cooperate as a supramolecular catalyst towards low-energy alternative pathways. We have shown that both hydrocarbon pool species and zeolite topology play a crucial role in the reaction kinetics for the initial C-C coupling step through shape selectivity and cation stabilization, to the extent that we should consider several separate mechanisms, each tailored to a different zeotype material. From this initiating step, we have mainly learnt that the zeolite topology can manifest itself in many different ways, going well beyond the geometric constraints imposed. The hydrocarbon pool reactions are, therefore, nowhere near a local phenomenon, which implies that current understanding of acid zeolite catalysis is in drastic need of modernization. Most importantly, though, it does indeed seem that the hydrocarbon pool model might provide an alternative route that bypasses the direct bottlenecks, but full theoretical evidence is yet to be provided. If we could succeed in pin-pointing the exact mechanism, the knowledge obtained from theoretical calculations could be used directly in finding ways to suppress secondary reactions and to obtain product control.

Control of the reactions might be obtained by suitable modifications to the zeolite framework. One of the major modifications that have been suggested in the literature for all kinds of zeolite-catalyzed processes is the creation of so-called 'zeozymes'. By incorporating small organic fragments directly into the inorganic zeolite framework it might be possible to combine the properties of zeolites with those of enzymes. Here we have studied the simplest of these modifications, i.e. methylene and amine functionalities, and their possible future importance in zeolite catalysis. Extensive investigation of typical properties of methylene functionalized zeolites shows how the methylene moiety influences adsorption properties. A study of proton mobility furthermore provides an explanation for the experimentally observed methyl end groups which result in local cleavage of the zeolite framework. Investigation of MTO-related reactions in amine-modified zeolites, on the other hand, show how the amine moiety provides an additional basic site at possibly more advantageous positions, thus allowing more favorable transition states for alkylammonium formation. This clearly demonstrates how organic moieties can alter and even improve the catalyst's properties.

Theoretical calculations have explained here existing experimental observations, provided new insights on the molecular level and are capable of giving guide-

lines for future synthesis. This has been performed right at the edge of what is currently feasible: this work would not have been possible without very high performance computers, state-of-the-art modeling techniques and an unprejudiced view on the zeolite catalyst. This thesis does not mark the end of a research direction and quite a few subjects are up for discussion. We close, therefore, by identifying several primary goals for further research, each of which we plan to pursue.

The road ahead

Since only the first step has been studied in detail so far, the entire reaction network of the hydrocarbon pool hypothesis should be validated theoretically. We are currently actively pursuing an entire low-energy pathway linking methanol all the way to ethene. By combining concepts from both heterogeneous and homogeneous catalysis, detailed insight into the hydrocarbon pool proposal will contribute to an improved understanding of a whole range of industrial applications in zeolites.

Once the reaction mechanism of MTO is fully understood, suitable improvements can be suggested and tested to answer the question of whether the best catalyst possible has already been assembled or not. The zeolite framework could be modified with organic and/or inorganic moieties which either take up necessary space and refine shape selectivity or provide a novel catalytically active site. The properties of these zeozymes and their applicability to MTO catalysis should be extensively investigated.

It is also unclear how the initial hydrocarbon pool is formed during the induction period. In an important topology like that of HSAPO-34 the relatively large aromatic species need to be formed through a 'ship-in-a-bottle' synthesis procedure: in most other acid-catalyzed reactions, however, these same aromatic species will not be the active center, but they will rather act as undesirable coke precursors. Ship-in-a-bottle reactions are furthermore vital in the design and synthesis of zeozymes. Therefore, theoretical insight into a whole range of ship-in-a-bottle type reactions will be important for the entire field of zeolite catalysis.

To solve these problems, several methodological issues will need to be addressed as well. For example, to include finite temperature effects properly, the free energy (that also accounts for entropic effects) must be monitored. Therefore,

we must go beyond TST towards molecular dynamics (MD) simulations. In addition, MD methods are ideally suited for determining global minima for systems with a large number of degrees of freedom. The DFT-based Car-Parrinello formalism is the most cost-effective ab initio MD method currently available. Though it is implemented in periodic codes, the unit cell of the industrially most important zeolites is too large to handle within computational limitations. Therefore, a suitable QM/MM MD code fit for zeolites should be developed. This code could then be used to study the docking positions of large aromatic species near the acid site and to evaluate the effect of solvating molecules like water or methanol on the reactivity of the supramolecular complex.

Last but not least, historically, MTO catalysis has most often been performed on HZSM-5, but more recently the excellent performance of HSAPO-34, which is an alumino-phosphate zeotype material, has rapidly been gaining interest. However, when full QM methods are applied to relatively small alumino-phosphate clusters, they are subject to unrealistic dipole moments created by the strong polarity of this material. Suitable models for all kinds of zeotype materials need to be built and validated experimentally, so that hydrocarbon pool reactions can be modeled in these as well, allowing for extraction of composition effects on the reaction mechanism.

Though this field of research has seen enormous progress in the last years, it is clear that we still have quite an adventurous road ahead of us...

N Nederlandstalige appendix

N.1 Algemene inleiding

Hoewel zuur-gekatalyseerde reacties over zeolieten een belangrijke schakel vormen voor allerlei processen in de petrochemische industrie, wordt hun reactief gedrag meestal slechts oppervlakkig begrepen. Om hieraan te verhelpen, worden in deze thesis enkele belangrijke elementaire reactiestappen uit de zeolietkatalyse gedetailleerd onderzocht met behulp van kwantumchemische modelleringstechnieken. Dit onderzoeksgebied heeft de laatste jaren enorme opgang gemaakt door de immense evolutie in computerkracht en de vele methodologische ontwikkelingen, waardoor vandaag de dag processen van industrieel belang bestudeerd kunnen worden. Het aldus verkregen inzicht wordt vervolgens aangewend om mogelijke verbeteringen aan het zeolietrooster vanuit submicroscopisch oogpunt te toetsen.

In het eerste luik van deze samenvatting worden enkele algemene begrippen verduidelijkt, zodat ze nadien doorheen dit hoofdstuk gebruikt kunnen worden. Dit zijn in eerste instantie begrippen die volgen uit de structuur en de samenstelling van zeolieten en zeotype materialen, zoals de vormselectieve eigenschappen en de aanwezigheid van zure sites. Vervolgens worden ook de gebruikte kwantumchemische methoden aangebracht, met speciale aandacht voor de specifieke technieken die nodig zijn voor het modelleren van elementaire reactiestappen in uitgebreide systemen zoals zeolieten. In deze thesis worden de belangrijkste conclusies gebaseerd op de reactiesnelheid van cruciale stappen. De chemische

kinetiek in het algemeen, en transitietoestandstheorie in het bijzonder, zijn daarvoor essentieel en worden ook summier besproken.

In het tweede deel wordt ingegaan op een zeer actuele problematiek, met name de zoektocht naar het reactiemechanisme van het methanol-to-olefin proces (MTO). Na een algemene inleiding over de rol van MTO in de petrochemie en een korte historiek van de talrijke studies op het mechanisme ervan, wordt er in dit deel een hele klasse van reactie-voorstellen onderzocht. Deze klasse zal dan in zijn totaliteit verworpen worden op grondige theoretische basis, waarna vervolgens het alternatief hydrocarbon pool model wordt ingeleid. De resultaten hierover leveren nieuwe inzichten op over de functie van het zeolietrooster en hoe het geheel van zeolietrooster en organisch actief centrum als een supramoleculair complex moet worden beschouwd.

De verworven kennis van deze elementaire reactiestappen wordt vervolgens in het derde deel ten volle benut door in detail na te gaan op welke manier organische veranderingen aan het zeolietrooster deze reacties kunnen beïnvloeden. De combinatie met een aluminium defect wordt voor zowel methyleen- als amine-gesubstitueerde zeolieten onderzocht. Daarna wordt de invloed van een amine groep op de kinetiek van enkele MTO-gerelateerde reacties verder nagegaan.

Tot slot worden alle conclusies gegroepeerd en worden er aanwijzigingen gegeven voor toekomstig onderzoek.

N.2 Terminologie en methodiek

In dit voorbereidend deel worden de termen en methoden verduidelijkt die later bij de toepassingen aangewend worden. Meer in het bijzonder wordt ingegaan op de katalytische eigenschappen van zeolieten, op de kwantumchemische en modelbenaderingen die moeten gemaakt worden en op de methoden om de reactiekinetiek op microscopische basis af te leiden.

N.2.1 Zeolieten en zeotype materialen

Zeolieten zijn nanoporeuze kristallijne aluminosilicaten, opgebouwd uit TO_4 tetrahedra (T=Si of Al), die een complex netwerk van 3-dimensionale holtes en kanalen vormen [1]. Vermits deze holtes en kanalen van moleculaire grootte

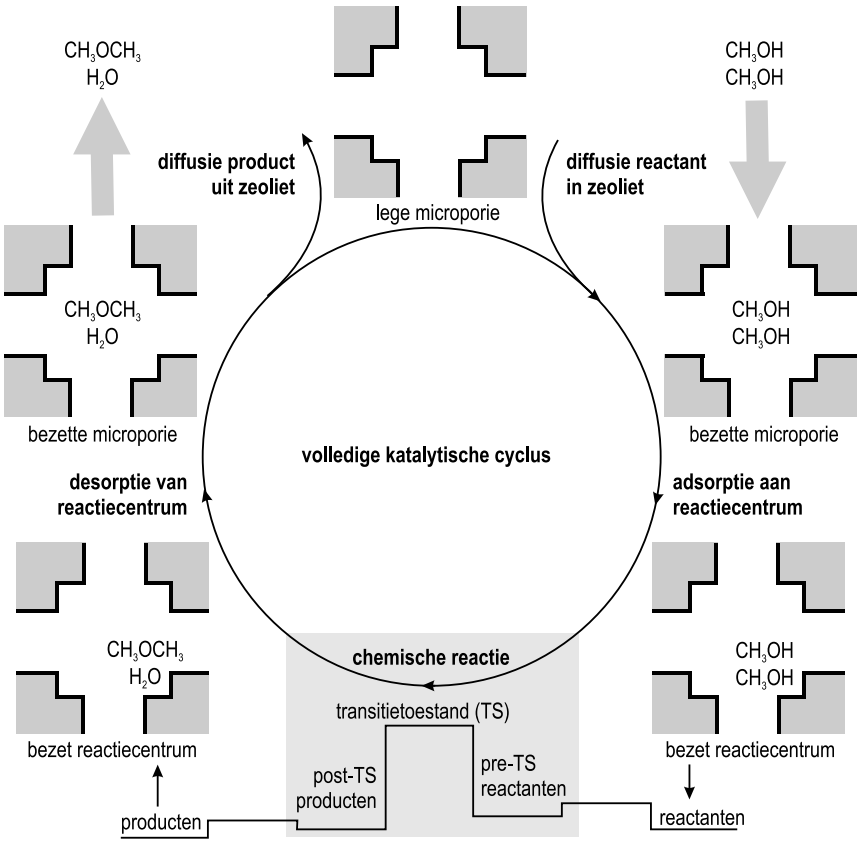

Figuur N.1: Volledige cyclus in een zeoliet-gebaseerd katalytisch proces [11].

zijn, staan zeolieten vooral bekend als moleculaire zeven. Dit komt vooral tot uiting wanneer ze gebruikt worden als vormselectieve katalysatoren:

- Wanneer kleine moleculen het zeoliet eenvoudig kunnen binnendringen terwijl grotere dat niet kunnen, dan spreekt men van vormselectiviteit op de reactanten.
- Wanneer verschillende producten in het zeoliet gevormd kunnen worden maar slechts enkele daarvan het materiaal ook daadwerkelijk kunnen verlaten, dan heeft men het over vormselectiviteit op de producten.
- Wanneer voor een bepaalde chemische reactie er een groot transitietoe-

standscomplex moet gevormd worden en de ruimte in de holten daarvoor ontbreekt, dan spreekt men van vormselectiviteit op de transitietoestand.

Indien in een puur silica-zeoliet een tetravalent silicium-atoom wordt vervangen door een trivalent aluminium-atoom, dan leidt dit tot een netto negatieve lading op het rooster. Dit defect kan ondermeer gecompenseerd worden door een positief geladen kation of door een Brønsted zuur proton (dat zich aan een aluminium-gebonden zuurstofbrug zal hechten). Terwijl striktgenomen enkel aluminosilicaten onder de noemer zeolieten geklasseerd worden, verwijst men naar materialen met een andere compositie maar een gelijkaardige topologie (zoals alumino-fosfaten) als zeotype materialen.

Zeolieten worden vooral gebruikt als zure katalysator in vele petrochemische processen [10]. De focus in deze thesis ligt vooral op elementaire reactiestappen voor dergelijke processen (grijze rechthoek in Figuur N.1), wat slechts een klein deel vormt van een volledige katalytische cyclus [11]. De overige stappen, zoals adsorptie en diffusie, worden het best beschreven aan de hand van (computationeel snelle) klassieke krachtveld-gebaseerde methoden. Chemische reacties daarentegen, moeten via meer veeleisende kwantummechanische (QM) technieken behandeld worden om de drastische wijzigingen in het elektronisch bindingspatroon correct te beschrijven. Verscheidene kwantumchemische benaderingen zijn in dit opzicht mogelijk, waarbij een hogere nauwkeurigheid meestal gepaard gaat met een hogere computationele kost.

N.2.2 Kwantumchemische benaderingen

Bij de keuze van een geschikte kwantumchemische methode moet steeds de balans gemaakt worden of voor een gegeven situatie de bijkomende nauwkeurigheid opweegt tegen de computationele meerkost. In deze thesis zal daarom vooral gebruik gemaakt worden van dichteidsfunctionaaltheorie (of kortweg DFT) [15], vermits deze voor het modelleren van reacties in zeolieten een uitstekend evenwicht tussen beide afwegingen oplevert. DFT heeft bovendien de laatste jaren een enorme opgang gemaakt en heeft ongetwijfeld bijgedragen tot de enorme toename aan toepassingen van de moleculaire modellering. Voor initiële geometrieën of voor rand-atomen die ver van het actief centrum verwijderd zijn, kan wel gegrepen worden naar minder nauwkeurige maar veel snellere semi-empirische methoden. Naast een geschikte keuze van kwantumchemische benadering, moet voor uitgestrekte systemen zoals zeolieten echter ook een bepaalde modelkeuze gemaakt worden. Zeolieten zijn immers uitgestrekte periodieke sytemen die op verscheidene manieren kunnen gemodelleerd worden.

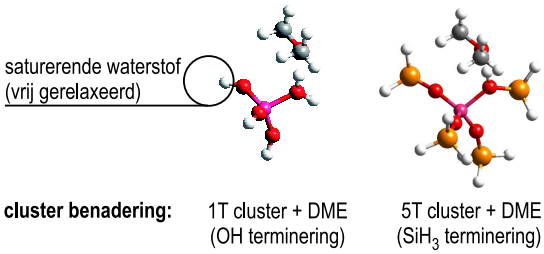

Figuur N.2: Kleine kwantummechanische clusters.

N.2.3 Atomaire modelkeuzes voor uitgebreide systemen

Zeolieten zijn zeer uitgestrekte materialen met een groot aantal atomen, waardoor een complete QM beschrijving van het volledige systeem binnen een aanvaardbare rekentijd niet haalbaar is. Dit heeft geleid tot de ontwikkeling van vergevorderde technieken die het toch mogelijk maken om een chemische reactie toch voldoende nauwkeurig te beschrijven binnen de huidige computationele beperkingen.

Kwantummechanische clusters

In de cluster-benadering wordt het periodieke rooster vervangen door een kleine cluster. Dit is de meest eenvoudige methode om snel en efficiënt reacties in zeolieten te modelleren. Het chemisch actieve deel van het kristalrooster wordt uitgeknipt, waarna alle gebroken bindingen gesatureerd worden met waterstofatomen (Figuur N.2). Dit heeft het enorme voordeel dat slechts een zeer beperkt aantal atomen in rekening gebracht wordt, wat de computationele kost aanzienlijk drukt. De basisveronderstelling hierbij is dat de invloed van het zeoliet zeer lokaal is. Later in deze thesis zal echter blijken dat dit beeld voor sommige reacties grondig moet bijgesteld worden. Vermits het zeoliet-kristal immers enkel gemodelleerd wordt door een kleine molecule in de gasfase, zijn aan deze techniek ook enkele serieuze nadelen verbonden:

Relaxatie van de cluster: Zowel wanneer de saturerende waterstofatomen volledig vrij gelaten worden als wanneer ze op kristallografische posities worden vastgepind, zal de cluster niet de ware inbedding in het zeolietrooster weergeven.

Langedracht-effecten: Alle effecten die eigen zijn aan het uitgebreid systeem (zoals elektrostatische interacties of vormselectiviteit) worden in de clusterbenadering volledig verwaarloosd.

Afhankelijk van de specifieke reactie zal de cluster-techniek al dan niet een vrij degelijke kwalitatieve informatie opleveren. In een aantal gevallen, vooral wanneer relatief grote en/of geladen moleculen een belangrijke rol spelen, zal naar meer geavanceerde technieken moeten uitgeweken worden [art. 3.5].

Periodieke codes

Een volledig periodieke beschrijving van het zeoliet lijkt de meest natuurlijk keuze. De eenheidscel van de industrieel belangrijkste zeolieten bevat echter vaak teveel atomen om nog op volledig kwantummechanische manier te behandelen (eenheidscel ZSM-5: 288 atomen). In de praktijk betekent dit dat er uitsluitend periodieke berekeningen kunnen uitgevoerd worden op een heel beperkte subset van zeoliet-topologieën. Gezien de aandacht in deze thesis uitgaat naar industriële processen wordt geen gebruik gemaakt van periodieke codes.

Hybride schillenmodellen (QM/MM of QM-hoog/QM-laag)

Idealiter zouden we de QM cluster simpelweg uitbreiden tot alle rooster-effecten voldoende in rekening gebracht worden. Deze clusters zijn echter te groot om volledig op een nauwkeurig QM niveau behandeld te worden. Een 'verdeel-en-heers' strategie biedt in dit geval de optimale oplossing: het relatief kleine actieve deel (waar chemische bindingen gebroken en gevormd worden) kan op een hoog niveau beschreven worden, terwijl het omringende rooster op een lager (en dus computationeel veel sneller) niveau mag behandeld worden. Deze opsplitsing van het moleculair systeem in meerdere delen, zoals voorgesteld in Figuur N.3, levert een volledig nieuw hybride potentiële-energie-oppervlak op.

De ONIOM methode [24] is een van de vele hybride methoden die momenteel op de markt zijn. Mits een geschikte keuze van hoog en laag niveau, kan deze methode even nauwkeurige resultaten opleveren als met een periodieke benadering, maar dan in een veel kortere rekentijd [31, 32]. Vermits deze methode bovendien alle zeoliet-topologieën probleemloos aankan, zal dit de methode zijn die in deze thesis de voorkeur geniet.

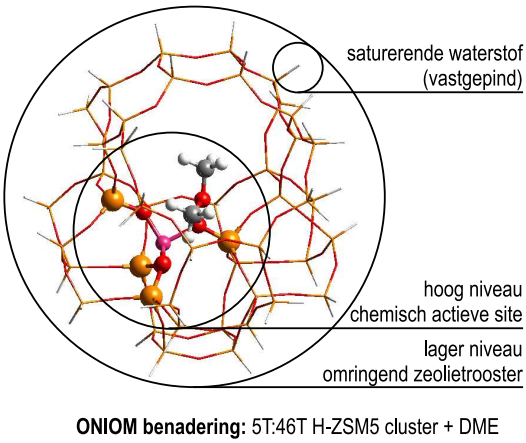

Figuur N.3: Twee-lagen ONIOM cluster die uit HZSM-5 gesneden werd.

N.2.4 Chemische kinetiek

Chemische kinetiek is een algemene term die in de fysische chemie gebruikt wordt om de studies aan te duiden die gerelateerd zijn aan de snelheid waarmee een chemische reactie verloopt. De microscopisch berekende snelheidscoëfficiënt vormt bovendien de link met dezelfde macroscopisch meetbare eenheid. In deze thesis zal enkel ingegaan worden op de kinetiek van unimoleculaire reacties, vermits deze benadering gebruikt mag worden voor een elementaire reactiestap na adsorptie van de reagentia aan de actieve site.

De sneheid van een unimoleculaire reactie v hangt af van de concentratie aan reagentia c_R (in $m^{-3}\ mol\ s^{-1}$) en de temperatuur T (in K):

$$v = k(T)c_R$$

met $k(T)$ de temperatuursafhankelijke snelheidscoëfficiënt (in s^{-1}). In de meeste gevallen zal deze snelheidscoëfficiënt exponentieel toenemen met stijgende temperatuur, waardoor binnen begrensde temperatuursintervallen de empirische Arrhenius-wet van toepassing is:

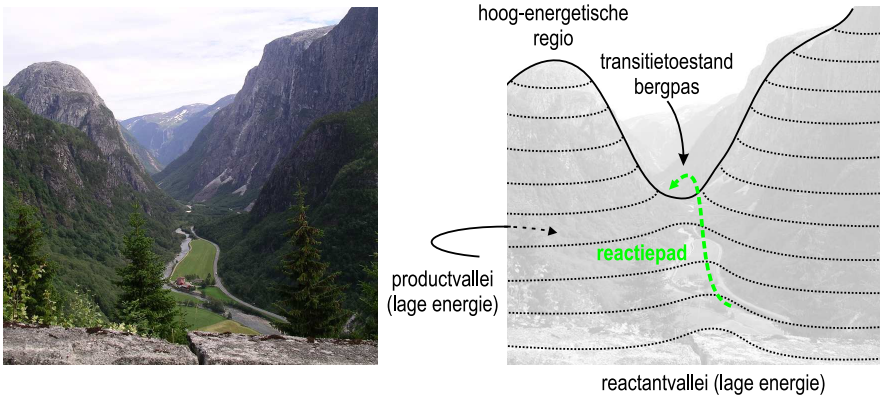

Figuur N.4: Analogie tussen een berglandschap en het potentiële-energie-oppervlak tijdens een chemische reactie.

$$k(T) = Ae^{-E_a/RT}$$

met R de universele gasconstante, E_a de activeringsenergie en A de pre-exponentiële factor.

Transitietoestandstheorie

Aan de hand van transitietoestandstheorie (TST) kunnen de Arrhenius-grootheden op microscopische basis berekend worden [37, 38]. Fundamentaal stelt TST dat er een kritisch punt bestaat (dat de transitietoestand genoemd wordt) dat op elk succesvol reactiepad ligt. Bovendien is dit punt een minimum-energie conformeer in alle vrijheidsgraden, behalve in de reactiecoördinaat, waar het een maximum is. Dit kan het best voorgesteld worden als een bergpas die twee valleien met elkaar verbindt (Figuur N.4).

De kracht van TST ligt vooral in het feit dat berekening van de snelheidscoëfficiënt slechts berust op drie stationaire punten: het reactant, de transitietoestand en het product. De voorwaartse snelheidscoëfficiënt kan bvb. als volgt berekend worden:

$$k(T) = \frac{k_B T}{h} \frac{q_\ddagger(T)}{q_R(T)} e^{-\Delta E_0/k_B T}$$

met k_B de constante van Boltzmann, h de constante van Planck, $q_{\ddagger}(T)$ en $q_R(T)$ de moleculaire partitiefuncties van de transitietoestand (op de beweging langsheen de reactiecoördinaat na) en het reactant respectievelijk, en ΔE_0 de energiebarrière op 0 Kelvin.

$$\Delta E_0 = E_0^{\ddagger} - E_0^R$$

Door deze microscopisch berekende snelheidscoëfficiënt in een $\ln(k)$ vs. $1/T$ diagram uit te zetten, kunnen de macroscopische Arrhenius-parameters A en E_a bepaald worden. Wanneer zeer gelijkaardige reacties vergeleken worden, zal men de pre-exponentiële factor vaak als identiek beschouwen en kan een kwalitatieve evaluatie gemaakt worden enkel op basis van ΔE_0. Deze benadering wordt in de literatuur meestal aangewend, maar in deze thesis zal blijken dat snelheidscoëfficiënten soms essentieel zijn om correcte resultaten te bekomen.

N.3 Conversie van methanol naar lichte olefines

De theoretische technieken zoals beschreven in het vorige luik, worden in dit deel aangewend om duidelijkheid te scheppen in één van de meest intrigerende discussies uit de heterogene katalyse, namelijk het mechanisme van het methanol-to-olefin proces (of kortweg MTO). Na een korte inleiding wordt de 30-jaar lang durende controverse over het mechanisme uit de doeken gedaan. De historisch belangrijke 'directe' mechanismes worden gedetailleerd geanalyseerd, wat finaal leidt tot de volledige verwerping ervan. Tot slot wordt een deel van de alternatieve 'hydrocarbon pool' hypothese onderzocht, waarvoor de initiële stap reeds vernieuwende inzichten oplevert aangaande de rol van het zeolietrooster.

N.3.1 Situering

Lichte olefines, die een cruciale grondstof zijn voor de hele petrochemische industrie [42], worden traditioneel verkregen door het kraken van ruwe olie-fracties. Aangezien de beperkte olie-reserve de steeds toenemende vraag naar deze grondstoffen (bvb. voor de productie van polyolefines) niet zal kunnen blijven ondersteunen, moet er gezocht worden naar alternatieve bronnen [43]. In de omzetting van methaan, gewonnen uit aardgas, naar polyolefines speelt het MTO proces een centrale rol. In dit proces wordt methanol katalytisch omgevormd tot lichte olefines zoals etheen en propeen [44–46]. Met behulp van MTO technologie kan men dus praktisch alles wat men normaalgezien uit ruwe olie produceert ook uit

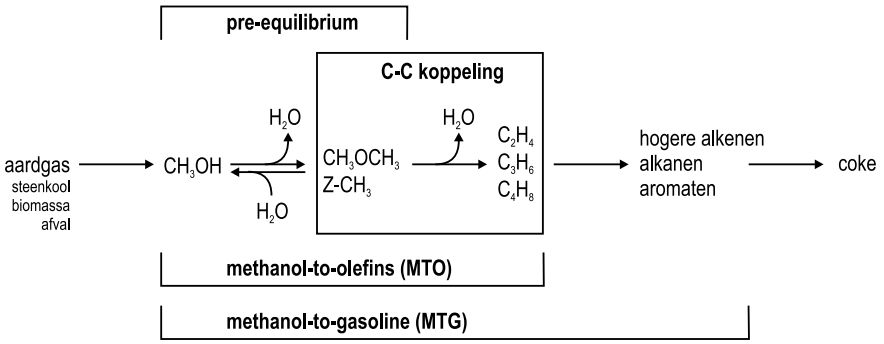

Figuur N.5: Conversie van methanol naar lichte olefines via het MTO proces.

methanol vervaardigen.

Figuur N.5 geeft een schematische weergave van de omzetting van aardgas naar grotere koolwaterstoffen, waarbij het MTO proces centraal staat. De conversie van methanol begint met de vorming van een tijdelijke evenwichtsfase waarin zowel water, dimethylether (DME) als rooster-gebonden methoxy species (Z-CH_3) aanwezig zijn. Dit pre-equilibrium zet zich vervolgens om naar lichte olefines en in een verder stadium zelfs naar zwaardere fracties (methanol-to-gasoline of MTG). De katalytische cyclus eindigt wanneer de poriën gevuld zijn met coke. Mogelijke verbeteringen aan de huidige katalysatoren, zoals HZSM-5 en HSAPO-34, zijn de preventie van deze cokesvorming en een maximalisatie van de productie aan lichte olefines. Bovendien is controle over de productselectiviteit uiterst gegeerd, waarbij de etheen tot propeen verhouding aangepast zou kunnen worden aan de specifieke marktvraag.

Discussie aangaande het reactie-mechanisme

Om controle over de productdistributie te verkrijgen, moet het reactiemechanisme eerst goed gekend zijn. Al meer dan 30 jaar is men echter op zoek naar een mechanisme dat alle experimentele observaties kan verklaren [46], met als voornaamste knelpunt de initiële C-C koppeling. De meeste aandacht ging hierin steevast uit naar de 'directe' mechanismes, waarbij lichte olefines gevormd worden op basis van co-reactie van 2 of meer C1-moleculen [46]. Onlangs hebben echter experimentele resultaten aangetoond dat zuiver methanol onreactief is

onder standaard MTO condities [53], wat in volledige tegenspraak is met de directe mechanismes. Een mogelijk alternatief is de 'hydrocarbon pool' hypothese [54, 55], waarin organische species, geklemd in de zeolietporiën, gemethyleerd worden en olefines afsplitsen. De laatste jaren krijgt dit model steeds meer voet aan de grond, waarbij vooral methylbenzenen als mogelijke hydrocarbon pool species vooruitgeschoven worden [56–58]. Desalniettemin bestaat er nog heel wat controverse over het al dan niet doorgaan van de directe mechanismes. Deze discussie wordt alleen maar versterkt door het sterk hypothetisch karakter en de geringe validatie van het hydrocarbon pool model.

N.3.2 Directe mechanismes

Door de extreme versnippering van alle theoretische studies op directe mechanismes en het brede spectrum aan kwantumchemische benaderingen en modelkeuzes, was rechtstreekse vergelijking tussen onderlinge resultaten tot voor kort onmogelijk. Hoewel het bestaan van individuele reacties steeds als bewijs aangevoerd werd voor de directe mechanismes, werd nooit ontegensprekelijk aangetoond dat de combinatie van deze elementaire stappen ook effectief een volledig succesvol reactiepad zou opleveren. Om dit complex probleem op te lossen, hebben we een uitgebreid reactieschema geconstrueerd (Figuur N.6) [art. 3.6], met opname van alle mogelijke directe reactiepaden naar etheen. Niet enkel reactiebarrières werden hiervoor berekend, maar ook snelheidscoëfficiënten op 720 K op basis van transitietoestandstheorie (Deel N.2.4).

Pre-equilibrium fase

Zoals voorgesteld in Figuren N.5 en N.6 begint de conversie van methanol met een snelle dehydratatie naar DME en de instelling van een pre-equilibrium [61–66]. Dit kan rechtstreeks gebeuren of in een 2-stapsmechanisme via een Z-CH_3 methoxy groep. Bijkomende methanol of water moleculen kunnen fungeren als assisterende moleculen, waardoor een minder verstoorde transitietoestand ontstaat met een lagere energiebarrière en een hogere snelheidscoëfficiënt tot gevolg.

Het trimethyl oxonium ion

Uit dit initieel pre-equilibrium wordt de vorming van het trimethyl oxonium ion (TMO) voorgesteld via verschillende routes [59, 60], zoals groen omkaderd in Figuur N.6. Het TMO kation vormt een ionenpaar met het negatief geladen

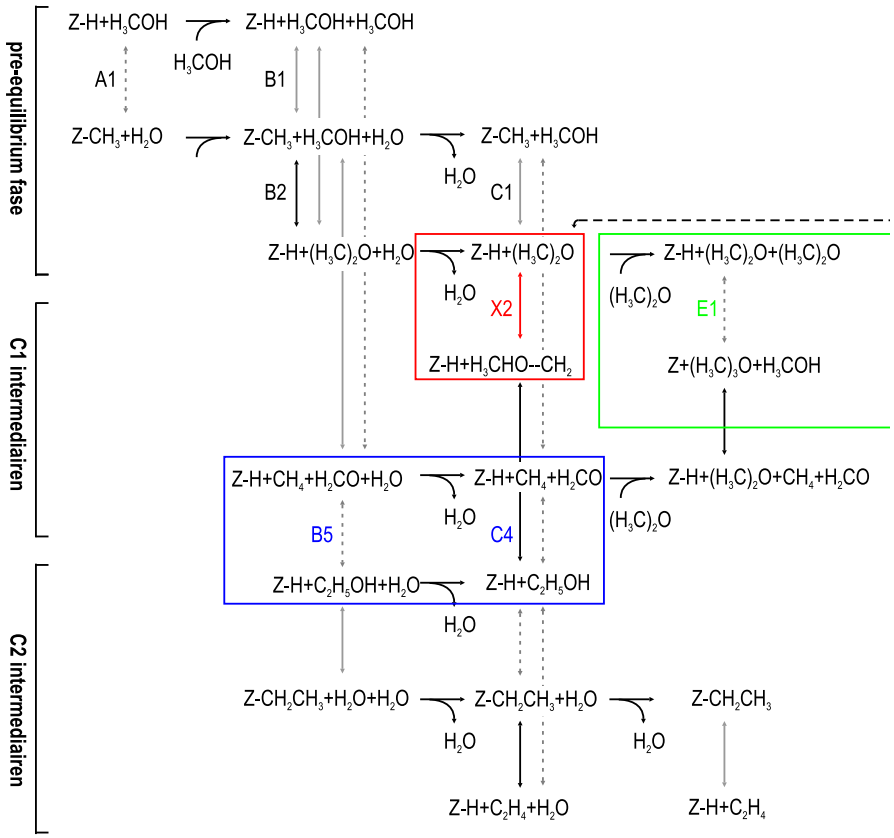

Figuur N.6: (deel 1/2) Compleet reactieschema voor de directe mechanismes.

zeolietrooster, waardoor de 5T clusterbenadering ontoereikend is. Meer geavanceerde ONIOM-berekeningen op grotere 46T clusters tonen aan dat TMO 70 kJ mol^{-1} bijkomend gestabiliseerd wordt door het zeolietrooster [art. 3.5].

Ylide en carbeen intermediairen

Na de vorming van TMO worden de oxonium ylides voorgesteld als mogelijke intermediairen (rode rechthoek in Figuur N.6) [art. 3.5], waarbij de CH_2 carbeen groep in een C-C of C-H binding kan inserteren. Zelfs met de ONIOM methode kon er geen route gevonden worden, terwijl optimalisatie van de yli-

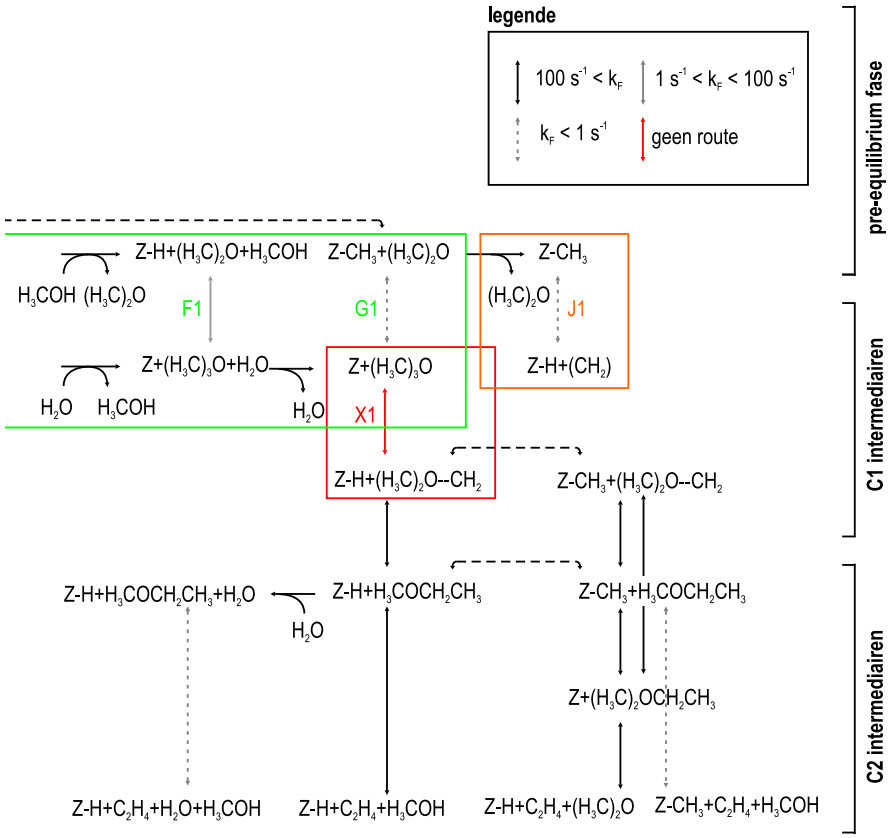

Figuur N.6: (deel 2/2) Compleet reactieschema voor de directe mechanismes.

des zelf aantoonde dat dit zeer hoog energetische species zijn. Een alternatief carbeen kan ook gevormd worden door deprotonering van een Z-CH_3 methoxy groep (bruine rechthoek in Figuur N.6) [69]. Door de enorm hoge barrière is de snelheidscoëfficiënt voor deze stap zeer klein [art. 3.7]. De grote instabiliteit van de ylides en het roostergebonden carbeen vormen het eerste knelpunt voor de directe mechanismes. Een H/D uitwisselingsstudie bevestigde ondertussen het niet bestaan van deze intermediairen [50].

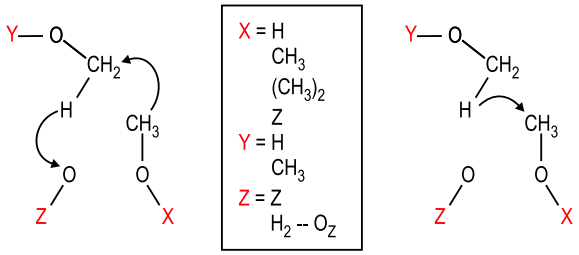

Figuur N.7: Hoog-geactiveerde geconcerteerde C-C koppeling (links) en competitieve vorming van methaan (rechts).

Methaan/formaldehyde route

Enkele alternatieve routes lopen langs methaan en formaldehyde [59, 67, 68]. Eens gevormd, vinden we enkel extreem trage reacties naar ethanol (blauwe rechthoek in Figuur N.6) [art. 3.6]. Dus zelfs al worden methaan en formaldehyde gevormd, de omzetting van dit mengsel naar ethanol zal te traag verlopen. Dit is een tweede knelpunt voor de directe routes in MTO.

Geconcerteerde C-C koppeling

Om Figuur N.6 niet te overbelasten, werden reactiestappen niet opgenomen wanneer zowel de voorwaartse als achterwaartse barrière meer dan 200 kJ mol^{-1} bedroeg. Deze reacties volgen bovendien allemaal een gelijkaardig geconcerteerd reactiemechanisme, zoals voorgesteld in de linkerzijde van Figuur N.7 [art. 3.6]. Een concurrerende reactie, waarbij het proton niet naar het zeoliet migreert, maar integendeel een gelijkaardige C-H binding vormt, zal veel sneller verlopen (rechterzijde in Figuur N.7). Deze uitgesproken preferentie naar de vorming van methaan en formaldehyde werd vroeger reeds waargenomen in moleculaire dynamica simulaties [67, 68]. Zoals eerder vermeld, leidt dit mengsel niet tot de gezochte C-C binding. Het feit dat de geconcerteerde C-C koppelingsreacties zo hoog geactiveerd zijn vormt het derde en finale knelpunt voor de directe mechanismes.

Volledig falen

De reactiestappen in de directe mechanismes werden gecombineerd, waardoor de knelpunten geïdentificeerd konden worden. Wanneer nodig, werden meer geavanceerde technieken aangewend. Zolang enkel individuele reactiestappen beschouwd werden, leken er verschillende directe reactiepaden mogelijk, maar door ze te combineren is het duidelijk dat alle directe mechanismes verworpen moeten worden. Alternatieve routes, zoals mogelijks de hydrocarbon pool hypothese, zullen C-C koppelingsreacties moeten voorzien die deze knelpunten omzeilen.

N.3.3 De hydrocarbon pool hypothese

Het belangrijkste alternatief voor de directe mechanismes is de 'hydrocarbon pool' hypothese, waarbij organische species in de zeolietporiën fungeren als stellingen waaraan C1 species zich hechten. Daarna ondergaat de organische molecule enkele gerichte herschikkingen (desnoods met bijkomende methyleringsstappen) en worden lichte olefines afgesplitst [54, 55]. Verdere methyleringsstappen regenereren de originele startmolecule. Op deze manier zouden de hoog-geactiveerde routes uit de directe mechanismes omzeild kunnen worden.

De elementaire reactiestappen van dit proces zijn totnogtoe vrij speculatief en allerminst goed begrepen, waardoor ze een ideaal onderzoeksthema vormen voor theoretische berekeningen. Deze berekeningen zijn gebaseerd op de algemene consensus dat polymethylbenzenen cruciale HP species vormen [74–76]. Er is bovendien ook bijkomend bewijs voor de aanwezigheid van stabiele benzenium ionen in de zeolietomgeving [56, 78–80]. *Gem*-dimethylbenzenium ionen in het bijzonder vormen het startpunt van de 'paring' en 'side-chain' mechanismes, voorgesteld in Figuur N.8 [57]. Beide cycli worden geïnitieerd door een éénstaps geminale methylering van hexamethylbenzeen door methanol tot het heptamethylbenzenium kation ($7MB^+$).

De supramoleculaire katalysator

Door de complexe interactie tussen de grote HP species en de zeolietomgeving, stelden Haw en medewerkers voor dat de combinatie van anorganisch zeolietrooster met de organische species binnenin beschouwd moet worden als een supramoleculaire katalysator [81], zoals schematisch voorgesteld in Figuur N.9. Het zeolietrooster speelt natuurlijk een belangrijke rol, waarbij zowel compositie

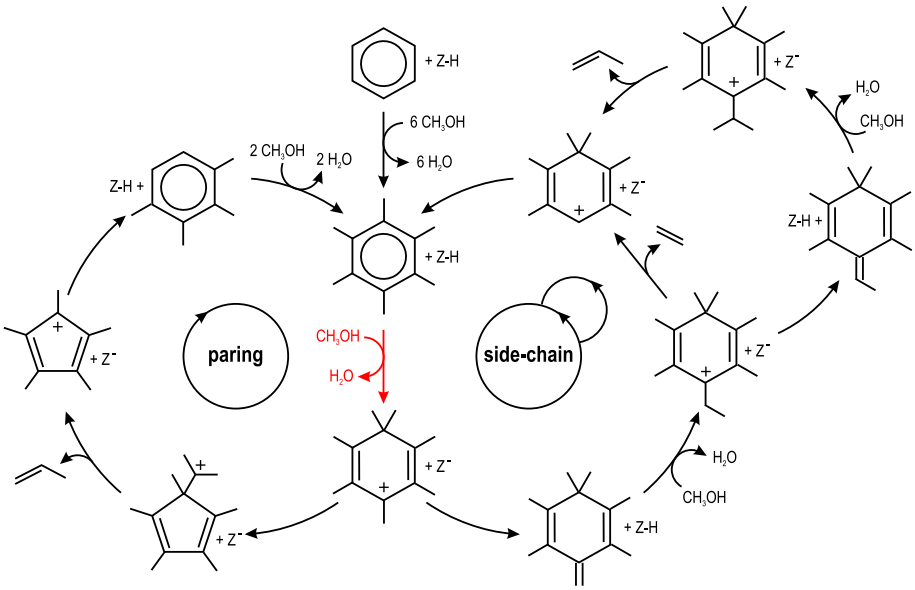

Figuur N.8: Katalytische cycli voor paring en side-chain routes, geïnitieerd door de *gem*-methylering van hexamethylbenzeen.

(R1), afmetingen van de holtes (R2) en diameter van de kanalen (R3) cruciaal zijn. Het organisch reactiecentrum (O1) vormt het platform waaraan C-C bindingen gevormd en gebroken kunnen worden. Verschillende organische species zullen een verschillende reactiviteit en productselectiviteit vertonen. Voor polymethylbenzenen in het bijzonder zal een toename in methylgroepen leiden tot een grotere propeen-selectiviteit [82]. Dit aantal methylgroepen zal afhangen van de rooster-afmetingen (R2), maar ook van de extra contributies getoond in Figuur N.9. De kooi-afmetingen kunnen immers gemodifieerd worden door ruimtevullende solvent-moleculen (E1) of anorganische modificaties aan het rooster (E2), die beiden het aantal methylgroepen beperken en bijgevolg de etheen-selectiviteit verhogen [82, 83].

De noodzakelijke aanwezigheid van de grote HP molecule impliceert dat zeolieten met kleine kooien en kanalen geen MTO activiteit zouden mogen vertonen (omdat daar enkel de directe mechanismes voor mogelijk zijn). Dit werd recent experimenteel geverifieerd [85], waarbij dit gedrag werd toegeschreven aan vormselectiviteit op de transitietoestand. In het volgend gedeelte zal de ex-

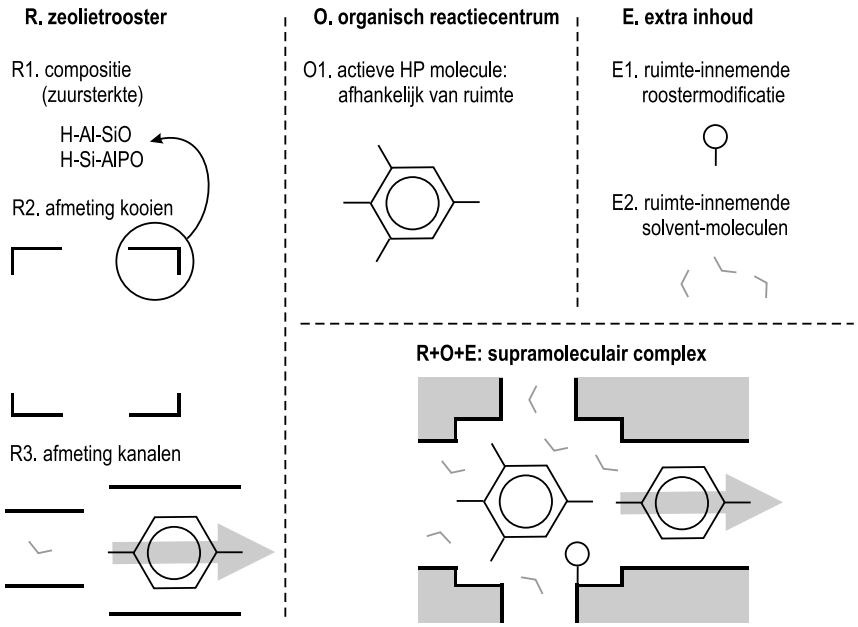

Figuur N.9: Contributies tot de supramoleculaire katalysator voorgesteld door Haw et al. [81].

pliciete rol van deze vormselectiviteit theoretisch aangetoond worden voor de initiërende stap uit Figuur N.8.

Kationische intermediairen in de supramolecule

Voor een zeoliet met middelmatige kooien, zoals HZSM-5 met de MFI topologie, is er onvoldoende ruimte om de hogere *gem*-dimethylbenzenium kationen te vormen. De reactiviteit van een polymethylbenzeen wordt dan vooral bepaald door de grootte van de transitietoestand voor geminale methylering [art. 3.8]. Deze theoretische conclusie werd bovendien experimenteel bevestigd: in MFI zijn het inderdaad de lagere methylbenzenen die vooral olefines afsplitsen [88].

Voor een zeoliet met grotere kooien (zoals de CHA topologie) is er voldoende ruimte voor de transitietoestand leidend tot het heptamethylbenzenium kation.

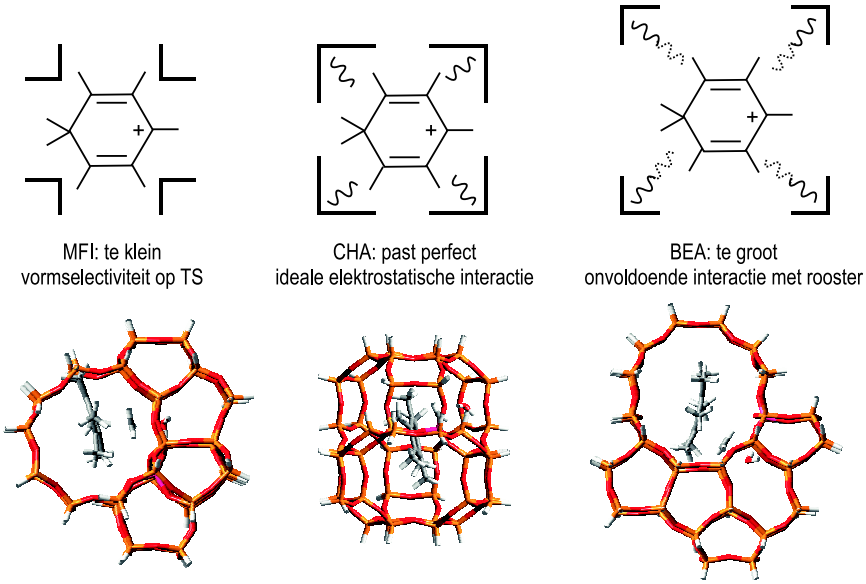

Figuur N.10: Verfijning van het supramoleculair karakter: elektrostatisch effect op het product (boven) en vormselectiviteit op de transitietoestand (onder), beide voor de *gem*-methylering van hexamethylbenzeen.

Zoals aangetoond in Figuur N.10, zal de omringende kooi de ideale elektrostatische stabilisering leveren aan het product [3.8]. In een ijle zeoliet zoals HBeta, is de kooi te groot om de nodige elektrostatische stabilisering te voorzien. Ook al is er meer dan voldoende ruimte voor de transitietoestand, het geladen product zal toch relatief onstabiel zijn ten opzichte van de neutrale reactanten. Blijkbaar moet verder gegaan worden dan enkel geometrische aspecten en speelt de volledige elektronische inbedding een minstens even belangrijke rol.

N.4 Organische functionalisering van zeolieten

Eerdere studies naar het reactie-mechanisme kunnen gebruikt worden om de katalysator te verbeteren door middel van geschikte functionalisering. In dit deel worden twee dergelijke substituties, met name methyleen en amine groepen, en hun invloed op het katalytisch gedrag van zeolieten bestudeerd. Een typische reactie uit het MTO proces, namelijk de vorming van een alkoxide groep, zal

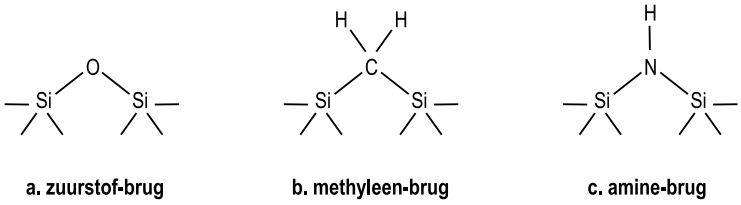

Figuur N.11: Functionalisering door de brug-zuurstofatomen te vervangen door kleine iso-elektronische organische groepen.

voor deze laatste materialen ook uitvoerig behandeld worden.

N.4.1 Situering

De meest recente pogingen om het toepassingsgebied van zeolieten te verbreden, bestaan erin welgekozen organische groepen in te bouwen. Dit is al vlot gelukt voor mesoporeuze silicaten [90–93], hoewel er nog niet zoveel gekend is over hun mogelijke toepassingen. Voor zeolieten is organische functionalisering bovendien iets moeilijker gebleken: grote organische groepen hebben immers de neiging om de holtes en kanalen volledig te blokkeren [94, 95]. Aan dit probleem kan verholpen worden door enkel kleine organische fragmenten in te bouwen, zoals geïllustreerd in Figuur N.11.

N.4.2 Methyleen-gesubstitueerde zeolieten

Eén van de eenvoudigste organische groepen is de methyleen-groep, die perfect past als brug tussen twee silicium atomen en zo een functionele Si-CH_2-Si groep vormt. Hoewel eerder al gelijkaardige organosilica materialen gesynthetiseerd werden [96–98], is maar uiterst recent een onderzoeksteam erin geslaagd om ook methyleen-gesubstitueerde zeolieten te produceren [99, 100]. Periodieke berekeningen toonden aan dat dergelijke structuren inderdaad stabiel zijn [101], maar er kon tot heden geen verklaring gevonden worden voor de waargenomen imperfecties in het rooster, zoals de aanwezigheid van eindstandige Si-CH_3 groepen.

Adsorptie van water en ammoniak

Vanuit katalytisch standpunt wordt algemeen aangenomen dat methyleen-groepen vrij inert zijn. Daarom zullen er voor deze materialen geen typische MTO re-

acties gemodelleerd worden, maar zullen meer algemene zeoliet-eigenschappen aan bod komen. Als eerste belangrijke eigenschap blijkt dat de adsorptie van zowel water als ammoniak (twee typische probe moleculen) sterk toeneemt als organisch silicaliet vergeleken wordt met traditioneel silicaliet. Dit is te wijten aan het feit dat de waterstof-atomen van de methyleen groep kunnen bijdragen tot bijkomende waterstofbruggen met het zuurstof en stikstof atoom van water en ammoniak respectievelijk [art. 4.5]. De concentratie van methyleen-groepen zal dus de adsorptie-capaciteit op bulk niveau rechtstreeks beïnvloeden.

Ladingscompensatie

Wanneer in een zuiver silica-rooster een Si atoom vervangen wordt door een Al atoom, dan zal het ladingsdefect gecompenseerd kunnen worden door een zuur proton, maar bijvoorbeeld ook door alkali kationen, zoals Li^+, Na^+ en K^+. Wanneer in diezelfde Al tetraëder ook een methyleen-groep wordt geplaatst, zal dat uiteraard zijn invloed hebben op het bindingspatroon van het ladingscompenserend ion. Voor de alkali-kationen die normaalgezien met 2 of zelfs met 3 brug-zuurstofatomen coördineren, zal de sterische hinder van de methyleengroep leiden tot een verzwakt adsorptie-patroon [art. 4.5]. Voor een zuur proton op een naburig zuurstofatoom daarentegen, wordt de deprotoneringsenergie nauwelijks beïnvloed. Desalniettemin zal deze combinatie niet thermodynamisch stabiel zijn, zoals verder verduidelijkt wordt in de volgende paragraaf.

Protonmobiliteit

In Figuur N.12, wordt de proton sprong van een zuurstofatoom naar de methyleengroep beschouwd. Deze sprong is sterk exotherm [art. 4.5] en geeft aan hoe eindstandige methylgroepen gevormd worden. Hierdoor zal de combinatie van een methyleen-groep en een zuur proton op het zuurstofatoom niet meer mogelijk zijn. Dit is bovendien een logische verklaring voor de experimenteel geobserveerde eindstandige methylgroepen [99].

N.4.3 Amine-gesubstitueerde zeolieten

Geïnspireerd door de succesvolle synthese van methyleen-gesubstitueerde zeolieten [99], bevestigden periodieke berekeningen dat amine-gesubstitueerde zeolieten ook zouden kunnen bestaan [101]. Deze zijn katalytisch veel interessanter, vermits Si-NH-Si groepen sterkere Lewis base sites zijn vergeleken met Si-O-Si bruggen. Recent zijn verschillende groepen erin geslaagd om stikstofhoudende

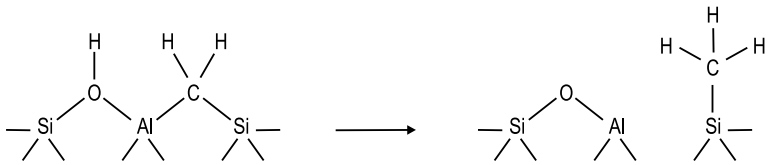

Figuur N.12: Proton sprong naar methyleengroep die aanleiding geeft tot het opbreken van het rooster.

nano- en mesoporeuze materialen te synthetiseren [102–105]. In dit onderdeel wordt nagegaan wat het gecombineerd effect is van een dergelijke basische site met een traditionele Brønsted zure site.

Protonmobiliteit en zuur-base gedrag

Net zoals bij de methyleen-gesubstitueerde zeolieten zal de combinatie van zowel een amine als een OH-groep op eenzelfde aluminium tetraëder aanleiding geven tot protonering van de organische groep [art. 4.6]. De combinatie van een zwak basische Al-O-Si groep met een zwak zure Al-NH_2-Si groep geeft aanleiding tot niet-optimale zuur-base eigenschappen. Als de amine groep echter 1 T-atoom verwijderd wordt van het aluminium defect, dan zal protonering een stuk minder waarschijnlijker zijn [art. 4.6]. Op die manier kan er wel een co-existentie ontstaan van een zure OH groep met de basische NH groep (rechterzijde van Figuur N.13).

In het MTO proces speelt basiciteit een belangrijke rol bij de vorming van een rooster-gebonden methoxide of ethoxide groep. Hoewel het falen van de directe mechanismes reeds aangetoond werd, zijn deze stappen ook belangrijk bij een stapsgewijze methylering of ethylering van grote aromaten in de hydrocarbon pool hypothese. NH substituties aan het aluminium atoom (site (1) in Figuur N.13) zullen automatisch geprotoneerd worden. Daarom moeten ze minstens op site (2) staan. Als de basiciteit van een Al-O-Si site (1) vergeleken wordt met die van een Si-NH-Si site (2), dan is deze identiek (en beduidend hoger dan de basiciteit van een Si-O-Si site (2)) [art. 4.7]. Blijkbaar zijn er twee tegenovergestelde effecten die hier spelen:

Intrinsieke basiciteit: de intrinsieke basiciteit van een N tegenover een O atoom

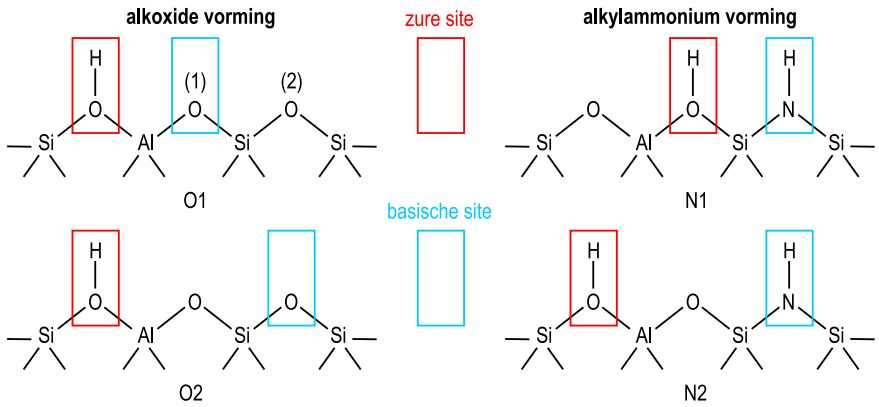

Figuur N.13: Definiëring van actieve sites voor zeolieten met en zonder amine substitutie.

> **Ladingsseparatie:** de energiekost die gepaard gaat met een grotere ladingsscheiding tussen CH_3^+ en de AlO_4^- tetraëder.

Deze effecten lijken elkaar op te heffen. De amine subsitutie voorziet dus geen sterkere basische site, maar wel één op een nieuwe locatie.

Alkylammonium of alkoxide?

Deze verschillende contributies zullen ook een belangrijke rol spelen bij alkylammonium vorming. Het eerste punt zal alkylammonium bevoordelen ten opzichte van alkoxide vorming, terwijl het tweede punt net het omgekeerde doet. Vermits beide contributies elkaar opheffen, geldt bij het reactiemechanisme nog één bijkomend verschil:

> **Geometrische structuurveranderingen:** doordat de basische site niet meer verplicht op dezelfde tetraëder staat, zullen andere transitietoestanden mogelijk zijn.

In dit deel zal vooral op dit effect geconcentreerd worden, door alkoxide-vorming rechtstreeks te vergelijken met alkylammonium-vorming uitgaande van enkele MTO-gerelateerde moleculen, zoals methanol, chloormethaan en etheen.

De vorming van een methoxide species uit methanol verloopt volgens een geconcerteerd mechanisme zoals geïllustreerd in Figuur N.14a. De transitietoe-

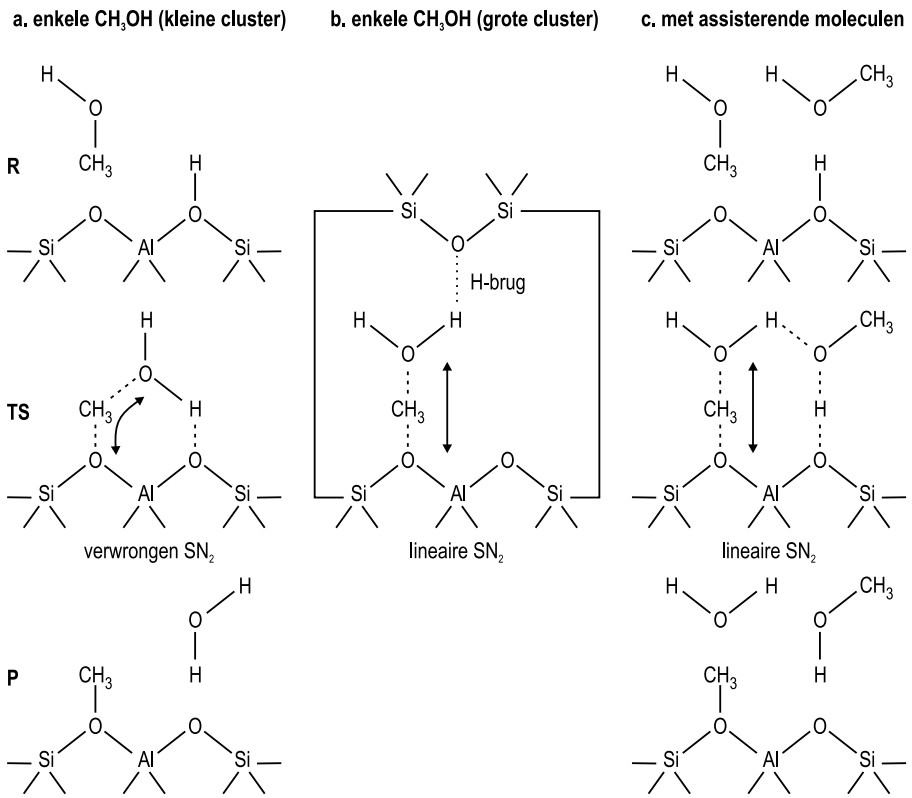

Figuur N.14: Methoxide vorming uit methanol.

stand vormt een methoxonium-achtig complex, waarbij waterstofbruggen gevormd worden met de rooster O-atomen. In een kleine cluster zijn er slechts beperkte mogelijkheden voor een dergelijke waterstofbrug, waardoor de transitietoestand niet de optimale lineaire SN_2 configuratie inneemt maar sterk verstoord is (Figuur N.14a). Hierdoor zal de barrière ontzettend hoog lijken. Dit kan verholpen worden door een grotere cluster in rekening te nemen, zodat deze optimale transitietoestand kan aangenomen worden (Figuur N.14b). Anderzijds kan ook een assisterende molecule, zoals water of methanol een gelijkaardige optimale transitietoestands-geometrie mogelijk maken (Figuur N.14c). Vermits in deze twee laatste situaties de optimale structuur reeds mogelijk is, zal amine modificatie van het zeolietrooster niet bijdragen tot een betere transitietoestand-

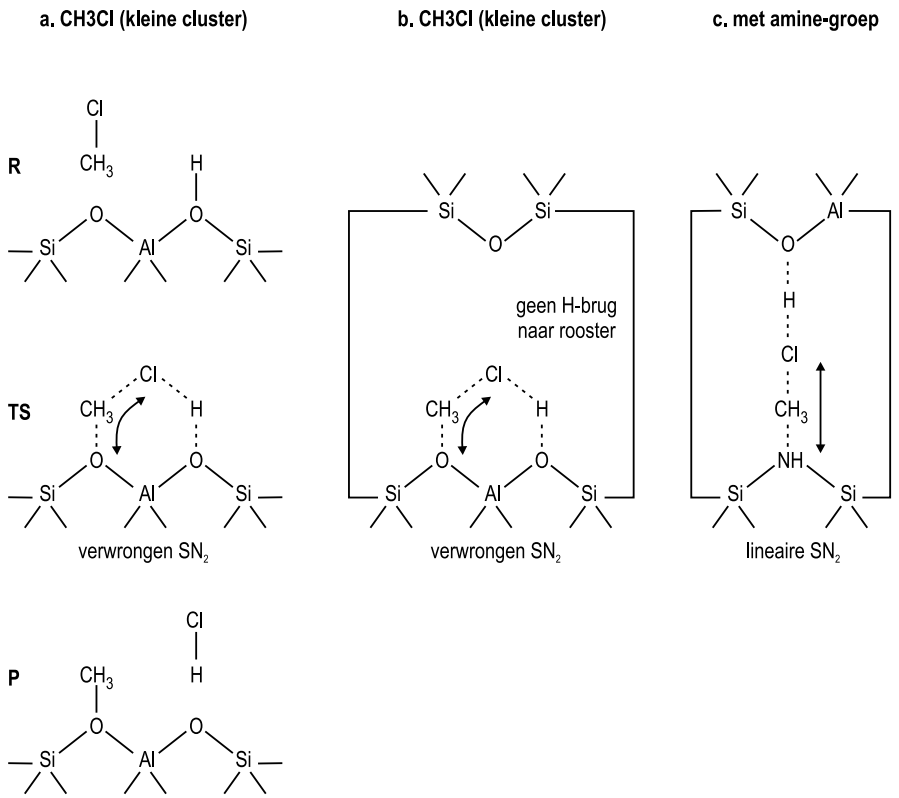

Figuur N.15: Methoxide vorming uit chloormethaan.

structuur [art. 4.7].

Alternatief aan methanol, wordt ook de conversie van halomethanen naar olefines voorgesteld [118]. Voor conventionele zeolieten zal de transitietoestand er uitzien als in Figuur N.15a . Het grote verschil met methanol is het feit dat het zure proton in de transitietoestand aan de basische zuurstof gebonden blijft, zodat vergroting van de cluster geometrisch en energetisch niets opbrengt (Figuur N.15b). Door het bijvoegen van een amine-site, kan de transitietoestand nu wel meer dan één tetraëder omspannen N.15c. Dit heeft een aanzienlijk verlagend effect op de reactiebarrière tot gevolg [art. 4.6].

De protonering van lichte olefines zoals etheen verloopt niet volgens een lineair SN_2 mechanisme. Vermits de bijkomende basische site geen betere transitietoestand kan opleveren, zullen reactiebarrières niet verlaagd worden.

N.5 Algemeen besluit

In deze thesis werd aangetoond hoe moleculaire modellering een substantiële bijdrage kan leveren tot een verbeterd begrip van industriële katalytische processen. Veelal worden katalysatoren ad hoc voorgesteld, zonder een gedetailleerd begrip van hun werking op microscopische schaal. Experimenteel is het vaak bijzonder moeilijk om het volledig reactienetwerk te ontrafelen. Theoretische berekeningen kunnen, mits ze accuraat genoeg zijn, hier een wezenlijke bijdrage in leveren. Door de grote toename aan computercapaciteit en de ontwikkeling van geavanceerde theoretische methoden is het sedert een aantal jaar mogelijk geworden om complexe processen over zeolieten te modelleren. Zelfs tijdens dit doctoraatswerk werden vele nieuwe technieken voorgesteld, wat een duidelijk bewijs is voor de uiterst snelle evolutie in deze discipline.

Theoretische berekeningen in deze thesis hebben bewezen dat de vaak gesuggereerde directe mechanismes voor het MTO proces onmogelijk een verklaring kunnen bieden voor de initiële C-C koppeling. De meerwaarde van snelheidcoëfficiënten ten opzichte van reactiebarrières is ook duidelijk aangetoond. Drie knelpunten kunnen geïdentificeerd worden:

- de instabiliteit van de ylide of carbeen intermediairen,
- de uiterst trage omzetting van het methaan/formaldehyde mengsel,
- en de extreem hoge barrière voor geconcerteerde C-C koppelingsreacties.

Het feit dat hiermee een lang aanslepend probleem eindelijk is opgelost kan zonder twijfel beschouwd worden als de belangrijkste verwezenlijking van deze thesis. Bovendien werd ook verduidelijkt hoe de organische HP species en het anorganisch zeolietrooster samenwerken als een supramoleculaire katalysator om alternatieve routes mogelijk te maken. Het supramoleculair beeld is zelfs verder uitgebreid naar vormselectiviteit op de transitietoestand en de rol van het zeolietrooster op cruciale kationen. Bijkomend inzicht in het volledige HP netwerk is echter nog nodig om de katalysator te optimaliseren. Hierin zal een sterke interactie tussen theoretisch en experimenteel werk een uitermate belangrijke rol spelen.

Deze studie toont ook aan hoe kleine organische modificaties aan het zeolietrooster de fundamentele eigenschappen en MTO-gerelateerde reactiviteit op nano-schaal kunnen beïnvloeden. Zowel methyleen als amine groepen kunnen echter niet op aluminium tetraëders gesynthetiseerd worden zonder dat het zure proton de organische groep contamineert, en zelfs aanleiding kan geven tot het klieven van het rooster. Hoewel katalytisch inert, zullen methyleengroepen wel de adsorptie-eigenschappen van probe-molecules water en ammoniak of van ladingscompenserende alkali kationen merkbaar beïnvloeden. Aminegesubstitueerde zeolieten, daarentegen, zullen er voor zorgen dat er bijkomende basische sites zijn, vergelijkbaar met een Al-O-Si site, maar dan niet beperkt tot het aluminiumdefect. Dit laat meer protonposities toe, alsook de mogelijkheid om meer gunstige transitietoestanden aan te nemen. Dit veroorzaakt een sterk reducerend effect op de reactiebarrière voor reacties die een anders te vervormde transitietoestand zouden vertonen. Het is dan ook zeker interessant om deze weg verder te zetten, waarbij theorie en experiment opnieuw complementair zijn in de zoektocht naar nieuwe materialen en bijhorende toepassingen. Hierdoor moet het mogelijk zijn om de eigenschappen van zeolieten te combineren met deze van enzymen, om op die manier een nieuwe klasse katalysatoren, de zeozymen, te produceren.

Deze thesis geeft reeds een eerste indruk van de mogelijkheden die theoretische modellering biedt op het vlak van zuurgekatalyseerde reacties in zeolieten. De toepassingen die hier beschouwd worden, bevinden zich al op de limiet van wat huidig in dit onderzoeksdomein mogelijk is, zowel qua computerkracht, methodologie en de vertrouwdheid met het supramoleculair karakter. De snelle evolutie van dit onderzoeksdomein, zelfs tijdens dit doctoraatswerk, biedt rooskleurige toekomstperspectieven. Deze onderzoekspiste loopt dus nog lang niet ten einde en er is nog een lange weg af te leggen...

Bibliography

[1] P. Payra and P. K. Dutta; Zeolites: a primer; In S. M. Auerbach, K. A. Carrado, and P. K. Dutta, Ed., *Handbook of zeolite science and technology*, pages 1–19. Marcel Dekker, Inc., New York, **2003**.

[2] Ch. Baerlocher, W. M. Meier, and D. H. Olson, *Atlas of Zeolite Framework Types;* Elsevier, Amsterdam, **2001**.

[3] C. R. Marcilly, *Topics in Catalysis*, **2000**, *13*(4), 357–366.

[4] J. Weitkamp, *Solid State Ionics*, **2000**, *131*(1-2), 175–188.

[5] D. Dubbeldam, S. Calero, T. L. M. Maesen, and B. Smit, *Angewandte Chemie - International Edition*, **2003**, *42*(31), 3624–3626.

[6] M. Schenk, S. Calero, T. L. M. Maesen, L. L. van Benthem, M. G. Verbeek, and B. Smit, *Angewandte Chemie - International Edition*, **2002**, *41*(14), 2500–2502.

[7] J. A. Martens, G. Vanbutsele, P. A. Jacobs, J. Denayer, R. Ocakoglu, G. Baron, J. A. M. Arroyo, J. Thybaut, and G. B. Marin, *Catalysis Today*, **2001**, *65*(2-4), 111–116.

[8] W. Lowenstein, *American Mineralogist*, **1954**, *39*, 92–96.

[9] H. O. Pastore, S. Coluccia, and L. Marchese, *Annual Review of Materials Research*, **2005**, *35*, 351–395.

[10] M. Stocker, *Microporous and Mesoporous Materials*, **2005**, *82*(3), 257–292.

[11] X. Rozanska and R. A. van Santen; Reaction mechanisms in zeolite catalysis; In S. M. Auerbach, K. A. Carrado, and P. K. Dutta, Ed., *Handbook of zeolite science and technology*, pages 785–832. Marcel Dekker, Inc., New York, **2003**.

[12] A. H. Fuchs and A. K. Cheetham, *Journal of Physical Chemistry B*, **2001**, *105*(31), 7375–7383.

[13] R. J. Bartlett, *Annual Review of Physical Chemistry*, **1981**, *32*, 359–401.

[14] A. D. Boese, M. Oren, O. Atasoylu, J. M. L. Martin, M. Kallay, and J. Gauss, *Journal of Chemical Physics*, **2004**, *120*(9), 4129–4141.

[15] R. G. Parr, *Annual Review of Physical Chemistry*, **1983**, *34*, 631–656.

[16] M. J. S. Dewar and W. Thiel, *Journal of the American Chemical Society*, **1977**, *99*(15), 4899–4907.

[17] J. J. P. Stewart, *Journal of Computational Chemistry*, **1989**, *10*, 209–220.

[18] R. A. van Santen and G. J. Kramer, *Chemical Reviews*, **1995**, *95*(3), 637–660.

[19] E. M. Morales, C. M. Zicovich-Wilson, J. E. S. Sanchez, and L. J. Alvarez, *Chemical Physics Letters*, **2000**, *327*(3-4), 224–229.

[20] R. Fricke, H. Kosslick, G. Lischke, and M. Richter, *Chemical Reviews*, **2000**, *100*(6), 2303–2405.

[21] Y. Zhao and D. G. Truhlar, *Journal of Physical Chemistry A*, **2006**, *110*(15), 5121–5129.

[22] K. P. Schroder and J. Sauer, *Journal of Physical Chemistry*, **1996**, *100*(26), 11043–11049.

[23] J. Sauer and M. Sierka, *Journal of Computational Chemistry*, **2000**, *21*(16), 1470–1493.

[24] S. Dapprich, I. Komaromi, K. S. Byun, K. Morokuma, and M. J. Frisch, *Journal of Molecular Structure - Theochem*, **1999**, *462*, 1–21.

[25] M. J. Frisch, G. W. Trucks, H. B. Schlegel, G. E. Scuseria, M. A. Robb, J. R. Cheeseman, J. A. Montgomery, Jr., T. Vreven, K. N. Kudin, J. C. Burant, J. M. Millam, S. S. Iyengar, J. Tomasi, V. Barone, B. Mennucci, M. Cossi, G. Scalmani, N. Rega, G. A. Petersson, H. Nakatsuji, M. Hada, M. Ehara, K. Toyota, R. Fukuda, J. Hasegawa, M. Ishida, T. Nakajima, Y. Honda, O. Kitao, H. Nakai, M. Klene, X. Li, J. E. Knox, H. P. Hratchian, J. B. Cross, V. Bakken, C. Adamo, J. Jaramillo, R. Gomperts, R. E. Stratmann, O. Yazyev, A. J. Austin, R. Cammi, C. Pomelli, J. W. Ochterski, P. Y. Ayala, K. Morokuma, G. A. Voth, P. Salvador, J. J. Dannenberg, V. G. Zakrzewski, S. Dapprich, A. D. Daniels, M. C.

Strain, O. Farkas, D. K. Malick, A. D. Rabuck, K. Raghavachari, J. B. Foresman, J. V. Ortiz, Q. Cui, A. G. Baboul, S. Clifford, J. Cioslowski, B. B. Stefanov, G. Liu, A. Liashenko, P. Piskorz, I. Komaromi, R. L. Martin, D. J. Fox, T. Keith, M. A. Al-Laham, C. Y. Peng, A. Nanayakkara, M. Challacombe, P. M. W. Gill, B. Johnson, W. Chen, M. W. Wong, C. Gonzalez, and J. A. Pople; Gaussian 03, Gaussian, Inc.; Wallingford, CT, **2004**.

[26] A. Damin, F. Bonino, G. Ricchiardi, S. Bordiga, A. Zecchina, and C. Lamberti, *Journal of Physical Chemistry B*, **2002**, *106*(30), 7524–7526.

[27] S. Kasuriya, S. Namuangruk, P. Treesukol, M. Tirtowidjojo, and J. Limtrakul, *Journal of Catalysis*, **2003**, *219*(2), 320–328.

[28] M. Boronat, P. M. Viruela, and A. Corma, *Journal of the American Chemical Society*, **2004**, *126*(10), 3300–3309.

[29] K. Sillar and P. Burk, *Journal of Physical Chemistry B*, **2004**, *108*(28), 9893–9899.

[30] B. Jansang, T. Nanok, and J. Limtrakul, *Journal of Physical Chemistry B*, **2006**, *110*(25), 12626–12631.

[31] J. T. Fermann, T. Moniz, O. Kiowski, T. J. McIntire, S. M. Auerbach, T. Vreven, and M. J. Frisch, *Journal of Chemical Theory and Computation*, **2005**, *1*(6), 1232–1239.

[32] X. Solans-Monfort, M. Sodupe, V. Branchadell, J. Sauer, R. Orlando, and P. Ugliengo, *Journal of Physical Chemistry B*, **2005**, *109*(8), 3539–3545.

[33] A. D. Becke, *Journal of Chemical Physics*, **1993**, *98*(7), 5648–5652.

[34] S. A. Zygmunt, R. M. Mueller, L. A. Curtiss, and L. E. Iton, *Journal of Molecular Structure - Theochem*, **1998**, *430*, 9–16.

[35] M. J. Frisch, J. A. Pople, and J. S. Binkley, *Journal of Chemical Physics*, **1984**, *80*(7), 3265–3269.

[36] C. Raksakoon and J. Limtrakul, *Journal of Molecular Structure - Theochem*, **2003**, *631*, 147–156.

[37] H. Eyring, *Journal of Chemical Physics*, **1935**, *3*, 107–115.

[38] M. G. Evans and M. Polanyi, *Transactions of the Faraday Society*, **1935**, *31*, 875–894.

[39] A. M. Vos, F. De Proft, R. A. Schoonheydt, and P. Geerlings, *Chemical Communications*, **2001**, (12), 1108–1109.

[40] A. M. Vos, K. H. L. Nulens, F. De Proft, R. A. Schoonheydt, and P. Geerlings, *Journal of Physical Chemistry B*, **2002**, *106*(8), 2026–2034.

[41] A. M. Vos, R. A. Schoonheydt, F. De Proft, and P. Geerlings, *Journal of Physical Chemistry B*, **2003**, *107*(9), 2001–2008.

[42] I. Chorkendorff and J. W. Niemantsverdriet; Oil refining and petrochemistry; In *Concepts of Modern Catalysis and Kinetics*, pages 349–376. **2005**.

[43] C. Okkerse and H. van Bekkum, *Green Chemistry*, **1999**, *1*(2), 107–114.

[44] S. L. Meisel, J. P. McCullough, C. H. Lechthaler, and P. B. Weisz, *Chemtech*, **1976**, *6*(2), 86–89.

[45] C. D. Chang, *Catalysis Reviews - Science and Engineering*, **1983**, *25*(1), 1–118.

[46] M. Stocker, *Microporous and Mesoporous Materials*, **1999**, *29*(1-2), 3–48.

[47] W. Wang, A. Buchholz, M. Seiler, and M. Hunger, *Journal of the American Chemical Society*, **2003**, *125*(49), 15260–15267.

[48] Y. J. Jiang, M. Hunger, and W. Wang, *Journal of the American Chemical Society*, **2006**, *128*(35), 11679–11692.

[49] Y. J. Jiang, W. Wang, V. R. R. Marthala, J. Huang, B. Sulikowski, and M. Hunger, *Journal of Catalysis*, **2006**, *238*(1), 21–27.

[50] D. M. Marcus, K. A. McLachlan, M. A. Wildman, J. O. Ehresmann, P. W. Kletnieks, and J. F. Haw, *Angewandte Chemie - International Edition*, **2006**, *45*(19), 3133–3136.

[51] J. F. Haw, D. M. Marcus, and P. W. Kletnieks, *Journal of Catalysis*, **2006**, *244*(1), 130–133.

[52] Y. J. Jiang, W. Wang, V. R. R. Marthala, J. Huang, B. Sulikowski, and M. Hunger, *Journal of Catalysis*, **2006**, *244*(1), 134–136.

[53] W. G. Song, D. M. Marcus, H. Fu, J. O. Ehresmann, and J. F. Haw, *Journal of the American Chemical Society*, **2002**, *124*(15), 3844–3845.

[54] R. M. Dessau, *Journal of Catalysis*, **1986**, *99*(1), 111–116.

[55] I. M. Dahl and S. Kolboe, *Journal of Catalysis*, **1994**, *149*(2), 458–464.

[56] J. F. Haw, J. B. Nicholas, W. G. Song, F. Deng, Z. K. Wang, T. Xu, and C. S. Heneghan, *Journal of the American Chemical Society*, **2000**, *122*(19), 4763–4775.

[57] B. Arstad, J. B. Nicholas, and J. F. Haw, *Journal of the American Chemical Society*, **2004**, *126*(9), 2991–3001.

[58] M. Bjorgen, U. Olsbye, S. Svelle, and S. Kolboe, *Catalysis Letters*, **2004**, *93*(1-2), 37–40.

[59] N. Tajima, T. Tsuneda, F. Toyama, and K. Hirao, *Journal of the American Chemical Society*, **1998**, *120*(32), 8222–8229.

[60] S. R. Blaszkowski and R. A. van Santen, *Journal of the American Chemical Society*, **1997**, *119*(21), 5020–5027.

[61] C. M. Zicovich-Wilson, P. Viruela, and A. Corma, *Journal of Physical Chemistry*, **1995**, *99*(35), 13224–13231.

[62] P. E. Sinclair and C. R. A. Catlow, *Journal of the Chemical Society - Faraday Transactions*, **1997**, *93*(2), 333–345.

[63] S. R. Blaszkowski and R. A. van Santen, *Journal of Physical Chemistry B*, **1997**, *101*(13), 2292–2305.

[64] E. Sandre, M. C. Payne, and J. D. Gale, *Chemical Communications*, **1998**, (22), 2445–2446.

[65] M. C. Payne, M. Hytha, I. Stich, J. D. Gale, and K. Terakura, *Microporous and Mesoporous Materials*, **2001**, *48*(1-3), 375–381, Sp. Iss. SI.

[66] M. Hytha, I. Stich, J. D. Gale, K. Terakura, and M. C. Payne, *Chemistry - A European Journal*, **2001**, *7*(12), 2521–2527.

[67] C. Lo, C. A. Giurumescu, R. Radhakrishnan, and B. L. Trout, *Molecular Physics*, **2004**, *102*(3), 281–288.

[68] C. S. Lo, R. Radhakrishnan, and B. L. Trout, *Catalysis Today*, **2005**, *105*(1), 93–105.

[69] P. E. Sinclair and C. R. A. Catlow, *Journal of Physical Chemistry B*, **1997**, *101*(3), 295–298.

[70] R. Shah, J. D. Gale, and M. C. Payne, *Journal of Physical Chemistry B*, **1997**, *101*(24), 4787–4797.

[71] O. Dewaele, V. L. Geers, G. F. Froment, and G. B. Marin, *Chemical Engineering Science*, **1999**, *54*(20), 4385–4395.

[72] B. Arstad and S. Kolboe, *Catalysis Letters*, **2001**, *71*(3-4), 209–212.

[73] H. A. Zaidi and K. K. Pant, *Catalysis Today*, **2004**, *96*(3), 155–160.

[74] W. G. Song, J. F. Haw, J. B. Nicholas, and C. S. Heneghan, *Journal of the American Chemical Society*, **2000**, *122*(43), 10726–10727.

[75] B. Arstad and S. Kolboe, *Journal of the American Chemical Society*, **2001**, *123*(33), 8137–8138.

[76] U. Olsbye, M. Bjorgen, S. Svelle, K. P. Lillerud, and S. Kolboe, *Catalysis Today*, **2005**, *106*(1-4), 108–111.

[77] A. Sassi, M. A. Wildman, H. J. Ahn, P. Prasad, J. B. Nicholas, and J. F. Haw, *Journal of Physical Chemistry B*, **2002**, *106*(9), 2294–2303.

[78] T. Xu, D. H. Barich, P. W. Goguen, W. G. Song, Z. K. Wang, J. B. Nicholas, and J. F. Haw, *Journal of the American Chemical Society*, **1998**, *120*(16), 4025–4026.

[79] M. Bjorgen, F. Bonino, S. Kolboe, K. P. Lillerud, A. Zecchina, and S. Bordiga, *Journal of the American Chemical Society*, **2003**, *125*(51), 15863–15868.

[80] W. G. Song, J. B. Nicholas, A. Sassi, and J. F. Haw, *Catalysis Letters*, **2002**, *81*(1-2), 49–53.

[81] J. F. Haw and D. M. Marcus, *Topics in Catalysis*, **2005**, *34*(1-4), 41–48.

[82] W. G. Song, H. Fu, and J. F. Haw, *Journal of the American Chemical Society*, **2001**, *123*(20), 4749–4754.

[83] W. G. Song and J. F. Haw, *Angewandte Chemie - International Edition*, **2003**, *42*(8), 892–894.

[84] F. D. P. Mees, P. Van Der Voort, P. Cool, L. R. M. Martens, M. J. G. Janssen, A. A. Verberckmoes, G. J. Kennedy, R. B. Hall, K. Wang, and E. F. Vansant, *Journal of Physical Chemistry B*, **2003**, *107*(14), 3161–3167.

[85] Z. M. Cui, Q. Liu, W. G. Song, and L. J. Wan, *Angewandte Chemie - International Edition*, **2006**, *45*(39), 6512–6515.

[86] L. A. Clark, M. Sierka, and J. Sauer, *Journal of the American Chemical Society*, **2004**, *126*(3), 936–947.

[87] A. M. Vos, X. Rozanska, R. A. Schoonheydt, R. A. van Santen, F. Hutschka, and J. Hafner, *Journal of the American Chemical Society*, **2001**, *123*(12), 2799–2809.

[88] S. Svelle, F. Joensen, J. Nerlov, U. Olsbye, K. P. Lillerud, S. Kolboe, and M. Bjorgen, *Journal of the American Chemical Society*, **2006**, *128*(46), 14770–14771.

[89] C. M. Zicovich-Wilson, A. Corma, and P. Viruela, *Journal of Physical Chemistry*, **1994**, *98*(42), 10863–10870.

[90] T. Asefa, M. J. MacLachan, N. Coombs, and G. A. Ozin, *Nature*, **1999**, *402*(6764), 867–871.

[91] S. Inagaki, S. Guan, T. Ohsuna, and O. Terasaki, *Nature*, **2002**, *416*(6878), 304–307.

[92] F. Fajula, A. Galarneau, and F. Di Renzo, *Microporous and Mesoporous Materials*, **2005**, *82*(3), 227–239.

[93] F. Hoffmann, M. Cornelius, J. Morell, and M. Froba, *Angewandte Chemie - International Edition*, **2006**, *45*(20), 3216–3251.

[94] C. W. Jones, K. Tsuji, and M. E. Davis, *Nature*, **1998**, *393*(6680), 52–54.

[95] C. W. Jones, M. Tsapatsis, T. Okubo, and M. E. Davis, *Microporous and Mesoporous Materials*, **2001**, *42*(1), 21–35.

[96] A. Shimojima and K. Kuroda, *Chemical Communications*, **2004**, (23), 2672–2673.

[97] K. Landskron, B. D. Hatton, D. D. Perovic, and G. A. Ozin, *Science*, **2003**, *302*(5643), 266–269.

[98] X. Y. Bao, X. Li, and X. S. Zhao, *Journal of Physical Chemistry B*, **2006**, *110*(6), 2656–2661.

[99] K. Yamamoto, Y. Sakata, Y. Nohara, Y. Takahashi, and T. Tatsumi, *Science*, **2003**, *300*(5618), 470–472.

[100] K. Yamamoto, Y. Nohara, Y. Domon, Y. Takahashi, Y. Sakata, J. Plevert, and T. Tatsumi, *Chemistry of Materials*, **2005**, *17*(15), 3913–3920.

[101] R. Astala and S. M. Auerbach, *Journal of the American Chemical Society*, **2004**, *126*(6), 1843–1848.

[102] S. Ernst, M. Hartmann, S. Sauerbeck, and T. Bongers, *Applied Catalysis A - General*, **2000**, *200*(1-2), 117–123.

[103] J. M. Xiong, Y. J. Ding, H. J. Zhu, L. Yan, X. M. Liu, and L. W. Lin, *Journal of Physical Chemistry B*, **2003**, *107*(6), 1366–1369.

[104] Y. D. Xia and R. Mokaya, *Angewandte Chemie - International Edition*, **2003**, *42*(23), 2639–2644.

[105] C. M. Zhang, Z. Xu, K. Wan, and Q. Liu, *Applied Catalysis A - General*, **2004**, *258*(1), 55–61.

[106] M. E. Franke, M. Sierka, U. Simon, and J. Sauer, *Physical Chemistry Chemical Physics*, **2002**, *4*(20), 5207–5216.

[107] M. T. Aronson, R. J. Gorte, W. E. Farneth, and D. White, *Journal of the American Chemical Society*, **1989**, *111*(3), 840–846.

[108] J. F. Haw, B. R. Richardson, I. S. Oshiro, N. D. Lazo, and J. A. Speed, *Journal of the American Chemical Society*, **1989**, *111*(6), 2052–2058.

[109] J. F. Haw, *Physical Chemistry Chemical Physics*, **2002**, *4*(22), 5431–5441.

[110] V. Bosacek, *Journal of Physical Chemistry*, **1993**, *97*(41), 10732–10737.

[111] A. Philippou, F. Salehirad, D. P. Luigi, and M. W. Anderson, *Journal of the Chemical Society - Faraday Transactions*, **1998**, *94*(18), 2851–2856.

[112] V. B. Kazansky, *Catalysis Today*, **1999**, *51*(3-4), 419–434.

[113] L. Benco, J. Hafner, F. Hutschka, and H. Toulhoat, *Journal of Physical Chemistry B*, **2003**, *107*(36), 9756–9762.

[114] A. Bhan, Y. V. Joshi, W. N. Delgass, and K. T. Thomson, *Journal of Physical Chemistry B*, **2003**, *107*(38), 10476–10487.

[115] J. W. Thybaut, C. S. L. Narasimhan, G. B. Marin, J. F. M. Denayer, G. V. Baron, P. A. Jacobs, and J. A. Martens, *Catalysis Letters*, **2004**, *94*(1-2), 81–88.

[116] G. Yaluris, R. J. Madon, and J. A. Dumesic, *Journal of Catalysis*, **1999**, *186*(1), 134–146.

[117] W. Wang, M. Seiler, and M. Hunger, *Journal of Physical Chemistry B*, **2001**, *105*(50), 12553–12558.

[118] S. Svelle, S. Kolboe, U. Olsbye, and O. Swang, *Journal of Physical Chemistry B*, **2003**, *107*(22), 5251–5260.

[119] S. Svelle, S. Aravinthan, M. Bjorgen, K. P. Lillerud, S. Kolboe, I. M. Dahl, and U. Olsbye, *Journal of Catalysis*, **2006**, *241*(2), 243–254.

[120] S. Namuangruk, P. Pantu, and J. Limtrakul, *Journal of Catalysis*, **2004**, *225*(2), 523–530.

[121] T. F. Degnan, C. M. Smith, and C. R. Venkat, *Applied Catalysis A - General*, **2001**, *221*(1-2), 283–294.

[122] S. R. Blaszkowski and R. A. van Santen, *Journal of Physical Chemistry*, **1995**, *99*(30), 11728–11738.

[123] P. Geerlings, F. De Proft, and W. Langenaeker, *Chemical Reviews*, **2003**, *103*(5), 1793–1873.